

# **Functional Characterization of Dynamin in Spermatozoa Epididymal Maturation and Acrosomal Exocytosis**

**Wei Zhou**

Master Degree of Science

*Thesis submitted to the Faculty of Science and Information  
Technology, The University of Newcastle, Australia in fulfillment of  
the requirement for the degree of Doctor of Philosophy*

December 2018

# Declaration

## *Statement of Originality*

I hereby certify that the work embodied in the thesis is my own work, conducted under normal supervision.

The thesis contains no material which has been accepted, or is being examined, for the award of any other degree or diploma in any university or other tertiary institution and, to the best of my knowledge and belief, contains no material previously published or written by another person, except where due reference has been made in the text. I give consent to the final version of my thesis being made available worldwide when deposited in the University's Digital Repository, subject to the provisions of the Copyright Act 1968 and any approved embargo.

## *Thesis by publication*

I hereby certify that this thesis is in the form of a series of papers. I have included as part of the thesis a written declaration from each co-author, endorsed in writing by the Faculty Assistant Dean (Research Training), attesting to my contribution to any jointly authored papers.

Signed: .....

Wei Zhou

## **Acknowledgments**

I still could not believe that three and a half years come to an end. As an international student, it is not an easy decision for me to come over to another country to conquer a PhD degree. However, this decision turns out to be the most right one in my life and now I feel Newcastle is my second hometown and it is really hard to say goodbye. To me, it has been a wonderful journey and I would like to express my sincere gratitude to all that have helped me during my PhD study.

First and foremost, to my principal supervisor Brett, there is no word to describe how lucky and grateful I am to be your student. Your passion and knowledge about science guide me into the epididymis research. I always feel enjoyable chatting with you in your office, and your interpretations and feedback on my projects are just beyond satisfaction. I wish I had more time under your supervision, there is so much I want to learn from you. Also, thank you for being so patient with my weak language background. I do not know how you find the time, but I really appreciate your patience to correct every single language error of my manuscript. Without your dedication, none of my work would be published smoothly. I am going to miss how quickly I could get feedback from you. To my co-supervisor Geoffry, thank you for all the amazing feedback on my projects and presentations.

To Amanda, I feel lucky that I have you around when I started the lab work. Thank you for all the “secret” tips and being so supportive when things did not work out so well. Your day-to-day enthusiasm and optimism make my lab life so much easier. To all my colleagues especially Jinwei, Natalie, Jacinta, Jess, Shenae and Caitlin. Thank you all for being so nice to me and there is no way I could conquer the PhD without the company of you guys. To the other members of the Nixon group Liz, Mona and Ilana. Thank you all for the generous and unreserved support during my PhD study.

To Mum, Dad, Sister and my nephew, thank you all for being so supportive when I told you guys I want to go to Australia for further education. All these cannot happen without your support and understanding.

Finally and most importantly, I would like to dedicate this thesis to my lovely wife Eva. Being married to a guy who is obsessed with biological science is miserable. Thank you for being so understandable and supportive all these years. You have always been my best listener and wonderful motivator.

# **Publications and awards arising from work in this thesis**

## 1. Publications

### Chapter 1: Introduction and literature review

**Zhou W**, De Iuliis GN, Dun MD, Nixon B (2018). Characteristics of the Epididymal Luminal Environment Responsible for Sperm Maturation and Storage. *Front Endocrinol*; 9: 59. DOI: 10.3389/fendo.2018.00059.

**Invited Review, Published | Frontiers in Endocrinology**

### Chapter 2:

**Zhou W**, Sipila P, De Iuliis GN, Dun MD, Nixon B (2018). Analysis of Epididymal Protein Synthesis and Secretion. *J Vis Exp*; 138: e58308. DOI: 10.3791/58308.

**Published | Journal of Visualized Experiments**

### Chapter 3:

**Zhou W**, De Iuliis GN, Turner AP, Reid AT, Anderson AL, McCluskey A, McLaughlin EA, Nixon B (2016). Developmental expression of the dynamin family of mechanoenzymes in the mouse epididymis. *Biol Reprod*; 96: 159-173. DOI: 10.1095/biolreprod.116.145433.

**Published | Biology of Reproduction**

### Chapter 4:

**Zhou W**, Stanger SJ, Anderson AL, De Iuliis GN, McCluskey A, McLaughlin EA, Dun MD, Nixon B (2018). Mechanistic insights into mouse epididymosome-sperm interactions.

**Submitted | BMC Biology**

### Chapter 5:

**Zhou W**, Anderson AL, Turner AP, De Iuliis GN, McCluskey A, McLaughlin EA, Nixon B (2017). Characterization of a novel role for the dynamin mechanoenzymes in the regulation of human sperm acrosomal exocytosis. *Mol Hum Reprod*; 23(10): 657-673. DOI: 10.1093/molehr/gax044.

**Published | Molecular Human Reproduction**

## 2. Statements of Contribution

I attest that the Research Higher Degree candidate Wei Zhou has contributed upward of 50% towards data collection/analysis and manuscript preparation for all the publications included in this thesis for which I am a co-author.

.....  
**Prof. Adam McCluskey**  
*Date:05/12/2018*

.....  
**Dr. Adrian P Turner**  
*Date:04/12/2018*

.....  
**Amanda L Anderson**  
*Date:30/11/2018*

.....  
**Dr. Andrew T Reid**  
*Date:04/12/2018*

.....  
**Prof. Brett Nixon**  
*Date:30/11/2018*

.....  
**Prof. Eileen A Mclaughlin**  
*Date:06/12/2018*

.....  
**Dr. Geoffry De Iuliis**  
*Date:03/12/2018*

.....  
**Dr. Matthew D Dun**  
*Date:30/11/2018*

.....  
**A/Prof. Petra Sipilä**  
*Date:07/12/2018*

.....  
**Simone J Stanger**  
*Date:04/12/2018*

.....  
**Prof. Frances Martin**  
Assistant Dean of Research Training  
*Date:11/12/2018*

### 3. Conference proceedings relevant to this thesis

**Zhou W**, Stanger SJ, Anderson AL, De Iuliis GN, McCluskey A, McLaughlin EA, Dun MD, Nixon B.

Mechanistic insights into epididymosome-sperm interactions. 7<sup>th</sup> International Conference on the Epididymis. Montreal, Canada. September 2018. *Poster presentation* | Travel award for the excellent quality of the abstract.

**Zhou W**, Stanger SJ, Anderson AL, De Iuliis GN, McCluskey A, McLaughlin EA, Dun MD, Nixon B.

Mechanistic insights into epididymosome-sperm interactions. 49<sup>th</sup> Annual Conference of the Society for Reproductive Biology. Adelaide, Australia. August 2018. *Oral presentation*.

**Zhou W**, Stanger SJ, Anderson AL, De Iuliis GN, McCluskey A, McLaughlin EA, Dun MD, Nixon B.

Elucidating the role of dynamin in epididymosome mediated transfer of fertility-modulating proteins to maturing spermatozoa. Australian Society for Medical Research Scientific Meeting. Newcastle, Australia. December 2017. *Oral presentation*.

**Zhou W**, Stanger SJ, Anderson AL, De Iuliis GN, McCluskey A, McLaughlin EA, Dun MD, Nixon B.

Elucidating the role of dynamin in epididymosome mediated transfer of fertility-modulating proteins to maturing spermatozoa. 22<sup>nd</sup> annual biology RHD conference. Newcastle, Australia. November 2017. *Oral presentation* | winner of best 3<sup>rd</sup>-year student presentation.

**Zhou W**, Anderson AL, Turner AP, De Iuliis GN, McCluskey A, McLaughlin EA, Nixon B.

Characterization of a novel role for the dynamin mechanoenzymes in the regulation of human sperm acrosomal exocytosis. 48<sup>th</sup> Annual Conference of the Society for Reproductive Biology. Perth, Australia. August 2017. *Oral presentation* | Finalist in Oozoa award section.

**Zhou W**, Reid AT, Anderson AL, De Iuliis GN, McCluskey A, McLaughlin EA, Nixon B.

Developmental expression of the dynamin family of mechanoenzymes in the mouse epididymis. 47<sup>th</sup> Annual Conference of the Society for Reproductive Biology. Gold Coast, Australia. August 2016. *Poster presentation*.

**Zhou W**, Reid AT, Anderson AL, De Iuliis GN, McCluskey A, McLaughlin EA, Nixon B.

Developmental expression of the dynamin family of mechanoenzymes in the mouse epididymis. 20<sup>th</sup> Annual biology RHD conference. Newcastle, Australia. November 2015. *Oral presentation*.

## 4. Additional publications

Nixon B, De Iuliis GN, Hart H, **Zhou W**, Mathe A, Bernstein I, Anderson A, Larsen MR, Dun MD (2018). Proteomic profiling of mouse epididymosomes reveals their contributions to post-testicular sperm maturation. *Mol Cell Proteomics*; pii: mcp.RA118.000946. DOI: 10.1074/mcp.RA118.000946.

**Published | Molecular & Cellular Proteomics**

## 5. Awards

Best HDR Publication Award “Highly Commended” | University of Newcastle | 2018

Travel award for the excellent quality of the abstract | 7<sup>th</sup> International Conference on the Epididymis | 2018

HDR International Conference Scholarship | University of Newcastle | 2018

Best HDR Publication Award | University of Newcastle | 2017

Best 3<sup>rd</sup> year Oral Presentation | 22<sup>nd</sup> Annual Biology RHD Conference | University of Newcastle | 2017

Finalist for Oozoa Award for best student presentation | Society for Reproductive Biology | 2017

## 6. Journal cover image

Biology of Reproduction, Volume 96, Issue 1 (January 2017).

Vol. 96, No. 1

# BOR

Volume 96 Issue 1 January 2017

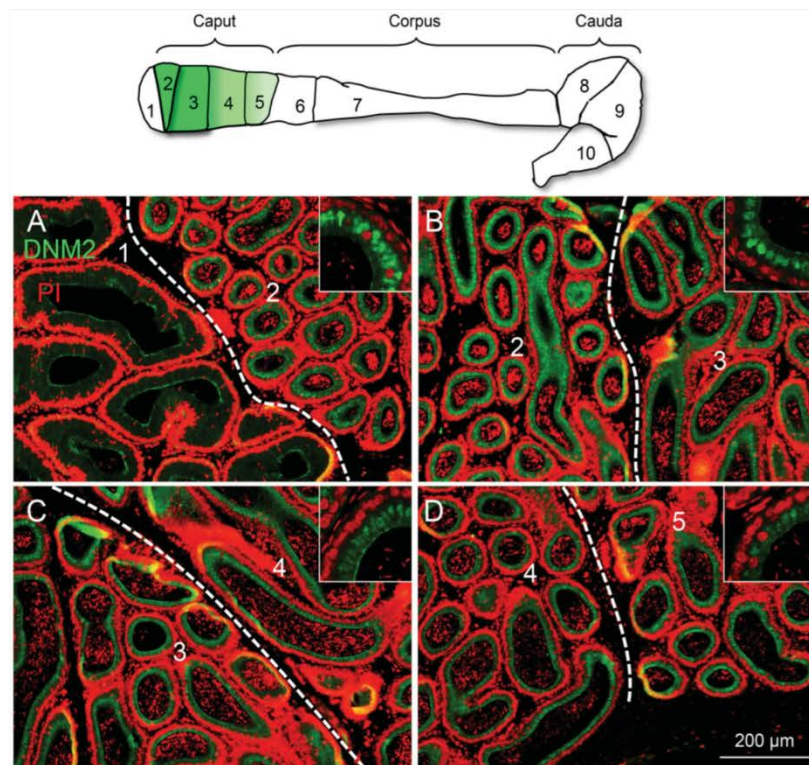
# Biology of Reproduction

OFFICIAL JOURNAL OF THE SOCIETY FOR THE STUDY OF REPRODUCTION

BIOLOGY of REPRODUCTION

Pages 1-265

January 2017



 **SSR**  
Society for the Study  
of Reproduction

# Table of contents

Declaration.....	2
Acknowledgments.....	3
Publication and awards arising from work in this thesis.....	4
Table of contents.....	9
Abstract.....	10

---

## CHAPTER 1: LITERATURE REVIEW

Characteristics of the Epididymal Luminal Environment Responsible for Sperm Maturation and Storage.....	13
---	----

## CHAPTER 2:

Analysis of Epididymal Protein Synthesis and Secretion.....	28
---	----

## CHAPTER 3:

Developmental expression of the dynamin family of mechanoenzymes in the mouse epididymis.....	40
---	----

## CHAPTER 4:

Mechanistic insights into epididymosome-sperm interactions.....	63
---	----

## CHAPTER 5:

Characterization of a novel role for the dynamin mechanoenzymes in the regulation of human sperm acrosomal exocytosis.....	103
--	-----

## CHAPTER 6: FINAL DISCUSSION AND FUTURE RESEARCH

DIRECTIONS.....	134
-----------------	-----

## Abstract

Human infertility is now a major clinical problem affecting approximately one in six couples; with a male factor contributing to nearly 50% of these cases. Clinical analysis has shown that a majority of male infertile patients are still able to produce enough spermatozoa to achieve fertilization. However, for reasons that remain poorly defined, the functionality of these cells has become compromised. Improved understanding of how sperm acquire functional maturity would not only be beneficial in terms of uncovering the causative basis of male gamete dysfunction, but also for the provision of urgently needed biomarkers of sperm quality to reliably predict the outcome of assisted reproductive technology treatments. In this context, it is generally accepted that spermatozoa released from the testes require additional phases of post-testicular development that occur during their transit through the epididymis and female reproductive tract before acquiring functional competence. Both biophysical and biochemical changes occur along this journey, eventually culminating in the ability of sperm to undergo an acrosome reaction and recognize the oocyte. Notably, due to spermatozoa being both transcriptionally and translationally silent, the acquisition of functional maturity is reliant on communication between the spermatozoa and the extrinsic factors that they encounter within the male and female reproductive tracts.

Our recent work has shown that the dynamin family of enzymes may regulate several key steps in these communication pathways. The dynamin family comprises a group of large GTPases responsible for the regulation of membrane trafficking events such as endocytosis, exocytosis and intracellular trafficking. Such diverse functionality relies on the ability of dynamin to polymerize into a helix structure around the template lipid membrane, whereupon GTP hydrolysis drives the lengthwise constriction of the helix structure and leads to scission of the connection between the two membrane templates. Dynamin has three canonical isoforms, namely dynamin 1, dynamin 2 and dynamin 3. Although sharing over 80% sequence homology, recent studies have shown that each isoform may play distinct roles in regulating membrane trafficking events, depending on their localization and ability to interact with other protein targets. This is especially the case in male reproduction with our previously published studies having shown that dynamin 1 and 2 putatively regulate acrosomal exocytosis whilst dynamin 2 plays an essential role in regulating spermatogenesis in the mouse model.

Herein, we have provided further evidence that dynamin is involved in sperm maturation through the regulation of epididymal epithelium secretion. Our detailed

characterization of the three canonical dynamin isoforms have revealed that each are highly expressed during the early development phases of epididymal differentiation. Interestingly however, the widespread localization of these isoforms in the juvenile epididymis is replaced by segment and cell specific patterns coinciding with the arrival of testicular sperm into the tract. Notably, the expression of dynamin 2 in the Golgi apparatus of caput epithelial cells ideally positions the enzyme to regulate the classical merocrine pathway of protein secretion. This hypothesis was tested through the use of an *in vitro* caput epithelial cell line; i.e. mECap18 cells. Accordingly, pharmacological inhibition of dynamin selectively inhibited the secretion of a subset of proteins, such as CCT3 and CCT8, from the mECap18 cells.

Having demonstrated that dynamin influences the secretion of epididymal proteins, we elected to explore if members of this family also participate in downstream communication between epididymal soma and sperm via the control of extracellular vesicle uptake. For this purpose, we elected to focus on epididymosomes, small membrane encapsulated vesicles that have been implicated in establishing the sperm proteomic and epigenetic landscape. Through the establishment of an *in vitro* co-culture model, we have documented the kinetics of epididymosome-mediated transfer of proteins to spermatozoa and identified the post-acrosomal sheath as the domain responsible for initial epididymosome – sperm adhesion. Such adhesion appears to be followed by the uptake of epididymosome cargo into the cell, a process that is reliant on both dynamin 1 and lipid rafts.

In continuing our investigation of dynamin, we also elected to study the role of this family of mechanoenzymes in regulating the acrosome reaction in human spermatozoa. Based on previous data generated in a mouse model, we hypothesized that dynamin 1 and 2 play a conserved role in facilitating acrosomal exocytosis in human spermatozoa, and that this activity is linked to the phosphorylation status of the dynamin proteins. Consistent with this hypothesis, dynamin 1 and 2 were localized to the acrosomal domain of human spermatozoa and their pharmacological inhibition significantly compromised the ability of human spermatozoa to complete an acrosome reaction. This activity appears to be tied to the phosphorylation of dynamin, with our data identifying CDK1 as an important targeting kinase for dynamin 2. Accordingly, we recorded a significant loss of dynamin 2 expression in the acrosomal domain of poor quality human spermatozoa; a loss that was accompanied by a significant reduction in the ability of these cells to complete an acrosome reaction. Collectively these data support a conserved role for dynamin in regulating the acrosome reaction in both mouse and human spermatozoa.

In summary, the data summarized in this thesis implicates dynamin as a key regulatory enzyme in both epididymal sperm maturation and downstream acrosomal exocytosis. In contrast to the overlapping role of the dynamin family members in somatic cells, our findings raise the prospect that different dynamin members fulfill distinct functions in the male reproductive system. Such distinctions raise the intriguing possibility of being able to target specific dynamin members for the purpose of male fertility regulation. Moreover, the functional conservation we observed between human and mouse models supports the utility of conditional knockout mouse models as an important tool with which to further dissect the role of dynamin in human male (in)fertility.

# CHAPTER 1: LITERATURE REVIEW

---

## *Characteristics of the Epididymal Luminal Environment Responsible for Sperm Maturation and Storage*

**Published:** Frontiers in Endocrinology (2018) 9: 59

**Authors:** Wei Zhou<sup>1</sup>, Geoffry N. De Iuliis<sup>1</sup>, Matthew D. Dun<sup>2,3</sup> and Brett Nixon<sup>1\*</sup>

<sup>1</sup>Priority Research Centre for Reproductive Biology, School of Environmental and Life Sciences,  
University of Newcastle, Callaghan, NSW 2308, Australia.

<sup>2</sup>Faculty of Health and Medicine, University of Newcastle, Callaghan, NSW, Australia.

<sup>3</sup>Cancer Research Program, School of Biomedical Sciences and Pharmacy, Hunter Medical Research  
Institute, University of Newcastle, New Lambton Heights, NSW, Australia.

\*Correspondence: [brett.nixon@newcastle.edu.au](mailto:brett.nixon@newcastle.edu.au)

## Chapter 1: Overview

The aim of the following manuscript was to review our current understanding of the molecular mechanisms that exert influence over the unique intraluminal environment of the male reproductive tract (the epididymis), with a particular focus on vesicle-dependent mechanisms that facilitate intracellular communication between the epididymal soma and maturing sperm cell population.

The mammalian epididymis is an exceptionally long, convoluted ductal system that provides an optimal environment to promote the functional transformation of spermatozoa and their subsequent storage in a viable state in readiness for ejaculation. What makes this process remarkable is that, as testicular spermatozoa are transcriptionally and translationally silent, it is entirely driven by the luminal microenvironment created by the combined secretory and absorptive activities of the epididymal epithelial cells. Here we summarize the regionalized characteristics of the epididymis, the luminal components, how secretory and absorptive pathways contribute to and maintain the complex luminal microenvironment and how specific gene knockout or depletion affects the luminal microenvironment. Furthermore, we place particular emphasis on recent work focusing on the evaluation of vesicle-dependent mechanisms (especially epididymosomes) that facilitate intercellular communication between the epididymal soma and maturing sperm cell population. This body of research has aroused broad interest as vesicle-dependent mechanisms not only afford a mechanism for the bulk delivery of macromolecular cargo to spermatozoa, but the membrane-bound structures also provide protection to such cargo against the deleterious outside environment. Moreover, this pathway has recently been implicated in the relay of epigenetic information (e.g. small non-protein coding RNA) to spermatozoa with the potential to influence early embryo development. Finally, we give consideration to our own novel findings regarding the role of the dynamin family of mechanoenzymes in the regulation of the epididymal luminal environment and in mediation of epididymosome-sperm interactions.



# Characteristics of the Epididymal Luminal Environment Responsible for Sperm Maturation and Storage

Wei Zhou<sup>1</sup>, Geoffry N. De Iulii<sup>1</sup>, Matthew D. Dun<sup>2,3</sup> and Brett Nixon<sup>1\*</sup>

<sup>1</sup> Priority Research Centre for Reproductive Science, School of Environmental and Life Sciences, University of Newcastle, Callaghan, NSW, Australia, <sup>2</sup> Faculty of Health and Medicine, University of Newcastle, Callaghan, NSW, Australia, <sup>3</sup> Cancer Research Program, School of Biomedical Sciences and Pharmacy, Hunter Medical Research Institute, University of Newcastle, New Lambton Heights, NSW, Australia

## OPEN ACCESS

### Edited by:

Marc Yeste,  
University of Girona, Spain

### Reviewed by:

Robert Sullivan,  
Laval University, Canada  
Jean-Louis Dacheux,  
UMR7247 Physiologie de la  
reproduction et des comportements  
(PRC), France

### \*Correspondence:

Brett Nixon  
brett.nixon@newcastle.edu.au

### Specialty section:

This article was submitted  
to Reproduction,  
a section of the journal  
Frontiers in Endocrinology

**Received:** 14 December 2017

**Accepted:** 09 February 2018

**Published:** 28 February 2018

### Citation:

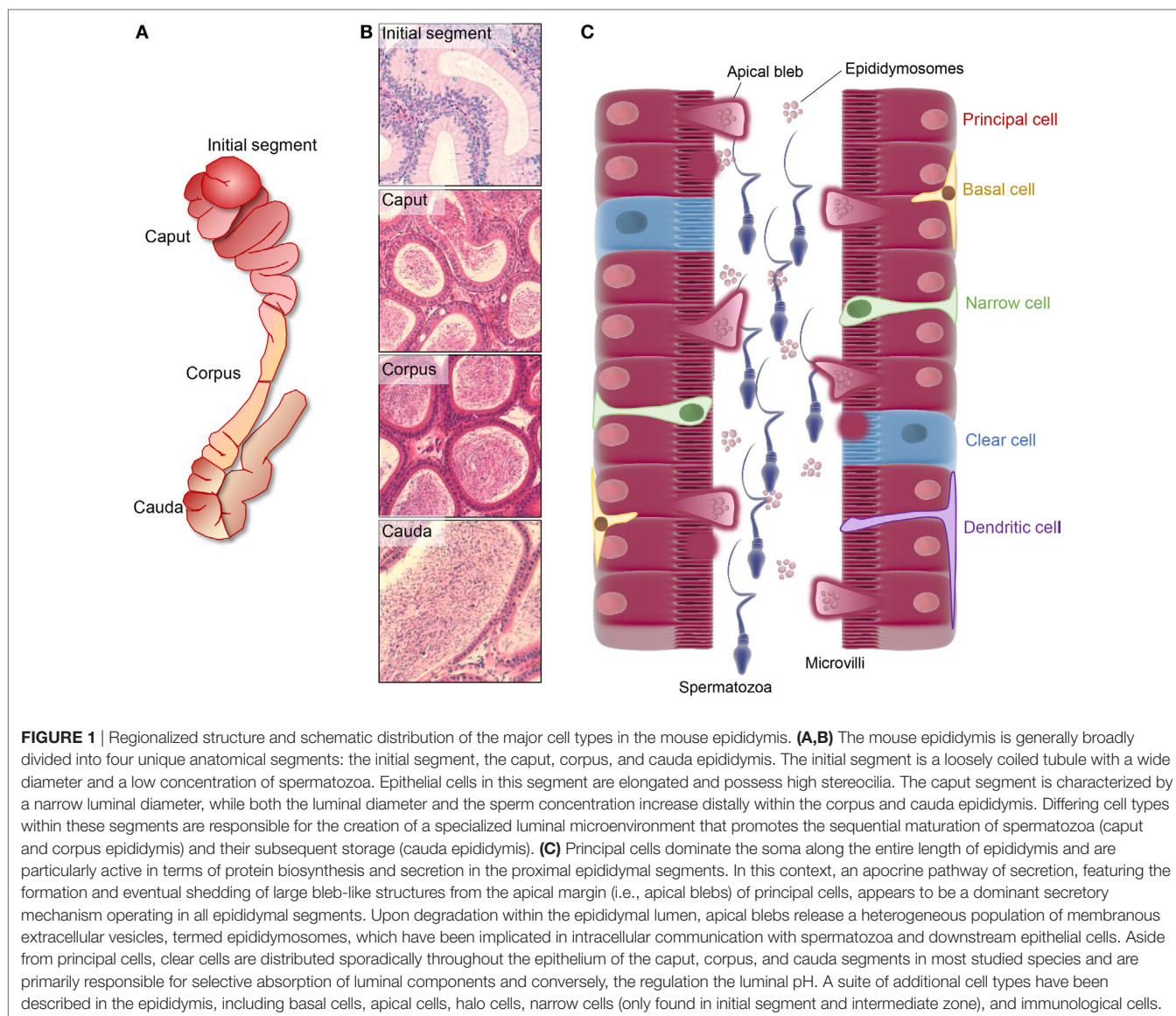
Zhou W, De Iulii GN, Dun MD  
and Nixon B (2018) Characteristics  
of the Epididymal Luminal  
Environment Responsible for  
Sperm Maturation and Storage.  
*Front. Endocrinol.* 9:59.  
doi: 10.3389/fendo.2018.00059

The testicular spermatozoa of all mammalian species are considered functionally immature owing to their inability to swim in a progressive manner and engage in productive interactions with the cumulus–oocyte complex. The ability to express these key functional attributes develops progressively during the cells' descent through the epididymis, a highly specialized ductal system that forms an integral part of the male reproductive tract. The functional maturation of the spermatozoon is achieved *via* continuous interactions with the epididymal luminal microenvironment and remarkably, occurs in the complete absence of *de novo* gene transcription or protein translation. Compositional analysis of the luminal fluids collected from the epididymis of a variety of species has revealed the complexity of this milieu, with a diversity of inorganic ions, proteins, and small non-coding RNA transcripts having been identified to date. Notably, both the quantitative and qualitative profile of each of these different luminal elements display substantial segment-to-segment variation, which in turn contribute to the regionalized functionality of this long tubule. Thus, spermatozoa acquire functional maturity in the proximal segments before being stored in a quiescent state in the distal segment in preparation for ejaculation. Such marked division of labor is achieved *via* the combined secretory and absorptive activity of the epithelial cells lining each segment. Here, we review our current understanding of the molecular mechanisms that exert influence over the unique intraluminal environment of the epididymis, with a particular focus on vesicle-dependent mechanisms that facilitate intercellular communication between the epididymal soma and maturing sperm cell population.

**Keywords:** epididymis, sperm maturation, intracellular communication, protein trafficking, apocrine secretion, merocrine secretion, epididymosome, dynamin

## INTRODUCTION

The mammalian epididymis is an exceptionally long, convoluted ductal system that serves to connect the ductuli efferentes, which drain the testes, to the ductus deferens. Anatomically, this highly specialized organ is generally divided into four broad segments: the initial segment, caput, corpus, and cauda epididymides (**Figures 1A,B**) (1); although this demarcation is not strictly adhered to in all mammalian species (2). Irrespective, the epididymis is responsible for the



provision of an optimal environment to promote the functional transformation of spermatozoa and their subsequent storage in viable state in readiness for ejaculation. Functional profiling studies indicate that the epididymis displays highly regionalized characteristics. Thus, the initial segment and upstream ductuli efferentes are responsible for the absorption of the majority of testicular fluid entering the duct leading to a pronounced concentration of the luminal spermatozoa (3). Thereafter, the caput epididymis is most active in terms of protein synthesis and secretion, and a small portion of the sperm passing through this region begin to exhibit the ability to swim in a progressive manner and to recognize an oocyte (4–6). These functional characteristics continue to develop in the corpus epididymis before reaching an optimal level in the distal caudal segment. This latter region is characterized by a relatively large lumen and its surrounding epithelial cells exhibit strong absorptive activity (7, 8). Such attributes align with the dominant function

of the cauda epididymis in terms of the formation of a sperm storage reservoir.

It is well established that the combined secretory and absorptive activities of the epididymal epithelial cells are responsible for the creation of the highly specialized luminal microenvironment that promotes the gradient of increasing fertility in the sperm population held therein (9). Systematic analysis of the composition of these luminal fluids has revealed a complex macromolecular landscape encompassing a myriad of soluble factors in addition to non-pathological amyloid matrices and exosome-like vesicles termed epididymosomes. The latter of these have come under increasing scrutiny owing to their potential to facilitate the efficient transfer of a variety of protein and small non-coding RNA cargo to the maturing sperm cells. Furthermore, there is emerging evidence that the epididymosome payload may be dynamically altered in response to paternal exposure to environment stressors. The implications of such changes in terms of

establishing the sperm epigenetic and proteomic signatures, and their potential to influence the downstream health and developmental trajectory of offspring, are only just beginning to be realized. It is therefore timely to review the changes associated with sperm maturation in the epididymal tract and the molecular mechanisms by which such changes are brought about. Here, we focus on the regulation of the epididymal luminal microenvironment and place particular emphasis on vesicle-dependent mechanisms that facilitate intercellular communication between the lining epididymal soma and the maturing sperm cell population.

## THE LUMINAL MICROENVIRONMENT OF THE EPIDIDYMIS

The process of post-testicular sperm maturation is reliant on the highly specialized intraluminal microenvironment of the epididymis, arguable one of the most complex milieus produced by any endocrine gland. Accordingly, the selective ablation of genes that lead to dysregulation of the epididymal microenvironment commonly results in male infertility/subfertility phenotypes (Table 1). The origin of these fluids rests with the pseudostratified epithelium lining the duct. This epithelium comprises a number of different cell types (Figure 1C) including, populations of principal, clear, narrow, apical, basal, halo, and immunological (macrophage and dendritic) cells; the abundance of which varies considerably between different epididymal segments (10). Detailed functional studies have confirmed spatial differences in the profile of each cell type and revealed that, under the precise control afforded by androgens and various other factors of testicular origin, they each make unique contributions to sperm maturation, protection, and storage (10).

## Epididymal Epithelium

Principal cells represent the major cell type throughout the entire epididymis, constituting as much as 80% of the peritubular interstitium (11). These cells are characterized by abundant secretory apparatus [endoplasmic reticulum (ER), Golgi and secretory granules] reflecting their high exocytotic activity, especially in the proximal portions of the epididymis (caput and corpus) (8, 12, 13). In more distal segments (cauda), the principal cells take on a predominantly endocytotic role in which they are actively responsible for the reabsorption of various components from the epididymal fluid, a function that is also shared with that of the clear cell population (12). Clear cells are the second most abundant cell type, being widely distributed in the caput and corpus segments but displaying most enrichment in the cauda. The apical domain of clear cells is replete with endocytotic apparatus and accordingly, these cells have a tremendous capacity for endocytosis (7, 12). This is particularly true of the clear cells that populate the distal epididymal segments, which have been implicated in the uptake and disposal of the cytoplasmic droplets that are shed from the maturing sperm cell population (7), as well as the recycling of various other luminal components. Also within their apical domain, clear cells possess key elements of the machinery [vacuolated (V)-ATPase, carbonic anhydrase II, and soluble adenylate cyclase] necessary for acidification of the luminal environment, thus highlighting their role in regulation of the pH of the epididymal environment (8, 14). Narrow and apical cells are mainly found within the initial segment (15, 16). However, their function is yet to be fully resolved (8). Basal cells display a hemispherical morphology and form intimate contact with the basement membrane and principal cells on both sides (8).

**TABLE 1** | Gene knockout or deletion strategies that impact the intraluminal environment of the mouse epididymis.

Gene knockout	Fertility phenotype	Changes to epididymal environment	References (PMID)
<i>Sed1</i>	Infertile	Hypo-osmotic and alkaline epididymal fluid, disrupted fluid reabsorption, increased intracellular vesicles	20122713
<i>Esr1</i>	Infertile	Hypo-osmotic fluid	20130266
<i>C-ros</i>	Infertile	Defective initial segment development, increased luminal pH	10645273, 15095336
<i>Dicer1</i>	Subfertile	Imbalanced lipid homeostasis in proximal segments. Dedifferentiation of the epithelium and imbalance in sex steroid signaling	25366345, 22701646
<i>Rlx</i>	Subfertile	Delayed maturation and growth associated with increased collagen deposition	15956703
<i>He6</i>	Infertile	Reduced in size and dysregulation of fluid reabsorption	15367682
<i>Lur</i> (testosterone treatment)	Subfertile	Inflammation in epididymis	15514086
<i>Era</i>	Infertile	Disruption in Na <sup>+</sup> reabsorption and passive water transport, abnormal epithelial ultrastructure	11698654
<i>Nhe3</i>	Infertile	Disruption in Na <sup>+</sup> reabsorption and passive water transport	11698654
<i>Lxr</i>	Infertile	Abnormal accumulation neutral lipids	15525595
<i>Apoer2</i>	Infertile	Dysfunction of clusterin and PHGPx protein impacting sperm maturation	12695510
<i>Fsh-r</i>	Subfertile	Smaller epithelial surface area in caput and corpus segments	15973687
<i>Gpx5</i>	Higher incidence of miscarriages and developmental defects	Excess of reactive oxygen species in the cauda segment leading to oxidative damage of spermatozoa	19546506
<i>Hoxa10</i>	Subfertile	Epididymis characterized by homeotic transformation	8787743
<i>Hoxa11</i>	Infertile	Epididymis characterized by homeotic transformation	7789268
<i>Hexa</i>	Infertile (age dependent)	Inability to degrade endocytosed substrates	12617783
<i>Tmf</i>	Infertile	Epithelial apoptosis and sperm stasis in the cauda segment	23000399
<i>Trpv6</i>	Subfertile	Defects in epididymal Ca <sup>2+</sup> absorption	22427671
<i>Slc9a3</i>	Infertile	Abnormally abundant secretions and calcification in the lumen	28384194

Ligation experiments in the rat have shown that basal cells possess the ability to change shape in order to adjust the luminal volume and pressure; features that are suggestive of a protective role in preserving the structural integrity of the lumen (17).

The remaining cell types comprising the epididymal epithelium are predominantly related to immune functions (8), an important consideration given the highly antigenic nature of the male germ cell. Indeed, the epididymal luminal environment and thus maturing spermatozoa are shielded from immune surveillance behind a blood–epididymal barrier. This barrier consists of a network of tight junctions that form between adjacent epithelial cells. The ductal system so created is further characterized by connective septa to form a number of distinct segments and thus facilitate the formation of successive, regionally distinct luminal microenvironments (18–20). Since a majority of testicular fluid is reabsorbed before reaching the proximal segments of the epididymis, most of the luminal components, other than the sperm cells themselves, originate from the secretory activity of the pseudostratified epithelial cells comprising the duct. Detailed compositional analysis of the epididymal fluid has revealed it contains a complex array of proteins, ions, and small non-coding RNA species (21, 22). While these molecules are present in all the epididymal segments, they nonetheless display an extraordinary level of regionalization, which reflect differential secretory and absorptive activity of the epithelial cells.

## Luminal Components

As previously mentioned, the proteome of maturing spermatozoa is substantially modified *via* the uptake, repositioning, and posttranslational modification of a significant portion of proteins. Such changes are mediated by direct exposure to the proteins secreted into the epididymal luminal environment, with a majority of these originating in the proximal segments of the caput and corpus epididymis (23). By contrast, proteins involved in the preservation of sperm viability, such as antioxidant enzyme defenses, and those responsible for suppression of humoral immune responses, tend to be enriched in the cauda epididymal secretome (23). Furthermore, detailed transcriptomic analysis in the mouse epididymis has identified a prominent theme of segment-dependent regulation, with the expression of 12.8% of the total 17,000 epididymal genes being characterized by changes of at least fourfold between any two segments (21). This ratio increases to 35.8% if the criterion is relaxed to include transcripts that vary by at least twofold. Consistent with these data, it has also been shown that protein and gene expression patterns display very discrete profiles that closely align with the borders of septa demarcating anatomically different segments of the epididymis (24–26). How this precise regulation is imposed is still unclear, but it is perhaps notable that grossly similar profiles of epididymal protein expression have been documented along the epididymal tract of many mammalian species, including large domestic species (27) and humans (28). One possible explanation rests with evidence for the expression of a myriad of small non-protein coding RNA transcripts in the epithelial cells (22, 29–33).

In this context, the focus for most investigations has been the microRNA (miRNA) class of RNA molecules (~21–25

nucleotides) that hold a key regulatory role in the repression of mRNA translation. Indeed, the use of microarray and next generation sequencing methodologies has led to the identification of a total of 545 and 370 miRNAs in the human and mouse epididymis, respectively (22, 29). A large portion of these miRNAs are conserved among different epididymal segments (75% in the mouse epididymis) and even between different species (31% between mouse and human), suggesting housekeeping roles in the regulation of epididymal homeostasis (22). In contrast, other miRNAs are characterized by pronounced segmental patterns of expression (15% in mouse epididymis). For example, *miR-204-5p* and *miR-196b-5p* are down and upregulated significantly, with approximately 39- and 45-fold differences in expression having been recorded between caput and caudal segments of the mouse epididymis (22). The biological implications of such differences are highlighted by the potential for each miRNA species to exert regulatory control over multiple targets. By way of illustration, target prediction algorithms indicate that an estimated 530 and 160 genes are putatively able to be targeted by *miR-204-5p* and *miR-196b-5p*, respectively (34). Thus, the differing miRNA expression profiles documented in each epididymal segment impose a daunting level of complexity to the regulation of unique segmental environments in the epididymis. The precise mechanisms responsible for differential miRNA expression profiles remains poorly understood but are undoubtedly influenced by androgens and other lumicrine factors of testicular origin (35). Alternatively, it has been proposed that epididymosomes may serve as vectors to selectively traffic miRNA cargo between their sites of production in the proximal epididymal segments to recipient epithelial cells lining downstream segments (36).

In any case, it is therefore perhaps not surprising that intraluminal proteome of the epididymis ranks among the most complex produced by any endocrine gland. In addition to a diversity of soluble proteins, electron-dense proteinaceous complexes have also been described in the epididymal lumen of rodents, rams and, recently humans (37–40). These are apparently non-pathological structures, with a diameter ranging from 500 nm to 1.2  $\mu\text{m}$ , which lack any obvious organelles, and similarly, are not delineated by a lipid bilayer (39). Despite these features, the formation/maintenance of these extracellular matrices appears to be a selective rather than stochastic process as evidenced by the conservation of their protein profile across several taxa. In this regard, the highly amyloidogenic cystatin-related epididymal spermatogenic (CRES) family appear to be critical constituents of these entities (41). Thus, a potential mechanism for formation is through self-assembly brought about by interaction of CRES subgroup members, small hydrophobic proteins and/or prion proteins (37, 41). Accordingly, pioneering work by the Cornwall laboratory has established that these extracellular matrices do possess amyloid structural properties, which change along the length of the epididymal tubule. Indeed, immature amyloid forms prevail in the proximal epididymis before taking on thinner “film-like” characteristics in the distal epididymis (41, 42). Notably, these changes in amyloid matrix structure parallel changes in epididymal function with proximal segments responsible for promoting sperm maturation and distal segments serving

primarily as a storage site for mature spermatozoa (please see Introduction). On the basis of these data, it has been suggested that epididymal amyloids are formed for functional purposes in sperm maturation and/or protection by coordinating interactions between the luminal fluid and spermatozoa. Interestingly, a similar role has also been proposed for “dense bodies” that have been documented in the lumen of the rodent epididymis (39, 43, 44), although at present it remains to be established whether these amorphous entities do equate to amyloid matrices. Irrespective, dense bodies are replete with proteins such as those of the molecular chaperone family (HSPD1 and HSP90B1) (39), bactericidal/permeability-increasing protein (43), and glycogen synthase kinase 3. While the precise function of the chaperone cargo remains obscure, it has been suggested that, similar to CRES, these proteins may assist in the aggregation of luminal proteins into large discrete entities, and thus increase the efficiency with which they are able to be delivered to the spermatozoa. In keeping with this notion, ultrastructural analyses have provided evidence that dense bodies form intimate contact with epididymal spermatozoa, and thereafter mediate the transfer of associated cargo (44). Further dissection of the structural and functional properties of these extracellular matrices promises to shed new light on the mechanisms by which the epididymal soma communicates with sperm to coordinate their maturation and storage.

In addition to amyloids/dense bodies, the epididymal lumen also features an impressive population of extracellular vesicles. Indeed, as early as 1985, Yanagimachi identified a population of small membranous vesicles residing near the surface of epididymal spermatozoa in the Chinese hamster, and subsequently predicted their potential role in cholesterol transfer to the maturing spermatozoa (45). The existence of these vesicles, now commonly referred to as “epididymosomes,” has subsequently been confirmed in the epididymal fluid of a variety of other mammalian species such as mice (46), rats (47), bull (48, 49), and human (50). With defining characteristics of a relatively small size (varying from 50–500 nm), a heterogeneous cargo of macromolecules, and a membrane that is highly enriched in cholesterol (51), epididymosomes have since been implicated in promoting various aspects of sperm maturation. Such influence is mediated through either direct interaction with the sperm themselves or *via* indirect mechanisms involving delivery of regulatory cargo (e.g., miRNAs; see below) to epithelial cells downstream of their site of genesis.

Proteomic analysis of bull and human epididymosomes has revealed they contain a complex cargo of several hundred proteins encompassing key classes of enzymes, chaperones, structural proteins, and many more with hitherto unknown function (52, 53). Some of these proteins have been shown to be directly transferred to specific sperm domains during their transit through the epididymis and are, in turn, essential for promoting the functional maturity of these cells. Notable examples include macrophage migration inhibitory factor (MIF), a cytokine with a broad distribution and diverse functions in multiple tissues. During epididymal transit in the rat and bovine, MIF is transferred from epididymosomes to the fibrous sheath of the sperm flagellum and subsequently influences the motility characteristics

of these cells (54, 55). Alternatively, P26h/P34H family members (P26h in hamster, P25b in bovine, and P34H in humans) are a group of glycosyl-phosphatidylinositol (GPI)-linked proteins that are initially found within epididymosomes before becoming firmly anchored to the surface of the sperm acrosomal domain. Functional studies have revealed that these proteins are indispensable for zona pellucida binding, which is a prerequisite for successful fertilization (56–58). Other transferred proteins include membrane-associated, transmembrane, and GPI-linked candidates, and it is likely that the epididymosomes afford an important mechanism for the bulk delivery of this cargo, possibly in the form of already assembled protein complexes to the sperm cell. Direct evidence for this form of transport has been provided through *in vitro* co-incubation studies between spermatozoa and epididymosomes focusing on protein complexes such as the MCA4a–PMCA4b–CASK complex, which has been directly co-immunoprecipitated from epididymosomes (59). This protein complex has been shown to be transferred to the acrosomal region and mid-piece of the flagellum (which are two key functional domains in the male gamete) under optimized *in vitro* incubation conditions featuring the physiologically relevant pH of 6.5 and a high concentration of zinc (60, 61).

In this sense, the ionic composition of epididymal fluids is markedly different from that documented in other bodily fluids (62). Thus, the epididymal fluid contains a lower overall concentration of  $\text{Na}^+$ ,  $\text{Cl}^-$ ,  $\text{Ca}^{2+}$  (except for human), and  $\text{HCO}_3^-$  ions than those that have been reported in blood plasma (62–65). These particular ionic concentrations are, in turn, tightly associated with the regulation of luminal acidification that helps keep spermatozoa in a dormant state (66, 67). Within the epididymal lumen, events such as sexual arousal stimulate principal cells to secrete  $\text{HCO}_3^-$  and  $\text{Cl}^-$ . This change is sensed by purinergic receptors in adjacent clear cells where it leads to activation of bicarbonate-sensitive adenylyl cyclase and the downstream relocalization of proton pumping ATPases to the apical region of these cells. These pumps subsequently secrete  $\text{H}^+$  (66) leading to further acidification of the epididymal luminal environment. This cell–cell cross talk is mediated by several membrane receptors including cystic fibrosis conductance transmembrane regulator positioned in the principal cells and cognate sodium bicarbonate cotransporters (NBC) in the clear cells. Intracellular  $\text{Ca}^{2+}$  is also required for ATPase sequestration within the apical domain of clear cells owing to its ability to dynamically modulate the actin cytoskeleton (68).  $\text{Ca}^{2+}$  also plays a more direct role in the regulation of sperm functionality by virtue of its ability to enter the cell through cation channels (CATSPER) that are located in the principal piece of the sperm flagellum. Accordingly, blocking  $\text{Ca}^{2+}$  influx *via* *CatSper* knockout strategies leads to impaired sperm motility (69).

Finally, in addition to the more well-studied proteomic and ionic components of the epididymal luminal fluids, a number of recent studies have provided compelling evidence for the existence of myriad of small non-protein coding RNA transcripts in epididymal fluid (29–33). Such entities appear predominantly, but perhaps not exclusively, to be associated with epididymosomes (33, 70–72). In the mouse model, we have confirmed that epididymosomes encapsulate >350 different

miRNAs. This inventory includes many miRNAs that are found in epididymosomes and epididymal spermatozoa but are apparently absent, or detected at significantly reduced levels, in the surrounding soma. Such findings are suggestive of selective packaging of the epididymosomes cargo (52). In keeping with this notion, substantial qualitative and quantitative changes have been documented in the epididymosome cargo along the length of the epididymis; including significant fold changes in the accumulation of almost half of their encapsulated miRNAs (70). These data accord with similar findings in the bull (33), and take on added significance in view of evidence that epididymosomes can convey their macromolecular payload to spermatozoa and downstream epididymal epithelial cells (33). Epididymosomes thus represent key conduits for the selective modification of the sperm proteome and epigenome during their post-testicular maturation (71, 73). A challenge for future studies will be to determine the extent to which this novel form of intercellular communication underpins the perturbation of the sperm epigenome arising in response to paternal environmental exposures (74).

## REGULATION OF THE EPIDIDYMAL LUMINAL ENVIRONMENT

Sequential modification of the epididymal luminal milieu demands the interchange of components between the lining epithelium and the lumen. As described previously, this form of intercellular communication is carefully orchestrated by the secretory and absorptive activity of the differing populations of epithelial cells (8). Logically, the interface for a majority of these interactions is the sperm plasma membrane, a structure that is known to undergo dramatic maturational changes mediated by either direct contact with the epithelial margin or by physical exchange of luminal components. Although such exchanges undoubtedly rely on membrane trafficking activity, the precise mechanisms and the machinery involved in these events remains to be fully elucidated.

### Epithelial Secretion: Merocrine versus Apocrine Secretory Pathways

Merocrine secretion is a classical pathway operative in glandular tissue whereby the endosomal network generates, packages, and finally exports cargo *via* exocytosis (Figure 2). The diverse proteins secreted in this fashion share the general properties of being soluble and containing a signal peptide sequence that directs them toward the ER in preparation for trafficking to the membrane (75). In the mammalian epididymis, merocrine secretion is believed to be one of the major pathways through which principal cells are able to regulate the composition of the intraluminal milieu. Accordingly, morphological characterization of this cell population has revealed they possess extremely long microvilli accompanied by numerous vesicles extending from the Golgi apparatus to the adluminal cell border; this is particularly true of the proximal caput segment, which is most active in terms of protein secretion into the lumen (76). Among the epididymal proteins secreted *via* the merocrine pathway, many have been implicated in forming loose electrostatic associations

with the periphery of the sperm surface (77). This appears to be true of proteins such as those implicated in holding sperm in a decapacitated state, i.e., the so-called decapacitation factors (77).

The precise mechanisms controlling merocrine secretion are still relatively poorly understood. Some studies have implicated regulatory elements of classical membrane trafficking machinery, such as the Rab superfamily of monomeric GTPases (78). Although various Rab proteins are highly, and differentially, expressed in the epididymal epithelium, their ability to exert similar regulation to that described in other somatic systems remains to be verified. Alternatively, recent work in our own laboratory has focused on the characterization of the temporal and spatial expression of the dynamin family of mechanoenzymes in the mouse epididymis (79). This family of proteins is of potential interest owing to their ability to couple both exo- and endocytotic processes. Indeed, while dynamin has been best studied in the context of clathrin-coated endocytosis from the plasma membrane, it is also implicated in formation and budding of transport vesicles from the Golgi network (80, 81), vesicle trafficking (82), orchestrating exocytotic events (83, 84), and in the regulation of microtubular and actin cytoskeletal dynamics (84, 85). Moreover, dynamin also has the potential to fine-tune exocytotic events by virtue of its ability to control the rate of fusion pore expansion, and thus the amount of cargo released from an exocytotic vesicle. In our analysis we found that, the dynamin 2 isoform is positioned within the vicinity of the Golgi apparatus of principal cells of the caput epididymis. Further, pharmacological inhibition of dynamin 2 selectively compromised the profile of proteins secreted from an immortalized caput epididymal cell line (79). On the basis of these data, we infer that dynamin 2 may contribute to the regulation of merocrine secretion by the mouse caput epididymal epithelium.

In addition to participating in merocrine secretion, there is also compelling evidence that the epididymal epithelium is heavily reliant on apocrine secretory pathways. Notably, apocrine secretion appears to underpin the transportation and release of epididymosomes into the epididymal lumen (Figure 2). This pathway, in turn, provides a mechanism for the release of proteins lacking an ER signal peptide and/or containing a glycosyl-phosphatidylinositol (GPI) anchor (86, 87); neither of which could be delivered to the epididymal luminal environment *via* the merocrine secretory pathway. As documented above, the epididymosomes released *via* apocrine secretion also contain a comprehensive profile of miRNAs and other sncRNAs, that themselves display marked segment specific differences (70). During intracellular transfer, the small epididymosome vesicles are first sequestered into large bleb-like structures that protrude from the apical margin of principal cells. The apical blebs eventually detach and disintegrate to release their encapsulated cargo within the lumen (11, 88). At present, the precise mechanisms by which the blebs are formed and detached remain to be determined. However, performed under conditions of stringent fixation, ultrastructural electron microscopy has revealed that the attachment of the apical blebs progressively narrows to form a stalk-like process that eventually undergoes scission to release the bleb into the lumen (88). This process

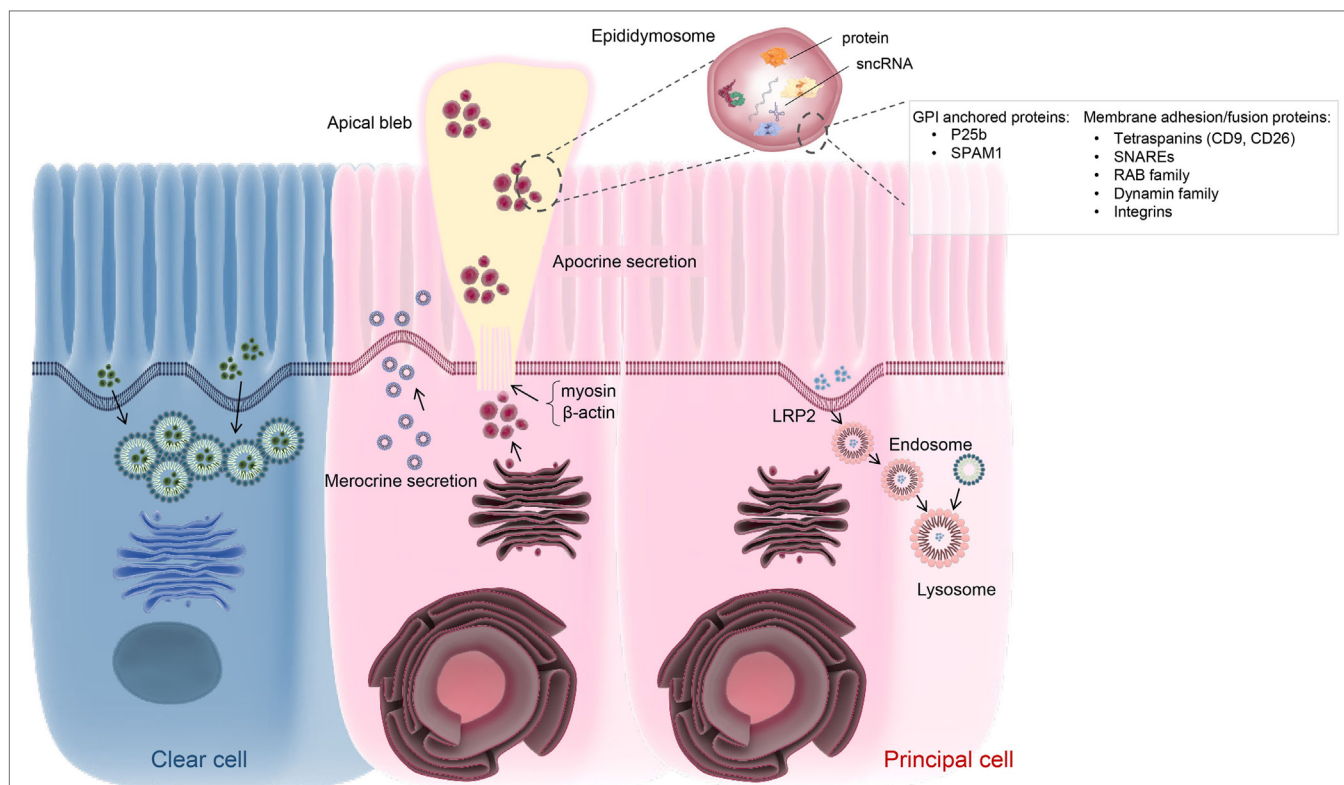


**FIGURE 2** | Schematic of vesicle-dependent mechanisms that contribute to the creation of the highly specialized epididymal intraluminal milieu. Principal cells represents the dominant cell type throughout the length of the epididymis and are particularly active in terms of protein biosynthesis and secretion. At least two active secretory pathways have been documented in these cells, namely classical merocrine secretion and an alternative apocrine secretory pathway. The former is characterized by secretory vesicles formed by the Golgi apparatus and leads to the release of a myriad of soluble proteins. In contrast, apocrine secretion provides a pathway for the secretion of glycosyl-phosphatidylinositol-linked proteins and other hydrophobic proteins. These proteins generally require posttranslational modification in the Golgi apparatus, prior to being selectively packaged into exosome-like vesicles referred to as epididymosomes. These small vesicles are sequestered into large bleb-like structures protruding from the apical margin of the epithelial cells. The attachment anchoring the blebs to their parent cell progressively narrows to form a stalk-like process (potentially through reorganization of cytoskeletal proteins such as myosin and  $\beta$ -actin) and eventually undergoes scission leading to their shedding into the lumen and eventual degradation. The epididymosomes so released provide a mechanism for intercellular communication, thereby enabling the delivery of a complex macromolecular payload to recipient cells in the form of luminal spermatozoa and/or downstream epithelial cells. Such cargo are known to include several hundred proteins as well as various species of small non-protein coding RNA (sncRNA). At present, the mechanisms by which epididymosomes are tethered, and deliver their cargo, to recipient cells remains to be equivocally determined although various proteins have been implicated in this process. Principal cells may also participate in endocytosis, involving the uptake of epididymal luminal contents via receptor (e.g., LRP2) mediated mechanism(s). A similar function has also been assigned to the clear cell population, which is mainly responsible for the recycling of luminal components.

appears to involve reorganization of cytoskeletal proteins such as myosin and  $\beta$ -actin (46, 89). In any case, the release of the epididymosomes into the luminal environment ideally positions this heterogeneous vesicle population to interact with the maturing spermatozoa.

### Epithelial Absorptive Pathways

The epithelial cells lining the initial segment of the mature mammalian epididymis have been shown to be very active in the uptake and recycling of the testicular contributions that enter the tract (3). One putative pathway for this absorption has been alluded to on the basis of apolipoprotein (apo) E receptor-2 (APOER2) expression in the principal cells of the initial segment. In this position, the APOER2 receptor is responsible for the clearance of clusterin, a glycoprotein implicated in lipid transport from spermatozoa to the principal cells. Accordingly, the inhibition of

APOER2 leads to the accumulation of clusterin in the epididymal fluid (90). Additional luminal components such as androgen binding protein, transferrin, and alpha2-macroglobulin also appear to be recycled following selective adhesion to receptors located in the adluminal domain of principal cells; a portion of which are located in the initial segment, while others present with more diffuse localization throughout the downstream segments of the epididymis. While a portion of these proteins appear destined for disposal (91–93), others such as androgen binding protein have proven to be indispensable for the normal functioning of the epididymal principal cells (91). The balance of evidence indicates that, in contrast to the initial segment, the bulk of the absorptive and recycling activity of the distal epididymal regions (and in particular the cauda epididymis) resides in clear cells. This is certainly the case for immobilin, a large glycoprotein that is responsible for the creating of the

viscoelastic luminal environment that serves to mechanically immobilize spermatozoa (94, 95). Immobilin is predominantly secreted into the proximal caput epididymis prior to the acquisition of the potential for sperm motility. Thereafter, immobilin forms an intimate association with the maturing sperm cells and physically restricts the propagation of a flagellar beat. In contrast, the principal cells of more distal segments secrete minimal immobilin, while the corresponding population of clear cells begins the task of absorbing excess immobilin (95). Differing patterns of absorption have been documented for alternative proteins such as that designated as epididymis-specific Inactive ribonuclease-like protein 10 (Protein Train A) (96); a protein that is secreted into the anterior segment of the bull epididymis *via* a classical merocrine pathway. Thereafter, Train A experiences a rapid reabsorption, such that this protein is unable to be detected in the epididymal lumen immediately adjacent to its site of secretion (96).

Receptor-mediated absorption is also involved in the recycling of the epididymal luminal contents (Figure 2). In this context, clusterin again serves as an interesting example. Indeed, in addition to the clusterin isoform that originates in the testes (and is subsequently absorbed by principal cells of the initial segment), an alternative isoform is abundantly secreted into the lumen of the proximal epididymis, whereupon it has been implicated in sperm maturation. Both *in vivo* and *in vitro* studies have revealed that epididymal sourced clusterin is recycled by downstream principal cells *via* interaction with low density lipoprotein receptor (LRP-2) (97). Accordingly, clusterin and LRP-2 are both found in association with the apical surface, coated pits, endocytic vesicles, and early endosomes of principal cells. Subsequently, only clusterin is detected in late endosomes and lysosomes, suggesting that LRP-2 is recycled back to the apical surface while clusterin is delivered to the lysosomes for degradation (97). This process can be prevented by presenting the cells with an excess of protein substrates that competitively bind to LRP-2. Such receptor-dependent recycling of luminal components is a commonly encountered phenomenon within the epididymis, with additional examples including transferrin and  $\alpha$ 2-macroglobulin (93). Epididymal epithelial cells also possess the ability to monitor the luminal environment and adjust their absorptive ability accordingly. In this context, the estrogen receptor  $\alpha$  (ER $\alpha$ ) has been identified as key sensor involved in the regulation of fluid reabsorption in the efferent ducts and initial segment of the epididymis. This system is apparently fine-tuned by a ubiquitin-dependent proteasome pathway that affords precise control over ER $\alpha$  turnover and degradation (98). Another interesting example of this phenomenon has been afforded by the analysis of an MFGE8 (formerly known as SED1) knockout mouse model (Table 1). The epididymal epithelial cells of these mice are characterized by increased accumulation of intracellular vesicles and an apical distribution of VATPase. Such changes are, in turn, reflected in epididymal luminal environment, which displays abnormal osmolarity (i.e., hypo-osmotic) and alkalinity; suggestive of the existence of a positive feedback loop responsible for regulating the behavior of the epithelial cells in response to changes in the luminal environment (99).

## Membrane Trafficking Machinery Involved in the Regulation of the Epididymal Environment

Despite recognition of the importance of bidirectional epithelial transport in regulating the epididymal luminal environment, little is currently known about the molecular machinery that controls these complementary pathways. Key elements are likely to include Soluble NSF Attachment Protein Receptor (SNARE) proteins, which have well-described roles in the regulation of membrane fusion activity in alternative tissue models. This activity requires the complementary action of different SNARE proteins contributed by vesicles (v-SNARE proteins) and target (t-SNARE proteins) membranes. Initiated by nucleation of the SNARE complex in response to calcium fluxes, the two opposing membranes are brought into close apposition and are thereafter able to engage in membrane fusion (100). The first evidence implicating SNARE proteins in the regulation of membrane fusion events in the epididymis arose from studies of the clear cell population (101). Functional analysis of these cells revealed that cellubrevin, a v-SNARE, is essential for acidification of the luminal environment. Accordingly, tetanus toxin-mediated cleavage of cellubrevin is able to inhibit proton secretion into the lumen (101). In addition to the lining epithelial cells, it is known that spermatozoa also harbor several t-SNARE and their cognate v-SNARE counterparts, which are localized to the plasma membrane and underlying outer acrosomal membranes, respectively. Such a location accords with the proposed role of SNARE proteins in regulating the membrane fusion events that underpin sperm acrosomal exocytosis (102–104). Notably however, this also ideally positions SNAREs to participate in the tethering of epididymosomes to the sperm surface and thereby facilitate the transfer of their cargo to the maturing cells. In agreement with this model, the requisite SNARE proteins necessary for constructing a functional membrane fusion complex have also been documented in epididymosomes (53, 101, 102). Nevertheless, there is currently limited experimental evidence to support the role of SNARE complexes in the regulation of sperm maturation.

Aside from SNARE proteins, recent proteomic analyses of luminal fluids obtained from the bovine epididymis have revealed the presence of at least 13 proteins implicated in clathrin-mediated endocytosis. Since this form of endocytosis is unlikely to occur in spermatozoa, these proteins may instead contribute the recycling of epididymal components *via* uptake into the surrounding epithelial cells (105). In this context, alternative regulators of membrane trafficking belonging to the Rab superfamily of GTPases have also been documented within epididymal luminal fluid, and more specifically, as part of the proteome of both human and bull epididymosomes (53, 106). Such findings are of interest as the Rab superfamily, which consists of some 30 members, have been implicated in regulating various membrane trafficking events including vesicle formation, sorting, release, and cargo transfer to recipient cells (100, 107). It is therefore tempting to speculate that Rab proteins may participate in epididymosome–sperm interaction/cargo transfer.

An additional family of membrane-trafficking proteins that warrant further investigation in the context of regulating

epididymal function is that of the dynamin family of large GTPases. Indeed, our recent studies have shown that canonical dynamin isoforms display both cell, and segment-specific, differences in their profile of expression in the mouse epididymis. Specifically, dynamin 1 and 3 are mainly expressed in the corpus and cauda segments where they localize within the clear cell and principal cell populations, respectively. Of note, the differential localization of these dynamin isoforms contrasts the overlapping and redundant roles they display in neuronal tissues (108), suggesting that they may fulfill discrete functions in the epididymal tubule. Moreover, dynamin 1 was shown to be delivered to human spermatozoa during epididymal transit, in a mechanism that may involve epididymosomes (109). This compares favorably with the mouse in which caput and cauda spermatozoa display different patterns of dynamin 1 labeling (79). At present however, it remains to be determined whether dynamin 1 forms part of the cargo transferred between epididymosomes and maturing spermatozoa, or alternatively if it is instead involved in the regulation of epididymosome docking/fusion with spermatozoa. In contrast to dynamin isoforms 1 and 3, dynamin 2 localizes strongly to the Golgi apparatus in principal cells of the proximal epididymal segments, consistent with a role in mediating post-Golgi vesicle trafficking in the most active secretory cells of the tract. In more distal segments, dynamin 2 is detected in the microvilli and apical blebs lining the luminal border, suggesting it may participate in the regulation of apocrine secretion (79).

## Epididymosome-Mediated Sperm-Soma Intracellular Communication

Among the varied molecular mechanisms that exert influence over the unique intraluminal environment of the epididymis, vesicle-dependent pathways of intercellular communication have emerged as being of fundamental importance. An obvious advantage afforded by the production of epididymosomes is the prospect of delivering macromolecular cargo to spermatozoa *en masse*. Additionally, the encapsulation of such cargo within a relatively stable membrane-bound structure could afford stability and protection against the potentially deleterious extracellular environment of the epididymal lumen. It is therefore perhaps not surprising that, in addition to their protein cargo, epididymosomes also comprise a heterogeneous population of small non-coding RNAs (sncRNA) including miRNA and tRNA fragments (70, 72). Like that of their protein cargo, these sncRNAs are available for direct transfer to the maturing spermatozoa. Accordingly, emerging work has shown that exposure of male mice to dietary perturbations (e.g., low protein diets) can markedly influence the sncRNA profiles of detected in the epididymis of these animals. Moreover, these changes are subsequently manifest in altered sperm sncRNA profiles, with epididymosomes having been implicated as the vector for delivery of this cargo to the maturing epididymal spermatozoa. Of some concern is the recognition that spermatozoa are subsequently able to relay these sncRNA to the oocyte during fertilization, whereupon they exert epigenetic control over early embryo development through targeting of a specific subset of genes (72). Such findings encourage a deeper

understanding of the mechanisms underpinning the selective packaging of epididymosome cargo, the way in which this cargo is delivered to recipient cells (i.e., maturing spermatozoa and/or downstream epithelial cells) and the degree to which these vectors regulate the acquisition of functional competence in maturing spermatozoa.

This field of research is somewhat confounded by the fact that epididymosomes represent a heterogeneous population of vesicles. In this context, it has been shown that bovine epididymosomes collected from different epididymal segments are capable of transferring differing protein repertoires to spermatozoa. Further, an excess of one population of epididymosomes (collected from caput segment) does not overtly influence the transfer efficacy of the alternative population (collected from cauda segment) during simultaneous co-incubation with spermatozoa (49). As an extension of this work, it has also recently been shown that epididymosomes can be subdivided into two discrete subpopulations owing to their size and molecular composition. The smaller of these populations measure ~10–100 nm in diameter and are distinguished based on the presence of tetraspanin-enriched microdomains containing both CD9 and its cooperative partner CD26. These epididymosomes also contain a relatively high concentration of proteins such as MIF and P25b, and display a preference to interact with live spermatozoa. These collective properties implicate this sub-class of epididymosomes in sperm maturation (110). The alternative subpopulation is characterized by the presence of epididymal sperm binding protein 1, and also by their propensity to interact with dead spermatozoa (52, 111). The overall heterogeneity of epididymosomes and their capacity to selectively interact with different sub-populations of spermatozoa suggests these interactions may be tightly regulated.

At present, however, the molecular mechanisms underpinning the biogenesis of different populations of epididymosomes, as well as those responsible for their interaction with spermatozoa remain to be established. Recent work has suggested the latter process may be initiated *via* the docking of GPI anchor(s) to the outer leaflet of the sperm surface lipid bilayer (87). Such docking is putatively followed by membrane fusion between the epididymosome and sperm membrane. In this regard, the adhesive/fusion properties of CD9 have identified this tetraspanin as a likely candidate in regulation of this fusion event (112, 113). Such a model is commensurate with the demonstration that anti-CD9 masking antibodies are able to reduce the efficacy of protein transfer from epididymosomes to spermatozoa (110). Notably, however, CD9 is unlikely to be the sole candidate since epididymosome–sperm interaction is characterized by a degree of selectivity in terms of the relayed content and their ability to discriminate between different populations of spermatozoa. As mentioned above, this is particularly the case in the bovine model where a subset of epididymosomes has been identified that do not possess CD9 and yet are still able to interact with spermatozoa (52). Owing to their role in receptor sequestration, lipid rafts have also been recently proposed as a “platform” to facilitate docking of the epididymosome and sperm membranes. Highly enriched in cholesterol and sphingolipid (114), these microdomains also compartmentalize GPI-anchored

proteins such as P25b and SPAM1 (87) that themselves have been implicated in epididymosome-sperm adhesion. Thus, the release of P25b and SPAM1 proteins from sperm lipid rafts, *via* trypsin/pronase proteolysis, leads to a significant reduction in the efficacy of epididymosome cargo transfer to the sperm cells (115). However, it remains to be determined if the disruption of lipid raft integrity (e.g., through cholesterol sequestration using methyl- $\beta$ -cyclodextrin) also compromises the docking of epididymosomes to the sperm surface.

Adding to this controversy is the suggestion that the interaction between epididymosomes and spermatozoa may not involve a complete fusion of their respective membranes (116). Rather, epididymosome adherence may be followed by creation of a transient fusion pore and subsequent release of the epididymosome once delivery of their cargo is complete. Accordingly, proteomic analyses of epididymosomes, and spermatozoa themselves, have identified a myriad of complementary trafficking proteins (e.g., SNARE proteins, Ras-like proteins, and dynamins) (53) that could regulate this form of intercellular communication. An intriguing aspect of this “kiss and run” model is that it could potentially facilitate bi-directional exchange of proteins and other macromolecules both into, and out of, the maturing sperm cell. It may also account for why a portion of epididymosomes persist in seminal fluids rather than being completely absorbed by spermatozoa within the duct. To the best of our knowledge, however, there is presently limited functional evidence linking any of the abovementioned trafficking proteins to a role in sperm-epididymosome interaction, and no evidence that epididymosomes can sequester proteins from spermatozoa. Irrespective, it has been shown that lipid labeled (Dilc12) epididymosomes originating from the median caput segment are able to be incorporated into distal caput epithelial cells *in vitro* (33). Such incorporation is time-dependent, with fluorescence imaging revealing a punctate distribution of Dilc12 within the epithelial cells after epididymosome interaction. This pattern of labeling is reminiscent of that observed after exosome interaction

with somatic cells in other tissue models (117), thus indicating that sperm are not the sole recipients of epididymosome cargo.

## CONCLUSION

The epididymal milieu is undoubtedly crucial for promoting sperm maturation as well as supporting their storage. Indeed, since sperm are transcriptionally and translationally silent cells, their functional transformation relies entirely on the creation and maintenance of a highly specialized epididymal luminal milieu. The establishment of this unique epididymal microenvironment features the varied endocytotic and exocytotic contributions of the epithelial cells that line the duct. Unfortunately, our understanding of the molecular machinery the epididymal epithelial cells employ to facilitate these processes remains incomplete, as does our knowledge of how these cells are precisely regulated in different segments. Resolving these questions promises to inform our understanding of male fertility regulation with implications for contraceptive intervention and infertility diagnostics.

## AUTHOR CONTRIBUTIONS

All authors made substantial contributions to the conception of this review and the critical appraisal of the literature summarized herein. WZ generated the initial draft of the manuscript, and this was critically revised by BN, GD, and MD. All authors approved the final version and submission of this article.

## FUNDING

This work was supported by National Health and Medical Research Council of Australia Project Grants (APP1103176 and APP1147932) to BN and MD. WZ is supported by a PhD scholarship awarded by the University of Newcastle. MD is supported by a Cancer Institute New South Wales Early Career Fellowship. BN is supported by an Australian Research Council Future Fellowship (FT140101368).

## REFERENCES

- Benoit J. Recherches anatomiques, cytologiques et histophysiologiques, sur les voies excrétrices du testicules chez les mammifères. *Arch Anat Histol Embryol* (1926) 5:173–412.
- Nixon B, Ecroyd H, Dacheux JL, Dacheux F, Labas V, Johnston SD, et al. Formation and dissociation of sperm bundles in monotremes. *Biol Reprod* (2016) 95:91. doi:10.1095/biolreprod.116.140491
- Abe K, Takano H, Ito T. Microvasculature of the mouse epididymis, with special reference to fenestrated capillaries localized in the initial segment. *Anat Rec* (1984) 209:209–18. doi:10.1002/ar.1092090208
- Aitken RJ, Nixon B, Lin M, Koppers AJ, Lee YH, Baker MA. Proteomic changes in mammalian spermatozoa during epididymal maturation. *Asian J Androl* (2007) 9:554–64. doi:10.1111/j.1745-7262.2007.00280.x
- Bork K, Chevrier C, Paquignon M, Jouannet P, Dacheux JL. [Flagellar motility and movement of boar spermatozoa during epididymal transit]. *Reprod Nutr Dev* (1988) 28:1307–15. doi:10.1051/rnd:19880811
- Chevrier C, Dacheux JL. Evolution of the flagellar waveform of ram spermatozoa in relation to the degree of epididymal maturation. *Cell Motil Cytoskeleton* (1992) 23:8–18. doi:10.1002/cm.970230103
- Hermo L, Dworkin J, Oko R. Role of epithelial clear cells of the rat epididymis in the disposal of the contents of cytoplasmic droplets detached from spermatozoa. *Am J Anat* (1988) 183:107–24. doi:10.1002/aja.1001830202
- Robaire B, Hinton B, Orgebin-Crist M. *The Epididymis, Knobil and Neill's Physiology of Reproduction*. New York: Elsevier (2006).
- Turner TT. Resorption versus secretion in the rat epididymis. *J Reprod Fertil* (1984) 72:509–14. doi:10.1530/jrf.0.0720509
- Cornwall GA. New insights into epididymal biology and function. *Hum Reprod Update* (2009) 15:213–27. doi:10.1093/humupd/dmn055
- Abe K, Takano H, Ito T. Ultrastructure of the mouse epididymal duct with special reference to the regional differences of the principal cells. *Arch Histol Jpn* (1983) 46:51–68. doi:10.1679/aohc.46.51
- Hermo L, Robaire B. Epididymal cell types and their functions. In: Robaire B, Hinton BT, editors. *The Epididymis: From Molecules to Clinical Practice*. Boston, MA: Springer (2002). p. 81–102.
- Dacheux JL, Belleannee C, Jones R, Labas V, Belghazi M, Guyonnet B, et al. Mammalian epididymal proteome. *Mol Cell Endocrinol* (2009) 306:45–50. doi:10.1016/j.mce.2009.03.007
- Brown D, Smith PJ, Breton S. Role of V-ATPase-rich cells in acidification of the male reproductive tract. *J Exp Biol* (1997) 200:257–62.
- Adamali HF, Hermo L. Apical and narrow cells are distinct cell types differing in their structure, distribution, and functions in the adult rat epididymis. *J Androl* (1996) 17:208–22.
- Sun EL, Flickinger CJ. Morphological characteristics of cells with apical nuclei in the initial segment of the adult rat epididymis. *Anat Rec* (1980) 196:285–93. doi:10.1002/ar.1091960304

17. Hermo L, Papp S. Effects of ligation, orchidectomy, and hypophysectomy on expression of the Yf subunit of GST-P in principal and basal cells of the adult rat epididymis and on basal cell shape and overall arrangement. *Anat Rec* (1996) 244:59–69. doi:10.1002/(SICI)1097-0185(199601)244:1<59::AID-AR6>3.0.CO;2-A
18. Jelinsky SA, Turner TT, Bang HJ, Finger JN, Solarz MK, Wilson E, et al. The rat epididymal transcriptome: comparison of segmental gene expression in the rat and mouse epididymides. *Biol Reprod* (2007) 76:561–70. doi:10.1095/biolreprod.106.057323
19. Wong PYD, Gong XD, Leung GPH, Cheuk BLY. Formation of the epididymal fluid microenvironment. In: Robaire B, Hinton BT, editors. *The Epididymis: From Molecules to Clinical Practice*. Boston, MA: Springer (2002). p. 119–30.
20. Turner TT, Hinton BT. *The Third International Conference on the Epididymis*. Charlottesville, VA: The Van Doren Company (2003).
21. Johnston DS, Jelinsky SA, Bang HJ, DiCandeloro P, Wilson E, Kopf GS, et al. The mouse epididymal transcriptome: transcriptional profiling of segmental gene expression in the epididymis. *Biol Reprod* (2005) 73:404–13. doi:10.1095/biolreprod.105.039719
22. Nixon B, Stanger SJ, Mihalas BP, Reilly JN, Anderson AL, Dun MD, et al. Next generation sequencing analysis reveals segmental patterns of microRNA expression in mouse epididymal epithelial cells. *PLoS One* (2015) 10:e0135605. doi:10.1371/journal.pone.0135605
23. Skerget S, Rosenow MA, Petritis K, Karr TL. Sperm proteome maturation in the mouse epididymis. *PLoS One* (2015) 10:e0140650. doi:10.1371/journal.pone.0140650
24. Garrett SH, Garrett JE, Douglass J. In situ histochemical analysis of region-specific gene expression in the adult rat epididymis. *Mol Reprod Dev* (1991) 30:1–17. doi:10.1002/mrd.1080300102
25. Cornwall GA, Orgebin-crist MC, Hann SR. The CRES gene – a unique testis-regulated gene related to the cystatin family is highly restricted in its expression to the proximal region of the mouse epididymis. *Mol Endocrinol* (1992) 6:1653–64. doi:10.1210/me.6.10.1653
26. Lareyre JJ, Thomas TZ, Zheng WL, Kasper S, Ong DE, Orgebin-Crist MC, et al. A 5-kilobase pair promoter fragment of the murine epididymal retinoic acid-binding protein gene drives the tissue-specific, cell-specific, and androgen-regulated expression of a foreign gene in the epididymis of transgenic mice. *J Biol Chem* (1999) 274:8282–90. doi:10.1074/jbc.274.12.8282
27. Guyonnet B, Marot G, Dacheux JL, Mercat MJ, Schwob S, Jaffrezic F, et al. The adult boar testicular and epididymal transcriptomes. *BMC Genomics* (2009) 10:369. doi:10.1186/1471-2164-10-369
28. Browne JA, Yang R, Leir SH, Eggen SE, Harris A. Expression profiles of human epididymis epithelial cells reveal the functional diversity of caput, corpus and cauda regions. *Mol Hum Reprod* (2016) 22:69–82. doi:10.1093/molehr/gav066
29. Li Y, Wang HY, Wan FC, Liu FJ, Liu J, Zhang N, et al. Deep sequencing analysis of small non-coding RNAs reveals the diversity of microRNAs and piRNAs in the human epididymis. *Gene* (2012) 497:330–5. doi:10.1016/j.gene.2012.01.038
30. Zhang J, Liu Q, Zhang W, Li J, Li Z, Tang Z, et al. Comparative profiling of genes and miRNAs expressed in the newborn, young adult, and aged human epididymides. *Acta Biochim Biophys Sin* (2010) 42:145–53. doi:10.1093/abbs/gmp116
31. Zhang YL, Zhang JS, Zhou YC, Zhao Y, Ni MJ. Identification of microRNAs and application of RNA interference for gene targeting in vivo in the rat epididymis. *J Androl* (2011) 32:587–91. doi:10.2164/jandrol.111.013060
32. Belleanne C, Calvo E, Thimon V, Cyr DG, Legare C, Garneau L, et al. Role of microRNAs in controlling gene expression in different segments of the human epididymis. *PLoS One* (2012) 7:e34996. doi:10.1371/journal.pone.0034996
33. Belleanne C, Calvo E, Caballero J, Sullivan R. Epididymosomes convey different repertoires of microRNAs throughout the bovine epididymis. *Biol Reprod* (2013) 89:30. doi:10.1095/biolreprod.113.110486
34. Wong N, Wang X. miRDB: an online resource for microRNA target prediction and functional annotations. *Nucleic Acids Res* (2015) 43:D146–52. doi:10.1093/nar/gku1104
35. Ma W, Hu S, Yao G, Xie S, Ni M, Liu Q, et al. An androgen receptor-microRNA-29a regulatory circuitry in mouse epididymis. *J Biol Chem* (2013) 288:29369–81. doi:10.1074/jbc.M113.454066
36. Villarroya-Beltri C, Gutiérrez-Vázquez C, Sánchez-Cabo F, Pérez-Hernández D, Vázquez J, Martín-Cofreces N, et al. Sumoylated hnRNPA2B1 controls the sorting of miRNAs into exosomes through binding to specific motifs. *Nat Commun* (2013) 4:2980. doi:10.1038/ncomms3980
37. Ecroyd H, Belghazi M, Dacheux JL, Gatti JL. The epididymal soluble prion protein forms a high-molecular-mass complex in association with hydrophobic proteins. *Biochem J* (2005) 392:211–9. doi:10.1042/BJ20050459
38. Díaz-Flores L, Gutiérrez R, del Pino García M, Gayoso MJ, Carrasco JL, Díaz-Flores L Jr, et al. Localized amyloidosis of the epididymis: a previously unreported phenomenon. *Diagn Pathol* (2017) 12:58. doi:10.1186/s13000-017-0646-z
39. Asquith KL, Harman AJ, McLaughlin EA, Nixon B, Aitken RJ. Localization and significance of molecular chaperones, heat shock protein 1, and tumor rejection antigen gp96 in the male reproductive tract and during capacitation and acrosome reaction. *Biol Reprod* (2005) 72:328–37. doi:10.1095/biolreprod.104.034470
40. Whelly S, Johnson S, Powell J, Borchardt C, Hastert MC, Cornwall GA. Nonpathological extracellular amyloid is present during normal epididymal sperm maturation. *PLoS One* (2012) 7:e36394. doi:10.1371/journal.pone.0036394
41. Whelly S, Muthusubramanian A, Powell J, Johnson S, Hastert MC, Cornwall GA. Cystatin-related epididymal spermatogenic subgroup members are part of an amyloid matrix and associated with extracellular vesicles in the mouse epididymal lumen. *Mol Hum Reprod* (2016) 22:729–44. doi:10.1093/molehr/gaw049
42. Hewetson A, Do HQ, Myers C, Muthusubramanian A, Sutton RB, Wylie BJ, et al. Functional amyloids in reproduction. *Biomolecules* (2017) 7:46. doi:10.3390/biom7030046
43. Yano R, Matsuyama T, Kaneko T, Kurio H, Murayama E, Toshimori K, et al. Bactericidal/permeability-increasing protein is associated with the acrosome region of rodent epididymal spermatozoa. *J Androl* (2010) 31:201–14. doi:10.2164/jandrol.109.007880
44. Reid AT, Anderson AL, Roman SD, McLaughlin EA, McCluskey A, Robinson PJ, et al. Glycogen synthase kinase 3 regulates acrosomal exocytosis in mouse spermatozoa via dynamin phosphorylation. *FASEB J* (2015) 29:2872–82. doi:10.1096/fj.14-265553
45. Yanagimachi R, Kamiguchi Y, Mikamo K, Suzuki F, Yanagimachi H. Maturation of spermatozoa in the epididymis of the Chinese hamster. *Am J Anat* (1985) 172:317–30. doi:10.1002/aja.1001720406
46. Rejraji H, Sion B, Prensier G, Carreras M, Motta C, Frenoux JM, et al. Lipid remodeling of murine epididymosomes and spermatozoa during epididymal maturation. *Biol Reprod* (2006) 74:1104–13. doi:10.1095/biolreprod.105.049304
47. Fornes MW, Barbieri A, Cavicchia JC. Morphological and enzymatic study of membrane-bound vesicles from the lumen of the rat epididymis. *Andrologia* (1995) 27:1–5. doi:10.1111/j.1439-0272.1995.tb02087.x
48. Frenette G, Sullivan R. Prostate-like particles are involved in the transfer of P25b from the bovine epididymal fluid to the sperm surface. *Mol Reprod Dev* (2001) 59:115–21. doi:10.1002/mrd.1013
49. Frenette G, Girouard J, Sullivan R. Comparison between epididymosomes collected in the intraluminal compartment of the bovine caput and cauda epididymidis. *Biol Reprod* (2006) 75:885–90. doi:10.1095/biolreprod.106.054692
50. Thimon V, Frenette G, Saez F, Thabet M, Sullivan R. Protein composition of human epididymosomes collected during surgical vasectomy reversal: a proteomic and genomic approach. *Hum Reprod* (2008) 23:1698–707. doi:10.1093/humrep/den181
51. Sullivan R, Saez F, Girouard J, Frenette G. Role of exosomes in sperm maturation during the transit along the male reproductive tract. *Blood Cells Mol Dis* (2005) 35:1–10. doi:10.1016/j.bcmd.2005.03.005
52. Sullivan R. Epididymosomes: a heterogeneous population of microvesicles with multiple functions in sperm maturation and storage. *Asian J Androl* (2015) 17:726–9. doi:10.4103/1008-682X.155255
53. Girouard J, Frenette G, Sullivan R. Comparative proteome and lipid profiles of bovine epididymosomes collected in the intraluminal compartment of the caput and cauda epididymidis. *Int J Androl* (2011) 34:e475–86. doi:10.1111/j.1365-2605.2011.01203.x
54. Frenette G, Lessard C, Madore E, Fortier MA, Sullivan R. Aldose reductase and macrophage migration inhibitory factor are associated with epididymosomes

- and spermatozoa in the bovine epididymis. *Biol Reprod* (2003) 69:1586–92. doi:10.1095/biolreprod.103.019216
55. Eickhoff R, Baldauf C, Koyro HW, Wennemuth G, Suga Y, Seitz J, et al. Influence of macrophage migration inhibitory factor (MIF) on the zinc content and redox state of protein-bound sulphhydryl groups in rat sperm: indications for a new role of MIF in sperm maturation. *Mol Hum Reprod* (2004) 10:605–11. doi:10.1093/molehr/gah075
  56. Légaré C, Bérubé B, Boué F, Lefèvre L, Morales CR, El-Alfy M, et al. Hamster sperm antigen P26h is a phosphatidylinositol-anchored protein. *Mol Reprod Dev* (1999) 52:225–33. doi:10.1002/(SICI)1098-2795(199902)52:2<225::AID-MRD14>3.0.CO;2-M
  57. Boue F, Blais J, Sullivan R. Surface localization of P34H an epididymal protein, during maturation, capacitation, and acrosome reaction of human spermatozoa. *Biol Reprod* (1996) 54:1009–17. doi:10.1095/biolreprod54.5.1009
  58. Berube B, Sullivan R. Inhibition of in vivo fertilization by active immunization of male hamsters against a 26-kDa sperm glycoprotein. *Biol Reprod* (1994) 51:1255–63. doi:10.1095/biolreprod51.6.1255
  59. Patel R, Al-Dossary AA, Stabley DL, Barone C, Galileo DS, Strehler EE, et al. Plasma membrane Ca<sup>2+</sup>-ATPase 4 in murine epididymis: secretion of splice variants in the luminal fluid and a role in sperm maturation. *Biol Reprod* (2013) 89:6. doi:10.1095/biolreprod.113.108712
  60. Mawson CA, Fischer MI. Zinc content of the genital organs of the rat. *Nature* (1951) 167:859. doi:10.1038/167859a0
  61. Wales RG, Wallace JC, White IG. Composition of bull epididymal and testicular fluid. *J Reprod Fertil* (1966) 12:139–44. doi:10.1530/jrf.0.0120139
  62. Levine N, Marsh DJ. Micropuncture studies of the electrochemical aspects of fluid and electrolyte transport in individual seminiferous tubules, the epididymis and the vas deferens in rats. *J Physiol* (1971) 213:557–70. doi:10.1113/jphysiol.1971.sp009400
  63. Jenkins AD, Lechene CP, Howards SS. Concentrations of seven elements in the intraluminal fluids of the rat seminiferous tubules, rete testis, and epididymis. *Biol Reprod* (1980) 23:981–7. doi:10.1095/biolreprod23.5.981
  64. Jones RC, Clulow J. Regulation of the elemental composition of the epididymal fluids in the tammar, *Macropus eugenii*. *J Reprod Fertil* (1987) 81:583–90. doi:10.1530/jrf.0.0810583
  65. Morton BE, Sagadraga R, Fraser C. Sperm motility within the mammalian epididymis: species variation and correlation with free calcium levels in epididymal plasma. *Fertil Steril* (1978) 29:695–8. doi:10.1016/S0015-0282(16)43348-0
  66. Shum WW, Ruan YC, Da Silva N, Breton S. Establishment of cell-cell cross talk in the epididymis: control of luminal acidification. *J Androl* (2011) 32:576–86. doi:10.2164/jandrol.111.012971
  67. Breton S, Ruan YC, Park YJ, Kim B. Regulation of epithelial function, differentiation, and remodeling in the epididymis. *Asian J Androl* (2016) 18:3–9. doi:10.4103/1008-682X.165946
  68. Beaulieu V, Da Silva N, Pastor-Soler N, Brown CR, Smith PJ, Brown D, et al. Modulation of the actin cytoskeleton via gelsolin regulates vacuolar H<sup>+</sup>-ATPase recycling. *J Biol Chem* (2005) 280:8452–63. doi:10.1074/jbc.M412750200
  69. Ren D, Navarro B, Perez G, Jackson AC, Hsu S, Shi Q, et al. A sperm ion channel required for sperm motility and male fertility. *Nature* (2001) 413:603–9. doi:10.1038/35098027
  70. Reilly JN, McLaughlin EA, Stanger SJ, Anderson AL, Hutcheon K, Church K, et al. Characterisation of mouse epididymosomes reveals a complex profile of microRNAs and a potential mechanism for modification of the sperm epigenome. *Sci Rep* (2016) 6:31794. doi:10.1038/srep31794
  71. Hutcheon K, McLaughlin EA, Stanger SJ, Bernstein IR, Dun MD, Eamens AL. Analysis of the small non-protein-coding RNA profile of mouse spermatozoa reveals specific enrichment of piRNAs within mature spermatozoa. *RNA Biol* (2017) 14:1–15. doi:10.1080/15476286.2017.1356569
  72. Sharma U, Conine CC, Shea JM, Boskovic A, Derr AG, Bing XY, et al. Biogenesis and function of tRNA fragments during sperm maturation and fertilization in mammals. *Science* (2016) 351:391–6. doi:10.1126/science.aad6780
  73. Nixon B, Stanger SJ, Mihalas BP, Reilly JN, Anderson AL, Tyagi S, et al. The microRNA signature of mouse spermatozoa is substantially modified during epididymal maturation. *Biol Reprod* (2015) 93(91):1–20. doi:10.1095/biolreprod.115.132209
  74. Eaton SA, Jayasooriah N, Buckland ME, Martin DI, Cropley JE, Suter CM. Roll over Weismann: extracellular vesicles in the transgenerational transmission of environmental effects. *Epigenomics* (2015) 7:1165–71. doi:10.2217/epi.15.58
  75. Hermo L, Oko R, Morales CR. Secretion and endocytosis in the male reproductive tract: a role in sperm maturation. *Int Rev Cytol* (1994) 154:106–89.
  76. Dacheux JL, Castella S, Gatti JL, Dacheux F. Epididymal cell secretory activities and the role of proteins in boar sperm maturation. *Theriogenology* (2005) 63:319–41. doi:10.1016/j.theriogenology.2004.09.015
  77. Cooper TG. Epididymal research: more warp than weft? *Asian J Androl* (2015) 17:699–703. doi:10.4103/1008-682X.146102
  78. Gomi H, Mori K, Itohara S, Izumi T. Rab27b is expressed in a wide range of exocytic cells and involved in the delivery of secretory granules near the plasma membrane. *Mol Biol Cell* (2007) 18:4377–86. doi:10.1091/mbc.E07-05-0409
  79. Zhou W, De Iulius GN, Turner AP, Reid AT, Anderson AL, McCluskey A, et al. Developmental expression of the dynamin family of mechanoenzymes in the mouse epididymis. *Biol Reprod* (2017) 96:159–73. doi:10.1095/biolreprod.116.145433
  80. Kreitzer G, Marmorstein A, Okamoto P, Vallee R, Rodriguez-Boulan E. Kinesin and dynamin are required for post-Golgi transport of a plasma-membrane protein. *Nat Cell Biol* (2000) 2:125–7. doi:10.1038/35000081
  81. Weller SG, Capitani M, Cao H, Micaroni M, Luini A, Sallèse M, et al. Src kinase regulates the integrity and function of the Golgi apparatus via activation of dynamin 2. *Proc Natl Acad Sci U S A* (2010) 107:5863–8. doi:10.1073/pnas.0915123107
  82. González-Jamett AM, Momboise F, Haro-Acuña V, Bevilacqua JA, Caviedes P, Cárdenas AM. Dynamin-2 function and dysfunction along the secretory pathway. *Front Endocrinol* (2013) 4:126. doi:10.3389/fendo.2013.00126
  83. Jackson J, Papadopoulos A, Meunier FA, McCluskey A, Robinson PJ, Keating DJ. Small molecules demonstrate the role of dynamin as a bi-directional regulator of the exocytosis fusion pore and vesicle release. *Mol Psychiatry* (2015) 20:810–9. doi:10.1038/mp.2015.56
  84. Williams M, Kim K. From membranes to organelles: emerging roles for dynamin-like proteins in diverse cellular processes. *Eur J Cell Biol* (2014) 93:267–77. doi:10.1016/j.ejcb.2014.05.002
  85. Menon M, Schafer DA. Dynamin: expanding its scope to the cytoskeleton. *Int Rev Cell Mol Biol* (2013) 302:187–219. doi:10.1016/B978-0-12-407699-0.00003-0
  86. Sullivan R, Frenette G, Girouard J. Epididymosomes are involved in the acquisition of new sperm proteins during epididymal transit. *Asian J Androl* (2007) 9:483–91. doi:10.1111/j.1745-7262.2007.00281.x
  87. Griffiths GS, Galileo DS, Reese K, Martin-Deleon PA. Investigating the role of murine epididymosomes and uterosomes in GPI-linked protein transfer to sperm using SPAM1 as a model. *Mol Reprod Dev* (2008) 75:1627–36. doi:10.1002/mrd.20907
  88. Hermo L, Jacks D. Nature's ingenuity: bypassing the classical secretory route via apocrine secretion. *Mol Reprod Dev* (2002) 63:394–410. doi:10.1002/mrd.90023
  89. Aumuller G, Wilhelm B, Seitz J. Apocrine secretion – fact or artifact? *Ann Anat* (1999) 181:437–46. doi:10.1016/S0940-9602(99)80020-X
  90. Andersen OM, Yeung CH, Vorum H, Wellner M, Andreassen TK, Erdmann B, et al. Essential role of the apolipoprotein E receptor-2 in sperm development. *J Biol Chem* (2003) 278:23989–95. doi:10.1074/jbc.M302157200
  91. Hermo L, Barin K, Oko R. Androgen binding protein secretion and endocytosis by principal cells in the adult rat epididymis and during postnatal development. *J Androl* (1998) 19:527–41.
  92. Djakiew D, Griswold MD, Lewis DM, Dym M. Micropuncture studies of receptor-mediated endocytosis of transferrin in the rat epididymis. *Biol Reprod* (1986) 34:691–9. doi:10.1095/biolreprod34.4.691
  93. Djakiew D, Byers SW, Lewis DM, Dym M. Receptor-mediated endocytosis of Alpha2-macroglobulin by principal cells in the proximal caput epididymidis in vivo. *J Androl* (1985) 6:190–6. doi:10.1002/j.1939-4640.1985.tb00835.x
  94. Axné E. Sperm maturation in the domestic cat. *Theriogenology* (2006) 66:14–24. doi:10.1016/j.theriogenology.2006.03.022
  95. Hermo L, Oko R, Robaire B. Epithelial-cells of the epididymis show regional variations with respect to the secretion or endocytosis of immobilin as revealed by light and electron-microscope immunocytochemistry. *Anat Rec* (1992) 232:202–20. doi:10.1002/ar.1092320206

96. Castella S, Benedetti H, de Llorens R, Dacheux JL, Dacheux F, Train A, et al. RNase A-like protein without RNase activity, is secreted and reabsorbed by the same epididymal cells under testicular control. *Biol Reprod* (2004) 71:1677–87. doi:10.1095/biolreprod.104.031666
97. Morales CR, Igdoura SA, Wosu UA, Boman J, Argraves WS. Low density lipoprotein receptor-related protein-2 expression in efferent duct and epididymal epithelia: evidence in rats for its in vivo role in endocytosis of apolipoprotein J/clusterin. *Biol Reprod* (1996) 55:676–83. doi:10.1095/biolreprod55.3.676
98. Oliveira CA, VictorCosta AB, Hess RA. Cellular and regional distributions of ubiquitin proteasome and endocytotic pathway components in the epithelium of rat efferent ductules and initial segment of the epididymis. *J Androl* (2009) 30:590–601. doi:10.2164/jandrol.108.007310
99. Raymond AS, Elder B, Ensslin M, Shur BD. Loss of SED1/MFG-E8 results in altered luminal physiology in the epididymis. *Mol Reprod Dev* (2010) 77:550–63. doi:10.1002/mrd.21189
100. Lin RC, Scheller RH. Mechanisms of synaptic vesicle exocytosis. *Annu Rev Cell Dev Biol* (2000) 16:19–49. doi:10.1146/annurev.cellbio.16.1.19
101. Breton S, Nsumu NN, Galli T, Sabolic I, Smith PJ, Brown D. Tetanus toxin-mediated cleavage of cellubrevin inhibits proton secretion in the male reproductive tract. *Am J Physiol Renal Physiol* (2000) 278:F717–25. doi:10.1152/ajprenal.2000.278.5.F717
102. Tomes CN, Michaut M, De Blas G, Visconti P, Matti U, Mayorga LS. SNARE complex assembly is required for human sperm acrosome reaction. *Dev Biol* (2002) 243:326–38. doi:10.1006/dbio.2002.0567
103. Zhao L, Shi X, Li L, Miller DJ. Dynamin 2 associates with complexins and is found in the acrosomal region of mammalian sperm. *Mol Reprod Dev* (2007) 74:750–7. doi:10.1002/mrd.20660
104. Garcia MA, Meizel S. Progesterone-mediated calcium influx and acrosome reaction of human spermatozoa: pharmacological investigation of T-type calcium channels. *Biol Reprod* (1999) 60:102–9. doi:10.1095/biolreprod60.1.102
105. Westfalewicz B, Dietrich MA, Mostek A, Partyka A, Bielas W, Nizański W, et al. Identification and functional analysis of bull (*Bos taurus*) cauda epididymal fluid proteome. *J Dairy Sci* (2017) 100:6707–19. doi:10.3168/jds.2016-12526
106. Belleannée C, Labas V, Teixeira-Gomes AP, Gatti JL, Dacheux JL, Dacheux F. Identification of luminal and secreted proteins in bull epididymis. *J Proteomics* (2011) 74:59–78. doi:10.1016/j.jprot.2010.07.013
107. Geppert M, Südhof TC. RAB3 and synaptotagmin: the yin and yang of synaptic membrane fusion. *Annu Rev Neurosci* (1998) 21:75–95. doi:10.1146/annurev.neuro.21.1.75
108. Raimondi A, Ferguson SM, Lou X, Armbruster M, Paradise S, Giovedi S, et al. Overlapping role of dynamin isoforms in synaptic vesicle endocytosis. *Neuron* (2011) 70:1100–14. doi:10.1016/j.neuron.2011.04.031
109. Zhou W, Anderson AL, Turner AP, De Iulius GN, McCluskey A, McLaughlin EA, et al. Characterization of a novel role for the dynamin mechanoenzymes in the regulation of human sperm acrosomal exocytosis. *Mol Hum Reprod* (2017) 23:657–73. doi:10.1093/molehr/gax044
110. Caballero JN, Frenette G, Belleannée C, Sullivan R. CD9-positive microvesicles mediate the transfer of molecules to bovine spermatozoa during epididymal maturation. *PLoS One* (2013) 8:e65364. doi:10.1371/journal.pone.0065364
111. D'Amours O, Frenette G, Caron P, Belleannée C, Guillemette C, Sullivan R. Evidences of biological functions of biliverdin reductase A in the bovine epididymis. *J Cell Physiol* (2016) 231:1077–89. doi:10.1002/jcp.25200
112. Thery C, Zitvogel L, Amigorena S. Exosomes: composition, biogenesis and function. *Nat Rev Immunol* (2002) 2:569–79. doi:10.1038/nri855
113. Thery C, Ostrowski M, Segura E. Membrane vesicles as conveyors of immune responses. *Nat Rev Immunol* (2009) 9:581–93. doi:10.1038/nri2567
114. Harroun TA, Katsaras J, Wassall SR. Cholesterol is found to reside in the center of a polyunsaturated lipid membrane. *Biochemistry* (2008) 47:7090–6. doi:10.1021/bi800123b
115. Girouard J, Frenette G, Sullivan R. Compartmentalization of proteins in epididymosomes coordinates the association of epididymal proteins with the different functional structures of bovine spermatozoa. *Biol Reprod* (2009) 80:965–72. doi:10.1095/biolreprod.108.073551
116. Gatti JL, Métayer S, Belghazi M, Dacheux F, Dacheux JL. Identification, proteomic profiling, and origin of ram epididymal fluid exosome-like vesicles. *Biol Reprod* (2005) 72:1452–65. doi:10.1095/biolreprod.104.036426
117. Tian T, Wang Y, Wang H, Zhu Z, Xiao Z. Visualizing of the cellular uptake and intracellular trafficking of exosomes by live-cell microscopy. *J Cell Biochem* (2010) 111:488–96. doi:10.1002/jcb.22733

**Conflict of Interest Statement:** The authors declare that this manuscript was prepared in the absence of any commercial or financial relationships or activities that could be construed as a potential conflict of interest.

Copyright © 2018 Zhou, De Iulius, Dun and Nixon. This is an open-access article distributed under the terms of the Creative Commons Attribution License (CC BY). The use, distribution or reproduction in other forums is permitted, provided the original author(s) and the copyright owner are credited and that the original publication in this journal is cited, in accordance with accepted academic practice. No use, distribution or reproduction is permitted which does not comply with these terms.

## CHAPTER 2

---

### *Analysis of Epididymal Protein Synthesis and Secretion*

**Published:** Journal of Visualized Experiments (2018) 138

**Authors:** Wei Zhou<sup>1,2</sup>, Petra Sipila<sup>3</sup>, Geoffrey N. De Iuliis<sup>1,2</sup>, Matthew D. Dun<sup>2,4</sup> and Brett Nixon<sup>1,2\*</sup>

<sup>1</sup>Priority Research Centre for Reproductive Biology, School of Environmental and Life Sciences, University of Newcastle, Callaghan, NSW 2308, Australia.

<sup>2</sup>Hunter Medical Research Institute, University of Newcastle, New Lambton Heights, NSW, Australia.

<sup>3</sup>Department of Physiology, Turku Center for Disease Modeling, Institute of Biomedicine, University of Turku, Kiinamylynkatu 10, 20520 Turku, Finland.

<sup>4</sup>School of Biomedical Sciences and Pharmacy, Faculty of Health and Medicine, University of Newcastle, Callaghan, NSW 2308, Australia.

\*Correspondence: [brett.nixon@newcastle.edu.au](mailto:brett.nixon@newcastle.edu.au)

## Chapter 2: Overview

The aim of this manuscript was to describe the techniques that were applied in this thesis to study the role of dynamin in regulating epididymal sperm maturation. This chapter has been published in the Journal of Visualized Experiments; a strategic decision to ensure repeatability of our experimental approaches via the generation of detailed videography to guide the intended reader through the main steps of each protocol. These protocols include the application of immunofluorescence localization techniques for the study of the spatial distribution of proteins in mouse epididymal tissue. The broad applicability of this protocol has been extended by summarizing information on antigen retrieval optimization and the selection of appropriate representative markers for different subtypes of epithelial cells. We also documented our recently optimized protocols for the isolation and characterization of epididymosomes; small exosome-like vesicles that constitute key elements of the epididymal secretory profile and appear to hold a prominent role in promoting sperm maturation. As a complementary approach, we also describe the immunofluorescence detection of target proteins in an immortalized mouse caput epididymal epithelial (mECap18) cell line and the use of this resource as a model with which to explore the regulation of epididymal secretory activity *in vitro*. These combined methods hold considerable potential to help resolve the mechanistic basis of epididymal function and have been used extensively in the following Chapters of this thesis.

## Video Article

# Analysis of Epididymal Protein Synthesis and Secretion

Wei Zhou<sup>1,2</sup>, Petra Sipilä<sup>3</sup>, Geoffry N. De Luliis<sup>1,2</sup>, Matthew D. Dun<sup>2,4</sup>, Brett Nixon<sup>1,2</sup><sup>1</sup>Priority Research Centre for Reproductive Science, School of Environmental and Life Sciences, University of Newcastle<sup>2</sup>Hunter Medical Research Institute<sup>3</sup>Department of Physiology, Turku Center for Disease Modeling, Institute of Biomedicine, University of Turku<sup>4</sup>School of Biomedical Sciences and Pharmacy, Faculty of Health and Medicine, University of NewcastleCorrespondence to: Brett Nixon at [brett.nixon@newcastle.edu.au](mailto:brett.nixon@newcastle.edu.au)URL: <https://www.jove.com/video/58308>DOI: [doi:10.3791/58308](https://doi.org/10.3791/58308)

Keywords: Developmental Biology, Issue 138, Dynamin, epididymis, epididymosome, exosome, immunofluorescence, protein secretion, sperm, sperm maturation

Date Published: 8/25/2018

Citation: Zhou, W., Sipilä, P., De Luliis, G.N., Dun, M.D., Nixon, B. Analysis of Epididymal Protein Synthesis and Secretion. *J. Vis. Exp.* (138), e58308, doi:10.3791/58308 (2018).

## Abstract

The mammalian epididymis generates one of the most complex intraluminal fluids of any endocrine gland in order to support the post-testicular maturation and storage of spermatozoa. Such complexity arises due to the combined secretory and absorptive activity of the lining epithelial cells. Here, we describe the techniques for the analysis of epididymal protein synthesis and secretion by focusing on the model protein family of dynamin (DNM) mechanoenzymes; large GTPases that have the potential to regulate bi-directional membrane trafficking events. For the study of protein expression in epididymal tissue, we describe robust methodology for immunofluorescence labeling of target proteins in paraffin-embedded sections and the subsequent detection of the spatial distribution of these proteins via immunofluorescence microscopy. We also describe optimized methodology for the isolation and characterization of exosome like vesicles, known as epididymosomes, which are secreted into the epididymal lumen to participate in intercellular communication with maturing sperm cells. As a complementary approach, we also describe the immunofluorescence detection of target proteins in an SV40-immortalized mouse caput epididymal epithelial (mECap18) cell line. Moreover, we discuss the utility of the mECap18 cell line as a suitable *in vitro* model with which to explore the regulation of epididymal secretory activity. For this purpose, we describe the culturing requirements for the maintenance of the mECap18 cell line and the use of selective pharmacological inhibition regimens that are capable of influencing their secretory protein profile. The latter are readily assessed via harvesting of conditioned culture medium, concentration of secreted proteins via trichloroacetic acid/acetone precipitation and their subsequent analysis via SDS-PAGE and immunoblotting. We contend that these combined methods are suitable for the analysis of alternative epididymal protein targets as a prelude to determining their functional role in sperm maturation and/or storage.

## Video Link

The video component of this article can be found at <https://www.jove.com/video/58308/>

## Introduction

The spermatozoa of all mammalian species acquire the potential to display forward progressive motility and to fertilize an ovum during their prolonged descent through the epididymis, a highly specialized region of the male extra-testicular duct system, which may take 7 - 14 days to navigate (depending on the species)<sup>1</sup>. Due to the extreme condensation of the paternal chromatin and the shedding of the majority of cytoplasm that accompanies the cytodifferentiation of spermatozoa within the testes, their subsequent functional maturation is driven exclusively by their interaction with the epididymal microenvironment. This milieu is, in turn, created by the secretory and absorptive activity of the lining epididymal soma and displays an exceptional level of segment-segment variation<sup>1</sup>. Thus, the most active segments in terms of protein synthesis and secretion are those located in the proximal portion of the epididymis (namely, the caput and corpus)<sup>2</sup>. This activity mirrors the functional profile of spermatozoa, with the cells first beginning to display hallmarks of functional competence (*i.e.*, progressive motility and the ability to bind to acid-solubilized zona glycoproteins) following their passage through the caput epididymis<sup>3</sup>. These functional attributes continue to develop before reaching optimal levels as the sperm reach the distal epididymal segment (cauda), wherein they are stored in a quiescent state in readiness for ejaculation. The formation and maintenance of this sperm storage reservoir is also intimately tied to the lining epithelium, which in the cauda is dominated by strong absorptive activity<sup>4,5</sup>. Although anatomical differences have been reported<sup>6,7,8</sup>, such regionalized division of labor appears to be a characteristic of the epididymis that is shared among the majority of mammalian species studied to date, including our own<sup>9,10</sup>. Indeed, from a clinical perspective, it is known that epididymal dysfunction makes an important contribution to the etiology of male factor infertility<sup>11</sup>, thus highlighting the importance of understanding the regulation of this specialized tissue.

It is therefore regrettable that our understanding of epididymal physiology, and the mechanisms that regulate the sequential phases of sperm maturation and storage within this tissue, remain to be fully resolved. Among the contributing factors, limiting advances in epididymal research are the overall complexity of this tissue and knowledge of the mechanisms that exert regulatory control over its luminal microenvironment. Anatomically, we know that beyond the distinction of caput, corpus and cauda segments, the epididymis can be further subdivided into several zones (**Figure 1A**), each separated by septa<sup>12</sup> and characterized by discrete profiles of gene/protein expression<sup>13,14,15,16,17,18</sup>. Indeed, on the

basis of detailed transcriptional profiling of segmental gene expression in the epididymis, as many as 6 and 9 distinct epididymal zones have been reported in the mouse and rat models, respectively<sup>19,20</sup>. Such complexity presumably reflects the composition of the epididymal soma, a pseudostratified epithelium comprising numerous different cell types; each differing with respect to their abundance, distribution and secretory/absorptive activities along the length of the tract. Thus, principal cells are by far the most abundant epididymal cell type constituting upwards of 80% of all epithelial cells. Accordingly, principal cells are responsible for the bulk of epididymal protein biosynthesis and secretion<sup>5</sup>. In contrast, the clear cell population, which rank as the second most abundant cell type within the epididymal soma, are primarily involved in selective absorption of luminal components and the acidification of this microenvironment<sup>5</sup>. Adding another tier of complexity, androgens and other lumicrine factors of testicular origin exert differential control over each of these epididymal cell types depending on their positioning along the tract.

Despite the limitations imposed by such complexity, significant inroads continue to be made into resolving the mechanistic basis of epididymal function. A key to these studies has been the application of advanced mass spectrometry strategies to establish broad scale inventories of the epididymal proteome, in tandem with detailed analyses of individual proteins selected from among these initial surveys. An illustration of this approach is our recent characterization of the DNM family of mechanoenzymes in the mouse model<sup>21</sup>. Our initial interest in DNM was fueled by its dual action in the coupling of exo- and endocytotic processes. Building on these observations, we were able to demonstrate that the three canonical isoforms of DNM (DNM1 - DNM3) are highly expressed in the mouse epididymis and appropriately positioned to fulfill regulatory roles in protein secretion and absorption<sup>21</sup>. Moreover, we were able to clearly differentiate each DNM isoform on the basis of their cellular and sub-cellular localization, thus suggesting that they possess complementary, as opposed to redundant, activity within the epididymal epithelium<sup>21</sup>.

Here, we describe the experimental methodology employed for the study of DNM expression in the mouse epididymis with the hope that this information will find wider application in the characterization of alternative epididymal proteins and thus contribute to our understanding of the function of this important element of the male reproductive tract. Specifically, we describe the development of robust methodology for immunofluorescence labeling of target proteins in paraffin-embedded epididymal sections and the subsequent detection of the spatial distribution of these proteins via immunofluorescence microscopy. We further document our recently optimized protocols<sup>22</sup> for the isolation and characterization of epididymosomes; small exosome-like vesicles that constitute key elements of the epididymal secretory profile and appear to hold a prominent role in promoting sperm maturation<sup>23</sup>. As a complementary approach, we also describe the immunofluorescence detection of target proteins in an immortalized mouse caput epididymal epithelial (mECap18) cell line and the use of this resource as a model with which to explore the regulation of epididymal secretory activity *in vitro*.

## Protocol

All experimental procedures involving animal tissue collection were approved by the University of Newcastle's Animal Care and Ethics Committee.

### 1. Immunofluorescence Staining of the Paraffin-embedded Epididymal Sections (Figures 1 and 2)

1. Immediately after the euthanasia of adult mice via CO<sub>2</sub> inhalation (Swiss mice, over 8 weeks old), carefully dissect the epididymis (using surgical scissors and tweezers) free of overlying connective tissue and fat and immerse in Bouin's fixative solution (> ten times volume/tissue weight) for overnight fixation.
2. Wash the tissue with 70% ethanol with 2× changes daily for 2 days and then dehydrate through graded ethanol (70%, 95% and 100%) in preparation for infiltration and embedding into a paraffin block.
3. Section the paraffin blocks at a thickness of 4-6 μm and mount on the slides in preparation for immunofluorescence staining.
4. In a fume hood, dewax the epididymal paraffin sections by adding a sufficient amount of xylene to the slide jar to completely immerse the tissue section (3× 5 min each time).
5. Rehydrate the tissue sections by the immersion in graded ethanol solutions diluted in purified H<sub>2</sub>O (100% ethanol 5 min, 100% ethanol 5 min, 90% ethanol 1 min, 80% ethanol 1 min, 70% ethanol 1 min, and 50% ethanol 1 min).
6. Wash the sections in a slide jar once for 5 min with sufficient phosphate buffered saline (PBS) to completely immerse the entire tissue section (follow these directions for all subsequent washes).
7. Decant appropriate antigen retrieval solution (*i.e.*, 10 mmol/L sodium citrate, 50 mmol/L Tris pH 10.5 or alternative antigen retrieval solution(s), depending on the antigen to be detected) into a slide rack and microwave until boiling. Immerse the slides into this solution and subject the tissue sections to heat-induced antigen retrieval conditions optimized for individual antibodies (see **Table 1**).  
Caution: Ensure that the slides are fully immersed in antigen retrieval solution during the antigen retrieval process.
8. Remove the slide container from the microwave and cool to room temperature.
9. Rinse the slides with PBS and use a liquid-repellent slide marker pen to trace around the tissue section.
10. Place the slides in a humidified container (created by a moistened tissue at the base of the container), and apply blocking solution (3% BSA/PBS, previously filtered through a 0.45 μm filter) for 1 h at 37 °C.
11. Rinse the slides once with PBS.
12. Incubate the sections with appropriate primary antibody diluted to an experimentally optimized concentration in filtered 1% BSA/PBS at 4 °C overnight (1:60 for anti-DNM1, DNM2 and DNM3 antibodies; 1:100 for anti-ATP6V1B1 antibody, see **Table of Materials** for antibody details).  
Note: To distinguish specific from non-specific antibody binding, it is necessary to include stringent negative (*i.e.*, secondary antibody only, primary antibody preabsorbed against immunizing peptide) and positive controls<sup>24</sup>.
13. Rewarm the slides by placing at room temperature for 30 min.
14. Wash the slides 3× with PBS on a shaking platform (60 rpm) for 10 min each.
15. Incubate the sections with appropriate secondary antibody diluted in 1% BSA/PBS (filtered through a 0.45 μm filter) at 37 °C for 1 h (1:400 dilution for all secondary antibodies, see **Table of Materials** for antibody details).  
CAUTION: Keep the slide container in the dark from this step onwards. For dual labeling, choose a compatible combination of secondary antibodies (*i.e.*, secondary antibodies must have been raised in different species).

16. Wash the slides 3× with PBS on a shaking platform (60 rpm) for 10 min each.
17. Counterstain the sections with propidium iodide (PI, 7.48 μmol/L) or 4',6-diamidino-2-phenylindole (DAPI, 4.37 μmol/L) for 2 min at room temperature to label the cell nucleus.
18. Wash the slides twice with PBS on a shaking platform (60 rpm) for 5 min each.
19. Mount the sections with 10% Mowiol 4-88 prepared in a solution of 30% glycerol in 0.2 mol/L Tris (pH 8.5) and 2.5% 1, 4-diazabicyclo-(2.2.2)-octane.
20. Seal the coverslip with nail varnish and store the slides at 4 °C for future observation.  
CAUTION: It is recommended to perform the imaging of the slides as soon as practical after the preparation to avoid excessive loss of fluorescence.

## 2 Isolation of Epididymosomes from the Mouse Caput Epididymis (Figure 3)

1. Immediately after the euthanasia of adult mice via CO<sub>2</sub> inhalation (Swiss mice over 8 weeks old), perfuse their vasculature with PBS (pre-warmed to 37 °C) to minimize the blood contamination of epididymal tissue.  
CAUTION: Blood plasma contains diverse populations of exosomes, which are of similar size to epididymosomes<sup>25</sup>. The efficacy of blood clearance from epididymal tissue can be accessed via the inspection of the initial segment, a highly vascularized epididymal segment located proximal to the caput segment (*i.e.*, zone 1 in **Figure 1A**)
2. Carefully dissect the epididymis free of overlying fat and connective tissue, and rinse with modified Biggers, Whitten, and Whittingham medium (BWW; pH 7.4, osmolality of 300 mmol/kg water<sup>26,27</sup>) to reduce any potential for surface blood contamination.
3. Blot the epididymal tissue to remove excess media, dissect the caput epididymis (*i.e.*, zones 2-5 in **Figure 1A**) and transfer to a fresh Petri dish (35 × 10 mm) containing BWW medium. Ensure that the amount of medium is sufficient for the final recovery.  
Note: For 6 caput epididymides, it is recommended to use 1.1 mL of the medium to allow for a recovery of ~900 μL, which is then evenly split and applied atop of 2 pre-prepared gradients (see step 2.9).
4. Make a number of small incisions into the caput tissue with a razor blade. Do not mince the tissue and thus avoid contaminating the sample with excessive cytosolic contents. Incubate the plate containing the tissue with mild agitation at 37 °C for 30 min to release the luminal contents.
5. Filter the resultant suspension through 70 μm membranes to remove the cellular debris.
6. Collect the filtrate and subject this to successive centrifugation steps at 4 °C with increasing velocity in order to eliminate cellular debris (*i.e.*, 500 × g, 2,000 × g, 4,000 × g, 8,000 × g, 5 min each; 17,000 × g for 20 min, and finally 17,000 × g for an additional 10 min or until no pellet is formed after centrifugation).  
CAUTION: It is important to assess the color of the pellet after the initial 500 × g centrifugation step to ensure minimal blood contamination is present. Discard any samples in which this pellet displays pink coloration.
7. Prepare discontinuous iodixanol gradients (comprising 40%, 20%, 10%, 5% layers) by diluting a density gradient medium (comprising 60% (w/v) aqueous iodixanol) with a solution of 0.25 mol/L sucrose and 10 mmol/L Tris (pH 7.5).
8. Prepare the gradient in an ultracentrifuge tube (11 × 35 mm), with each fraction of 450 μL (**Figure 3**). Visually inspect the gradient after the application of each fraction to ensure that the interfaces are successfully formed between each layer prior to loading the epididymal fluid sample. Prepare each gradient fresh on the day of use, however, the epididymal luminal fluid sample can be preserved at 4 °C for up to 2 h prior to loading.
9. Carefully add 450 μL of epididymal luminal fluid suspension (corresponding to the material collected from the caput of 3 epididymides) atop of a single gradient.
10. Ultracentrifuge the gradients at 160,000 × g at 4 °C for 18 h.  
CAUTION: Since this centrifugation is conducted at very high speed, all ultracentrifuge tubes must be paired and balanced precisely. Check the tubes to ensure that they are free of any visible damage that could compromise their integrity.
11. Gently remove 12 equal fractions (each consisting of 185 μL) starting from the uppermost layer and progressing toward the bottom of the gradient. Pool the equivalent fractions recovered from each gradient if applicable (up to two gradients).  
Note: Mouse epididymosomes are most highly enriched in fractions 9 - 11<sup>22</sup>, see **Figure 4** and Discussion.
12. After the recovery and pooling of fractions 9 – 11, dilute into 2 mL of PBS, and ultracentrifuge the samples at 100,000 × g at 4 °C for 3 h (13 × 56 mm tube) to pellet the epididymosomes.  
CAUTION: Since the epididymosome pellet can be difficult to see, ensure that the orientation of the tubes is noted as they are placed into the rotor and mark the tube to indicate the expectant position of the epididymosome pellet. Ensure that each tube contains a sufficient volume (*i.e.*, exceeding 50% of its total capacity) to preclude the risk of tube collapse.
13. Carefully aspirate and discard the supernatant without disturbing the epididymosome pellet.
14. Assess the epididymosome purity (**Figure 4**).
15. Resuspend the epididymosome pellet into desired medium according to the downstream application(s). For instance, BWW medium is generally used for the experiments involving co-incubation with spermatozoa or alternatively an appropriate lysis buffer in preparation for the resolution of the epididymal proteome via SDS-PAGE.

## 3. Immunofluorescence Staining of mECap18 Cells

1. Preparation of sterile coverslips (to be conducted in a cell culture hood)
  1. Soak the coverslips (12 × 12 mm) in 70% ethanol for 10 min and disinfect by drying under high temperature above an ethanol lamp.
  2. Cool the coverslip for 10 s before transferring to a 12 well plate.
  3. Apply sterile poly-L-lysine solution to cover the coverslip and settle for 10 min at room temperature.
  4. Discard the poly-L-lysine solution and rinse the coverslip with sterile H<sub>2</sub>O or appropriate medium.
2. Preparation mECap18 cells
  1. Passage the aliquots of 2 × 10<sup>5</sup> mECap18 cells in each well of the 12 well plate containing the coverslips.

2. Culture the cells with mECap18 cell medium (DMEM supplemented with 1% L-glutamine, 1% sodium pyruvate, 1% penicillin/streptomycin, and 50  $\mu\text{mol/L}$  5 $\alpha$ -androstan-17 $\beta$ -ol-3-oneC-IIIN) containing 10% fetal calf serum (FBS) in a 37 °C incubator under an atmosphere 5% CO<sub>2</sub> overnight.
  3. Once the cells adhere to the coverslip, discard the medium and rinse the cells twice with PBS.
  4. Add a sufficient amount of 4% paraformaldehyde (PFA) diluted in PBS to immerse the entire coverslip and fix the cells at room temperature for 15 min.
  5. Discard the PFA solution and rinse the coverslips twice in PBS.
3. Immunofluorescence staining
1. Permeabilize mECap18 cells by immersion in 0.1% Triton X-100 in PBS for 10 min.
  2. Rinse the coverslips with PBS.
  3. Block mECap18 cells with 3% BSA and proceed with immunolabeling of cells utilizing equivalent protocols to those described for epididymal tissue sections.

## 4. Isolation of Proteins from Conditioned Cell Culture Medium

1. Collection of conditioned cell culture medium
  1. Passage aliquots of  $4 \times 10^5$  mECap18 cells in each well of 6 well plate with mECap18 cell medium supplemented with 10% FBS for 24 h.
  2. Wash mECap18 cells three times with mECap18 cell medium (prepared without FBS) to remove residual FBS and any associated protein contaminants.
  3. Add 1.5 mL of mECap18 cell medium (prepared without FBS) to each well and incubate with mECap18 cells for 12 h in a 37°C incubator under 5% CO<sub>2</sub>.  
Note: mECap18 cells at this step can be assessed for different target antigens according to experimental design.
  4. After 12 h incubation, collect the cell medium and centrifuge at  $2,000 \times g$  for 10 min to remove all cellular debris.  
Note: The duration of incubation is able to be altered in accordance with experimental design/endpoint assessment and in consideration of the cell's tolerance to applied treatment(s). It is recommended to tailor the timing of incubation based on specific experimental regimens to ensure that optimal results are achieved.
  5. Assess mECap18 cell viability via the application of a standard trypan blue exclusion assay<sup>28</sup>. Discard all material in which cell viability has declined below 90% to eliminate bias introduced by proteins released from dead or moribund cells.
  6. Isolate proteins from cell medium as follows or preserve medium at -80 °C.
2. Protein isolation (to be conducted in a fume hood)
  1. Add 20% volume of chilled 100% trichloroacetic acid to 80% volume of conditioned cell medium to precipitate the proteins released from the cultured mECap18 cells. Incubate at 4 °C overnight with constant mixing.
  2. After the incubation, pellet precipitated protein by centrifugation ( $17,000 \times g$ , 4 °C for 10 min).  
Note: Due to the limited quantity of protein expected to be secreted into the medium, it is possible that the pellet will not be easily visualized after centrifugation. It is therefore imperative to correctly orientate the tube prior to the centrifugation and take care not to disturb the expectant pellet location during removal of the supernatant.
  3. Discard the supernatant and wash the pellet twice with chilled acetone prior to the re-centrifugation ( $17,000 \times g$ , 4 °C for 10 min).
  4. Carefully remove and discard the supernatant before air-drying any residual acetone within a fume hood.
  5. Resuspend the protein pellet in an appropriate extraction buffer in preparation for endpoint analysis to detect complete secretory protein profiles and/or individual target proteins (e.g., SDS-PAGE, immunoblotting).

## Representative Results

**Figure 1 and Figure 2** show representative results of immunofluorescence localization of DNM in the mouse caput epididymis. Each of the three DNM isoforms investigated display distinct localization profiles. Thus, DNM1 is characterized by relatively modest diffuse labeling of the epididymal cells throughout the initial segment and caput epididymis (**Figure 2A**). By contrast, the DNM2 isoform was first detected in the vicinity of the opposing basal and apical border of cells in the initial segment, before being repositioned to the supranuclear domain in cells within the adjacent downstream caput segment (*i.e.*, zones 2 - 5) (**Figure 1B, C**). Notably, however, the intensity of DNM2 labeling gradually decreased between zones 2 to 5 of the caput epididymis, a result that essentially mirrors the secretory activity of these epididymal segments<sup>21</sup> (**Figure 1B, C**). Accordingly, the supranuclear labeling of DNM2 was subsequently shown to correspond to the distribution of the Golgi apparatus within caput principal cells<sup>21</sup>. Spermatozoa isolated from the same epididymal region showed intense acrosomal labeling for DNM2 (**Figure 1D**). As a caveat, however, equivalent DNM2 labeling was not routinely detected on luminal spermatozoa within our tissue sections. This phenomenon is the one we have encountered on several occasions when applying a range of antibodies targeting different epididymal/sperm antigens and presumably arises due to issues associated with antigen presentation and/or masking in the paraffin-embedded tissue sections. In any case, such differences emphasize the importance of conducting parallel immunofluorescent labeling of isolated spermatozoa alongside that of the epididymal tissue itself. Differing from both DNM1 and DNM2, the DNM3 isoform was mainly detected in the apical domain of a small number of caput epithelial cells (**Figure 2B, green arrows**), which were shown to correspond to the clear cell sub-population by co-labeling with the recognized clear cell marker, ATP6V1B1 (**Figure 2B, red arrows**). In a similar manner, representative markers that have proven suitable for differentiating the different epididymal epithelial cell types are summarized in **Table 2**<sup>29,30,31,32,33,34</sup>.

In addition to the description of the techniques for the subcellular localization of proteins residing within the epididymal epithelium, here, we also report our recently optimized protocols for the study of secretory proteins encapsulated within epididymosomes, small extracellular vesicles that represent an important component of the luminal milieu responsible for supporting sperm maturation and storage<sup>22</sup>. Combined, step 2 and **Figure 3** provide a detailed step by step account of the methodology used for the isolation of highly enriched populations of epididymosomes from mouse caput epididymal tissue. Notably, however, these methods are readily applicable for the isolation of alternate populations of epididymosomes originating from more distal epididymal segments. Owing to the potential for contamination of these samples, we also described the stringent characterization protocols that we routinely employ for each epididymosome preparation. These include the assessment of the size and heterogeneity of the epididymosome populations using both high-resolution electron microscopy and dynamic light scattering techniques. In tandem, we also utilize immunoblotting strategies to assess the enrichment of recognized extracellular vesicle markers and the corresponding absence of proteins that are characteristic of potential contaminants (*i.e.*, anti-hemoglobin (HBB) as a marker of blood contamination and anti-arachidonate 15-lipoxygenase (ALOX15) and anti-IZUMO1 antibodies as markers of cytoplasmic droplet and sperm contamination, respectively)<sup>22</sup>. Although we have found that the contaminants are rare, if they are encountered, we immediately discard the epididymosome preparation.

The non-overlapping localization of DNM isoforms in the caput epididymis prompted a further investigation of their potential roles in regulating the epididymal microenvironment. For this purpose, an immortalized mECap18 cell line was utilized as an *in vitro* model to study epididymal cell secretory activity. Previous characterization of this cell line has shown that it harbors a mixed cell population, which stain positive for either principal or clear cell markers. Moreover, mECap18 cells have also proven suitable for reporting physiological profiles of epididymal gene and protein expression under different *in vitro* treatment regimens<sup>35</sup>. Prior to use, DNM localization was assessed in cultured mECap18 cells by settling these onto poly-L-lysine treated coverslips (**Figure 5A**) and subjecting them to immunofluorescence detection. Consistent with the distribution patterns recorded in caput epididymal tissue sections, DNM1 was detected throughout the cytoplasm of mECap18 cells, while DNM2 was concentrated within the supranuclear domain of these cells and DNM3 was characterized by discrete foci of membrane staining within a small sub-population number (*i.e.*, 11%) of the mECap18 cells which were ATP6V1B1 positive (**Figure 5B**). These data affirm the utility of the mECap18 cell line as a valuable resource for investigating the role of DNM in regulating epididymal cell secretory/absorptive activity.

Accordingly, step 4 describes the methodology for the analysis of mECap18 cell secretory activity; the techniques which are broadly amenable for assessing the impact of a range of different experimental conditions. In our study, we applied selective pharmacological interventions to suppress the activity of DNM1 and DNM2 prior to the visualization and quantification of the profile of proteins released from mECap18 cells into conditioned medium<sup>21</sup>. An important feature of this analysis, however, was to ensure that mECap18 cells were thoroughly washed and cultured in the absence of FBS supplementation. Whilst such a step was essential to preclude the contamination of conditioned medium with FBS derived proteins, it nevertheless carries the attendant risk of negatively impacting mECap18 cell growth and/or viability. In controlling for this possibility, we noted that the mECap18 cell line tolerated FBS free culture and the introduction of DNM inhibitors for the duration of our incubation window (*i.e.*, 12 h). Indeed, over this time course, cell viability remained above 90% in all experimental replicates. This approach could therefore serve as a useful proof-of-concept strategy to identify the function of specific epididymal proteins before committing to investment into gene manipulation strategies.

Heat induced epitope retrieval solution	10 mmol/L sodium citrate	50 mmol/L Tris (pH 10.5)
Time	3 min	3 min
	6 min	6 min
	9 min	9 min
	12 min	12 min

**Table 1: General conditions for the optimization of heat-induced antigen retrieval for the use with paraffin-embedded epididymal sections.** The fixation process can be problematic as different epitopes often require the use of different fixation techniques, thereby necessitating that the methodology is optimized for each antigen.

Epithelial cell type	Distribution	Marker	References (PMID)
Principal cell	Whole epididymis	AQP9	11027599, 17360690
Clear cell	Caput, corpus and cauda	V-ATPases, CIC-5	19448084, 12475763
Basal cell	Whole epididymis	CLDN1	11159859, 21441423
Narrow cell	Initial segment	V-ATPases, CIC-5	19448084, 12475763

**Table 2: Representative markers suitable for the detection of different primary epididymal epithelial cell types.**

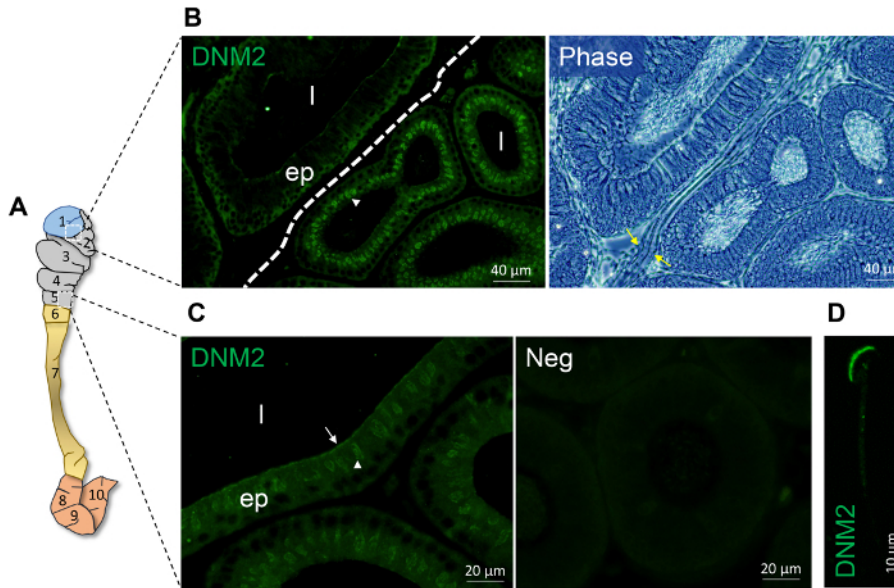


**Figure 1: Spatial expression of DNM 2 within the proximal mouse epididymis.** (A) Schematic model of epididymis depicting the partitioning on the mouse epididymis into 10 zones physically separated septa as reported by Turner and colleagues<sup>20</sup>. In this model, zone 1 corresponds to the initial segment, zones 2-5 correspond to the caput epididymis, zones 6-7 correspond to the corpus epididymis and zones 8-10 represent the cauda epididymis. (B-C) Immunofluorescence localization of DNM2 revealed zone-specific distribution patterns (indicated by white arrowhead and arrow). The border between zone 1 and 2 is demarcated by a dotted line or denoted by yellow arrows. (D) DNM2 is also expressed in the peri-acrosomal domain of spermatozoa isolated from the caput epididymis. However, no such staining was routinely detected in luminal spermatozoa within the corresponding epididymal sections. ep, epithelial cells; l, lumen; Neg, secondary antibody only control. Experiments were replicated on material from three animals and representative immunofluorescence images are presented. [Please click here to view a larger version of this figure.](#)

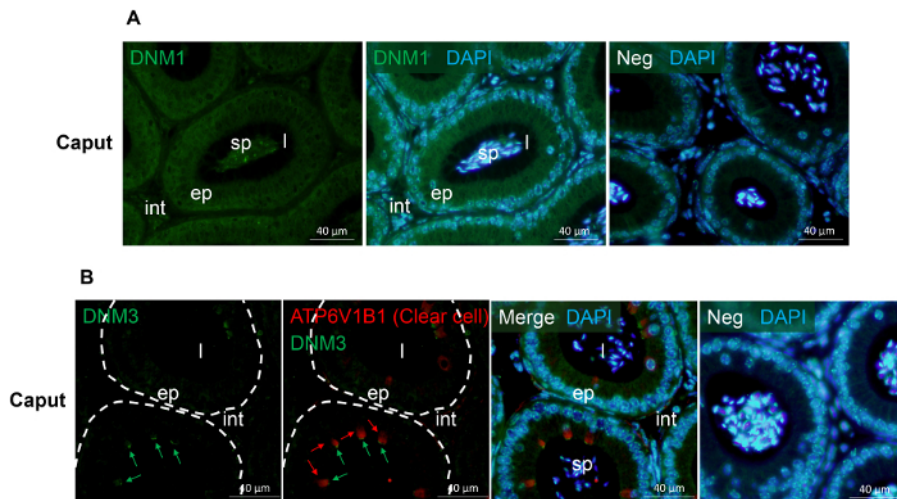


**Figure 2: Immunofluorescence detection of DNM 1 and DNM 3 in the mouse caput epididymis.** (A) The localization of DNM1<sup>36</sup> was examined in the mouse caput epididymis. (B) Co-localization of DNM3<sup>36</sup> and the clear cell marker, ATP6V1B1<sup>37</sup> in the mouse caput epididymis. This analysis confirmed that both DNM3 (green arrows) and ATP6V1B1 (red arrows) reside in the clear cell sub-population but display minimal sub-cellular overlap. ep, epithelial cells; int, interstitium; l, lumen; sp, sperm; Neg, secondary antibody only control. Cell nuclei were counterstained with DAPI (blue). Experiments were replicated on material from three animals and representative immunofluorescence images are presented. [Please click here to view a larger version of this figure.](#)

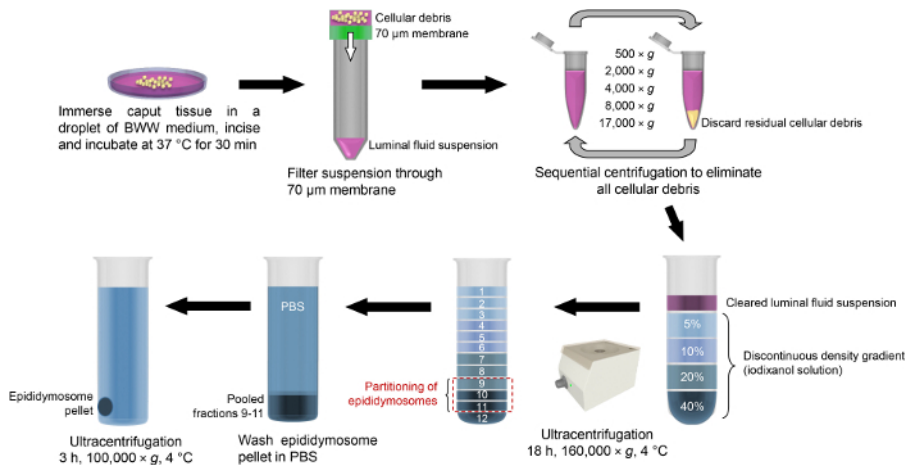


**Figure 3: Schematic of isolation protocols used for enrichment of mouse caput epididymosomes.** After the dissection, caput epididymal tissue is immersed into a droplet of BWV medium and incised to release the luminal contents. The luminal fluid is then filtered through a 70 µm membrane and the resultant suspension is centrifuged at increasing velocity in order to pellet any residual cell debris. The cleared suspension is then loaded atop of a discontinuous density gradient (iodixanol solution) and subjected to overnight ultracentrifugation. Epididymosomes partition into fractions 9 - 11, which are pooled, washed via dilution into PBS and returned to the ultracentrifuge to pellet the epididymosomes. [Please click here to view a larger version of this figure.](#)

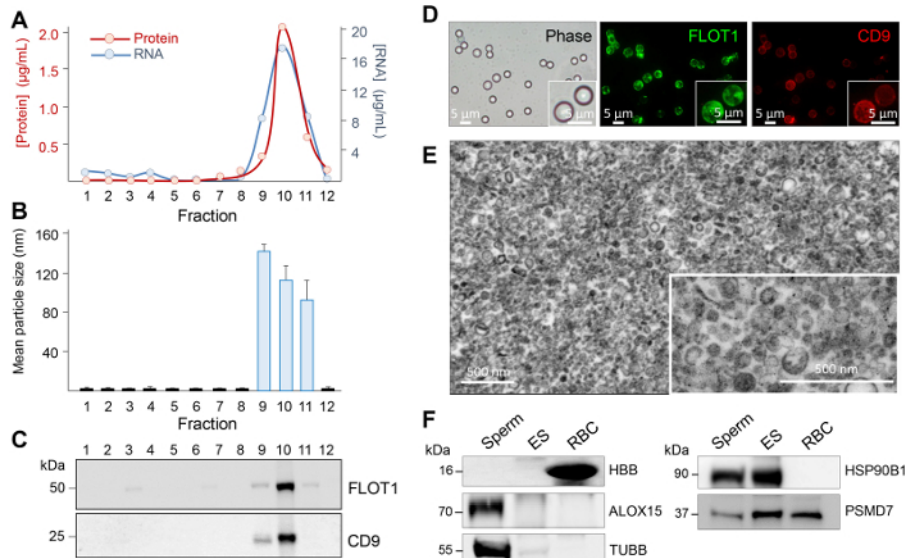


**Figure 4: Assessment of epididymosome purity.** Twelve equal fractions were recovered after the ultracentrifugation of the gradient and an aliquot of each prepared for (A) protein and RNA quantification, (B) size heterogeneity assessment by using dynamic light scattering, and (C) immunoblot analysis of epididymosome marker distribution. Additional characterization steps included (D) dual-labeling of epididymosomes concentrated onto aldehyde/sulphate latex beads, (E) transmission electron microscopy assessment, and (F) immunoblot assessment of spermatozoa (Sperm) and red blood cell (RBC) contamination by using either anti-arachidonate 15-lipoxygenase (ALOX15, cytoplasmic droplet/ sperm contamination) or anti-hemoglobin (HBB, RBC contamination). Immunoblots were also probed with known epididymosome cargo (26S proteasome non-ATPase regulatory subunit 7, PSMD7; heat shock protein 90kDa beta member 1, HSP90B1; and beta tubulin, TUBB). These data were originally published in Scientific Reports (PMID: 27549865) and have been reproduced here with the permission of the publisher, Springer Nature. [Please click here to view a larger version of this figure.](#)

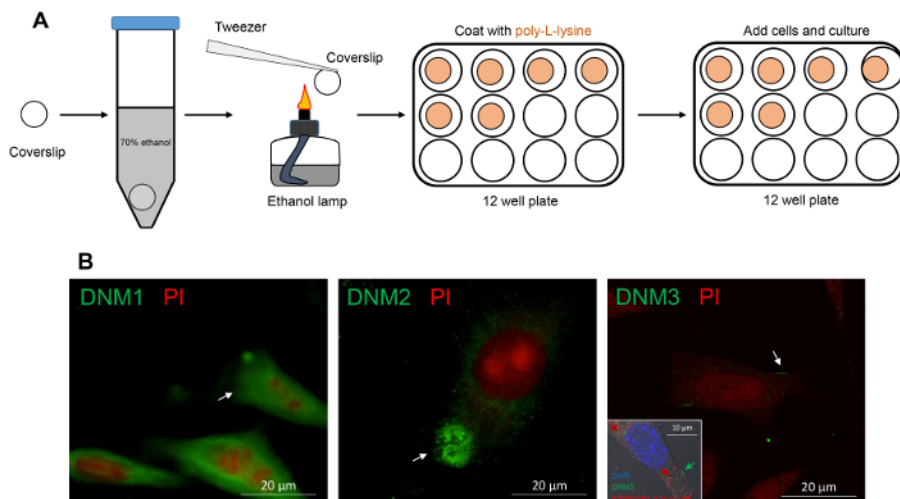


**Figure 5: Immunofluorescence detection of DNM isoforms in mECap18 cells reveal distribution patterns that accord with those detected in caput epididymal tissue. (A)** Schematic of coverslip preparation for sterile mECap18 cell culture. **(B)** Representative immunofluorescence images of DNM staining revealed cellular distribution patterns (arrows and inset (dual labeling of DNM3 and clear cell marker ATP6V1B1)) that mirrored those detected within epididymal tissue sections. Cell nuclei were counterstained with either propidium iodide (PI; red) or DAPI (blue). Experiments were replicated on material from three animals and representative immunofluorescence images are presented. [Please click here to view a larger version of this figure.](#)

## Discussion

These studies incorporated the use of Bouin's fixed epididymal tissue that had been subjected to paraffin embedding and standard sectioning protocols. Bouin's fixative solution comprises a mixture of formaldehyde, picric acid and acetic acid, with each component having a specific and complementary function. Thus, formaldehyde reacts with primary amines to form protein cross-links, picric acid slowly penetrates the tissue forming salts and hence coagulation of basic proteins and conversely, acetic acid rapidly penetrates the tissue and causes the coagulation of nucleic acids. These combined properties have engendered Bouin's as a fixative of choice for the preservation of morphological detail and its use is widely reported in the epididymal literature. However, Bouin's solution is not without its limitations, which include the propensity for fixative induced fluorescence and for formaldehyde induced cross-linking which may mask target antigens.

The potential for background fluorescence necessitates the use stringent negative controls, which in our studies include the omission of the primary antibody, omission of the secondary antibody and, where the reagents are available, the use of primary antibodies preabsorbed against the immunizing peptide from which they were generated. Details of the application of such controls are exemplified in our previous study of dynamin DNM expression in the mouse epididymis<sup>21</sup>. Ideally, such results should also be validated through the use of tissue derived from knockout animals, however, this material is not always readily available. In seeking to counter the secondary problem of cross-linked or chemically modified target antigens, it is frequently necessary to perform some form of antigen retrieval in order to unmask epitopes altered by fixation and thus restore their potential for antibody binding. The methodology used for retrieval depends on many variables, including the target antigen, antibody, tissue type, and the method of fixation. However, the most widely adopted techniques feature the application of either heat-mediated or proteolytic induced antigen retrieval. The former features as our favored approach owing to a higher success rate for restoring immunoreactivity, with the details of the heat regimens and retrieval solutions we commonly utilize being documented in **Table 1**. We caution however, that this is by no means an exhaustive list and ultimately the optimization of antigen retrieval for each protein target/antibody combination requires preliminary studies using a matrix of time, temperature, and pH combinations. Additional considerations include the potential for heat retrieval to elicit tissue damage and/or cause artefactual labeling. Thus, in addition to the application of the negative controls documented above, we also routinely incorporate positive controls featuring antibodies, such as anti-Golgin-97, which recognize distinct cellular organelles.

In seeking to establish whether proteins such as those belonging to the DNM family fulfill redundant, as opposed to complementary, functions in epididymal tissue, we have found it particularly informative to perform dual labeling experiments such as those illustrated in **Figure 2B**. This strategy involves sequential labeling of tissue sections with pairs of primary antibodies (raised in different species) followed appropriate secondary antibodies conjugated to different fluorophores. However, a confounding feature that occasionally arises in seeking to perform these dual labeling studies is the incompatibility of the antigen retrieval protocols needed for optimal labeling with each primary antibody. This limitation was encountered in the case of co-labeling of DNM 2 and Golgin-97 in the mouse caput epididymis, leading us to use consecutive serial sections (as opposed to the same section)<sup>21</sup>. Nevertheless, either of these approaches are extremely useful in the context of ascribing protein expression to a particular cell type among those represented in the pseudostratified epididymal epithelium. With this goal in mind, we have included a list of representative cell type markers and their reported distribution patterns along the length of the epididymal tubule (**Table 2**). When one wishes to go beyond cell type and begin to explore the subcellular distribution of target proteins, the use of dual labeling with recognized organelle markers, such as Golgin-97, offers distinct advantages. Alternatively, the application of high-resolution electron microscopy in tandem with immunogold labeling remains the method of choice for detailed ultrastructural localization and validation of staining patterns achieved using immunofluorescence<sup>21</sup>.

Among the limitations posed by the study of epididymosomes are their small size and the difficulty of obtaining sufficient quantities for detailed end point analyses, particularly in commonly used laboratory species such as the mouse. However, by capitalizing on the pioneering studies of Sullivan and colleagues<sup>38,39,40</sup>, we have been able to optimize robust methodology for epididymosome isolation from the mouse model (see

step 2). We do stress, however, the need to impose stringent controls to assess and physical characteristics of the enriched epididymosome populations<sup>41</sup> due to the potential contamination from spermatozoa, cytoplasmic droplets and/or blood-borne exosomes (see **Figure 4**). For this purpose, we routinely use a combination of: (i) high resolution electron microscopy to visualize the size and heterogeneity of the epididymosome preparation, (ii) calculation of the mean particle size and heterogeneity (iii) concentration of the epididymosomes onto 4 µm aldehyde/sulphate latex beads and fluorescent labeling of recognized exosome surface markers, including CD9 and FLOT1, and (iv) immunoblotting of isolated epididymosomes with a suite of antibodies recommended for experimental validation of exosomes (e.g., anti-CD9, anti-FLOT1), as well as negative controls corresponding to antigens that should be restricted to spermatozoa (anti-IZUMO1), sperm cytoplasmic droplets (anti-ALOX15), or blood (anti-HBB)<sup>22</sup>. If these standards are met, then the epididymosome preparations isolated are readily amenable for use in downstream applications including co-incubation with spermatozoa and/or cargo profiling analyses<sup>22,42</sup>, both of which are powerful approaches for enhancing our understanding of the role of epididymosomes in regulating epididymal sperm maturation<sup>1</sup>.

In this study, we describe the application of an SV40-immortalized mouse caput epididymal epithelial (mECap18) cell line, which we have utilized to study the involvement of DNM in the regulation of epididymal secretory activity<sup>21</sup> as well as the impact of environmental toxicants on epididymal physiology<sup>43</sup>. An important feature of the mECap18 cell line is that it displays phenotypic stability between passages and features a representative population of both principal and clear cells<sup>21,35,44</sup>. Compared to primary epididymal cell cultures, the mECap18 cell line also displays tolerance to culturing in fetal calf serum free medium, which extends the duration and nature of experimental interventions these cells can be exposed to, whilst also being permissive of recovering a higher abundance of secreted proteins from the conditioned medium. A limitation of the mECap18 cell line, however, is that it has been immortalized and may thus respond differently to stress and / or immune-related stimuli compared to that of primary cell cultures or those cells present *in vivo*. With this limitation in mind, it is recommended to compare the results obtained using mECap18 cells to *in vivo* responses whenever possible. In summary, the protocols we describe highlight the utility of this cell line as a tool with which to begin to study the functionality of target proteins within the caput epididymis. Indeed, in combination with the use of commercial protein inhibitors and/or genome-editing tools (such as CRISPR-Cas9), the mECap18 cell line holds considerable potential to help resolve the mechanistic basis of epididymal function.

## Disclosures

The authors have nothing to disclose.

## Acknowledgements

The authors would like to acknowledge the National Health and Medical Research Council of Australia Project Grant APP1103176 for the support of this work.

## References

- Zhou, W., De Iulius, G. N., Dun, M. D., & Nixon, B. Characteristics of the Epididymal Luminal Environment Responsible for Sperm Maturation and Storage. *Frontiers in Endocrinology*. **9** 59, (2018).
- Dacheux, J. L., Gatti, J. L., & Dacheux, F. Contribution of epididymal secretory proteins for spermatozoa maturation. *Microscopy research and technique*. **61**(1), 7-17, (2003).
- Aitken, R. J. *et al.* Proteomic changes in mammalian spermatozoa during epididymal maturation. *Asian journal of andrology*. **9**(4), 554-564, (2007).
- Hermo, L., Dworkin, J., & Oko, R. Role of epithelial clear cells of the rat epididymis in the disposal of the contents of cytoplasmic droplets detached from spermatozoa. *The American journal of anatomy*. **183**(2), 107-124, (1988).
- Robaire, B., Hinton, B., & Orgebin-Crist, M. *The epididymis*. Vol. **3** Knobil and Neill's Physiology of Reproduction (2006).
- Nixon, B. *et al.* Formation and dissociation of sperm bundles in monotremes. *Biology of Reproduction*. **95**(4), (2016).
- Cleland, K. The structure and function of the Epididymis. 1. The histology of the Rat Epididymis. *Australian Journal of Zoology*. **5**(3), 223-246, (1957).
- Belleannée, C. *et al.* Identification of luminal and secreted proteins in bull epididymis. *Journal of proteomics*. **74**(1), 59-78, (2011).
- Turner, T. T. De Graaf's thread: the human epididymis. *Journal of andrology*. **29**(3), 237-250, (2008).
- Holland, M. K., & Nixon, B. The specificity of epididymal secretory proteins. *Journal of reproduction and fertility*. **53** 197-210, (1998).
- Cooper, T. G., Hing-Heiyeung, C., Nashan, D., & Nieschlag, E. Epididymal markers in human infertility. *Journal of andrology*. **9**(2), 91-101, (1988).
- Turner, T. T., Johnston, D. S., Jelinsky, S. A., Tomsig, J. L., & Finger, J. N. Segment boundaries of the adult rat epididymis limit interstitial signaling by potential paracrine factors and segments lose differential gene expression after efferent duct ligation. *Asian journal of andrology*. **9**(4), 565-573, (2007).
- Garrett, S. H., Garrett, J. E., & Douglass, J. In situ histochemical analysis of region-specific gene expression in the adult rat epididymis. *Molecular reproduction and development*. **30**(1), 1-17, (1991).
- Lareyre, J. J. *et al.* A 5-kilobase pair promoter fragment of the murine epididymal retinoic acid-binding protein gene drives the tissue-specific, cell-specific, and androgen-regulated expression of a foreign gene in the epididymis of transgenic mice. *Journal of Biological Chemistry*. **274**(12), 8282-8290, (1999).
- Cornwall, G. A., Orgebin-Crist, M. C., & Hann, S. R. The CRES gene: a unique testis-regulated gene related to the cystatin family is highly restricted in its expression to the proximal region of the mouse epididymis. *Molecular Endocrinology*. **6**(10), 1653-1664, (1992).
- Nixon, B., Jones, R. C., Hansen, L. A., & Holland, M. K. Rabbit epididymal secretory proteins. I. Characterization and hormonal regulation. *Biology of Reproduction*. **67**(1), 133-139, (2002).
- Nixon, B., Jones, R. C., Clarke, H. G., & Holland, M. K. Rabbit epididymal secretory proteins. II. Immunolocalization and sperm association of REP38. *Biology of Reproduction*. **67**(1), 140-146, (2002).

18. Nixon, B., Hardy, C. M., Jones, R. C., Andrews, J. B., & Holland, M. K. Rabbit epididymal secretory proteins. III. Molecular cloning and characterization of the complementary DNA for REP38. *Biology of Reproduction*. **67**(1), 147-153, (2002).
19. Jelinsky, S. A. *et al.* The rat epididymal transcriptome: comparison of segmental gene expression in the rat and mouse epididymides. *Biology of Reproduction*. **76**(4), 561-570, (2007).
20. Johnston, D. S. *et al.* The Mouse Epididymal Transcriptome: Transcriptional Profiling of Segmental Gene Expression in the Epididymis 1. *Biology of Reproduction*. **73**(3), 404-413, (2005).
21. Zhou, W. *et al.* Developmental expression of the dynamin family of mechanoenzymes in the mouse epididymis. *Biology of Reproduction*. **96**(1), 159-173, (2017).
22. Reilly, J. N. *et al.* Characterisation of mouse epididymosomes reveals a complex profile of microRNAs and a potential mechanism for modification of the sperm epigenome. *Scientific reports*. **6**, (2016).
23. Sullivan, R. Epididymosomes: a heterogeneous population of microvesicles with multiple functions in sperm maturation and storage. *Asian journal of andrology*. **17**(5), 726-729, (2015).
24. Reid, A. T. *et al.* Glycogen synthase kinase 3 regulates acrosomal exocytosis in mouse spermatozoa via dynamin phosphorylation. *The FASEB Journal*. **29**(7), 2872-2882, (2015).
25. Danesh, A. *et al.* Exosomes from red blood cell units bind to monocytes and induce proinflammatory cytokines, boosting T-cell responses in vitro. *Blood*. **123**(5), 687-696, (2014).
26. Anderson, A. L. *et al.* Assessment of microRNA expression in mouse epididymal epithelial cells and spermatozoa by next generation sequencing. *Genomics data*. **6** 208-211, (2015).
27. Biggers, J., Whitten, W., Whittingham, D. The culture of mouse embryos in vitro. In: Daniels J (ed.), *Methods in mammalian embryology*. San Francisco: Freeman, 86 – 116, (1971).
28. Strober, W. Trypan blue exclusion test of cell viability. *Current protocols in immunology*. A3. B. 1-A3. B. 3, (2001).
29. Elkjær, M.-L. *et al.* Immunolocalization of AQP9 in liver, epididymis, testis, spleen, and brain. *Biochemical and biophysical research communications*. **276**(3), 1118-1128, (2000).
30. Gregory, M., Dufresne, J., Hermo, L., & Cyr, D. G. Claudin-1 is not restricted to tight junctions in the rat epididymis. *Endocrinology*. **142**(2), 854-863, (2001).
31. Isnard-Bagnis, C. *et al.* Detection of CIC-3 and CIC-5 in epididymal epithelium: immunofluorescence and RT-PCR after LCM. *American Journal of Physiology-Cell Physiology*. **284**(1), C220-C232, (2003).
32. Rojek, A. M. *et al.* Defective glycerol metabolism in aquaporin 9 (AQP9) knockout mice. *Proceedings of the National Academy of Sciences*. **104**(9), 3609-3614, (2007).
33. Shum, W. W., Da Silva, N., Brown, D., & Breton, S. Regulation of luminal acidification in the male reproductive tract via cell-cell crosstalk. *Journal of Experimental Biology*. **212**(11), 1753-1761, (2009).
34. Shum, W. W., Ruan, Y. C., Silva, N., & Breton, S. Establishment of cell-cell cross talk in the epididymis: Control of luminal acidification. *Journal of Andrology*. **32**(6), 576-586, (2011).
35. Sipilä, P., Shariatmadari, R., Huhtaniemi, I. T., & Poutanen, M. Immortalization of epididymal epithelium in transgenic mice expressing simian virus 40 T antigen: characterization of cell lines and regulation of the polyoma enhancer activator 3. *Endocrinology*. **145**(1), 437-446, (2004).
36. Feugang, J. M. *et al.* Profiling of relaxin and its receptor proteins in boar reproductive tissues and spermatozoa. *Reproductive Biology and Endocrinology*. **13**(1), 46, (2015).
37. Gullberg, M. *et al.* Cytokine detection by antibody-based proximity ligation. *Proceedings of the National Academy of Sciences*. **101**(22), 8420-8424, (2004).
38. Frenette, G., Girouard, J., & Sullivan, R. Comparison between epididymosomes collected in the intraluminal compartment of the bovine caput and cauda epididymidis. *Biology of Reproduction*. **75**(6), 885-890, (2006).
39. Fornes, M., Barbieri, A., Sosa, M., & Bertini, F. First observations on enzymatic activity and protein content of vesicles separated from rat epididymal fluid. *Andrologia*. **23**(5), 347-351, (1991).
40. Eickhoff, R. *et al.* Influence of macrophage migration inhibitory factor (MIF) on the zinc content and redox state of protein-bound sulphhydryl groups in rat sperm: indications for a new role of MIF in sperm maturation. *Molecular human reproduction*. **10**(8), 605-611, (2004).
41. Lötvall, J. *et al.* Minimal experimental requirements for definition of extracellular vesicles and their functions: a position statement from the International Society for Extracellular Vesicles. *Journal of Extracellular Vesicles*. **3**, 26913, (2014).
42. Hutcheon, K. *et al.* Analysis of the small non-protein-coding RNA profile of mouse spermatozoa reveals specific enrichment of piRNAs within mature spermatozoa. *RNA biology*. **14**(12), 1776-1790, (2017).
43. Bennett, P. Genetic basis of the spread of antibiotic resistance genes. *Annali dell'Istituto superiore di sanita*. **23**(4), 819, (1987).
44. Nixon, B. *et al.* Next generation sequencing analysis reveals segmental patterns of microRNA expression in mouse epididymal epithelial cells. *PLoS one*. **10**(8), e0135605, (2015).

## CHAPTER 3

---

### *Developmental expression of the dynamin family of mechanoenzymes in the mouse epididymis*

**Published:** Biology of Reproduction (2017) 96 (1): 159-173

**Authors:** Wei Zhou<sup>1</sup>, Geoffry N. De Iuliis<sup>1</sup>, Adrian P. Turner<sup>2</sup>, Andrew T. Reid<sup>1</sup>, Amanda L. Anderson<sup>1</sup>, Adam McCluskey<sup>3</sup>, Eileen A. McLaughlin<sup>1,2,3</sup>, and Brett Nixon<sup>1\*</sup>

<sup>1</sup>Priority Research Centre for Reproductive Biology, School of Environmental and Life Sciences, University of Newcastle, Callaghan, NSW 2308, Australia.

<sup>2</sup>School of Biological Sciences, University of Auckland, Auckland, New Zealand.

<sup>3</sup>Priority Research Centre for Chemical Biology, School of Environmental and Life Sciences, University of Newcastle, Callaghan, NSW 2308, Australia.

\*Correspondence: [brett.nixon@newcastle.edu.au](mailto:brett.nixon@newcastle.edu.au)

## Chapter 3: Overview

The epididymis generates one of the most complex of all intraluminal fluids in order to support sperm maturation and storage. The creation of this specialised luminal microenvironment is apparently strictly regulated through the combined secretory and absorptive activity of the surrounding epithelium such that sperm acquire functional maturity in a sequential manner. While considerable effort has focused on defining the luminal composition, relatively less is known about the mechanistic basis by which this environment is tightly regulated. In recent studies, we have begun to characterize the expression of the dynamin family of enzymes and explore their contribution to male reproduction. This interest was seeded by the ability of dynamin to regulate membrane trafficking events, such as those that predominate in the epididymis. Thus, the aim of this study was to characterize the spatial and temporal expression of dynamin in the mouse epididymis. Based on the promising results of these studies, we elected to use an *in vitro* cell culture model (as discussed in Chapter 2) to document the impact of pharmacological dynamin inhibition on the secretion of epididymal proteins.

Accordingly, we have shown that the three canonical dynamin isoforms (DNM1, DNM2 and DNM3) are abundantly expressed in the early developmental stages of mouse epididymal differentiation. However, upon sexual maturation ( $\geq 30$ d after birth) the conserved pattern of dynamin expression was replaced by one in which both segment- and cell-specific localization was recorded among different isoforms. Thus, DNM1 and DNM3 were predominately localized to the distal segment of the epididymis (corpus and cauda), where they resided in clear cells and principal cells. In marked contrast, DNM2 was mainly found within the proximal segment of the epididymis (caput), with its localization overlapping with that of the Golgi apparatus of the principal cells. Such findings are of potential significance as the caput segment is most active in terms of protein synthesis and secretion. Through the use of an *in vitro* culture of caput epithelial cells (mECap18 cells) we were able to demonstrate that dynamin inhibition significantly reduced the secretion of a subset, but certainly not all, epididymal proteins into the culture medium.

The results of this chapter support the segment specific and non-redundant roles of different dynamin isoforms in regulating the epididymal milieu. Such regulation aligns with the segment specific characteristics of the epididymal environment in terms of supporting sperm maturation and storage. Given that the spermatozoa lack the ability to participate in

gene transcription or *de novo* protein translation, an important direction for future research will be to investigate the functional impact of dynamin inhibition on sperm maturation.

Research Article

# Developmental expression of the dynamin family of mechanoenzymes in the mouse epididymis<sup>†</sup>

Wei Zhou<sup>1</sup>, Geoffry N. De Iuliis<sup>1</sup>, Adrian P. Turner<sup>2</sup>, Andrew T. Reid<sup>1</sup>,  
Amanda L. Anderson<sup>1</sup>, Adam McCluskey<sup>3</sup>, Eileen A. McLaughlin<sup>1,2,3</sup>  
and Brett Nixon<sup>1,\*</sup>

<sup>1</sup>Priority Research Centre for Reproductive Science, School of Environmental and Life Sciences, The University of Newcastle, Callaghan, New South Wales, Australia; <sup>2</sup>School of Biological Sciences, University of Auckland, Auckland, New Zealand and <sup>3</sup>Priority Research Centre for Chemical Biology, School of Environmental and Life Sciences, The University of Newcastle, Callaghan, New South Wales, Australia

\*Correspondence: School of Environmental and Life Sciences, The University of Newcastle, University Drive, Callaghan, NSW 2308, Australia. Tel: + 61-2-4921-6977; Fax: + 61-2-4921-6308; E-mail: [Brett.Nixon@newcastle.edu.au](mailto:Brett.Nixon@newcastle.edu.au)

<sup>†</sup>**Grant Support:** This project was supported by a National Health and Medical Research Council of Australia Project Grant (APP1103176) to Brett Nixon and Eileen A. McLaughlin.

Received 4 October 2016; Revised 2 November 2016; Accepted 7 November 2016

## Abstract

The mammalian epididymis is an exceptionally long ductal system tasked with the provision of one of the most complex intraluminal fluids found in any exocrine gland. This specialized milieu is continuously modified by the combined secretory and absorptive of the surrounding epithelium and thus finely tuned for its essential roles in promoting sperm maturation and storage. While considerable effort has been focused on defining the composition of the epididymal fluid, relatively less is known about the intracellular trafficking machinery that regulates this luminal environment. Here, we characterize the ontogeny of expression of a master regulator of this machinery, the dynamin family of mechanoenzymes. Our data show that canonical dynamin isoforms were abundantly expressed in the juvenile mouse epididymis. However, in peripubertal and adult animals dynamin takes on a heterogeneous pattern of expression such that the different isoforms displayed both cell- and segment-specific localization. Thus, dynamin 1 and 3 were predominately localized in the distal epididymal segments (corpus and cauda), where they were found within clear and principal cells, respectively. In contrast, dynamin 2 was expressed throughout the epididymis, but localized to the Golgi apparatus of the principal cells in the proximal (caput) segment and the luminal border of these cells in more distal segments. These dynamin isoforms are therefore ideally positioned to play complementary, nonredundant roles in the regulation of the epididymal milieu. In support of this hypothesis, selective inhibition of dynamin altered the profile of proteins secreted from an immortalized caput epididymal cell line.

## Summary Sentence

The dynamin family of mechanoenzymes is differentially expressed in the mouse epididymal epithelium and selectively regulates protein secretion.

**Key words:** epididymis, sperm maturation, dynamin, epididymal milieu, protein trafficking, exosomes, epididymosomes, apocrine secretion, merocrine secretion.

## Introduction

The mammalian epididymis is of fundamental importance to reproduction owing to its specialized roles in promoting the functional maturation of spermatozoa and their prolonged storage prior to ejaculation [1]. Both functions rely on the production of a complex intraluminal milieu [2] that is continuously modified by the combined secretory and absorptive activity of the epithelium lining this extraordinarily long tubule [3,4]. This pseudostratified epithelium comprises multiple cell types, each of which possesses discrete roles and unique patterns of distribution.

Principal cells dominate along the entire length of epididymis, constituting as much as 80% of the peritubular interstitium [5]. Despite some segment–segment variation in the structural and functional properties of these cells, a defining feature is their highly developed secretory and endocytotic machinery [5]. Such machinery encompasses key elements of the endocytic apparatus including abundant coated pits, endosomes, and lysosomes. Similarly, these cells are also decorated with extensive networks of rough endoplasmic reticulum, Golgi apparatus, small vesicular aggregates, and blebs of cytoplasm originating from their apical cell surface [6–8]. The presence of such elaborate trafficking machinery accords with an active role in the synthesis of proteins and their subsequent secretion into the lumen, particularly in the proximal epididymal segments (caput and corpus) where sperm acquire their potential for fertilization [9,10]. Throughout the epididymis, these cells also display endocytotic activity, thus facilitating the recycling of proteins and other luminal contents and contributing to an optimal environment for protracted periods of sperm maturation and storage [6–8]. Such endocytotic activity is also shared with clear cells, the second most abundant cell type in the epididymis [11,12]. Accordingly, clear cells also feature numerous coated pits, vesicles, endosomes, multivesicular bodies, and lysosomes [7,11]. While comparatively less is known of the function of the remaining subsets of basal, narrow, apical, halo, and immunological (macrophage and dendritic) cell types, it is widely recognized that the careful integration of their activities is essential to maintain the fidelity of post-testicular sperm development, protection, and storage [3,13].

It follows that an understanding of the mechanisms that underpin the creation of the epididymal luminal milieu is of key interest for fertility regulation both in the context of resolving the causes of male factor infertility [14] and as a target for contraceptive intervention [15]. Despite this, our knowledge of the precise molecular machinery and, in particular, the vesicle trafficking and fusogenic proteins that underpin the dynamic secretory and endocytotic activity of these cells is incomplete. In recent studies, we have begun to characterize novel roles for the dynamin family of large GTPases in the context of mammalian reproduction [16,17]. Here, we have sought to extend this work by examining the spatial and temporal expression of dynamin within the mouse epididymis. Our interest in dynamin reflects the central role the mechanochemical enzyme holds in the coupling of exo- and endocytotic processes [18–21]. While dynamin has been best studied in the context of clathrin-coated endocytosis from the plasma membrane [22], it is also implicated in formation and budding of transport vesicles from the Golgi network [23–26], vesicle trafficking [27], orchestrating exocytotic events [28,29], and in the regulation of microtubular, and actin cytoskeletal dynamics [29–33]. Such diverse functions rely on the ability of dynamin to spontaneously polymerize into high-order oligomers in the presence of a variety of tubular templates such as lipid membranes [34], microtubules [35,36], and actin bundles [37,38]. In the case of membrane remodeling and scission, this polymerization leads to the formation

of rings and/or helices [20]. In one of the most widely accepted models of action, guanosine triphosphate (GTP) hydrolysis drives conformational change and constriction of the dynamin helix, thus leading to membrane fission and physical separation of nascent vesicles from the parent membrane [18]. It has also recently been shown that dynamin has the potential to fine-tune exocytotic events by virtue of its ability to control the rate of fusion-pore expansion, and thus the amount of cargo released from an exocytotic vesicle [28,39].

In mammals, dynamin is encoded by three different genes (*Dnm1*, *Dnm2*, and *Dnm3*) whose products undergo alternative splicing to generate a several variants [21,40]. These isoforms are characterized by differential expression within distinct tissues of the body. Thus, dynamin 1 is primarily found within neural tissue [41], dynamin 2 is ubiquitously expressed throughout the body [42], and dynamin 3 (the most structurally divergent of the canonical isoforms) resides mainly within lung, brain, heart, and testis tissue [40]. It has also been shown that dynamin 1 and dynamin 2 localize to developing germ cells (spermatocytes and spermatids) as well as nurse Sertoli cells of the murine testes [43–46], leading to speculation of a novel role for the GTPase in the production of spermatozoa during the process of spermatogenesis. The role of dynamin 3 within this tissue appears to center on its participation in the formation of a tubulobulbar structure responsible for the release of spermatozoa from Sertoli cells [47]. Dynamin 1 and 2, but not dynamin 3, have also been implicated in the post-testicular functional maturation of spermatozoa [16,17,48]; yet, to the best of our knowledge there are no reports of any of these dynamin isoforms in the context of the mammalian epididymis. This study was therefore undertaken to characterize the epididymal expression of the canonical dynamin family and investigate their contribution to the function of this important endocrine system.

## Materials and methods

### Animals

All experimental procedures involving animals were conducted with the approval of the University of Newcastle's Animal Care and Ethics Committee in accordance with the Society for the Study of Reproduction's specific guidelines and standards. Mice were obtained from a breeding colony held at the institute's Central Animal House and raised under a controlled-lighting regime (16-h light:8-h dark) at 21–22°C and supplied with food and water ad libitum. Prior to dissection, animals were sacrificed by CO<sub>2</sub> inhalation.

### Antibodies and reagents

Unless otherwise stated, chemicals were purchased from Sigma-Aldrich (St. Louis, MO, USA) and were of molecular biology or research grade. A summary of the antibodies used in this study as well as the final antibody concentrations employed for each application is supplied in Supplemental Table S1. Briefly, rabbit polyclonal antibody against dynamin 1 (ab108458) and PSMD7 (ab11436) were purchased from Abcam (Cambridge, England, UK); rabbit polyclonal antibody against CCT3 (sc-33145), rat monoclonal antibody against CCT8 (sc-13891), goat polyclonal dynamin 2 (sc-6400) and its immunizing peptide (sc-6400 P), IZUMO1 (sc-79543), and ATP6V1B1 (sc-21206) were from Santa Cruz Biotechnology (Santa Cruz, CA, USA); mouse monoclonal antibody against dynamin 1 (MA5-15285), sheep polyclonal antibody against dynamin pSer778 (PA1-4621), and rabbit polyclonal antibody against dynamin 2 (PA5-19800) were purchased from Thermo Fisher

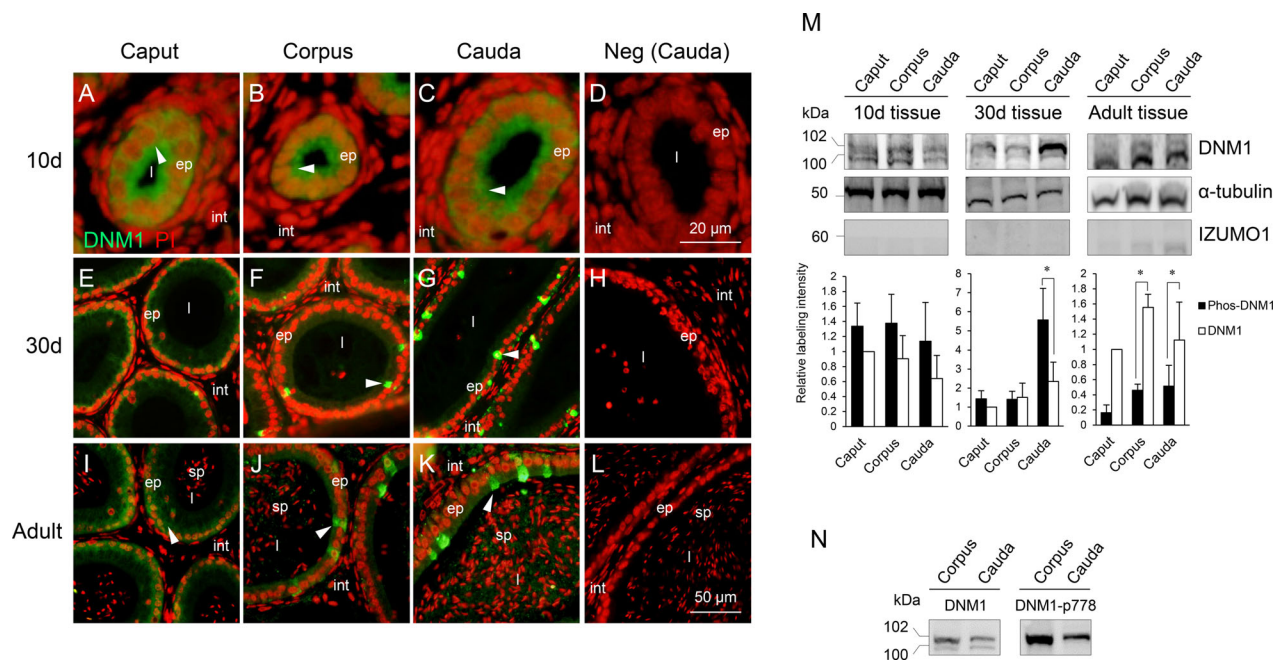


**Figure 1.** Detection of dynamin 1 in the mouse epididymis. (A–L) The spatial and temporal localization of dynamin 1 (arrowheads) was examined in the mouse epididymis at key developmental stages (day 10, 30, and >8 weeks postnatum) by sequential labeling with antidynamin 1 (DNM1, green) and the propidium iodide (PI, red) nuclear stain. Representative negative control (Neg, secondary antibody only) images are included to demonstrate the specificity of antibody labeling (D, H, L). ep, epithelial cells; sp, sperm; int, interstitium; l, lumen. (M) The relative levels of dynamin 1 expression were quantified by immunoblotting of tissue homogenates prepared from epididymides at equivalent developmental time points. Blots were subsequently stripped and reprobed with anti- $\alpha$ -tubulin antibody to confirm equivalent protein loading and enable densitometric analysis of band intensity ( $n = 3$ ;  $p < 0.05$ ). For the purpose of this analysis the labeling intensity of DNM1, or phosphorylated-DNM1 (Phos-DNM1), was normalized relative to that of  $\alpha$ -tubulin with the band intensity in caput tissue at each time point being nominally set to a value of 1. Prior to protein extraction, tissue was cleared of contaminating epididymal fluid and spermatozoa, and the efficacy of this treatment was assessed by labeling with anti-IZUMO1 antibodies (an intrinsic sperm protein that is not expressed in epididymal epithelium). (N) The detection of a doublet (of ~100 and 102 kDa) with antidynamin 1 antibodies prompted an investigation of the potential for post-translational phosphorylation of the dynamin 1 protein. For this purpose, blots were probed with antidynamin 1 pSer778 antibodies, revealing cross-reactivity with the higher molecular weight band only. These experiments were replicated on material from three animals and representative immunofluorescence images, and immunoblots are presented.

Scientific (Waltham, MA, USA); rabbit polyclonal antibody against dynamin 3 (14737-1-AP) and its immunizing peptide (ag6381) were from Proteintech Group (Chicago, IL, USA). Rabbit polyclonal antibody against flotillin 1 (F1180), rabbit polyclonal antibody against androgen receptor (SAB4501575), and mouse monoclonal antibody against  $\alpha$  tubulin (T5168) were from Sigma-Aldrich. Rabbit monoclonal antibody against Golgin-97 (#13192) was from Cell Signaling Technology (Arundel, QLD, Australia). Alexa Fluor 488-conjugated goat antirabbit, Alexa Fluor 594 or 488-conjugated donkey antigoat, and Alexa Fluor 594-conjugated goat antimouse were from Thermo Fisher Scientific. Antirabbit IgG-HRP was supplied by Millipore (Chicago, IL, USA), antisheep IgG-HRP was supplied by Abcam, and antirabbit IgG-HRP was supplied by Santa Cruz Biotechnology. Cell culture reagents (Dulbecco's Modified Eagle's Medium (DMEM), L-glutamine, penicillin/streptomycin, sodium pyruvate, Trypsin-ethylenediaminetetraacetic acid (EDTA)) were from Thermo Fisher Scientific; fetal bovine serum (FBS) was from Bovogen (Keilor, VIC, Australia). Nitrocellulose was supplied by GE Healthcare (Buckinghamshire, England, UK); minicomplete protease inhibitor cocktail tablets were obtained from Roche (Sandhoferstrasse, Mannheim, Germany). Bovine serum albumin (BSA) was purchased from Research Organics (Cleveland, OH, USA). Mowiol 4-88 was from Millipore; paraformaldehyde (PFA) was obtained from ProSciTech (Thuringowa, QLD, Australia). Dynamin inhibitors, Dynasore, and Dyngo 4a were purchased from Tocris Bioscience (Bristol, England, UK) and Abcam, respectively.

### Immunofluorescent localization

Mouse epididymides were fixed in fresh Bouin's solution, embedded in paraffin and sectioned at 5- $\mu$ m thickness. Embedded tissue was dewaxed, rehydrated, and then subjected to antigen retrieval under optimized conditions: microwaving in 10 mM sodium citrate at 1,100 W for either 6 min (antidynamin 1, ab108458) or 9 min (antidynamin 2); microwaving in 50 mM Tris (pH 10.5) for 9 min [antidynamin 1 (MA5-15285); antidynamin 3; antiATP6V1B1; anti-Golgin-97]. After being blocked with 3% BSA/phosphate-buffered saline (PBS) in a humid chamber (1 h at 37°C), the slides were then incubated with primary antibodies diluted in 1% BSA/PBS (4°C, overnight). After three washes in PBS, slides were incubated with Alexa Fluor 555 and/or Alexa Fluor 488-conjugated secondary antibodies diluted in 1% BSA/PBS (37°C, 1 h; Supplemental Table S1). The sections were then washed and counterstained with nuclear dyes; propidium iodide (5  $\mu$ g/ml) or 4', 6-diamidino-2-phenylindole (2  $\mu$ g/ml). After an additional wash in PBS, slides were mounted in 10% Mowiol 4-88 (Merck Millipore, Darmstadt, Germany) with 30% glycerol in 0.2 M Tris (pH 8.5) and 2.5% 1, 4-diazabicyclo-(2.2.2)-octane, and labeling patterns for all tissue sections recorded using fluorescence microscopy (Zeiss Axio Imager A1, Jena, Thuringia, Germany; Figures 1–5). The wavelengths of the microscopic filters used for excitation and emission were 474 and ~527 nm (Alexa Fluor 488 and propidium iodide), and 585 and ~615 nm (Alexa Fluor 594). Alternatively, confocal microscopy (Olympus IX81, Sydney, Australia) was used for

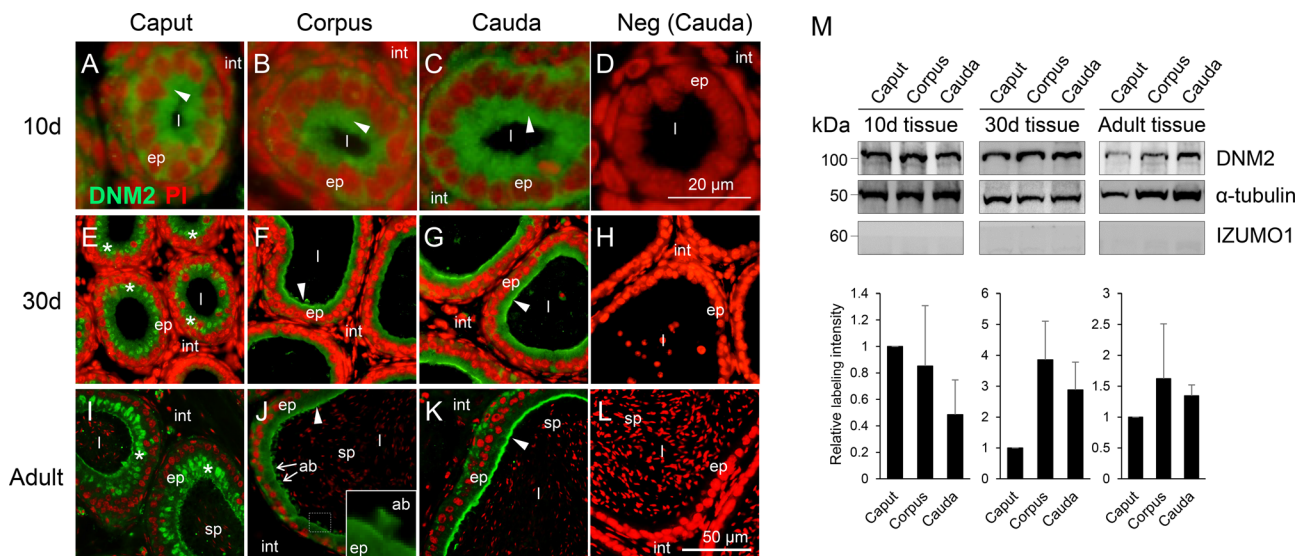


**Figure 2.** Detection of dynamin 2 in the mouse epididymis. (A–L) Immunofluorescence localization of dynamin 2 (arrowheads) was undertaken in the mouse epididymis (day 10, 30, and >8 weeks postnatum) by sequential labeling with antidynamin 2 (DNM2, green) and propidium iodide (PI, red). By 30 days postnatum, dynamin 2 localization was detected in the supranuclear region of caput epithelial cells (asterisks) and around the adluminal border and extending into apical blebs (ab) (arrows and inset in adult corpus) in the corpus and cauda epididymal segments. Representative negative control (Neg, secondary antibody only) images are included to demonstrate the specificity of antibody labeling (D, H, L). ep, epithelial cells; sp, sperm; int, interstitium; l, lumen. (M) The relative levels of dynamin 2 expression were quantified by immunoblotting of tissue homogenates prepared from epididymides at equivalent developmental time points. Blots were subsequently stripped and re probed with anti- $\alpha$ -tubulin antibody to confirm equivalent protein loading and enable densitometric analysis of band intensity ( $n = 3$ ). For the purpose of this analysis, the labeling intensity of DNM2 was normalized relative to that of  $\alpha$ -tubulin with the band intensity in caput tissue at each time point being nominally set to a value of 1. Immunoblots were also probed with anti-IZUMO1 antibodies to control for sperm contamination. These experiments were replicated on material from three animals and representative immunofluorescence images and immunoblots are presented.

detection of fluorescent-labeling patterns observed in mEcap18 cells (Figures 6 and 8) using excitation and emission filters of wavelength 473 and 485–545 nm (Alexa Fluor 488), and 559 and 570–670 nm (propidium iodide).

For immunofluorescent staining of mouse caput epididymal (mEcap18) cell cultures [49], the cells were settled onto poly-L-lysine-coated coverslips. They were then fixed in 4% PFA for 15 min and permeabilized by incubation in 0.1% Triton X-100 for 10 min. Following washing in PBS, cells were blocked with 3% BSA in PBS and immunolabeled as described for epididymal tissue sections.

All immunolocalization studies were replicated a minimum of three times, with epididymal tissue sections being prepared from more than three different male mice or mEcap18 cells being isolated from three separate cell cultures. The negative controls used in each of these experiments included tissues or cells that were prepared under the same conditions except that the primary antibody was substituted with antibody buffer (i.e., secondary antibody only controls). Where the immunizing peptide was available (i.e., for anti-DNM2 and anti-DNM3 antibodies), an additional control was included in which the antidynamin antibodies were pre-absorbed with excess immunizing peptide prior to use.

#### mEcap18 cell culture and dynamin inhibition assays

The SV40-immortalized mouse caput epididymal epithelial (mEcap18) cells were a generous gift from Dr Petra Sipila (Turku University, Turku, Finland) [49]. Aliquots of  $4 \times 10^5$  cells were passaged in each well of six well plates and cultured with mEcap18 medium (DMEM supplemented with 1% L-glutamine, 1% sodium pyruvate, 1% penicillin/streptomycin, and 50  $\mu$ M 5 $\alpha$ -androstano-17 $\beta$ -ol-3-oneC-IIIN) containing 10% FBS for 24 h. Cells were then washed three times with DMEM to remove FBS and thus the potential of this protein to bind dynamin inhibitors [50,51].

Thereafter, equal volumes of mEcap18 medium (FBS free) containing Dynasore, Dyngo 4a, Dyngo- $\Theta$  (an inactive isoform control for both Dynasore and Dyngo 4a), or a dimethyl sulfoxide (DMSO) vehicle control were added to each well for further incubation. The working concentration of each inhibitor (10  $\mu$ M for Dyngo 4a and 100  $\mu$ M for Dynasore) was selected on the basis of effective doses in previous work [52]. After 12 h of incubation, media were carefully aspirated from each of the different treatment groups and centrifuged under  $2,000 \times g$  for 10 min to remove all the cellular debris. Proteins released into the media during the incubation were then concentrated via precipitation with one-fifth volume of chilled 100% trichloroacetic acid (4°C, overnight). The precipitated protein was pelleted by centrifugation ( $17,000 \times g$ , 4°C, 10 min) and washed twice with chilled acetone prior to being recentrifuged under identical conditions. The resultant pellet was air-dried before being resuspended in SDS extraction buffer (0.375 M Tris pH 6.8, 2% w/v SDS, 10% w/v sucrose, protease inhibitor cocktail). To ensure that proteins were not simply released from dead or moribund cells, cell vitality was assessed via a trypan blue exclusion assay prior to, during, and after incubation with dynamin inhibitors. Importantly, none of the treatments used in this study compromised mEcap18 cell viability, which consistently remained >90% across the 12 h of incubation.

#### Sodium dodecyl sulfate-polyacrylamide gel electrophoresis (SDS-PAGE), silver staining, and immunoblotting

Epididymal dissection and fluids removal were conducted as previously described [53]. Following treatment, epididymal proteins were separately extracted from the caput, corpus, and caudal segments via boiling in SDS extraction buffer at 100°C for 5 min. Insoluble material was pelleted by centrifugation ( $17,000 \times g$ , 10 min,

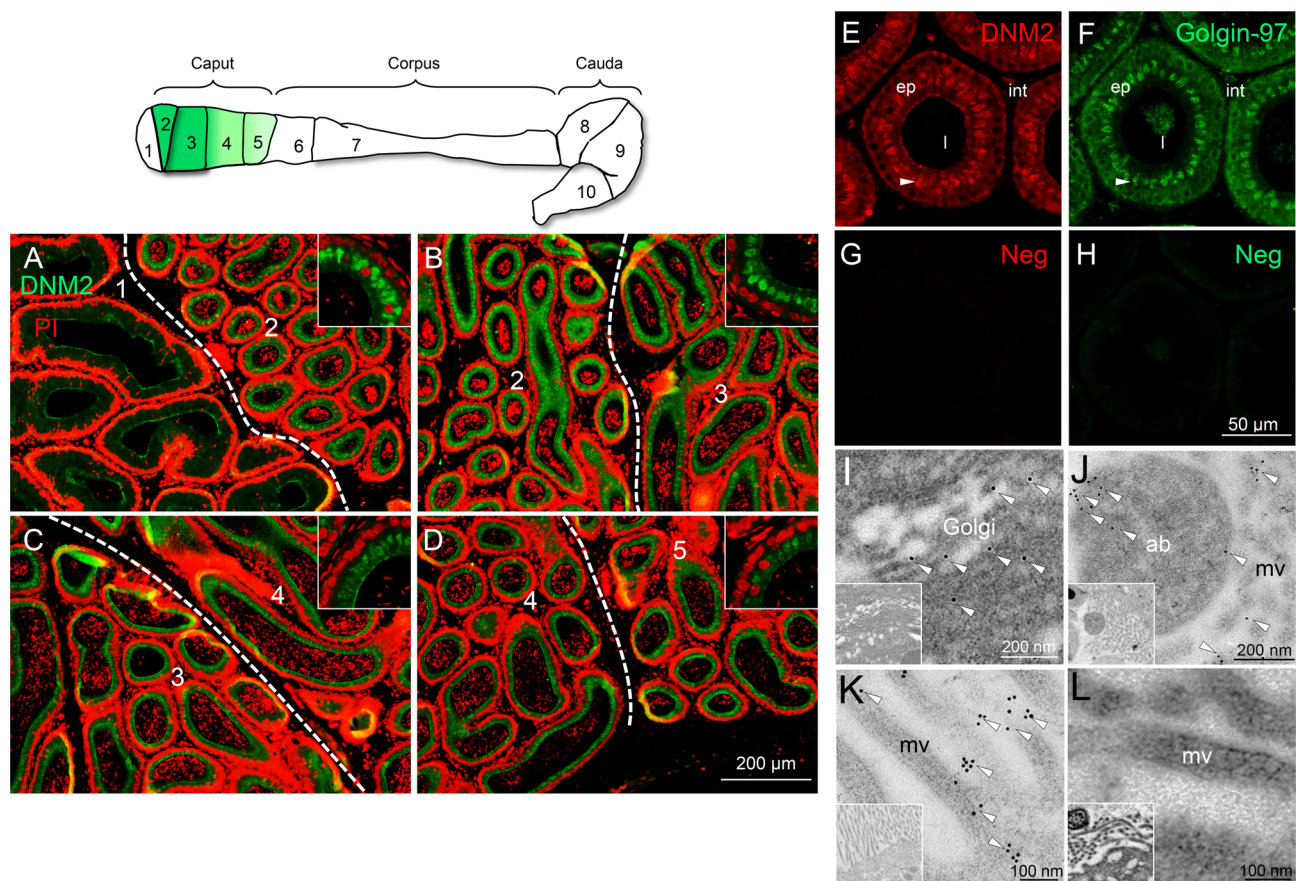


**Figure 3.** Dynamín 2 localizes to the Golgi apparatus of principal cells in the caput epithelium. (A–D) The spatial conservation of dynamín 2 supranuclear localization was assessed throughout zones 1–5 (corresponding to the initial segment and caput epididymis, respectively) of the adult mouse epididymis, with the border of different zones being demarcated by dotted lines. This analysis revealed a gradient of supranuclear staining, being initially detected in zone 2 and most intense staining in zones 2 and 3, before gradually decreasing distally in zones 4 and 5, and being undetectable in zone 6 (corpus). (E–H) Confirmation that this pattern of supranuclear localization corresponded to the positioning of the Golgi apparatus (arrowheads) was afforded by labeling of consecutive epididymal sections with anti-DNM2 (E, red) and Golgin-97 (a recognized Golgi marker; F, green). This approach was favored over that of dual labeling owing to incompatible antigen retrieval conditions necessary for optimal labeling with these antibodies. (G, H) NC: negative controls (secondary antibody only). (I, J) These studies were complemented with the use of immunogold ultrastructural analyses to confirm the presence of DNM2 in the Golgi apparatus of the caput (I), and in association with the microvilli (mv) and apical blebs (ab) in both the corpus and cauda epididymis (J, I) (arrowheads). (L) No such labeling was observed in control sections probed with secondary antibody only. v, vesicle; mv, microvilli; ab, apical blebs. These experiments were replicated on material from three animals, and representative immunofluorescence and immunogold images are presented.

4°C), and the soluble proteins present in the supernatant were quantified using a bicinchoninic acid (BCA) protein assay kit (Thermo Scientific). Equivalent amounts of protein were boiled in SDS-PAGE sample buffer (2% v/v mercaptoethanol, 2% w/v SDS, and 10% w/v sucrose in 0.375 M Tris, pH 6.8, with bromophenol blue) at 100°C for 5 min, prior to being resolved by SDS-PAGE and either silver stained or transferred to nitrocellulose membranes. Before detecting proteins of interest, membranes were blocked under optimized conditions of 3% BSA in PBS with 0.5% (v/v) Tween-20 (PBST; dynamín 1), 3% BSA in Tris-buffered saline with 0.1% (v/v) Tween-20 (TBST; IZUMO1, CCT8,  $\alpha$ -tubulin, dynamín 3, and dynamín pSer778), 5% skim milk in 0.1% (v/v) TBST (dynamín 2, FLOT1, and PSMD7), or 5% skim milk in 0.05% PBST (CCT3) for 1 h. Membranes were then incubated with primary antibody prepared in either 1% BSA or 1% skim milk in an equivalent diluent to that used for blocking. Blots were subsequently washed with 0.5% PBST (dynamín 1), 0.1% TBST (dynamín 2, dynamín 3, FLOT1, IZUMO1, CCT8,  $\alpha$ -tubulin, PSMD7, and dynamín pSer778), or 0.05% PBST (CCT3), followed by incubation with appropriate horse radish

peroxidase (HRP)-conjugated secondary antibodies (Supplemental Table S1). After three additional washes, labeled proteins were detected using an enhanced chemiluminescence kit (GE Healthcare). The specificity of dynamín 3 antibody was assessed by preincubating the antibody with excess immunizing peptide at 4°C for 2 h prior to immunoblotting. For quantification of dynamín expression, appropriate bands were assessed by densitometry, normalized against an  $\alpha$ -tubulin loading control, and nominally expressed relative to the amount of the protein appearing in the caput epididymal tissue within the same developmental time point (Figures 1M, 2M, and 4M). Alternatively, dynamín expression was also quantified based on normalization against the  $\alpha$ -tubulin loading control across all epididymal segments and developmental time points examined (Supplemental Figure S2).

### Electron microscopy

Samples were fixed and processed for electron microscopy as previously described [54]. Briefly, epididymal tissue and mEcap18 cells were fixed in 4% (w/v) PFA containing 0.5% (v/v) glutaraldehyde.

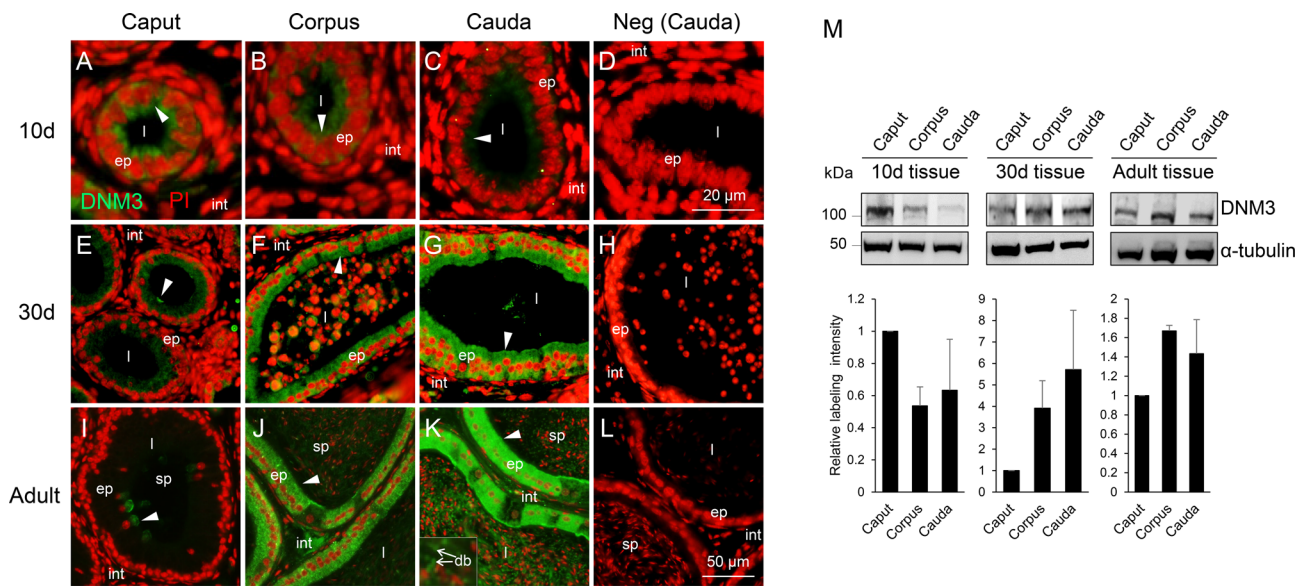


**Figure 4.** Detection of dynamin 3 in the mouse epididymis. (A–L) Immunofluorescence localization of dynamin 3 was undertaken in the mouse epididymis (day 10, 30, and >8 weeks postnatum) by sequential labeling with antidynamin 3 (DNM3, green) and propidium iodide (PI, red). Representative negative control (Neg, secondary antibody only) images are also shown to demonstrate the specificity of antibody labeling. (M) The relative levels of dynamin 3 expression were quantified by immunoblotting of tissue homogenates prepared from epididymides at equivalent developmental time points. Blots were subsequently stripped and reprobbed with anti- $\alpha$ -tubulin antibody to confirm equivalent protein loading and enable densitometric analysis of band intensity ( $n = 3$ ). For the purpose of this analysis the labeling intensity of DNM3 was normalized relative to that of  $\alpha$ -tubulin, with the band intensity in caput tissue at each time point being nominally set to a value of 1. These experiments were replicated on material from three animals, and representative immunofluorescence images and immunoblots are presented.

Epididymal tissue and mEcap18 cell [embedded in 2% (w/v) agarose] were processed via dehydration, infiltration, and embedding in LR (London Resin) White resin. Sections (80 nm) were cut with a diamond knife (Diatome Ltd., Bienne, Switzerland) on an EM UC6 ultramicrotome (Leica Microsystems, Vienna, Austria) and placed on 200-mesh nickel grids. Sections were blocked in 3% (w/v) BSA in PBS (30 min). Subsequent washes were performed in PBS (pH 7.4) containing 1% BSA. Sections were sequentially incubated with primary antibodies (overnight at 4°C), and an appropriate secondary antibody conjugated to 10-nm gold particles (90 min at 37°C). Labeled sections were then counterstained in 2% (w/v) uranyl acetate. Micrographs were taken on a Philips CM12 transmission electron microscope at 120 kV.

### Statistics

All experiments were replicated a minimum of three times, with tissue samples obtained from more than three different male mice. Graphical data are presented as mean values  $\pm$  SEM, which were calculated from the variance between samples. Statistical significance was determined analysis of variance.

## RESULTS

### Localization and ontogeny of dynamin expression in the mouse epididymis

#### Dynamin 1

Low-magnification fluorescence micrographs illustrating the overall expression patterns of dynamin 1 in the initial segment and epididymis are presented in Supplemental Figure S1 and Figure 1A–L, respectively. In the prepubertal epididymis (postnatal 10 days), positive dynamin 1 labeling was detected uniformly throughout the ep-

ithelium of all epididymal segments. In marked contrast, by peripubertal development (30 days) and extending into adulthood (>8 weeks), only weak diffuse dynamin 1 labeling was observed in the cytosol of cells in the initial segment (Supplemental Figure S1D and G) and caput epididymis (Figure 1E and I). Upon transitioning into the distal epididymal regions of the corpus and cauda, the pattern of dynamin 1 expression was abruptly replaced by one in which a majority of cells were completely devoid of the enzyme. Notably, however, dynamin 1 was intensely labeled in a small number of discrete, randomly distributed cells in both the corpus and cauda epididymal segments. The labeling of these large cells generally extended from the apical to the basal surfaces of the tubule, consistent with the distribution pattern expected of clear cells, a possibility that was directly assessed in subsequent experiments. The specificity of antibody labeling was confirmed by the complete absence of labeling in equivalent tissue sections probed with secondary antibody alone (Figure 1D, H, and L).

Immunoblotting of epididymal tissue homogenates confirmed the expression of dynamin 1 in all segments and at all developmental time points examined (Figure 1M). Of note was the labeling of two discrete protein bands of approximate molecular weight  $\sim$ 100 and  $\sim$ 102 kDa in a majority of the tissue samples. The lower of these bands corresponds to the known molecular weight (100 kDa) of dynamin 1, raising the possibility that higher band may reflect the presence of a post-translationally modified form of the parent protein. Such a scenario was assessed through the labeling of tissue homogenates with phospho-specific antibodies that detect dynamin 1 serine 778 phosphorylation. These antibodies consistently labeled the higher molecular weight band only (Figure 1N), a finding that is of potential significance in view of the ability of phosphorylation to modulate dynamin 1 activity [55,56]. In this context, the higher molecular weight (phosphorylated) form of dynamin 1 predominated

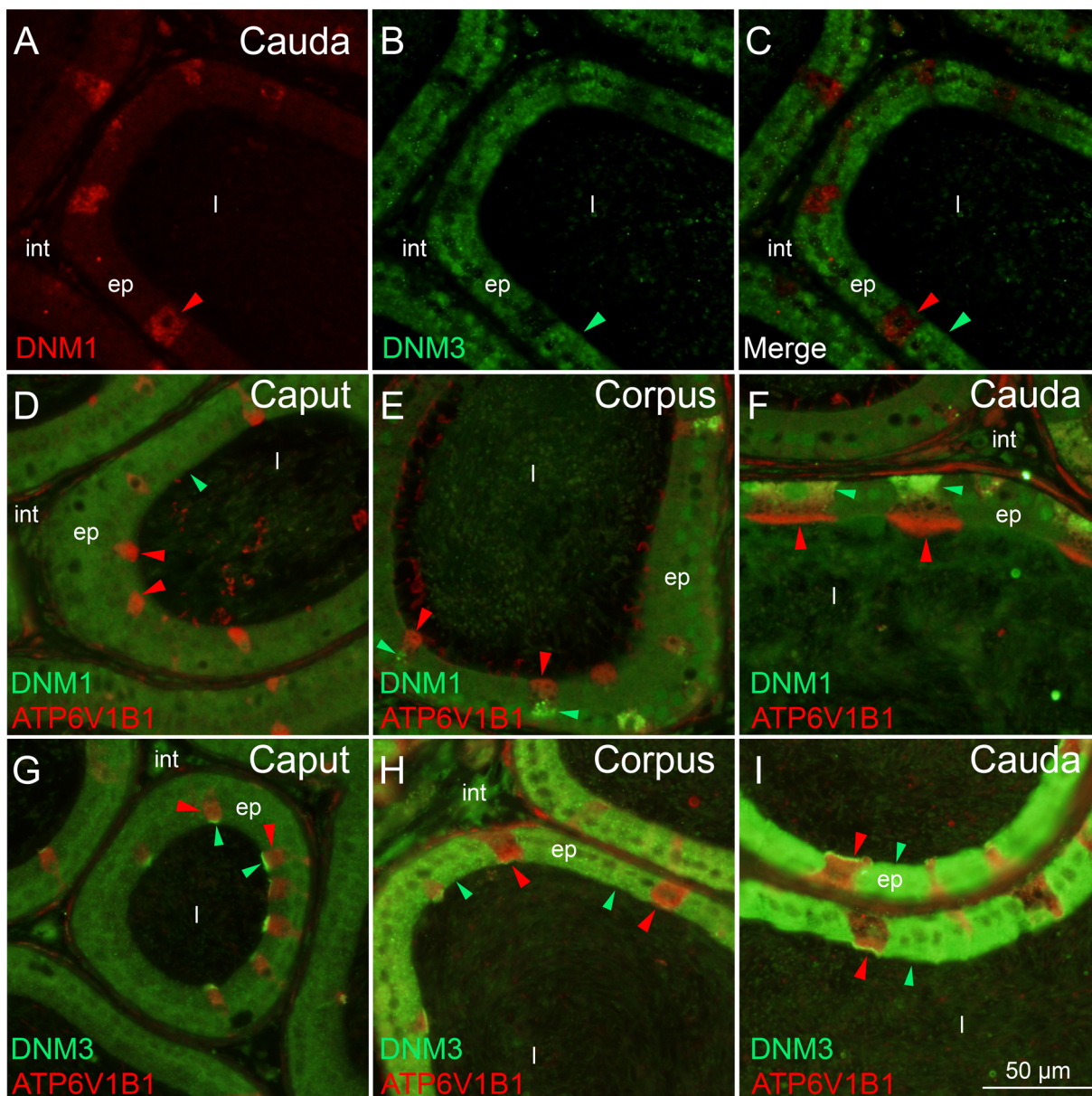


**Figure 5.** Colocalization of dynamin 1 and dynamin 3 with the clear cell marker, ATP6V1B1. (A–C) Representative immunofluorescence images of dual staining of dynamin 1 (red arrowhead) and dynamin 3 (green arrowhead) in the cauda epididymis of adult mice. Dynamin 1 and 3 clearly resided in different epithelial cell populations with no colocalization being detected. (D–F) Representative immunofluorescence images of dual staining of dynamin 1 (green arrowheads) and ATP6V1B1 (red arrowheads) in the adult mouse epididymis. Dynamin 1 colocalized with ATP6V1B1 in the clear cells of the corpus and cauda but not caput epididymis. (G–I) Representative immunofluorescence images of dual staining of dynamin 3 (green arrowheads) and ATP6V1B1 (red arrowheads) in the adult mouse epididymis. Dynamin 3 colocalized with ATP6V1B1 in the clear cells of the caput epithelium, but displayed minimal overlap in the cells and instead occupied a distinct subcellular location. This localization pattern was altered in the corpus and cauda epithelium such that dynamin 3 was uniquely detected in the principal cells in these segments. ep, epithelial cells; int, interstitium; l, lumen.

in the epididymides of 10- and 30-day-old animals; yet, the lower molecular weight unmodified protein was intensely stained in the epididymis of adult animals. The highest expression of phosphorylated dynamin 1 was recorded in the cauda epididymides of 30-day-old animals (Supplemental Figure S2). Since dynamin 1 and dynamin 2 are known to reside in mouse spermatozoa, all immunoblots were reprobed with antibodies against IZUMO1 (a protein expressed in spermatozoa but not epididymal tissue) to control for the possibility of sperm contamination. As anticipated, no IZUMO1 was detected in any of our preparations of epididymal tissue (Figures 1M and 2Q).

### Dynamin 2

Similar to the expression profile of dynamin 1, the second isoform of the dynamin family was also readily detected throughout the epithelium of the entire epididymis of prepubertal animals (Supplemental Figure S1B; Figure 2A–L). However, in peripubertal and adult animals, dynamin 2 was predominantly localized to the supranuclear region of caput epithelial cells, where it appeared to be concentrated within dense aggregates most likely corresponding to the Golgi apparatus (Figure 2E and I, asterisks). In the corpus, and particularly the cauda, epididymides of these animals, the majority of staining was

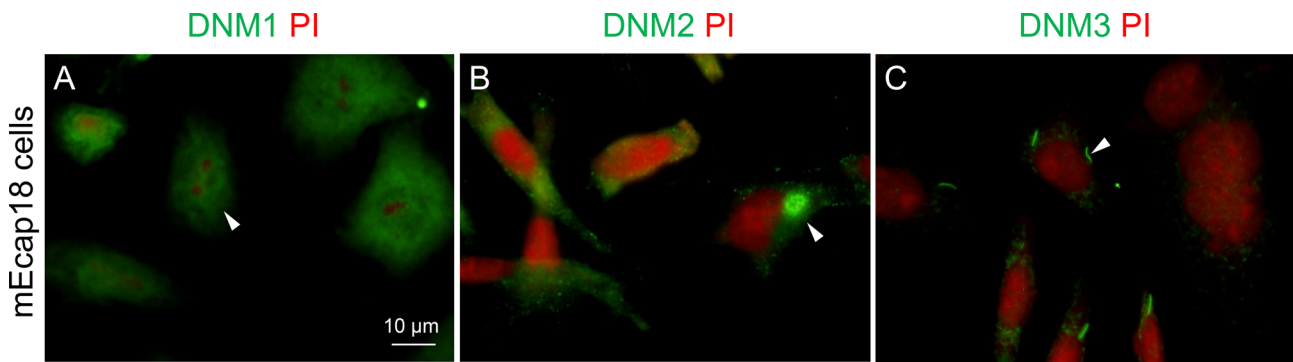


**Figure 6.** Mouse mEcap 18 cells and epididymal epithelial tissue possess conserved patterns of dynamin expression. (A–C) Immunofluorescence localization was conducted for each dynamin isoform (1–3) in fixed mEcap 18 cells (A: dynamin 1; B: dynamin 2; C: dynamin 3). (A) Staining for dynamin 1 (DNM1) was localized throughout the cytosol. (B) Dynamin 2 (DNM2) localized to the supranuclear domain in the majority of the cells. (C) Dynamin 3 (DNM3) localized exclusively to a portion of the plasma membrane in ~11% of the cell population. For A–C, nuclei are labeled with PI (red). Arrowheads indicate representative labeling patterns observed across three independent experiments.

detected in the immediate vicinity of luminal border (Figure 2F, G, J, and K) and extending into apical blebs that appear to decorate these cells (Figure 2J, see inset in lower panel). Presumably due to issues associated with antigen retrieval [16], luminal spermatozoa were not routinely labeled with dynamin 2 in the adult epididymal sections. Immunoblotting confirmed the abundant epididymal expression of dynamin 2 and revealed that the greatest increase in dynamin 2 expression along the epididymis was detected in the caudal segment of 30-day-old animals (Supplemental Figure S2). In the prepubertal and adult stage, the enzyme was expressed at similar overall levels in each epididymal segment examined (Figure 2M; Supplemental Figure S2).

The localization we recorded for dynamin 2, particularly within the caput segment of the adult epididymis, ideally positions the enzyme to contribute to the trafficking of secretory proteins to the luminal environment [57]. We therefore sought to assess the spatial expression profile and the subcellular localization of dynamin 2 within this segment in greater detail. This analysis revealed that in the initial segment (zone 1) [55], dynamin 2 was exclusively restricted to the apical membrane (Figure 3A; Supplemental Figure S1). Notably, supranuclear labeling was first detected immediately distal to the septa delineating the initial segment from that of the caput epididymis (Figure 3A–D; zones 2–5), and appeared most intense within zones 2 and 3 before gradually declining to be virtually undetectable in this subcellular domain by zone 6 (corpus epididymis). Confirmation that this pattern of supranuclear localization corresponded to the positioning of the Golgi apparatus was afforded by labeling of consecutive epididymal sections with anti-DNM2 (Figure 3E, red) and Golgin-97 (a recognized Golgi marker; Figure 3F, green). This approach was favored over that of dual labeling owing to incompatible antigen retrieval conditions necessary for optimal labeling with these antibodies. Importantly, no such staining was recorded in negative control sections (secondary antibody only; Figure 3G and H). Similarly, pre-absorption of the antidynamin 2 antibody with excess immunizing peptide also effectively eliminated all immunolabeling of epididymal tissue sections (Supplemental Figure S3).

Consistent with the localization of dynamin 2 detected by immunofluorescence, ultrastructural analyses confirmed the presence of immunogold-labeled dynamin 2 within the cisternae of the Golgi apparatus in the caput epididymis (Figure 3I, arrowheads). In the more distal segments of the corpus and cauda epididymis, immunogold-labeled dynamin 2 was not detected within the Golgi apparatus

(data not shown), being instead localized to the microvilli and apical blebs extending from the luminal margin of principal cells (Figure 3J and K). Gold-labeled dynamin 2 was also routinely found in the acrosomal region of sperm residing in the epididymal lumen (data not shown). The specificity of immunogold labeling was confirmed through the use of sections stained with secondary antibody alone, none of which revealed any staining (Figure 3L).

### Dynamin 3

Unlike dynamin isoforms 1 and 2, only relatively weak dynamin 3 staining was observed in the cytosol of the prepubertal epididymis epithelial cells (Figure 4A–C; Supplemental Figure S1). This labeling pattern subsequently underwent substantial changes in the epididymis of peripubertal and adult animals. Thus, dynamin 3 was localized to the apical domain/luminal margin of a small number of epithelial cells that were randomly dispersed through the tubules of the caput epididymis (Figure 4E and I). Upon entry into more distal epididymal segments, dynamin 3 gradually took on a unique expression profile in which virtually all corpus and cauda epididymal epithelial cells, save those likely to be clear cells, were uniformly stained throughout their cytosol (Figure 4F, G, J, and K). Interestingly, dynamin 3 was also labeled in granule-like luminal structures previously referred to as “epididymal dense bodies” [58] that lie juxtaposed with spermatozoa in the corpus and cauda epididymis (Figure 4K, inset). Few such structures were labeled for dynamin 3 in the epididymis of peripubertal animals, and similarly, no such labeling was observed in the lumen of the caput epididymis at any developmental time point. Since our previous work has shown that mature mouse sperm does not harbor the dynamin 3 isoform [59], it is unlikely that it features among the proteins that are putatively transferred between dense bodies and the maturing spermatozoa [58,60,61]. Importantly, no staining was recorded in negative control sections (secondary antibody only; Figure 4D, H, and L). Similarly, pre-absorption of the antidynamin 3 antibody with excess immunizing peptide also effectively eliminated all immunolabeling of epididymal tissue sections (Supplemental Figure S3).

Immunoblotting of epididymal tissue homogenates confirmed the expression of dynamin 3 in all segments and at all developmental time points examined (Figure 4M). Similar to the dynamin 1 and dynamin 2 isoforms, increased expression of the dynamin 3 protein was apparent within the epididymides of 30-day-old animals (Supplemental Figure S2). The conserved increase in expression

documented at this particular developmental stage may reflect the epididymis preparing for the arrival of first wave of spermatozoa.

### Colocalization of dynamin 1 and 3 with ATP6V1B1 in clear cells of the adult mouse epididymis

A notable finding from our immunolocalization studies was that the dynamin isoforms examined did not appear to show a high degree of colocalization. This was particularly true of the labeling patterns of dynamins 1 and 3 within the corpus and cauda epididymis of mature animals (Figure 1J and K; Figure 4J and K). To investigate whether dynamin isoforms are indeed expressed in unique cell populations, dual staining of epididymal tissue was conducted with antidynamin 1 and 3 antibodies. This strategy revealed that the distribution of dynamin 1 and 3 perfectly complemented each other with no colocalization apparent in either the corpus (not shown) or cauda epididymis (Figure 5A–C). The most logical explanation for such an expression profile is that dynamin 1 and 3 are exclusively produced in clear and principal cells, respectively. This possibility was examined through colabeling experiments with ATP6V1B1 (ATPase, H<sup>+</sup> transporting, lysosomal 56/58kDa, V1 subunit B1), a clear cell marker that mediates the acidification of the luminal environment [62]. As anticipated, dynamin 1 colocalized with ATP6V1B1 in the clear cells of the corpus and cauda epididymis (Figure 5E and F), but was not detected in this cell population in the caput epididymis (Figure 5D). By contrast, dynamin 3 colocalized with ATP6V1B1 in the clear cells of the caput epididymis (Figure 5G) but failed to overlap with the clear cells in more distal epididymal segments (Figure 5H and I).

### Selective inhibition of dynamin influences epididymal protein secretion in vitro

The existence of unique, nonoverlapping profiles of dynamin expression raises the prospect that this family of enzymes may be of fundamental importance in regulating the specialized functions of the epididymis. We therefore sought to document changes in protein trafficking brought about by selective pharmacological inhibition of dynamin. For this purpose, we elected to use a tractable in vitro assay employing an immortalized mouse caput epididymal (mEcap18) cell line that has previously been characterized in relation to its ability to faithfully report physiological profiles of epididymal gene and protein expression [49]. Prior to use, these cells were assessed for their expression of dynamin 1, 2, and 3 isoforms (Figure 6A–C) as well as androgen receptor and ATP6V1B1 (Supplemental Figure S4). Consistent with our labeling of caput epididymal tissue sections (Figures 11 and 21), dynamin 1 was localized throughout the cytosol (Figure 6A), and dynamin 2 was found within the supranuclear domain of a majority of mEcap18 cells (Figure 6B). Dynamin 3, by contrast, exhibited discrete foci of membrane staining in a small number of these cells (Figure 6C), the proportion of which compared favorably to those expressing ATP6V1B1 (Supplemental Figure S4). On the basis of these conserved expression patterns, the mEcap18 cells were deemed a suitable model to explore dynamin function.

Following incubation of mEcap18 cells in media supplemented with and without the dynamin inhibitors of Dynasore and Dyngo 4a (both of which target dynamin 1 and dynamin 2 with similar efficacy [63,64]), an equivalent volume of culture medium was recovered for assessment via SDS-PAGE. As shown in Figure 7A, mEcap18 cells readily secreted a number of proteins into the medium during the course of a 12-h incubation. However, the secretion of several of these proteins appeared to be reduced by the introduction of dy-

namin inhibitors (Figure 7A). This result was confirmed through the quantification of band intensity, normalized against an internal loading control (green arrowhead) (Figure 7B), which illustrated bands of  $M_r$  ~26, 30, 34, 42, 45, 47, 65, 80, 110, 115, and 250 kDa were all substantially reduced following dynamin inhibition (Figure 7A, white arrowheads; Figure 7B, green trace). In the majority of instances, this inhibitory effect proved selective such that the proteins were detected at similar levels in the medium sampled from either untreated control populations of cells (Figure 7B, orange trace) or those cells treated with Dyngo- $\Theta$  (an inactive analog of Dynasore and Dyngo 4a; Figure 7B, black trace). From these data, we infer that a subset of epididymal proteins may rely on dynamin-mediated pathways for their secretion.

In support of this hypothesis, we investigated the release of two representative 65 kDa proteins and one 47 kDa protein [namely chaperonin containing TCP1, subunit 3 (CCT3); chaperonin containing TCP1, subunit 8 (CCT8); flotillin 1 (FLOT1), respectively] that are secreted in the caput epididymis (Nixon, unpublished). Using a similar strategy to that reported above, dynamin inhibition was shown to effectively reduce the amount of both CCT3 and CCT8 that was detectable in the incubation media following 12 h of mEcap18 cell culture (Figure 8A). Notably, dynamin inhibition was also accompanied by an apparent increase in the amount of both proteins detected within the cytosol of mEcap18 cells compared to that of untreated controls (Figure 8B). In a majority of these cells, the staining of the CCT3 and CCT8 appeared to concentrate in numerous punctate foci. While such localization is consistent with that expected of proteins that had been packaged into secretory vesicles, in the absence of direct evidence the precise nature of the reaction foci remains to be determined. In contrast, no such inhibition was detected for PSMD7, a protein that has previously been detected in the proteome of bovine caput epididymosomes [65]. Importantly, dynamin inhibition did not have a detrimental impact on mEcap18 cell viability, which remained above 90% in all treatments. In the case of Dynasore, we did note a reduction in the number cells before ( $\sim 4 \times 10^5$ ) and after ( $\sim 2.9 \times 10^5$ ) incubation. However, no such reduction was evident in cells treated with Dyngo 4a.

## Discussion

The mammalian epididymis holds an essential role in promoting the functional maturation of spermatozoa, in addition to their prolonged storage in a viable state [3,13]. Both processes are supported by a highly specialized luminal microenvironment that is created, and maintained, by the combined secretory and absorptive activity of the lining epithelium. While elegant ultrastructural studies have defined the key cytological features of this epithelia [6–8], the molecular machinery it employs to regulate the tightly coupled processes of exocytosis and endocytosis remain poorly understood. In this study, we have explored the epididymal expression of dynamin, revealing a number of unique insights into the localization and putative function(s) of this mechanoenzyme. Namely, we show that the three canonical dynamin isoforms possess different spatial and temporal profiles of expression within the mouse epididymis. Thus, in juvenile animals at a time when the epididymis is undergoing considerable elongation and expansion, dynamins 1–3 displayed virtually ubiquitous patterns of localization raising the possibility that they have overlapping roles in regulating the differentiation of the tract. However, with the notable exception of the initial segment, each dynamin partitioned into distinct cell types and/or subcellular compartments prior to entry of the first wave of the spermatozoa,

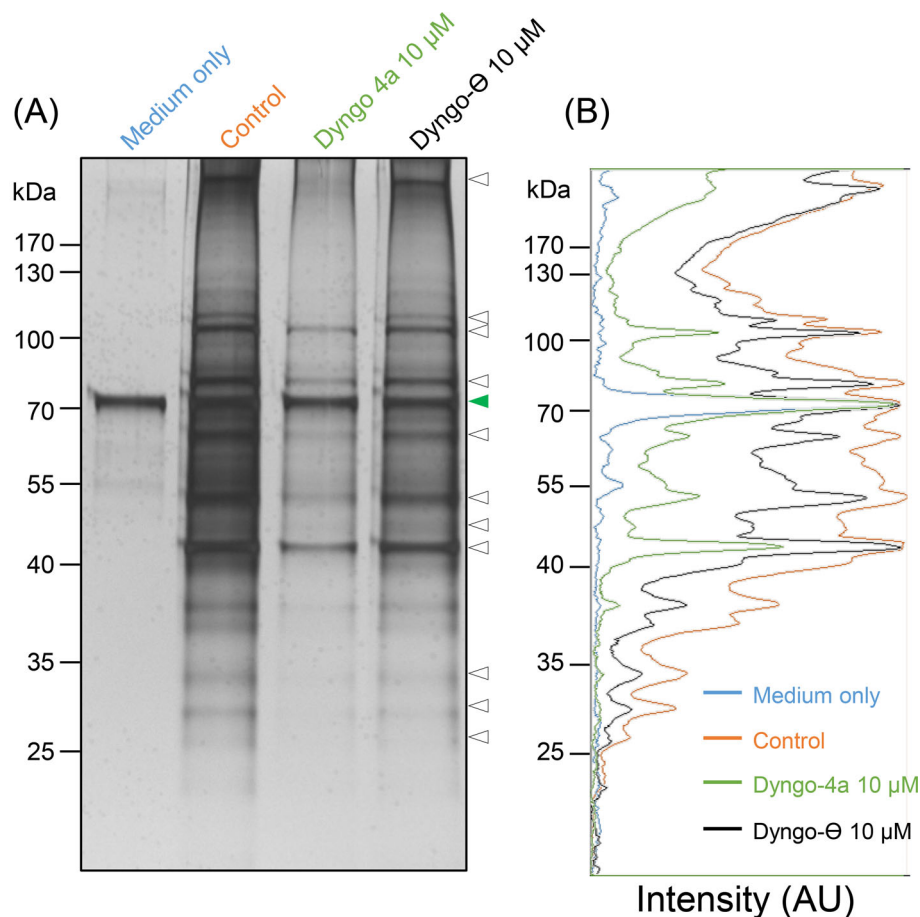


**Figure 7.** Dynamin inhibitors selectively modulate the secretion of proteins by cultured mouse mEcap18 cells. (A) Silver-stained gel illustrating the complement of proteins recovered from an equivalent volume of medium after 12 h of mEcap18 cell culture in the absence (control), or presence of Dyngo 4a ( $10 \mu\text{M}$ ; an inhibitor of dynamin isoforms 1 and 2) or Dyngo- $\Theta$  ( $10 \mu\text{M}$ , inactive isoform of Dyngo 4a). (B) The density of the bands was quantified by Image J and normalized to an internal control band (green arrow head) contributed by the culture medium. Dyngo 4a treatment selectively inhibited the secretion of a subset of protein bands such that they were substantially reduced (denoted by white arrowheads).

thus suggesting that they may possess fundamentally distinct roles in the secretory and absorptive pathways that dominate the functioning of the adult epididymis. This interpretation is consistent with our ability to selectively manipulate protein secretion through pharmacological inhibition of dynamin in an immortalized caput epididymal cell line.

The exceptional metabolic and secretory activity of the epididymal epithelium is well established, with conservative estimates indicating it is capable of synthesizing and selectively releasing several hundred proteins into the luminal environment [2,9,66]. Such activity predominantly resides within the anterior portion of the organ; the principal cells of the caput epididymis being responsible for the synthesis of  $\sim 70$ – $80\%$  of the overall epididymal secretome [67,68]. These proteins enter the epididymal lumen via one of two key secretory pathways: (i) a classical merocrine pathway or (ii) an alternative form of apocrine secretion [69]. The former of these is a highly regulated exocytotic process whereby proteins are synthesized in the endoplasmic reticulum before being modified and packaged into large secretory vesicles in the Golgi apparatus [70]. Upon receipt of appropriate physiological stimuli, these vesicles move toward the plasma membrane and release their contents into the epididymal lumen via the formation of transient fusion pores [70]. On the basis of

its localization within the Golgi apparatus of caput principal cells, we infer that the dynamin 2 isoform may be a key component of the trafficking machinery involved in regulating the merocrine secretory pathway. Specifically, we postulate that dynamin 2 mediates the production and/or scission of post-Golgi secretory vesicles. Consistent with this notion, independent studies have proven the necessity of dynamin 2 for protein processing in the Golgi apparatus [25,26] as well in the post-Golgi transportation of secretory proteins [23]. Such roles are also commensurate with our demonstration that dynamin inhibition suppresses the release of a subset, but certainly not all, proteins from an immortalized caput epididymal cell line. It is noteworthy that these proteins include members of the chaperonin containing T-complex protein 1 (TCP1) complex (i.e., CCT3 and CCT8) that have previously been implicated in regulating key aspects of sperm function [71].

Although dynamin 2 retained its association with principal cells in epididymal segments that lie immediate proximal (initial segment) and distal (corpus and cauda) to that of the caput, it was characterized by a marked redistribution to the adluminal border of these cells. Notably, this location is compatible with dynamin 2 fulfilling ancillary roles in either the endocytotic uptake of luminal contents and/or in modulating the fusion of intracellular secretory vesicles with the

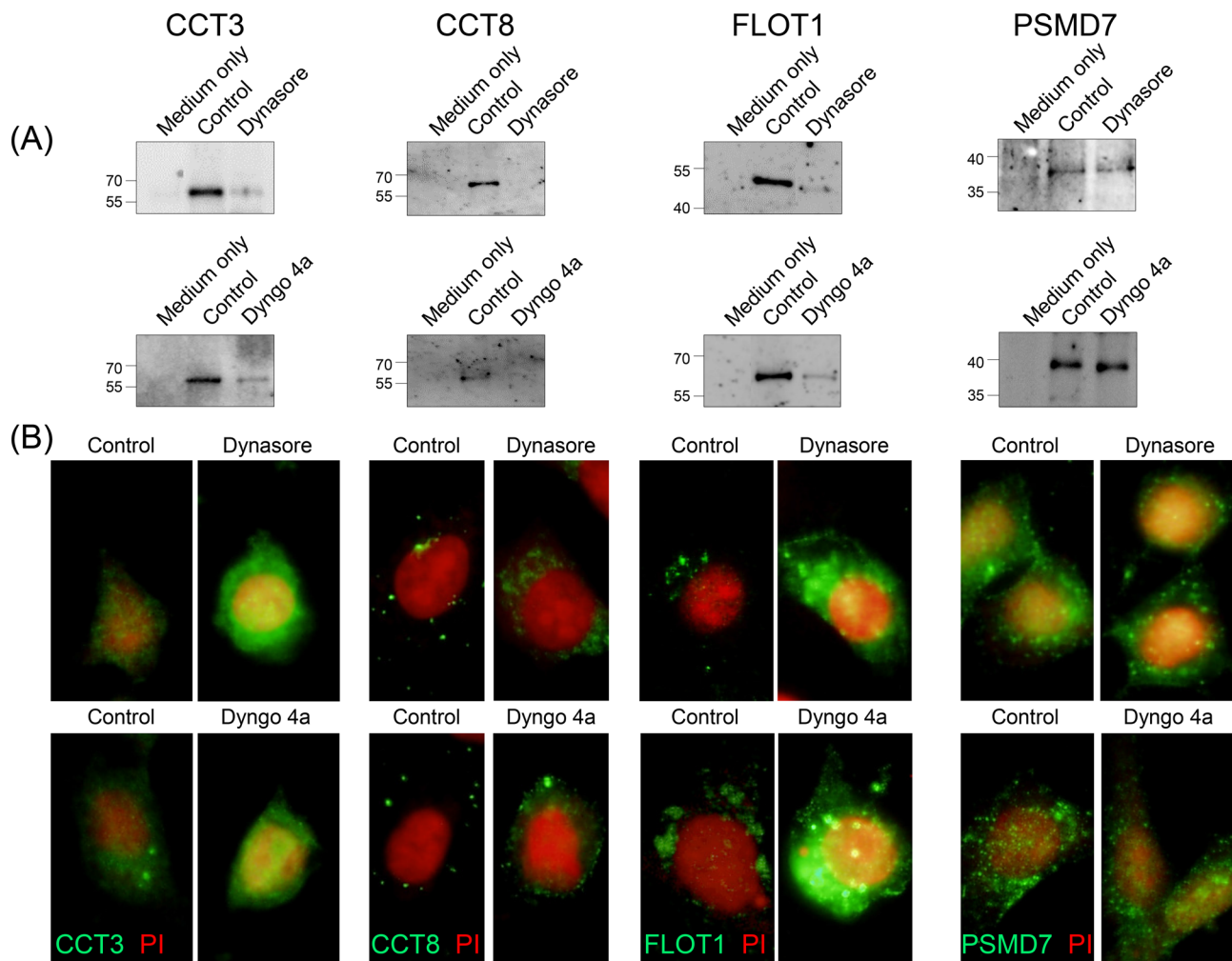


**Figure 8.** Dynamin inhibitors selectively modulate the secretion of proteins by cultured mouse mEcap18 cells. (A) Immunoblotting of three representative epididymal secretory proteins: CCT3, CCT8, and FLOT1 confirmed a significant decrease in abundance within the medium following treatment of mEcap18 cells with either Dynasore or Dyngo-4a dynamin inhibitors. By contrast, the abundance of an alternative epididymal secretory protein, PSMD7, was not influenced by the presence of dynamin inhibitors. These blots also feature protein recovered from mEcap18 cells treated with the DMSO vehicle control (control) as well as an equivalent volume of cell-free medium (medium only). (B) Immunofluorescence detection of CCT3, CCT8, and FLOT1 within mEcap18 cells treated with Dynasore, Dyngo-4a, or the DMSO vehicle control (control) for 12 h. Substantially more CCT3, CCT8, and FLOT1 were detected in mEcap18 cells treated with Dynasore or Dyngo-4a compared to that of the vehicle controls. In contrast, the abundance of PSMD7 was not influenced by the presence of dynamin inhibitors. These experiments were replicated three times, and representative gels, immunofluorescence images, and immunoblots are presented.

plasma membrane [7]. In support of the latter mechanism, recent evidence indicates that dynamin can control the rate of fusion-pore expansion [39,72] and thus fine-tune the amount of cargo released to the extracellular space during exocytosis [28]. Nevertheless, the detection of dynamin 2 in apical protrusions extending from the principal cells of the corpus and cauda epididymis raise the prospect that it may contribute to the apocrine mode of secretion employed by these cells [69]. This pathway serves as a secretory mechanism for proteins synthesized on free ribosomes and lacking an endoplasmic reticulum signal peptide sequence. Such proteins are believed to be either synthesized in or directed to apical blebs, large protrusions that project from the apical cytoplasm into the lumen before detaching from the cell surface and subsequently fragmenting to generate a highly heterogeneous population of small membrane-bound vesicles known as epididymosomes [73]. Although the mechanism(s) underpinning the detachment of apical blebs is yet to be fully resolved, the

relatively large areas of continuity that exist between these structures and the apical plasma membrane of principal cells [69] would appear to be incompatible with dynamin-mediated scission. Indeed, when assembled in the absence of GTP, the nonconstricted dynamin helix is capable of surrounding a membrane tube with an inner and outer radius of only 10 and 25 nm, respectively [18]. Despite this, detailed ultrastructural studies have revealed that the scission of apical blebs is likely to proceed gradually in a process characterized by involution of the plasma membrane and formation of multiple fissures between the blebs and apical cytoplasm [69]. This eventually yields narrow stalk-like attachments, the diameter of which may be more in keeping with the structural characteristics of dynamin helices.

In marked contrast to dynamin 2, the localization of dynamin 1 and dynamin 3 isoforms alternated between the principal cell population in some segments and that of the clear cells in other segments of the adult epididymis. Specifically, dynamin 1 was

detected throughout the cytosol of caput principal cells before being found exclusively within clear cells in more distal regions (corpus and cauda). Conversely, dynamin 3 was characterized by a reciprocal pattern of expression whereby it was detected in clear cells in the caput epididymis before localizing throughout the cytosol of corpus and cauda principal cells. This intriguing relationship was confirmed through dual labeling experiments, which demonstrated that the two proteins localized to distinct, nonoverlapping cell populations. These data contrast the overlapping localization and the concomitant redundant functions that have previously been described for dynamin 1 and 3 in neuronal tissues [74], but are similar to that of dynamin 1 and 3 in mammalian germ cells and their supporting Sertoli cell population in the testes [17,47,75]. We remain uncertain why this situation may have arisen in the male reproductive tissue and whether these variants fulfil similar or unique functions in these cells. Nevertheless, we did note that dynamin 3 expression was restricted to the apical membrane and subapical domain of clear cells, whereas this polarity was not shared with dynamin 1; this isoform was instead preferentially located throughout the cytosol of clear cells.

The significance of dynamin expression in clear cells is emphasized by the key role this population of cells plays in luminal acidification as well as their pronounced endocytotic activity [11,76,77]. The latter of these has been linked to the selective clearance of proteins [77] and other macromolecular entities from the epididymal lumen, including cytoplasmic droplets that are shed from maturing spermatozoa [11]. Thus, the apical membrane/subapical domains of clear cells are known to be populated with a heterogeneous assembly of endocytotic structures including coated and uncoated pits, numerous small vesicular elements (150–200 nm), and larger membrane-bound endosomes [11]. It is therefore tempting to speculate that dynamin 3 may contribute to the selective uptake and recycling of luminal material. By contrast, the diffuse cytosolic labeling of dynamin 1 is consistent with that observed for ATP6V1B1, a subunit of the proton-pumping ATPase (V-ATPase) that is highly enriched in clear cells and responsible for luminal acidification [78,79]. The positioning of the V-ATPase enzyme complex within the apical pole of cells has previously been shown to be tied to the dynamic remodeling of the actin cytoskeleton [80,81], as well as being acutely sensitive to inhibition of exocytotic events, such that treatment with microtubule-disrupting agents (colchicine) or cleavage of cellubrevin [a vesicle soluble N-ethylmaleimide-sensitive factor attachment protein receptor (v-SNARE)] [82], both lead to a redistribution of the complex throughout the cytosol. Such findings are of interest owing to the fact that dynamin is known to collaborate with SNARE proteins to mediate vesicle trafficking, as well as having been implicated in the regulation of actin cytoskeleton dynamics [27]. Taken together, these data raise the possibility that the cytosolic localization of dynamin 1 in clear cells may be linked to V-ATPase positioning/recycling within these cells, and thus the acidification of the epididymal lumen.

In conclusion, we have shown that three canonical isoforms of dynamin are highly expressed in the mouse epididymis and appropriately positioned to fulfil regulatory roles in vesicle trafficking events that underpin the extraordinary secretory and abortive activity of this specialized region of the male reproductive tract. Despite sharing more than 80% sequence homology, this family of mechanoenzymes was clearly distinguishable on the basis of their cellular and subcellular localization, thus arguing that they possess unique, rather than overlapping, modes of action within the epididymal epithelium. These results challenge the redundant roles proposed for dynamin isoforms in other tissues and encourage further investigation of the

mechanism that regulates the differential expression profiles of dynamin expression within the epididymis. It will also be of considerable interest to determine the functional implications of dynamin in the context of sperm maturation and storage.

## Supplementary data

Supplementary data are available at *BIOLRE* online.

**Supplemental Figure S1.** Detection of dynamin isoforms in the initial segment of the mouse epididymis. (A–I) Immunofluorescence localization of each dynamin isoform (1–3) was undertaken in the mouse epididymis (day 10, 30, and >8 weeks postnatum) by sequential labeling with antidynamin antibodies (green) and propidium iodide (PI, red). ep, epithelial cells; sp, sperm; int, interstitium; l, lumen. These experiments were replicated on material from three animals and representative immunofluorescence images are presented.

**Supplemental Figure S2.** Expression levels of dynamin protein in the developing mouse epididymis. The relative levels of dynamin protein expression were quantified by immunoblotting of tissue homogenates prepared from epididymides at key developmental time points (10 days, 30 days, >8 weeks). Blots were subsequently stripped and reprobbed with anti- $\alpha$ -tubulin antibody to confirm equivalent protein loading and enable densitometric analysis of band intensity ( $n = 3$ ). For the purpose of this analysis, the labeling intensity of each dynamin isoform was normalized relative to that of  $\alpha$ -tubulin across all epididymal segments and developmental time points examined. In this instance, band intensity in the day 10 caput tissue was nominally set to a value of 1.

**Supplemental Figure S3.** Examination of the specificity of dynamin antibodies. (A) The specificity of antidynamin 1, antidynamin 2, and antidynamin 3 antibodies was initially examined by immunoblotting of tissue homogenates prepared from mouse epididymal tissue alongside that of mouse brain (positive control for dynamin expression). In all instances, the antidynamin antibodies labeled a predominant band of the appropriate molecular weight (~100 kDa, denoted by arrows) in both brain and epididymal tissue. (B–J) Where available (antidynamin 2 and antidynamin 3), antibody specificity was also assessed by pre-absorption of the antibody with excess immunizing peptide prior to conducting immunolabeling of epididymal tissue sections. (B–E) In the case of antidynamin 2 (DNM2) antibody, immunofluorescence localization in both the caput (B) and corpus epididymis (C) was selectively eliminated (D, E) by preabsorption of the antibody with immunizing peptide (+IP). (F–I) Similarly, in the case of anti-DNM3 antibody, immunofluorescence localization in both the caput (F) and corpus epididymis (G) were also eliminated (H, I) following preabsorption of anti-DNM3 antibody with immunizing peptide (+IP). (J, K) Given the detection of additional cross-reactive bands in antidynamin 3 immunoblots (as shown in A), the specificity of DNM3 antibody was further examined by (J) immunoblotting of both epididymis and brain tissue lysates following pre-absorption of DNM3 antibody with immunizing peptide (+IP). While this treatment effectively eliminated labeling of the ~100 kDa protein in both cell lysates, this band was able to be detected once the same membrane was stripped and reprobbed with nonabsorbed antibody (K).

**Supplemental Figure S4.** The mouse mEcap 18 cell line represents a heterogenous culture featuring a predominance of principal cells as well as clear cells that stained positive for ATP6V1B1. Immunofluorescent staining of the mEcap 18 cell line with the clear cell marker ATP6V1B1 (A, green) and the epithelial cell marker androgen

receptor (B, green). Nuclei are labeled in red with propidium iodide (PI).

**Supplemental Table S1.** Details of antibodies used throughout this study.

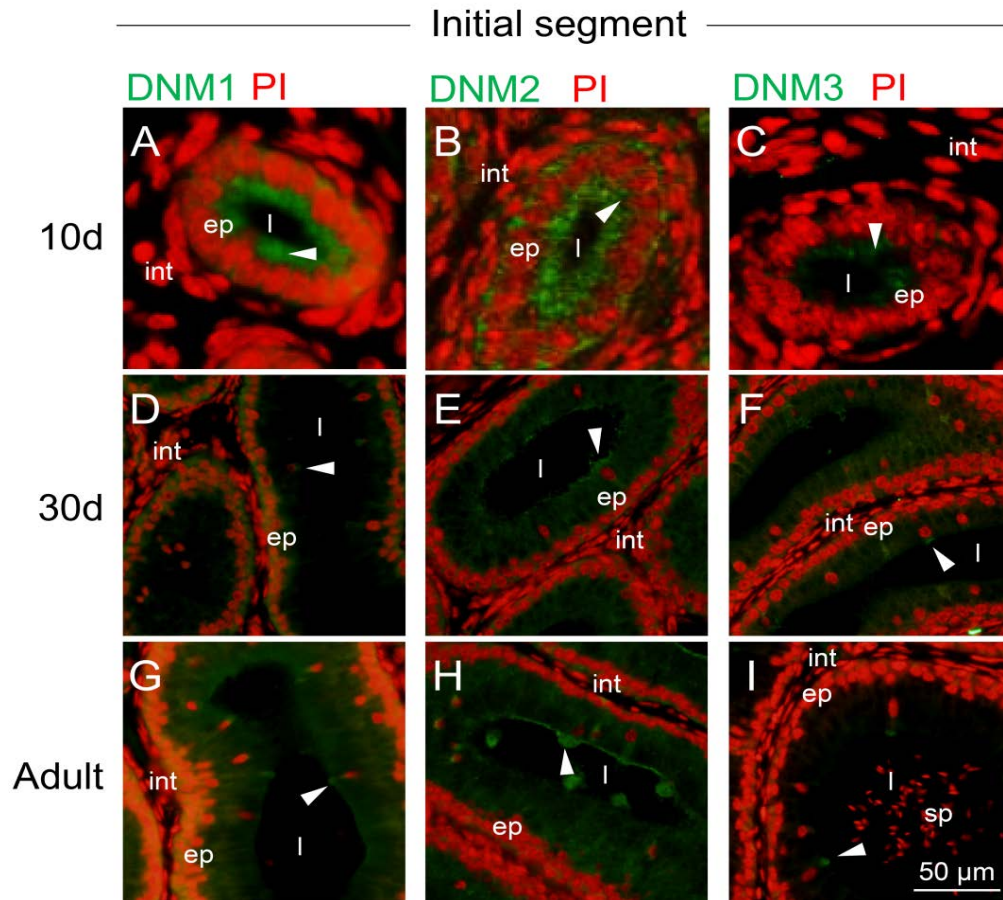
## References

- Cooper TG. *The Epididymis, Sperm Maturation and Fertilisation*. Berlin: Springer-Verlag; 1986; 1–281.
- Dacheux JL, Dacheux F, Druart X. Epididymal protein markers and fertility. *Anim Reprod Sci* 2016; **169**:76–87.
- Cornwall GA. New insights into epididymal biology and function. *Hum Reprod Update* 2009; **15**:213–227.
- Hinton BT, Palladino MA. Epididymal epithelium: its contribution to the formation of a luminal fluid microenvironment. *Microsc Res Tech* 1995; **30**:67–81.
- Abe K, Takano H, Ito T. Ultrastructure of the mouse epididymal duct with special reference to the regional differences of the principal cells. *Arch Histol Jpn* 1983; **46**:51–68.
- Hamilton DW, Greep RO. Structure and function of the epithelium lining the ductuli efferentes, ductus epididymidis, and ductus deferens in the rat. In: Greep RO, Astwood EB (eds.), *Handbook of Physiology*. Washington, D.C.: American Physiological Society; 1975:259–301.
- Hermo L, Robaire B. Epididymis cell types and their function. In: Robaire B, Hinton BT (eds.), *The Epididymis: From Molecules to Clinical Practice*. New York: Kluwer Academic/Plenum; 2002:81–102.
- Robaire B, Hermo L. Efferent ducts, epididymis, and vas deferens: structure, functions, and their regulation. In: Knobil E, Neill J (eds.), *The Physiology of Reproduction*, 1st ed. New York: Raven Press, Ltd.; 1988:999–1080.
- Dacheux JL, Belleanne C, Jones R, Labas V, Belghazi M, Guyonnet B, Druart X, Gatti JL, Dacheux F. Mammalian epididymal proteome. *Mol Cell Endocrinol* 2009; **306**:45–50.
- Dacheux JL, Dacheux F. New insights into epididymal function in relation to sperm maturation. *Reproduction* 2014; **147**:R27–R42.
- Hermo L, Dworkin J, Oko R. Role of epithelial clear cells of the rat epididymis in the disposal of the contents of cytoplasmic droplets detached from spermatozoa. *Am J Anat* 1988; **183**:107–124.
- Moore HDM, Bedford JM. Short-term effects of androgen withdrawal on the structure of different epithelial cells in the rat epididymis. *Anat Rec* 1979; **193**:293–312.
- Robaire B, Hinton BT, Orgebin-Crist MC. The Epididymis. In: Neill JD (ed.) *Knobil and Neill's Physiology of Reproduction*, 3rd ed. New York: Elsevier; 2006:1071–1148.
- Hamamah S, Miesusset R, Dacheux JL. *Epididymis: Role and Importance in Male Infertility Treatment*. Rome, Italy: Ares-Serono Symposia Publications; 1995:1–275.
- Hinton BT, Cooper TG. The epididymis as a target for male contraceptive development. *Handb Exp Pharmacol* 2010; **198**:117–137.
- Reid AT, Anderson AL, Roman SD, McLaughlin EA, McCluskey A, Robinson PJ, Aitken RJ, Nixon B. Glycogen synthase kinase 3 regulates acrosomal exocytosis in mouse spermatozoa via dynamin phosphorylation. *FASEB J* 2015; **29**:2872–2882.
- Reid AT, Lord T, Stanger SJ, Roman SD, McCluskey A, Robinson PJ, Aitken RJ, Nixon B. Dynamin regulates specific membrane fusion events necessary for acrosomal exocytosis in mouse spermatozoa. *J Biol Chem* 2012; **287**:37659–37672.
- Morlot S, Roux A. Mechanics of dynamin-mediated membrane fission. *Annu Rev Biophys* 2013; **42**:629–649.
- Danino D, Hinshaw JE. Dynamin family of mechanoenzymes. *Curr Opin Cell Biol* 2001; **13**:454–460.
- Hinshaw JE. Dynamin and its role in membrane fission. *Annu Rev Cell Dev Biol* 2000; **16**:483–519.
- Ferguson SM, De Camilli P. Dynamin, a membrane-remodelling GTPase. *Nat Rev Mol Cell Biol* 2012; **13**:75–88.
- Baba T, Damke H, Hinshaw JE, Ikeda K, Schmid SL, Warnock DE. Role of dynamin in clathrin-coated vesicle formation. *Cold Spring Harb Symp Quant Biol* 1995; **60**:235–242.
- Kreitzer G, Marmorstein A, Okamoto P, Vallee R, Rodriguez-Boulant E. Kinesin and dynamin are required for post-Golgi transport of a plasma-membrane protein. *Nat Cell Biol* 2000; **2**:125–127.
- Weller SG, Capitani M, Cao H, Micaroni M, Luini A, Sallèse M, McNiven MA. Src kinase regulates the integrity and function of the Golgi apparatus via activation of dynamin 2. *Proc Natl Acad Sci USA* 2010; **107**:5863–5868.
- Cao H, Thompson HM, Krueger EW, McNiven MA. Disruption of Golgi structure and function in mammalian cells expressing a mutant dynamin. *J Cell Sci* 2000; **113**:1993–2002.
- Jones SM, Howell KE, Henley JR, Cao H, McNiven MA. Role of dynamin in the formation of transport vesicles from the trans-Golgi network. *Science* 1998; **279**:573–577.
- Gonzalez-Jamett AM, Momboisse F, Haro-Acuna V, Bevilacqua JA, Caviedes P, Cardenas AM. Dynamin-2 function and dysfunction along the secretory pathway. *Front Endocrinol* 2013; **4**:1–9.
- Jackson J, Papadopoulos A, Meunier FA, McCluskey A, Robinson PJ, Keating DJ. Small molecules demonstrate the role of dynamin as a bidirectional regulator of the exocytosis fusion pore and vesicle release. *Mol Psychiatry* 2015; **20**:810–819.
- Williams M, Kim K. From membranes to organelles: emerging roles for dynamin-like proteins in diverse cellular processes. *Eur J Cell Biol* 2014; **93**:267–277.
- Menon M, Schafer DA. Dynamin: expanding its scope to the cytoskeleton. *Int Rev Cell Mol Biol* 2013; **302**:187–219.
- Ochoa GC, Slepnev VI, Neff L, Ringstad N, Takei K, Daniell L, Kim W, Cao H, McNiven M, Baron R, De Camilli P. A functional link between dynamin and the actin cytoskeleton at podosomes. *J Cell Biol* 2000; **150**:377–389.
- Orth JD, Krueger EW, Cao H, McNiven MA. The large GTPase dynamin regulates actin comet formation and movement in living cells. *Proc Natl Acad Sci USA* 2002; **99**:167–172.
- Palmer SE, Smaczynska-de R, Marklew CJ, Allwood EG, Mishra R, Johnson S, Goldberg MW, Ayscough KR. A dynamin-actin interaction is required for vesicle scission during endocytosis in yeast. *Curr Biol* 2015; **25**:868–878.
- Tuma PL, Stachniak MC, Collins CA. Activation of dynamin GTPase by acidic phospholipids and endogenous rat brain vesicles. *J Biol Chem* 1993; **268**:17240–17246.
- Sphetner HS, Vallee RB. Dynamin is a GTPase stimulated to high levels of activity by microtubules. *Nature* 1992; **355**:733–735.
- Maeda K, Nakata T, Noda Y, Sato-Yoshitake R, Hirokawa N. Interaction of dynamin with microtubules: its structure and GTPase activity investigated by using highly purified dynamin. *Mol Biol Cell* 1992; **3**:1181–1194.
- Mooren OL, Kotova TI, Moore AJ, Schafer DA. Dynamin2 GTPase and cortactin remodel actin filaments. *J Biol Chem* 2009; **284**:23995–24005.
- Gu C, Yaddanapudi S, Weins A, Osborn T, Reiser J, Pollak M, Hartwig J, Sever S. Direct dynamin-actin interactions regulate the actin cytoskeleton. *EMBO J* 2010; **29**:3593–3606.
- Anantharam A, Bittner MA, Aikman RL, Stuenkel EL, Schmid SL, Axelrod D, Holz RW. A new role for the dynamin GTPase in the regulation of fusion pore expansion. *Mol Biol Cell* 2011; **22**:1907–1918.
- Cao H, Garcia F, McNiven MA. Differential distribution of dynamin isoforms in mammalian cells. *Mol Biol Cell* 1998; **9**:2595–2609.
- Ferguson SM, Brasnjo G, Hayashi M, Wolfel M, Collesi C, Giovedi S, Raimondi A, Gong LW, Ariel P, Paradise S, O'Toole E, Flavell R et al. A selective activity-dependent requirement for dynamin 1 in synaptic vesicle endocytosis. *Science* 2007; **316**:570–574.
- Cook TA, Urrutia R, McNiven MA. Identification of dynamin 2, an isoform ubiquitously expressed in rat tissues. *Proc Natl Acad Sci USA* 1994; **91**:644–648.

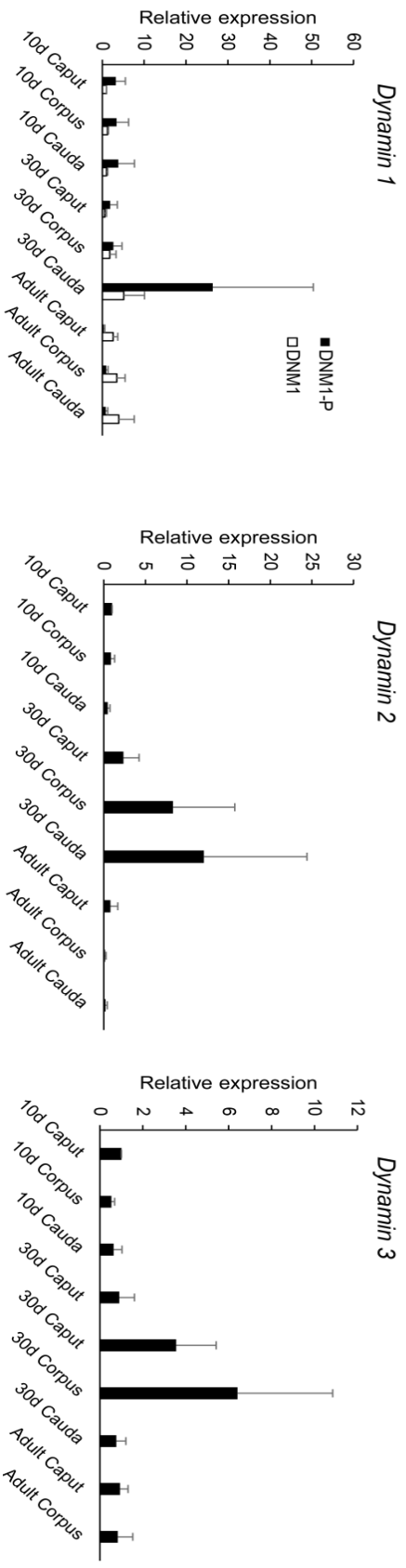
43. Otsuka A, Abe T, Watanabe M, Yagisawa H, Takei K, Yamada H. Dynamin 2 is required for actin assembly in phagocytosis in Sertoli cells. *Biochem Biophys Res Commun* 2009; 378:478–482.
44. Kusumi N, Watanabe M, Yamada H, Li SA, Kashiwakura Y, Matsukawa T, Nagai A, Nasu Y, Kumon H, Takei K. Implication of amphiphysin 1 and dynamin 2 in tubulobulbar complex formation and spermatid release. *Cell Struct Funct* 2007; 32:101–113.
45. Lie PP, Xia W, Wang CQ, Mruk DD, Yan HH, Wong CH, Lee WM, Cheng CY. Dynamin II interacts with the cadherin- and occludin-based protein complexes at the blood-testis barrier in adult rat testes. *J Endocrinol* 2006; 191:571–586.
46. Iguchi H, Watanabe M, Kamitani A, Nagai A, Hosoya O, Tsutsui K, Kumon H. Localization of dynamin 2 in rat seminiferous tubules during the spermatogenic cycle. *Acta Med Okayama* 2002; 56:205–209.
47. Vaid KS, Guttman JA, Babyak N, Deng W, McNiven MA, Mochizuki N, Finlay BB, Vogl AW. The role of dynamin 3 in the testis. *J Cell Physiol* 2007; 210:644–654.
48. Zhao L, Shi X, Li L, Miller DJ. Dynamin 2 associates with complexins and is found in the acrosomal region of mammalian sperm. *Mol Reprod Dev* 2007; 74:750–757.
49. Sipilä P, Shariatmadari R, Huhtaniemi IT, Poutanen M. Immortalization of epididymal epithelium in transgenic mice expressing simian virus 40 T antigen: characterization of cell lines and regulation of the polyoma enhancer activator 3. *Endocrinology* 2004; 145: 437–446.
50. Irannejad R, Kotowski SJ, von Zastrow M. Investigating signaling consequences of GPCR trafficking in the endocytic pathway. *Meth Enzymol* 2014; 535:403–418.
51. Kirchhausen T, Macia E, Pelish HE. Use of dynasore, the small molecule inhibitor of dynamin, in the regulation of endocytosis. *Meth Enzymol* 2008; 438:77–93.
52. Harper CB, Martin S, Nguyen TH, Daniels SJ, Lavidis NA, Popoff MR, Hadzic G, Mariana A, Chau N, McCluskey A. Dynamin inhibition blocks botulinum neurotoxin type A endocytosis in neurons and delays botulism. *J Biol Chem* 2011; 286:35966–35976.
53. Anderson AL, Stanger SJ, Mihalas BP, Tyagi S, Holt JE, McLaughlin EA, Nixon B. Assessment of microRNA expression in mouse epididymal epithelial cells and spermatozoa by next generation sequencing. *Gen Data* 2015; 6:208–211.
54. Asquith KL, Harman AJ, McLaughlin EA, Nixon B, Aitken RJ. Localization and significance of molecular chaperones, heat shock protein 1, and tumor rejection antigen GP96 in the male reproductive tract and during capacitation and acrosome reaction. *Biol Reprod* 2005; 72: 328–337.
55. Johnston DS, Jelinsky SA, Bang HJ, DiCandeloro P, Wilson E, Kopf GS, Turner TT. The mouse epididymal transcriptome: transcriptional profiling of segmental gene expression in the epididymis. *Biol Reprod* 2005; 73:404–413.
56. Tan TC, Valova VA, Malladi CS, Graham ME, Berven LA, Jupp OJ, Hansra G, McClure SJ, Sarcevic B, Boadle RA. Cdk5 is essential for synaptic vesicle endocytosis. *Nat Cell Biol* 2003; 5: 701–710.
57. Sullivan R, Saez F, Girouard J, Frenette G. Role of exosomes in sperm maturation during the transit along the male reproductive tract. *Blood Cells Mol Dis* 2005; 35:1–10.
58. Asquith KL, Harman AJ, McLaughlin EA, Nixon B, Aitken RJ. Localization and significance of molecular chaperones, heat shock protein 1, and tumor rejection antigen gp96 in the male reproductive tract and during capacitation and acrosome reaction. *Biol Reprod* 2005; 72: 328–337.
59. Reid AT, Lord T, Stanger SJ, Roman SD, McCluskey A, Robinson PJ, Aitken RJ, Nixon B. Dynamin regulates specific membrane fusion events necessary for acrosomal exocytosis in mouse spermatozoa. *J Biol Chem* 2012; 287:37659–37672.
60. Dun MD, Anderson AL, Bromfield EG, Asquith KL, Emmett B, McLaughlin EA, Aitken RJ, Nixon B. Investigation of the expression and functional significance of the novel mouse sperm protein, a disintegrin and metalloprotease with thrombospondin type 1 motifs number 10 (ADAMTS10). *Int J Androl* 2012; 35: 572–589.
61. Yano R, Matsuyama T, Kaneko T, Kurio H, Murayama E, Toshimori K, Iida H. Bactericidal/Permeability-increasing protein is associated with the acrosome region of rodent epididymal spermatozoa. *J Androl* 2010; 31:201–214.
62. Da Silva N, Shum WW, Breton S. Regulation of vacuolar proton pumping ATPase-dependent luminal acidification in the epididymis. *Asian J Androl* 2007; 9:476–482.
63. Macia E, Ehrlich M, Massol R, Boucrot E, Brunner C, Kirchhausen T. Dynasore, a cell-permeable inhibitor of dynamin. *Dev Cell* 2006; 10:839–850.
64. McCluskey A, Daniel JA, Hadzic G, Chau N, Clayton EL, Mariana A, Whiting A, Gorgani NN, Lloyd J, Quan A, Moshkanbaryans L, Krishnan S et al. Building a better dynasore: the dyngo compounds potentially inhibit dynamin and endocytosis. *Traffic* 2013; 14: 1272–1289.
65. Girouard J, Frenette G, Sullivan R. Comparative proteome and lipid profiles of bovine epididymosomes collected in the intraluminal compartment of the caput and cauda epididymidis. *Int J Androl* 2011; 34: e475–e486.
66. Dacheux JL, Belleannee C, Guyonnet B, Labas V, Teixeira-Gomes AP, Ecroyd H, Druart X, Gatti JL, Dacheux F. The contribution of proteomics to understanding epididymal maturation of mammalian spermatozoa. *Syst Biol Reprod Med* 2012; 58:197–210.
67. Fouchécourt S, Métayer S, Locatelli A, Dacheux F, Dacheux J-L. Stallion epididymal fluid proteome: qualitative and quantitative characterization; secretion and dynamic changes of major proteins. *Biol Reprod* 2000; 62:1790–1803.
68. Syntin P, Dacheux F, Druart X, Gatti JL, Okamura N, Dacheux J-L. Characterization and identification of proteins secreted in the various regions of the adult boar epididymis. *Biol Reprod* 1996; 55:956–974.
69. Hermo L, Jacks D. Nature's ingenuity: bypassing the classical secretory route via apocrine secretion. *Mol Reprod Dev* 2002; 63:394–410.
70. Kelly RB. Pathways of protein secretion in eukaryotes. *Science* 1985; 230:25–32.
71. Dun MD, Smith ND, Baker MA, Lin M, Aitken RJ, Nixon B. The chaperonin containing TCP1 complex (CCT/TRIC) is involved in mediating sperm-oocyte interaction. *J Biol Chem* 2011; 286: 36875–36887.
72. Anantharam A, Axelrod D, Holz RW. Real-time imaging of plasma membrane deformations reveals pre-fusion membrane curvature changes and a role for dynamin in the regulation of fusion pore expansion. *J Neurochem* 2012; 122:661–671.
73. Aumuller G, Wilhelm B, Seitz J. Apocrine secretion—fact or artifact? *Ann Anat* 1999; 181:437–446.
74. Raimondi A, Ferguson SM, Lou X, Armbruster M, Paradise S, Giovedi S, Messa M, Kono N, Takasaki J, Cappello V, O'Toole E, Ryan TA et al. Overlapping role of dynamin isoforms in synaptic vesicle endocytosis. *Neuron* 2011; 70:1100–1114.
75. Kamitani A, Yamada H, Kinuta M, Watanabe M, Li SA, Matsukawa T, McNiven M, Kumon H, Takei K. Distribution of dynamins in testis and their possible relation to spermatogenesis. *Biochem Biophys Res Commun* 2002; 294:261–267.
76. Hermo L, Adamali HI, Andonian S. Immunolocalization of CA II and H<sup>+</sup>-V-ATPase in epithelial cells of the mouse and rat epididymis. *J Androl* 2000; 21:376–391.
77. Vierula ME, Rankin TL, Orgebin-Crist M-C. Electron microscopic immunolocalization of the 18 and 29 kilodalton secretory proteins in the mouse epididymis: evidence for differential uptake by clear cells. *Microsc Res Tech* 1995; 30:24–36.
78. Miller RL, Zhang P, Smith M, Beaulieu V, Paunescu TG, Brown D, Breton S, Nelson RD. V-ATPase B1-subunit promoter drives

- expression of EGFP in intercalated cells of kidney, clear cells of epididymis and airway cells of lung in transgenic mice. *Am J Physiol Cell Physiol* 2005; 288:C1134–C1144.
79. Pietrement C, Sun-Wada GH, Silva ND, McKee M, Marshansky V, Brown D, Futai M, Breton S. Distinct expression patterns of different subunit isoforms of the V-ATPase in the rat epididymis. *Biol Reprod* 2006; 74:185–194.
80. Holliday LS, Lu M, Lee BS, Nelson RD, Solivan S, Zhang L, Gluck SL. The amino-terminal domain of the B subunit of vacuolar H<sup>+</sup>-ATPase contains a filamentous actin binding site. *J Biol Chem* 2000; 275:32331–32337.
81. Vitavska O, Wiczorek H, Merzendorfer H. A novel role for subunit C in mediating binding of the H<sup>+</sup>-V-ATPase to the actin cytoskeleton. *J Biol Chem* 2003; 278:18499–18505.
82. Breton S, Nsumu NN, Galli T, Sabolic I, Smith PJ, Brown D. Tetanus toxin-mediated cleavage of cellubrevin inhibits proton secretion in the male reproductive tract. *Am J Physiol Renal Physiol* 2000; 278:F717–F725.

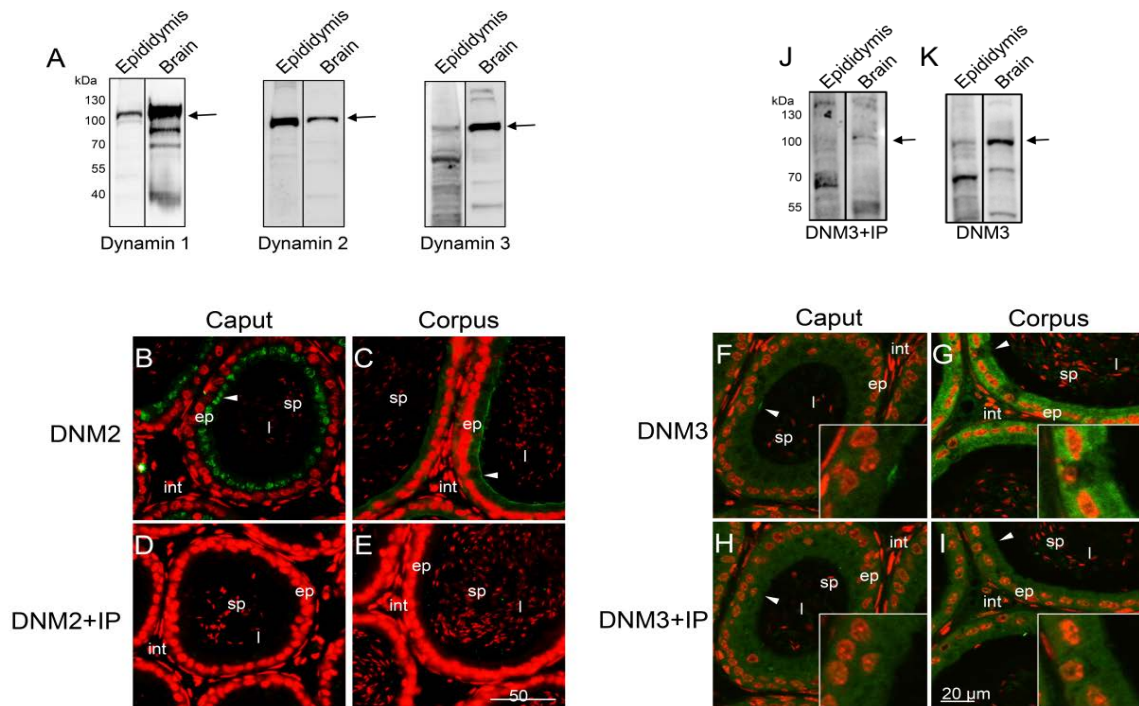
## Chapter 3: Supplementary material



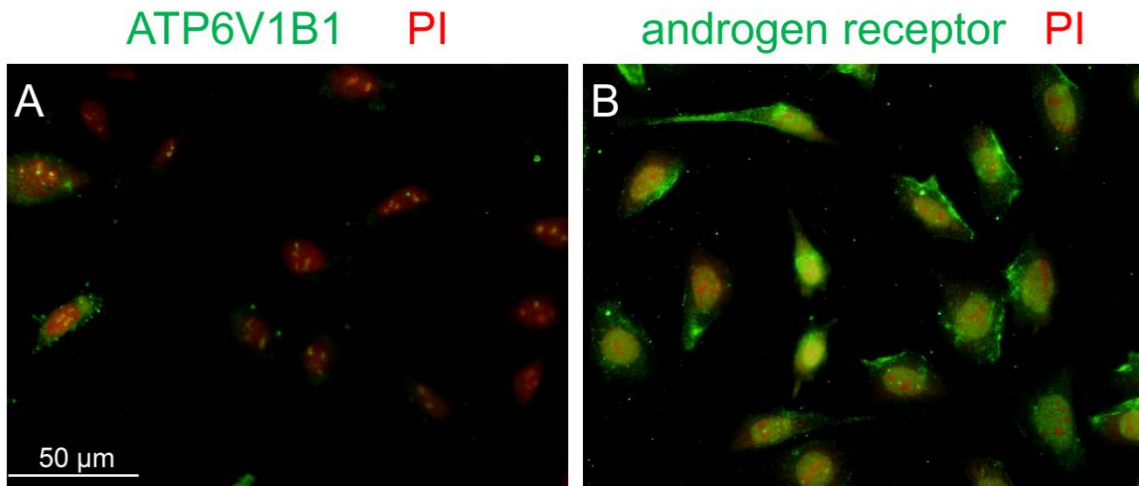
**Supplemental Figure S1** Detection of dynamin isoforms in the initial segment of the mouse epididymis. (A–I) Immunofluorescence localization of each dynamin isoform (1–3) was undertaken in the mouse epididymis (day 10, 30, and >8 weeks postnatum) by sequential labeling with antidynamin antibodies (green) and propidium iodide (PI, red). ep, epithelial cells; sp, sperm; int, interstitium; l, lumen. These experiments were replicated on material from three animals and representative immunofluorescence images are presented.



**Supplemental Figure S2** Expression levels of dynamin protein in the developing mouse epididymis. The relative levels of dynamin protein expression were quantified by immunoblotting of tissue homogenates prepared from epididymides at key developmental time points (10 days, 30 days, >8 weeks). Blots were subsequently stripped and reprobed with anti- $\alpha$ -tubulin antibody to confirm equivalent protein loading and enable densitometric analysis of band intensity ( $n = 3$ ). For the purpose of this analysis, the labeling intensity of each dynamin isoform was normalized relative to that of  $\alpha$ -tubulin across all epididymal segments and developmental time points examined. In this instance, band intensity in the day 10 caput tissue was nominally set to a value of 1.



**Supplemental Figure S3** Examination of the specificity of dynamin antibodies. (A) The specificity of antidynamin 1, antidynamin 2, and antidynamin 3 antibodies was initially examined by immunoblotting of tissue homogenates prepared from mouse epididymal tissue alongside that of mouse brain (positive control for dynamin expression). In all instances, the antidynamin antibodies labeled a predominant band of the appropriate molecular weight (~100 kDa, denoted by arrows) in both brain and epididymal tissue. (B–J) Where available (antidynamin 2 and antidynamin 3), antibody specificity was also assessed by pre-absorption of the antibody with excess immunizing peptide prior to conducting immunolabeling of epididymal tissue sections. (B–E) In the case of antidynamin 2 (DNM2) antibody, immunofluorescence localization in both the caput (B) and corpus epididymis (C) was selectively eliminated (D, E) by preabsorption of the antibody with immunizing peptide (+IP). (F–I) Similarly, in the case of anti-DNM3 antibody, immunofluorescence localization in both the caput (F) and corpus epididymis (G) were also eliminated (H, I) following preabsorption of anti-DNM3 antibody with immunizing peptide (+IP). (J, K) Given the detection of additional cross-reactive bands in antidynamin 3 immunoblots (as shown in A), the specificity of DNM3 antibody was further examined by (J) immunoblotting of both epididymis and brain tissue lysates following pre-absorption of DNM3 antibody with immunizing peptide (+IP). While this treatment effectively eliminated labeling of the ~100 kDa protein in both cell lysates, this band was able to be detected once the same membrane was stripped and re-probed with nonabsorbed antibody (K).



**Supplemental Figure S4** The mouse mEcap 18 cell line represents a heterogenous culture featuring a predominance of principal cells as well as clear cells that stained positive for ATP6V1B1. Immunofluorescent staining of the mEcap 18 cell line with the clear cell marker ATP6V1B1 (A, green) and the epithelial cell marker androgen receptor (B, green). Nuclei are labeled in red with propidium iodide (PI).

Antibody	Final concentration (dilution of stock solution) <sup>1</sup>			Company	Catalogue N°	Batch N°	Stock Concentration
	IF	IB	EM				
<b>Primary antibodies</b>							
Dynamin 1	1 µg (1:50)	1.5 µg (1:1000)	-	Abcam	ab108458	GR107528-1	1 mg/ml
Dynamin 1	N/A (1:50)	-	-	Thermo Fisher	MA5-15285	N/A	N/A
Dynamin 2	0.2 µg (1:50)	-	0.08 µg (1:100)	Santa Cruz	sc-6400	L0712	0.2 mg/ml
Dynamin 2	-	0.4 µg (1:1000)	-	Thermo	PA5-19800	QK2113152	0.27 mg/ml
Dynamin 3	0.15 µg (1:50)	0.225 µg (1:1000)	-	Proteintech	14737-1-AP	N/A	0.15 mg/ml
IZUMO1	-	0.3 µg (1:1000)	-	Santa Cruz	sc-79543	B1309	0.2 mg/ml
CCT3	0.2 µg (1:50)	0.3 µg (1:1000)	-	Santa Cruz	sc-33145	K0805	0.2 mg/ml
CCT8	0.2 µg (1:50)	0.3 µg (1:1000)	-	Santa Cruz	sc-13891	K1710	0.2 mg/ml
Flotillin 1	1 µg (1:50)	1.5 µg (1:1000)	-	Santa Cruz	F1180	124M4804V	1 mg/ml
PSMD7	1 µg (1:50)	1.5 µg (1:1000)	-	Abcam	ab11436	GR29448-3	1 mg/ml
ATP6V1B1	0.2 µg (1:50)	-	-	Santa Cruz	sc-21206	H2313	0.2 mg/ml
α-Tubulin	-	2.85 µg (1:1000)	-	Sigma	T5168	103M4773V	5.7 mg/ml
Dynamin pSer778	-	5.78 µg (1:1000)	-	Thermo	PA1-4621	QJ2096151	5.78 mg/ml
Androgen receptor	1 µg (1:50)	-	-	Sigma	SAB4501575	217009	1 mg/ml
Golgin-97	0.56 µg (1:100)	-	-	Cell Signaling Technology	13192	N/A	1.12 mg/ml
<b>Secondary antibodies</b>							
Anti rabbit Alexa Fluor 488	0.25 µg (1:400)	-	-	Thermo	A11008	1678787	2 mg/ml
Anti goat Alexa Fluor 488	0.25 µg (1:400)	-	-	Thermo	A11055	1369678	2 mg/ml
Anti goat Alexa Fluor 594	0.25 µg (1:400)	-	-	Thermo	A11058	1180089	2 mg/ml
Anti mouse Alexa Fluor 594	0.25 µg (1:400)	-	-	Thermo	A11005	1219862	2 mg/ml
Anti rabbit HRP	-	1.3 µg (1:1000)	-	Millipore	DC03L	N/A	0.13 mg/ml
Anti goat HRP	-	4 µg (1:400)	-	Santa Cruz	sc-2768	J0713	0.4 mg/ml
Anti mouse HRP	-	1.2 µg (1:400)	-	Santa Cruz	sc-2005	B1616	0.4 mg/ml
Anti goat gold label (10 nm)	-	-	N/A (1:10)	Sigma	G5402	SLBP7446V	N/A

<sup>1</sup> IF, immunofluorescence; IB, immunoblot; EM, electron microscopy; -, not applicable; N/A, information not available from manufacturer

**Supplemental Table S1** Details of antibodies used throughout this study.

# CHAPTER 4

---

## *Mechanistic insights into epididymosome-sperm interactions*

**Submitted:** BMC Biology (2018)

**Authors:** Wei Zhou<sup>1</sup>, Simone J. Stanger<sup>1</sup>, Amanda L. Anderson<sup>1</sup>, Geoffrey N. De Iuliis<sup>1</sup>, Adam McCluskey<sup>2</sup>, Eileen A. McLaughlin<sup>1,3</sup>, Matthew D. Dun<sup>4,5</sup> and Brett Nixon<sup>1\*</sup>

<sup>1</sup>Priority Research Centre for Reproductive Biology, School of Environmental and Life Sciences, University of Newcastle, Callaghan, NSW 2308, Australia.

<sup>2</sup> Priority Research Centre for Chemical Biology, School of Environmental and Life Sciences, University of Newcastle, Callaghan, NSW 2308, Australia.

<sup>3</sup>School of Biological Sciences, University of Auckland, Auckland, New Zealand.

<sup>4</sup>School of Biomedical Sciences and Pharmacy, Faculty of Health and Medicine, The University of Newcastle, Callaghan, NSW 2308, Australia.

<sup>5</sup>Hunter Medical Research Institute, Cancer Research Program, New Lambton Heights, NSW 2305, Australia.

\*Correspondence: [brett.nixon@newcastle.edu.au](mailto:brett.nixon@newcastle.edu.au)

## Chapter 4: Overview

In Chapter 3, we established that dynamin isoforms show both cell and segment specific localization in the mouse epididymis, suggesting that different family members play complementary and non-redundant roles in regulating the epididymal environment. Here we sought to extend our understanding of the epididymal soma-sperm communication by specifically focusing on epididymosomes, small extracellular vesicles released from the epididymal soma that contribute to sperm maturation and storage via interaction with luminal spermatozoa. The importance of epididymosomes is illustrated by their ability to influence the sperm epigenetic and proteomic landscapes during the epididymal maturation. However, much less is currently known about the mechanistic basis of how these vesicles interact with spermatozoa. Here we have utilized an *in vitro* co-culture system to track the transfer of biotinylated protein cargo and lipophilic dye-labeled lipids from mouse epididymosomes to recipient spermatozoa. We also applied pharmacological inhibition strategies to investigate the involvement of dynamin and lipid rafts in the regulation of these epididymosome-sperm interactions.

Our data indicate that epididymosome-sperm interactions are initiated via tethering of the epididymosome to receptors restricted to the post-acrosomal sheath of the sperm head. Thereafter, epididymosomes mediate the transfer of cargo to spermatozoa via a process that is dependent on dynamin. Notably, upon co-culture of sperm with epididymosomes, dynamin 1 undergoes a pronounced relocation between the peri- and post-acrosomal domains of the sperm head. This repositioning of dynamin 1 is potentially mediated via its association with lipid rafts and ideally locates the enzyme to facilitate the uptake of epididymosome-borne proteins. Accordingly, disruption of lipid raft integrity or pharmacological inhibition of dynamin both potently suppress the transfer of biotinylated epididymosome proteins to spermatozoa. In contrast, dynamin 2 was retained in the acrosomal domain during epididymosome-sperm interactions, suggesting this isoform may not be involved in the process. Together, these data provide new mechanistic insight into epididymosome-sperm interactions, bringing us closer to a molecular understanding of the process of sperm maturation with potential implications extending to the diagnosis and treatment of male infertility.

<b>Manuscript Number:</b>	BMCB-D-18-01006R1	
<b>Full Title:</b>	Mechanistic insights into mouse epididymosome-sperm interactions	
<b>Article Type:</b>	Research article	
<b>Funding Information:</b>	National Health and Medical Research Council (APP1103176)	Prof Brett Nixon
	National Health and Medical Research Council (APP1147932)	Prof Brett Nixon
<b>Abstract:</b>	<p><b>Background</b></p> <p>The mammalian epididymis is responsible for the provision of a highly specialized environment in which spermatozoa acquire functional maturity and are subsequently stored in preparation for ejaculation. Making important contributions to both processes are epididymosomes, small extracellular vesicles released from the epididymal soma via an apocrine secretory pathway. While considerable effort has been focused on defining the cargo transferred between epididymosomes and spermatozoa, comparatively less is known about the mechanistic basis of these interactions. To investigate this phenomenon, we have utilized an in vitro co-culture system to track the transfer of biotinylated protein cargo between mouse epididymosomes and recipient spermatozoa.</p> <p><b>Results</b></p> <p>Our data indicate that epididymosome-sperm interactions are initiated via tethering of the epididymosome to receptors restricted to the post-acrosomal domain of the sperm head. Thereafter, epididymosomes mediate the transfer of protein cargo to spermatozoa via a process that is dependent on dynamin, a family of mechanoenzymes that direct intercellular vesicle trafficking. Notably, upon co-culture of sperm with epididymosomes, dynamin 1 undergoes a pronounced relocation between the peri- and post-acrosomal domains of the sperm head. This repositioning of dynamin 1 is potentially mediated via its association with membrane rafts and ideally locates the enzyme to facilitate the uptake of epididymosome-borne proteins. Accordingly, disruption of membrane raft integrity or pharmacological inhibition of dynamin both potently suppress the transfer of biotinylated epididymosome proteins to spermatozoa.</p> <p><b>Conclusion</b></p> <p>Together, these data provide new mechanistic insight into epididymosome-sperm interactions with potential implications extending to the manipulation of sperm maturation for the purpose of fertility regulation.</p>	
<b>Corresponding Author:</b>	Wei Zhou Newcastle University Newcastle, AUSTRALIA	
<b>Corresponding Author Secondary Information:</b>		
<b>Corresponding Author's Institution:</b>	Newcastle University	
<b>Corresponding Author's Secondary Institution:</b>		
<b>First Author:</b>	Wei Zhou	
<b>First Author Secondary Information:</b>		

## **Title: Mechanistic insights into mouse epididymosome-sperm interactions**

**Authors:** Wei Zhou<sup>1</sup>, Simone J. Stanger<sup>1</sup>, Amanda L. Anderson<sup>1</sup>, Ilana R. Bernstein<sup>1</sup>, Geoffry N. De Iuliis<sup>1</sup>, Adam McCluskey<sup>2</sup>, Eileen A. McLaughlin<sup>1,3</sup>, Matthew D. Dun<sup>4,5</sup>, Brett Nixon<sup>1\*</sup>

5

**Affiliations:** <sup>1</sup>Priority Research Centre for Reproductive Science, School of Environmental and Life Sciences, The University of Newcastle, Callaghan, NSW 2308, Australia.

<sup>2</sup>Priority Research Centre for Chemical Biology, School of Environmental and Life Sciences, The University of Newcastle, Callaghan, NSW 2308, Australia.

10 <sup>3</sup>School of Biological Sciences, University of Auckland, Auckland 1142, New Zealand

<sup>4</sup>School of Biomedical Sciences and Pharmacy, Faculty of Health and Medicine, The University of Newcastle, Callaghan, NSW 2308, Australia.

<sup>5</sup>Hunter Medical Research Institute, Cancer Research Program, New Lambton Heights, NSW 2305, Australia.

**\*Corresponding author:** Brett Nixon, Priority Research Centre for Reproductive Science, School of Environmental and Life Sciences, Discipline of Biological Sciences, University of Newcastle, University Drive, Callaghan, NSW 2308, Australia.

15

Ph: + 61 2 4921 6977

Fax: + 61 2 4921 6308

Email: [Brett.Nixon@newcastle.edu.au](mailto:Brett.Nixon@newcastle.edu.au)

20 **Email address for each author:**

Wei Zhou: [WZhou3@uon.edu.au](mailto:WZhou3@uon.edu.au)

Simone J. Stanger: [simone.stanger@newcastle.edu.au](mailto:simone.stanger@newcastle.edu.au)

Amanda L. Anderson: [amanda.anderson@newcastle.edu.au](mailto:amanda.anderson@newcastle.edu.au)

Ilana R. Bernstein: [ilana.bernstein@newcastle.edu.au](mailto:ilana.bernstein@newcastle.edu.au)

25

Geoffry N. De Iuliis: [geoffry.deiuliis@newcastle.edu.au](mailto:geoffry.deiuliis@newcastle.edu.au)

Adam McCluskey: [adam.mccluskey@newcastle.edu.au](mailto:adam.mccluskey@newcastle.edu.au)

Eileen A. McLaughlin: [eileen.mclaughlin@auckland.ac.nz](mailto:eileen.mclaughlin@auckland.ac.nz)

Matthew D. Dun: [matt.dun@newcastle.edu.au](mailto:matt.dun@newcastle.edu.au)

## 30 ABSTRACT

**Background:** The mammalian epididymis is responsible for the provision of a highly specialized environment in which spermatozoa acquire functional maturity and are subsequently stored in preparation for ejaculation. Making important contributions to both processes are epididymosomes, small extracellular vesicles released from the epididymal soma via an apocrine secretory pathway. While considerable effort has been focused on defining the cargo transferred between epididymosomes and spermatozoa, comparatively less is known about the mechanistic basis of these interactions. To investigate this phenomenon, we have utilized an *in vitro* co-culture system to track the transfer of biotinylated protein cargo between mouse epididymosomes and recipient spermatozoa isolated from the caput epididymis; an epididymal segment that is of critical importance for promoting sperm maturation

**Results:** Our data indicate that epididymosome-sperm interactions are initiated via tethering of the epididymosome to receptors restricted to the post-acrosomal domain of the sperm head. Thereafter, epididymosomes mediate the transfer of protein cargo to spermatozoa via a process that is dependent on dynamin, a family of mechanoenzymes that direct intercellular vesicle trafficking. Notably, upon co-culture of sperm with epididymosomes, dynamin 1 undergoes a pronounced relocation between the peri- and post-acrosomal domains of the sperm head. This repositioning of dynamin 1 is potentially mediated via its association with membrane rafts and ideally locates the enzyme to facilitate the uptake of epididymosome-borne proteins. Accordingly, disruption of membrane raft integrity or pharmacological inhibition of dynamin both potently suppress the transfer of biotinylated epididymosome proteins to spermatozoa.

**Conclusion:** Together, these data provide new mechanistic insight into epididymosome-sperm interactions with potential implications extending to the manipulation of sperm maturation for the purpose of fertility regulation.

**Key words:** dynamin, epididymis, epididymosome, extracellular vesicle, exosome, intercellular trafficking, membrane raft, spermatozoa, sperm maturation

## BACKGROUND

Mammalian spermatozoa acquire motility and the potential to fertilize an ovum during their descent through the epididymis, an exceptionally long and highly regionalized tubule that connects the testis to the vas deferens. A distinctive hallmark of this process of functional maturation is that it proceeds in the complete absence of *de novo* gene transcription or protein translation. Rather, it is driven exclusively via extrinsic factors that sperm encounter within the luminal microenvironment of the epididymal tubule. Key elements of this environment are epididymosomes, small membrane bound vesicles that are released from the surrounding epididymal soma via an apocrine secretory pathway [1, 2]. These entities not only protect their encapsulated cargo against the potentially deleterious luminal microenvironment, but also provide a mechanism to affect the bulk delivery of this cargo to maturing spermatozoa. It is therefore not surprising that epididymosomes have been implicated in the trafficking of a broad range of enzymes, structural proteins, chaperones, cytokines, and immunological proteins [3-6], which collectively contribute to sperm function, protection and subsequent storage prior to ejaculation. In a similar context, epididymosomes have recently begun to attract considerable attention as vehicles for the delivery of alternative cargo, including small non-coding RNAs (sncRNA), to spermatozoa and to epididymal epithelial cells situated downstream of their site of secretion [7-10].

It follows that an understanding of the mechanisms by which epididymosomes are targeted to, and interact with, their recipient cells is of fundamental importance to the field of reproductive biology as well as those seeking to resolve the pathway(s) by which paternal exposures alter the sperm epigenome [11]. A defining feature of epididymosome-sperm interactions is their apparent specificity. Thus, in model species such as the bovine, at least two heterogeneous populations of epididymosomes have been characterized, with each possessing the ability to differentiate their investment between live and dead spermatozoa [12]. One such population are defined by their smaller diameter (~10 – 100 nm) and an abundance of CD9, a tetraspanin that decorates the surface of not only epididymosomes, but also the exosomes released from a variety of non-reproductive tissues [13]. This sub-class of epididymosomes display preferential interaction with live spermatozoa, thus implicating them in sperm maturation / storage [14]. The alternative population, lack CD9, but feature an abundance of epididymal sperm binding protein 1 and a propensity to interact with dead

spermatozoa. This latter population may therefore be involved in protecting viable spermatozoa from degradation products released from dead cells [15]. The selective nature of these interactions suggests that the adherence of epididymosomes to spermatozoa and the subsequent delivery of their encapsulated cargo are tightly regulated events. This accords with evidence that epididymosomes isolated from different epididymal segments possess discrete proteomic [16], lipid [16, 17] and sncRNA profiles [7, 9, 10], and may thus be responsible for sequential modification of the macromolecular composition of the sperm cells they encounter. It also agrees with evidence that, as recipient cells for epididymosome cargo, spermatozoa present a number of unique characteristics not typically found in somatic cell populations. Not the least of these are a highly polarized morphology and specialized membrane architecture. Thus, mature sperm cells possess three distinct domains, the: (i) head, involved in sperm-oocyte interaction; (ii) mid-piece, which houses the mitochondria and therefore contributes to the cell's metabolic demands; and (iii) flagellum, which facilitates sperm movement. Differences in membrane protein and lipid composition provide the basis for further subdivision of the sperm head surface topology into the apical and the post-acrosomal (overlying the post-acrosomal sheath) plasma membrane domains.

Previous work has revealed that epididymosomes appear to preferentially interact with the post-acrosomal domain of the sperm head [18, 19]. However, the mechanism(s) by which such selectivity is mediated remain to be fully resolved. Current evidence implicates the involvement of a variety of proteinaceous receptors and their complementary ligands [18]. In this context, our recent studies have identified milk fat globule-EGF factor 8 protein (MFGE8) as a potential ligand for epididymosome-sperm interaction. Accordingly, ultrastructural analyses confirmed the localization of MFGE8 on the epididymosome surface and extending into stalk-like projections associated with sites of epididymosome-sperm interaction. Furthermore, antibody masking of MFGE8 ligands compromised the efficiency of epididymosome-mediated protein transfer to recipient spermatozoa [19]. Downstream of this initial adhesion event it has been postulated that the epididymosome and sperm membranes undergo a transient fusion leading to delivery of the epididymosome cargo and a subsequent detachment of the epididymosome [20, 21]. Although several membrane-trafficking protein families have been identified within the epididymosome proteome [3, 16, 22], there remains a dearth of evidence concerning their precise functional roles. Similarly, specialized

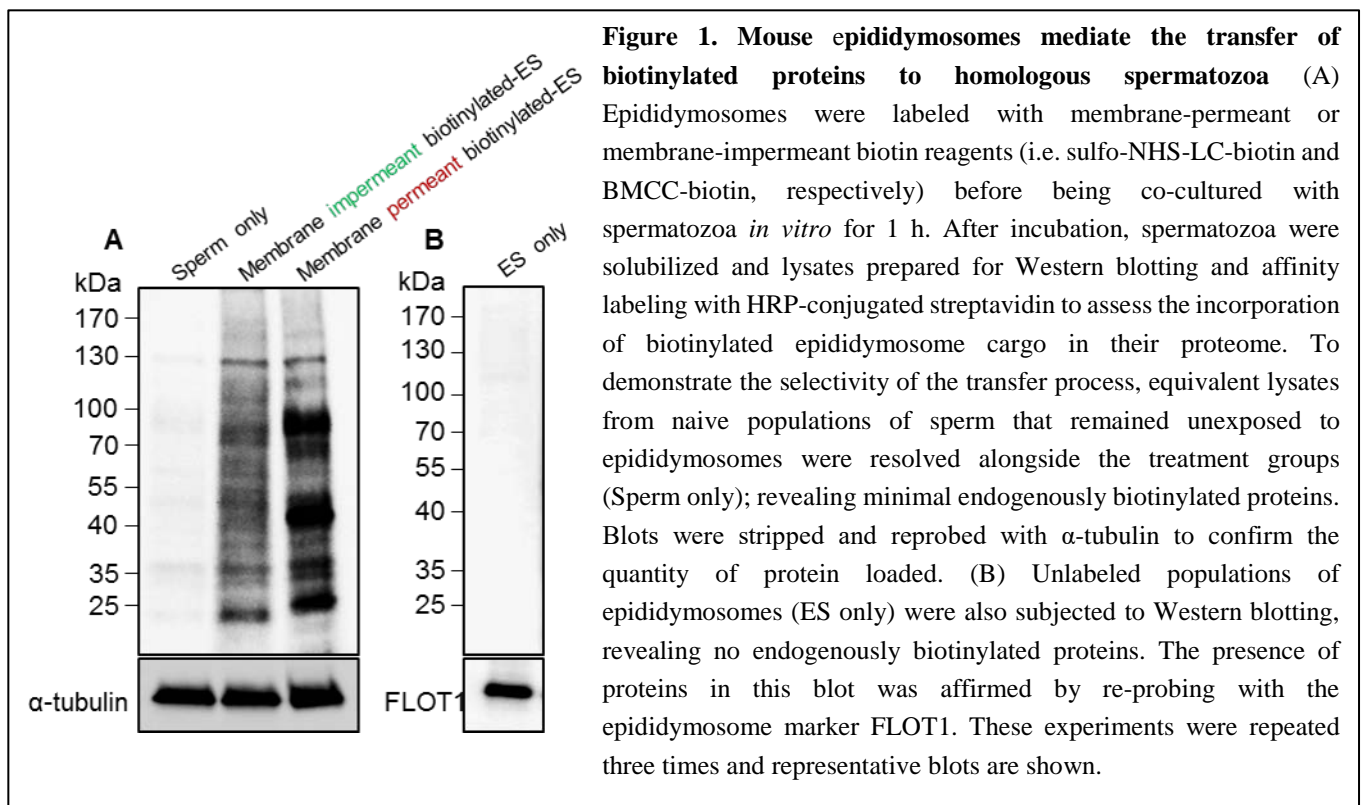
microdomains known as membrane or lipid rafts [23] have also been shown to play a role in coordinating the initial docking of sperm and epididymosome membranes [24], an interaction that results in the direct transfer of a subset of epididymosome raft-associated (i.e. glycosylphosphatidylinositol-linked) proteins into the cognate raft domains of the maturing sperm cell [2]. It is also conceivable that raft microdomains could facilitate the sequestration of complementary receptors / ligands and downstream fusion machinery within the respective epididymosome and sperm membranes to enable transfer of non-raft proteins. While this latter model of epididymosome-sperm interaction draws analogy with similar interactions recorded between exosomes and recipient somatic cells, much of the mechanistic detail remains elusive. This is particularly the case in species such as the mouse in which there are currently only limited reports of epididymosome characterization. In seeking to address this paucity of knowledge, here we report the use of an *in vitro* co-culture system to track the transfer of biotinylated protein cargo between mouse epididymosomes and recipient spermatozoa from the caput epididymis; the most active epididymal segment in terms of protein secretion and one that is of critical importance for promoting sperm maturation [21]. Moreover, we have utilized pharmacological inhibition strategies in an effort to characterize key elements of the sperm proteome responsible for the selective uptake of epididymosome cargo.

## RESULTS

### **Mouse caput epididymosomes selectively transfer biotinylated proteins to the head and mid-piece of homologous spermatozoa**

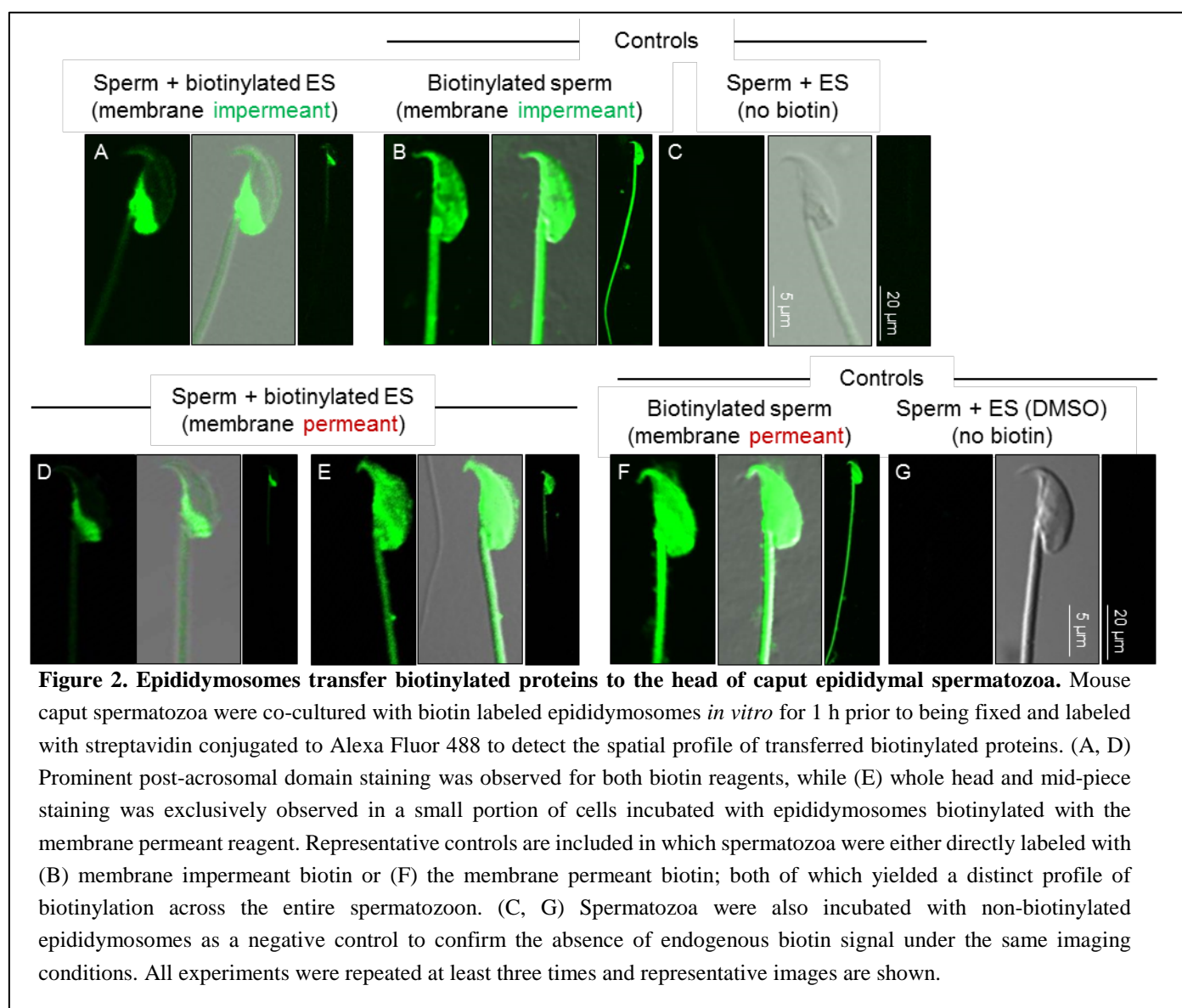
To begin to characterize the molecular mechanisms underpinning mouse epididymosome-sperm interactions we employed a previously optimized co-culture system [7] to track the transfer of biotinylated protein cargo to spermatozoa. For this purpose, both membrane impermeant (sulfo-NHS-LC-biotin) and membrane permeant (BMCC-biotin) reagents were applied to label the caput epididymosome proteome prior to their co-culture with isolated populations of caput spermatozoa. Thereafter, the efficacy of biotinylated protein transfer was assessed via affinity labeling of sperm lysates with streptavidin-HRP, revealing a substantive delivery of proteins ranging in size from ~15 – 150 kDa. As anticipated on the basis of their differential targeting of membrane vs whole epididymosome proteins, and reactivity toward primary amine (sulfo-NHS-LC-biotin) vs

sulfhydryl groups (BMCC-biotin), the profile of biotinylated epididymosome proteins transferred to the spermatozoa displayed marked differences (Fig. 1A). Indeed, as anticipated based on its propensity to label both membrane and encapsulated protein cargo, substantially more of the membrane permeant biotin appeared to be transferred to spermatozoa (Fig. 1A). These data confirm that caput epididymal spermatozoa are readily able to incorporate epididymosome proteins into their proteome after even a relatively brief period (i.e. 1 h) of *in vitro* co-culture. Attesting to the selectivity of this transfer process, we detected minimal endogenously biotinylated proteins within lysates prepared from either naïve populations of spermatozoa that had not encountered epididymosomes or within the epididymosomes themselves (Fig. 1B).



Having confirmed that mouse epididymosomes are capable of transferring proteins to caput spermatozoa, we next performed affinity labeling of the cells with streptavidin conjugated to Alexa Fluor 488 to determine the sperm domain(s) to which this cargo was targeted (Fig. 2). This analysis confirmed the selectivity of epididymosome-sperm interactions, with the post-acrosomal sheath of the sperm head serving as the dominant site for protein uptake after a 1 h co-incubation irrespective of the biotin labeling regimen used (Fig. 2A, D). In the case of epididymosomes subjected to membrane impermeant biotinylation (i.e. sulfo-NHS-LC-biotin), additional sperm labeling, albeit far less intense, was detected within the anterior domain of the head and mid-piece of the flagellum (Fig. 2A). Using the alternative pool of epididymosomes labeled with

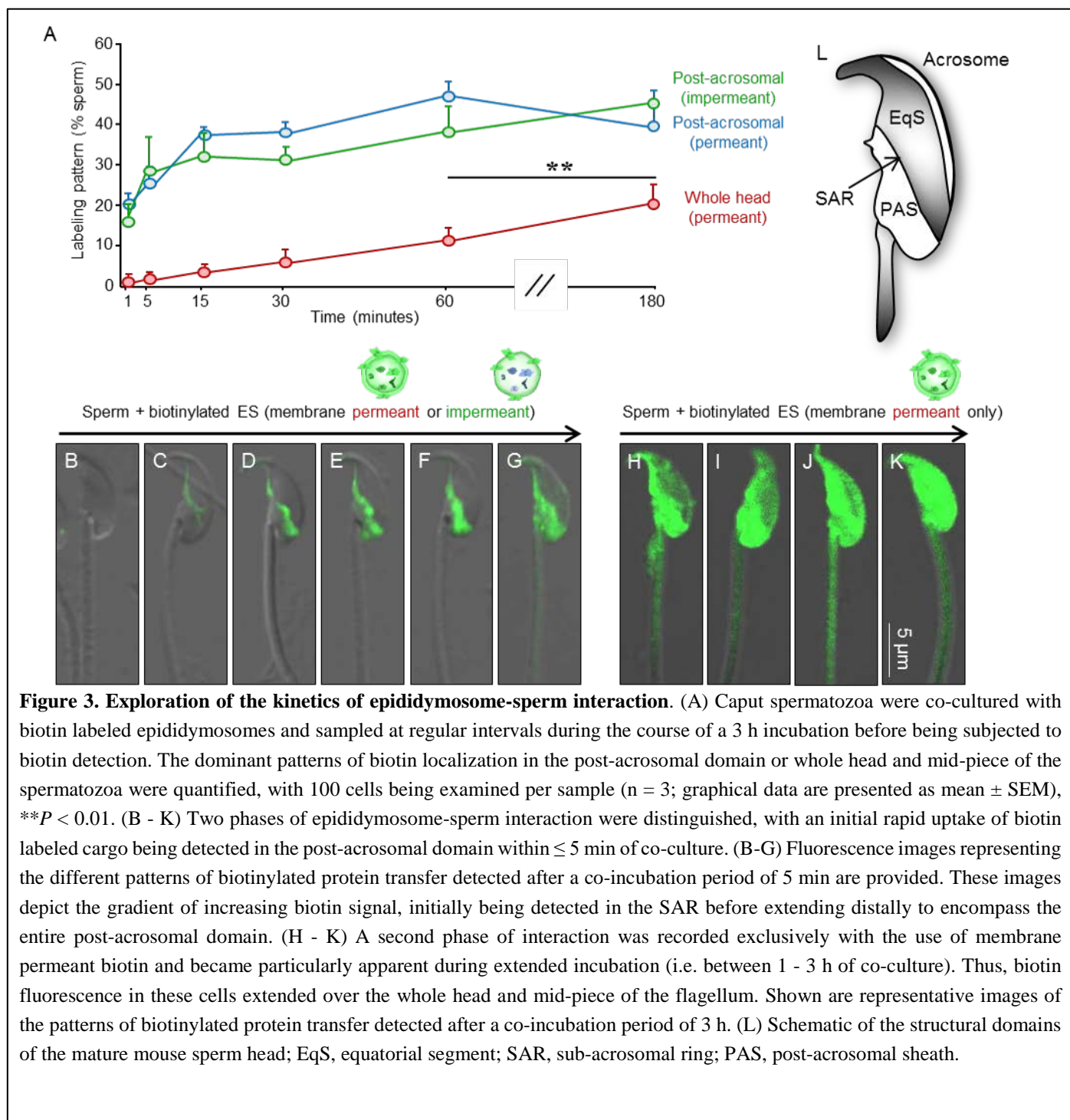
155 membrane permeant biotin (i.e. BMCC-biotin), ~10% of the spermatozoa presented with additional foci of intense labeling throughout the head and extending into the mid-piece of the flagellum (Fig. 2E). To discount the possibility of nonspecific labeling, spermatozoa were subjected to direct biotinylation, yielding a distinct pattern of labeling uniformly distributed across all sperm domains (i.e. head and flagellum) (Fig. 2B, F). Additionally, we failed to detect any endogenous biotin signal in sperm incubated with non-biotin-labeled epididymosomes (Fig. 2C, G).



160

**Caput epididymosome-sperm interactions can be discriminated into sequential adhesion and transient fusion / dispersal of cargo events**

In seeking to account for the appearance of additional diffuse localization of membrane permeant (but not impermeant) biotin throughout the sperm head and mid-piece, we elected to study the kinetics of protein transfer between caput epididymosomes and recipient caput spermatozoa. As shown in Fig. 3A, both forms of biotinylated protein were incorporated into the post-acrosomal sheath of the sperm head with similar overall kinetics and efficiency. Thus, within as little as 1 min of co-culture, ~16 - 20% of the sperm population displayed positive post-acrosomal sheath labeling. Thereafter, the percentage of positively labeled cells continued to gradually increase such that at 1 h of co-culture, ~40 - 50% of the sperm population were



170 characterized by positive post-acrosomal sheath labeling (Fig. 3A). In the case of epididymosome proteins  
labeled with the membrane impermeant (i.e. sulfo-NHS-LC-biotin), the post-acrosomal sheath appeared to be  
their final repository. Indeed, in the majority of cells, membrane impermeant biotin was not detected at  
appreciable levels in any alternative domains irrespective of extending the duration of co-incubation for up to  
3 h (i.e. only 3% of the cells featured whole head and mid-piece labeling after 3 h incubation, data not shown)  
175 (Fig. 3A). In marked contrast, spermatozoa incubated with the alternative pool of membrane permeant  
biotinylated epididymosomes (BMCC-biotin) experienced a reduction in post-acrosomal labeling between 1  
- 3 h of co-incubation. This apparent loss of post-acrosomal labeling was accompanied by a reciprocal increase  
in those cells displaying whole head and mid-piece labeling; effectively doubling to account for ~ 20% of the  
sperm population at 3 h compared to 10% at 1 h ( $P < 0.01$ , Fig. 3A).

180 On the basis of these data we infer that epididymosome-sperm interactions may encompass an  
adhesion event (detected by both forms of biotin transfer) followed by transient fusion and dispersal of cargo  
(detected by the membrane permeant biotin transfer only). To explore the validity of this model, we examined  
profiles of biotin labeling in spermatozoa isolated during both early (i.e. 5 min; Fig. 3B - G) and late phases  
(3 h; Fig. 3H - K) of co-incubation with epididymosomes. This analysis identified two putatively discrete  
185 stages of sperm-epididymosome interaction. Thus, during the early phases of co-incubation (1 min),  
biotinylated epididymosome proteins were mainly found to populate the sub-acrosomal ring (SAR; Fig. 3L)  
of the sperm head (similar to the image presented in Fig. 3C). This labeling pattern was however, replaced  
(within 5 min) as the majority of labeled sperm appeared to accumulate biotinylated proteins distally to the  
point where they eventually occupied the entire post-acrosomal sheath (representative images of this gradient  
of increasing labeling are depicted in Fig. 3D - G). Such staining characteristics were conserved between both  
190 forms of biotin utilized in this study. By contrast, the latter phases of co-incubation (3 h) saw a clear  
differentiation in terms of the fate of the epididymosome proteins. Thus, those proteins labeled with membrane  
impermeant biotin remained exclusively within the post-acrosomal sheath of the sperm head. The alternative  
sub-population of proteins labeled with membrane permeant biotin proceeded to undergo bidirectional  
195 dispersal into both the anterior region of the sperm head (equatorial segment and acrosomal domain) and mid-  
piece of the flagellum with similar overall kinetics (Fig. 3H - K). These data accord with those documented

during our previous application of carboxyfluorescein diacetate succinimidyl ester (CFSE), a dye that we have also traced from epididymosomes into the sperm head and mid-piece after 3 h co-incubation *in vitro* [7]. The lack of an equivalent dispersal when using membrane impermeant biotin, suggests this phenomenon may be restricted to proteins encapsulated within, as opposed to on the surface, of epididymosomes.

We elected to explore this possibility using a lipophilic dye PKH26, which incorporates directly into the membrane bilayer of the epididymosome. Following co-incubation of PKH26 labeled epididymosomes with spermatozoa, we documented a rapid transfer of the dye into the SAR of the sperm head (Fig. 4B - E). Thereafter, intense PKH26 labeling was documented throughout the post-acrosomal sheath (Fig. 4F - G). Notably, real-time imaging of live cells confirmed that both the spatial and temporal characteristics of

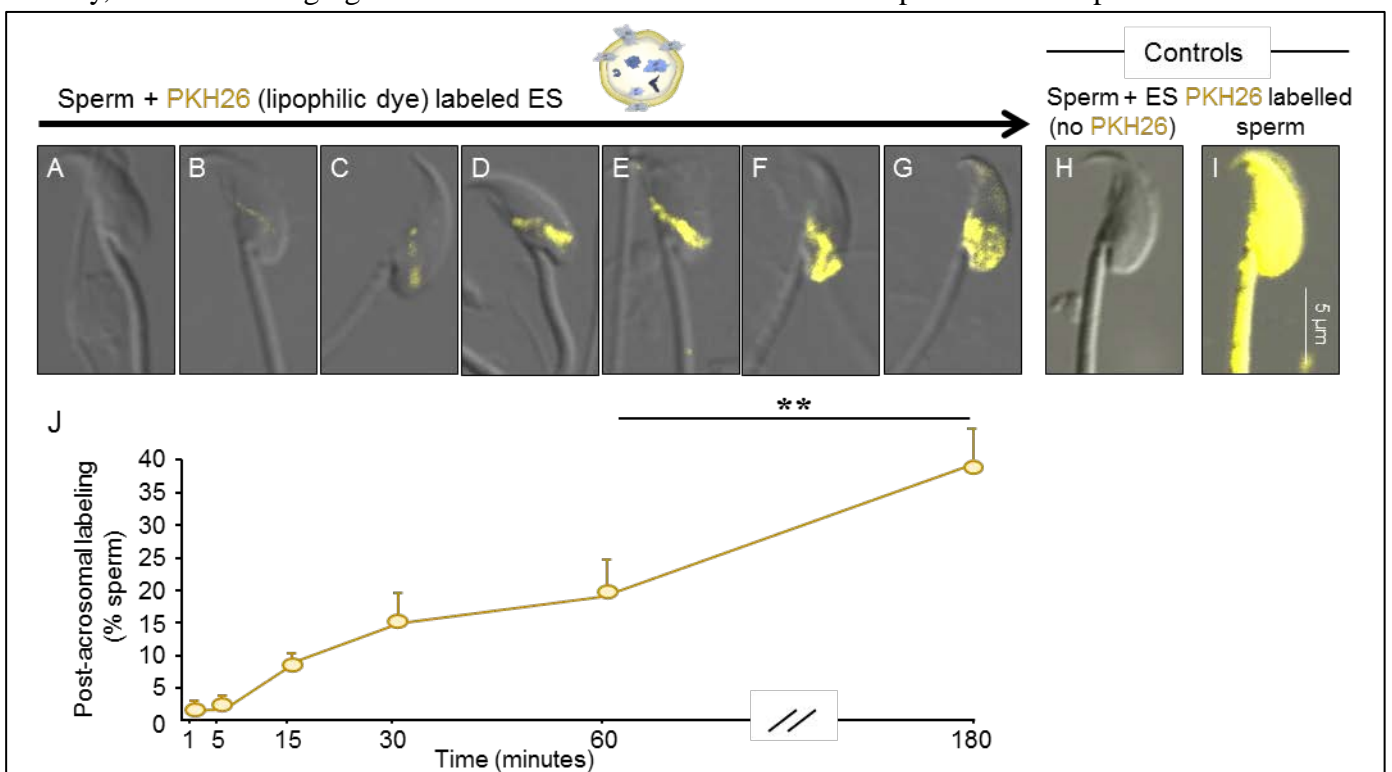


**Figure 4. Examination of the transfer of lipophilic dye (PKH26) between epididymosomes and spermatozoa.** (A - G) Caput spermatozoa were briefly co-cultured ( $\leq 5$  min) with populations of epididymosomes preloaded with the lipophilic dye, PKH26. After incubation spermatozoa, were washed and fixed prior to the analysis of PKH26 labeling profiles via immunofluorescence microscopy. Representative immunofluorescence images of different spermatozoa confirmed the incorporation of PKH26 dye, with staining patterns appearing broadly similar to those documented for proteins labeled with membrane impermeant biotin. That is, PKH26 labeled lipids were predominantly transferred to the SAR and post-acrosomal domain of the sperm. Representative controls were included in which spermatozoa were either (H) incubated with non-labeled epididymosomes to confirm no auto-fluorescence or alternatively, (I) directly labeled with PKH26 dye (independent of epididymosomes), which resulted in staining of the whole spermatozoon. (J) To examine the kinetics of PKH26 transfer, caput spermatozoa were co-cultured with PKH26 labeled epididymosomes and sampled at regular intervals during the course of a 3 h incubation. The dominant pattern of post-acrosomal labeling of the spermatozoa were quantified, with 100 cells being examined per sample ( $n = 3$ ; graphical data are presented as mean  $\pm$  SEM).  $**P < 0.01$ .

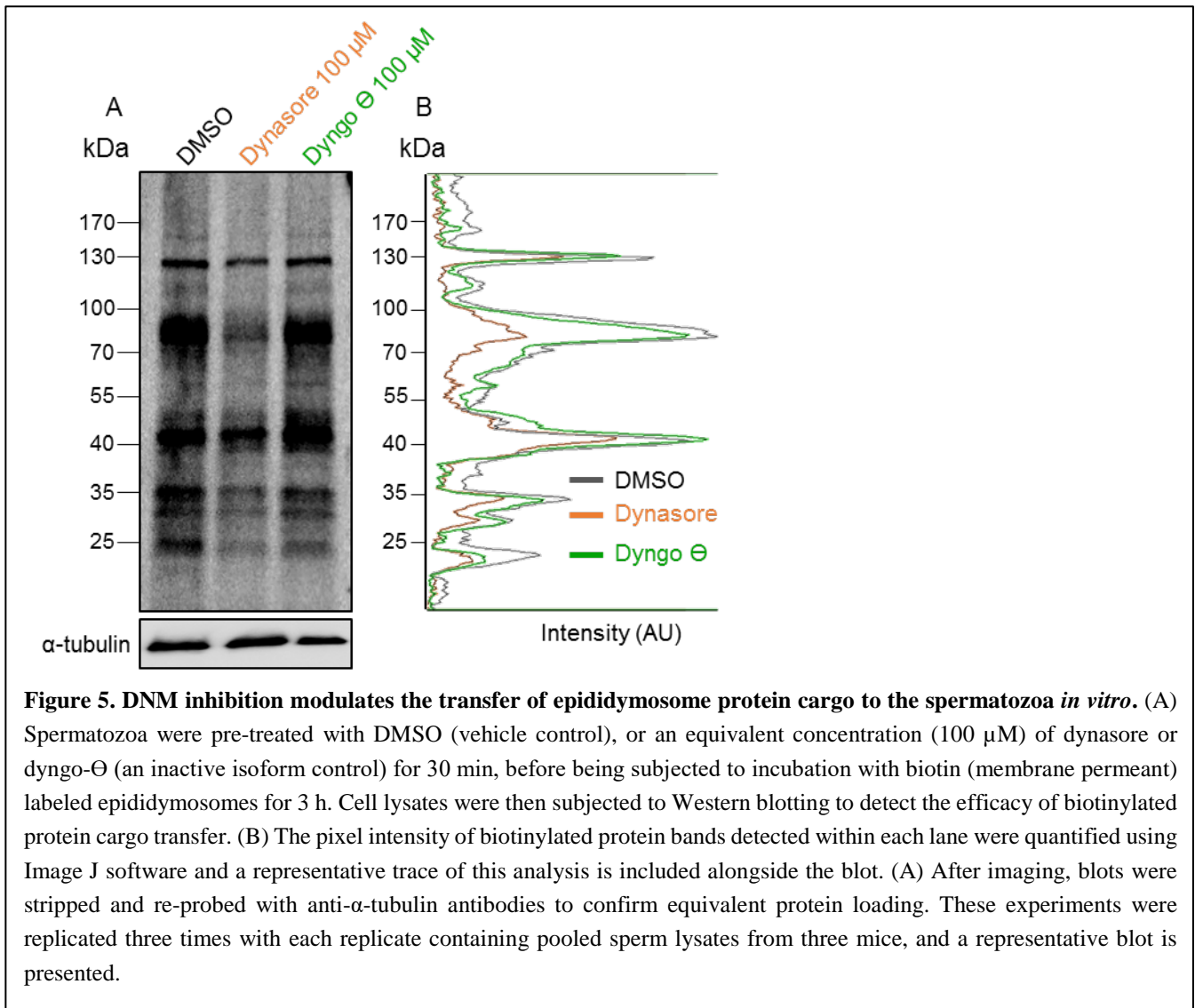
epididymosome-mediated transfer of PKH26 closely approximated those of the biotinylated epididymosome

proteins reported above (Additional file 1: Figure S1). An additional foci of PKH26 labeling was also detected within the anterior domain of the head, albeit far less intense than that of the post-acrosomal domain (Fig. 4G and Additional file 1: Figure S1). Moreover, while the initial transfer of PKH26 labeled lipids proceeded slower (Fig. 4J) than that recorded for biotinylated protein transfer (Fig 3A), the percentage of labeled spermatozoa proved equivalent after 3 h of co-culture. The specificity of epididymosome-mediated transfer of PKH26 labeling was confirmed by the absence of any endogenous fluorescence signals after co-incubation of sperm with non-labeled epididymosomes (Fig. 4H). By contrast, sperm labeled directly with PKH26 (i.e. in the absence of epididymosomes) readily incorporated the dye over their entire surface (Fig. 4I).

### **Dynamin mechanoenzymes are implicated epididymosome-mediated transfer of proteins to caput spermatozoa**

In view of the ability to differentiate caput epididymosome-sperm interactions into initial adhesion and downstream transient fusion events, we sought to capitalize on somatic cell literature implicating the dynamin (DNM) family of mechanoenzymes as master regulators of analogous forms of intercellular vesicle trafficking. As a caveat however, our previous work has established that the dynamin1 (DNM1) and dynamin2 (DNM2) isoforms, which are present in the mouse sperm proteome, appear to concentrate within the anterior acrosomal domain of the mature cell [25]; a location seemingly incompatible with the tethering of epididymosomes in the SAR / post-acrosomal domain. We therefore elected to track the efficacy of biotinylated epididymosome protein transfer to populations of spermatozoa that had been pre-incubated with Dynasore, a DNM inhibitor that targets DNM1 and DNM2 with equivalent efficacy, or Dyngo- $\Theta$ , an inactive isoform control. Since we anticipate that DNM would likely regulate epididymosome fusion, as opposed to adhesion, this study featured the use of membrane permeant biotin reagent for epididymosome labeling and was conducted over an incubation of 3 h to coincide with protein uptake and dispersal (Fig. 3H - K). This strategy revealed that pharmacological inhibition of DNM1 / DNM2 had no discernible impact on the ability of spermatozoa to incorporate biotinylated epididymosome proteins into their post-acrosomal domain, with ~40% of the cells displaying this pattern of labeling irrespective of the treatment group from which they originated (i.e. untreated, Dynasore or Dyngo- $\Theta$ ). By contrast, dynamin inhibition effectively halved the number of recipient

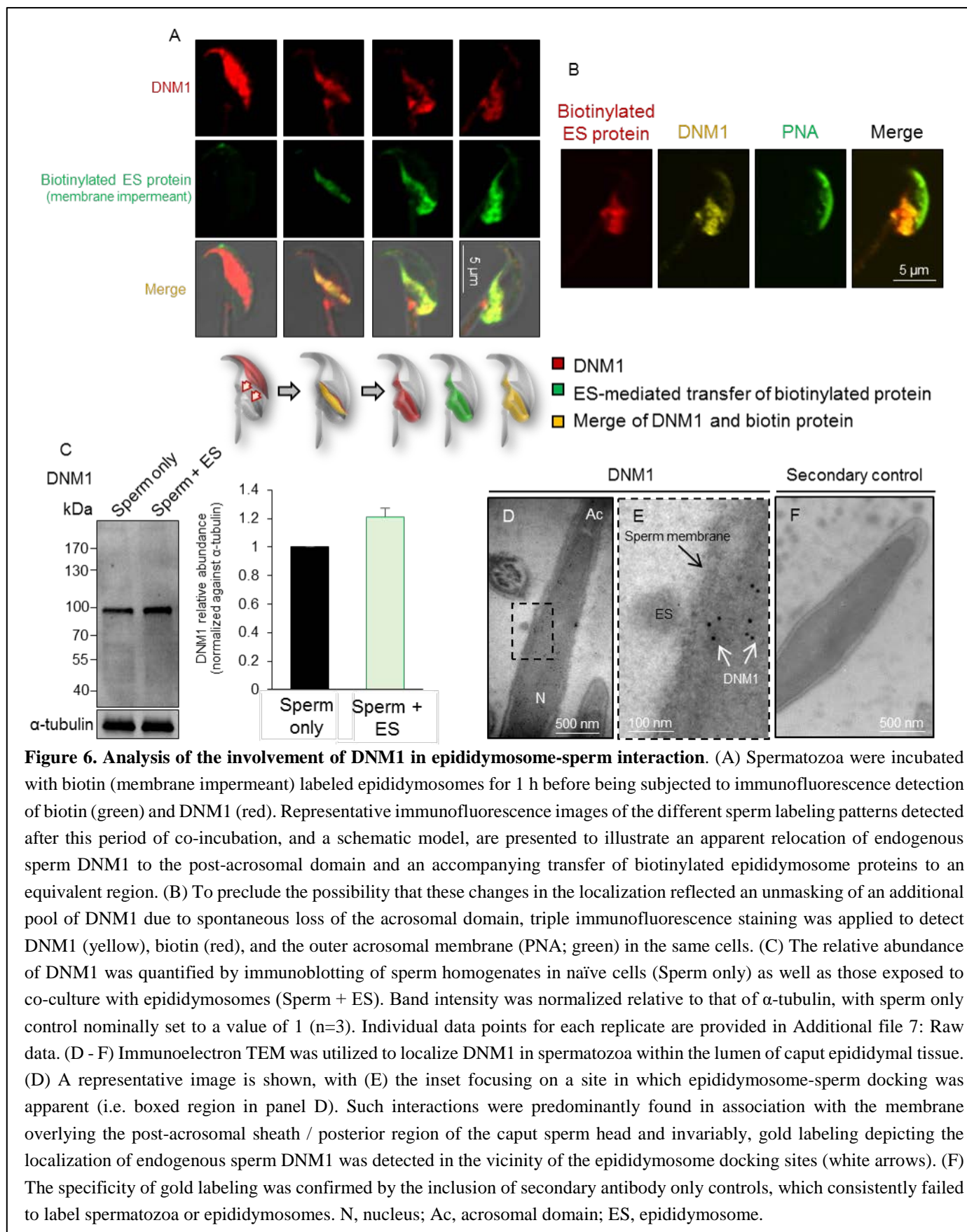
spermatozoa in which the biotinylated proteins were redistributed throughout the anterior region of the head and into the mid-piece of the tail (down from ~20% in the untreated group to ~10% in the Dynasore treatment group). Consistent with these data, densitometric quantification confirmed that dynamin inhibition significantly reduced, but did not eliminate, the transfer of biotinylated proteins from epididymosomes to spermatozoa (Fig. 5A, B). Importantly, no such reduction was witnessed in spermatozoa pre-treated with



Dyngo- $\Theta$ , thus precluding the possibility of non-specific pharmacological inhibition. Similarly, neither the DNM inhibitor nor the inactive isoform control had a detrimental impact on spermatozoa viability, which remain above 60% in all treatments.

Having implicated DNM-dependent mechanisms in the transfer of epididymosome cargo to spermatozoa, we next sought a more detailed characterization of DNM localization in the immature population of caput epididymal sperm used throughout this study.

*DNM1* - The DNMI protein was exclusively localized to the peri-acrosomal domain of naïve caput spermatozoa as well as those sampled immediately after the introduction of epididymosomes (Fig. 6A).



Unexpectedly however, DNMI was found to have undergone an apparent relocation; initially to the SAR

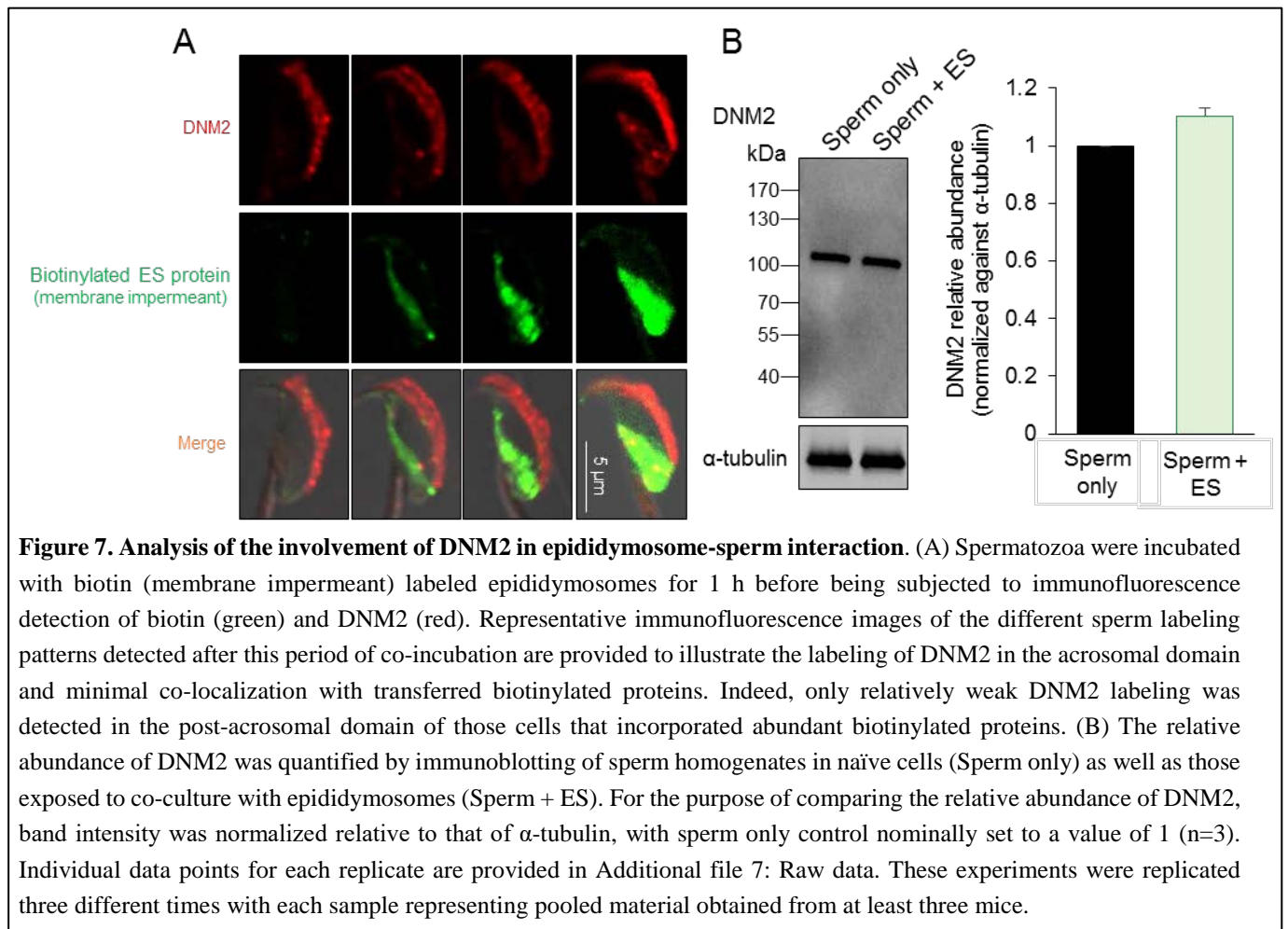
and thereafter to the post-acrosomal domain of sperm sampled at more advanced stages of co-incubation. Notably, the number of sperm experiencing these changes in DNMI localization mirrored those that had incorporated biotinylated epididymosome proteins (data not shown), prompting us to investigate the co-localization of DNMI and biotinylated proteins during representative stages of epididymosome protein transfer. With the exception of those cells in which DNMI was restricted to the anterior (peri-acrosomal) domain of the sperm head (and consequently displayed minimal biotin labeling), this strategy revealed strong overlapping distribution of DNMI and biotinylated epididymosome proteins (Fig. 6A). Illustrative of this, after 1 h of co-incubation with epididymosomes, ~3% and ~40% of spermatozoa displayed colocalization of DNMI and biotin labeling within either the sub-acrosomal ring or the post-acrosomal domain of the sperm head, respectively. To discount the possibility that DNMI under-representation in the peri-acrosomal domain was caused by the cells experiencing a premature or spontaneous loss of their acrosomal contents, triple immunofluorescence staining was applied to detect DNMI, biotin labeled epididymosome proteins and peanut agglutinin (PNA); a recognized marker of the outer acrosomal membrane (Fig. 6B). This analysis confirmed the co-localization of DNMI and biotin labeled protein in the post-acrosomal domain while PNA was clearly retained in the acrosomal domain, proving these cells possess an intact acrosome. As an additional control, we also investigated the relative levels of endogenous DNMI versus those present in the cell after co-incubation with epididymosomes. Densitometric analysis on the resultant immunoblots revealed no significant difference in DNMI levels in either cell population (Fig. 6C). Thus, despite the presence of DNMI in mouse epididymosomes (Additional file 2: Figure S2), the modest levels these vesicles contain are unlikely to account for the altered profile of DNMI labeling in sperm post-epididymosome incubation.

Having documented an apparent relocation of DNMI to coincide with the site of epididymosome adhesion in the post-acrosomal sheath, we next sought to strengthen the physiological relevance of this observation through the application of transmission immunoelectron microscopy to track DNMI localization during epididymosome-sperm interactions *in situ*. As shown in Fig. 6, we consistently observed epididymosome docking to the post-acrosomal sheath of the caput sperm head. Such events were commonly accompanied by immunogold labeling of endogenous sperm DNMI within the sperm vicinity of the membrane docking site. To preclude the possibility of non-specific labeling, sections were incubated with

secondary antibody only revealing no appreciable staining of the spermatozoa (Fig. 6F).

*DNM2* - Similar to *DNM1*, endogenous *DNM2* was also readily detected in the peri-acrosomal domain of caput spermatozoa (Fig. 7A). However, the *DNM2* isoform did not appear to undergo any pronounced change in location upon co-incubation with epididymosomes (Fig. 7A). In this context, only weak *DNM2* labeling was observed in the post-acrosomal sheath coinciding with those cells in which a substantial amount of biotinylated protein transfer was detected; raising the prospect that this additional pool of *DNM2* may have

280



been transferred to the cells as part of the epididymosome cargo. However, despite the detection of *DNM2* within caput epididymosomes (Additional file 2: Figure S2), densitometric analysis revealed only a modest, non-significant, increase in the abundance of *DNM2* before and after epididymosome co-incubation (Fig. 7B).

285

### ***DNM1* relocation is linked to lipid raft association**

To explore the mechanism(s) involved in the relocation of *DNM1* to a position compatible with regulation of epididymosome interaction, we elected to focus on lipid rafts, specialized membrane subdomains that have been implicated in the compartmentalization of proteins required for epididymosome docking to the sperm

290 surface [24, 26]. Strengthening the rationale for this approach, DNM contains a pleckstrin homology domain, which is commonly involved in the recruitment of proteins to specific membrane domains [27]. For these studies, we first characterized the localization of the abundant sperm lipid raft marker,  $G_{M1}$  ganglioside (via staining with Alexa Fluor 594 conjugated cholera toxin B subunit) [28], in naïve populations of caput spermatozoa as well as those exposed to in vitro epididymosome co-culture. This strategy revealed that lipid  
295 rafts were initially distributed throughout the head of caput spermatozoa, but that the pattern of  $G_{M1}$  localization was quite variable (Additional file 3: Figure S3). Notably, the subset of sperm presenting with diffuse labeling of  $G_{M1}$  throughout the whole head were generally refractory to the incorporation of biotinylated protein from epididymosomes (Fig. 8A). By contrast, we did document alternative  $G_{M1}$  labeling patterns, which were reminiscent of those observed for transferred epididymosomes proteins (Fig. 8B - E).

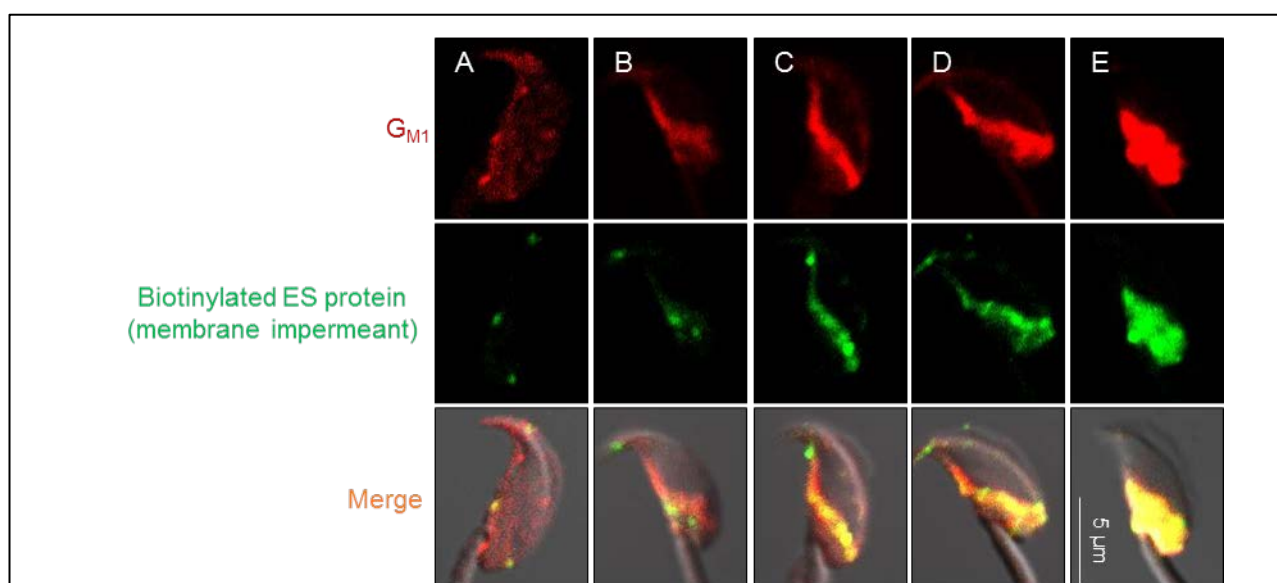


**Figure 8. Lipid raft microdomains facilitate epididymosome-sperm interaction.** The caput spermatozoa were co-cultured to biotinylated (membrane impermeant) epididymosomes for 5 min before being subjected to dual labeling for  $G_{M1}$  (lipid raft marker) and biotin (A – E). This strategy revealed spermatozoa harboring the anticipated spatial profiles of transferred biotinylated protein (green) and illustrated strong overlapping co-localization of  $G_{M1}$  (red) in these domains. Representative immunofluorescence images are presented to illustrate co-localization of  $G_{M1}$  and biotinylated protein in the SAR and post-acrosomal domain of the sperm head. These experiments were replicated three different times with each sample representing pooled material obtained from at least three mice.

300 Accordingly, strong overlapping co-localization of  $G_{M1}$  and biotinylated epididymosome proteins were detected in the SAR (Fig. 8C) and extending distally into the post-acrosomal sheath (Fig. 8E). Importantly, triple labeling of spermatozoa with  $G_{M1}$ , streptavidin conjugated to Alexa Fluor 488 and anti-DNM1 antibodies also confirmed strong co-localization of their respective targets (Fig. 9B). Based on these data we infer that the relocation of endogenous sperm DNM1 may be reliant on lipid raft association.

To test this hypothesis, spermatozoa were treated with methyl- $\beta$ -cyclodextrin (m $\beta$ CD) to sequester cholesterol and disrupt raft integrity [29] prior to their incubation with biotin-labeled epididymosomes. Triple immunofluorescence staining was then applied to detect DNMI, biotin labeled protein and G<sub>M1</sub> distribution. In the control group, we routinely observed ~35% - 40% of the spermatozoa with post-acrosomal labeling for biotin (Fig. 9A), and each of these cells also displayed strong colocalization with DNMI and G<sub>M1</sub> in the same domain (Fig. 9B). By contrast, m $\beta$ CD treatment disrupted lipid raft distribution, effectively preventing the accumulation of G<sub>M1</sub> within the post-acrosomal sheath (Fig. 9C). In parallel, we also documented a marked reduction in DNMI relocalization, with the protein instead being retained predominantly within the anterior peri-acrosomal domain of m $\beta$ CD treated spermatozoa (Fig. 9C); suggesting that lipid raft integrity is

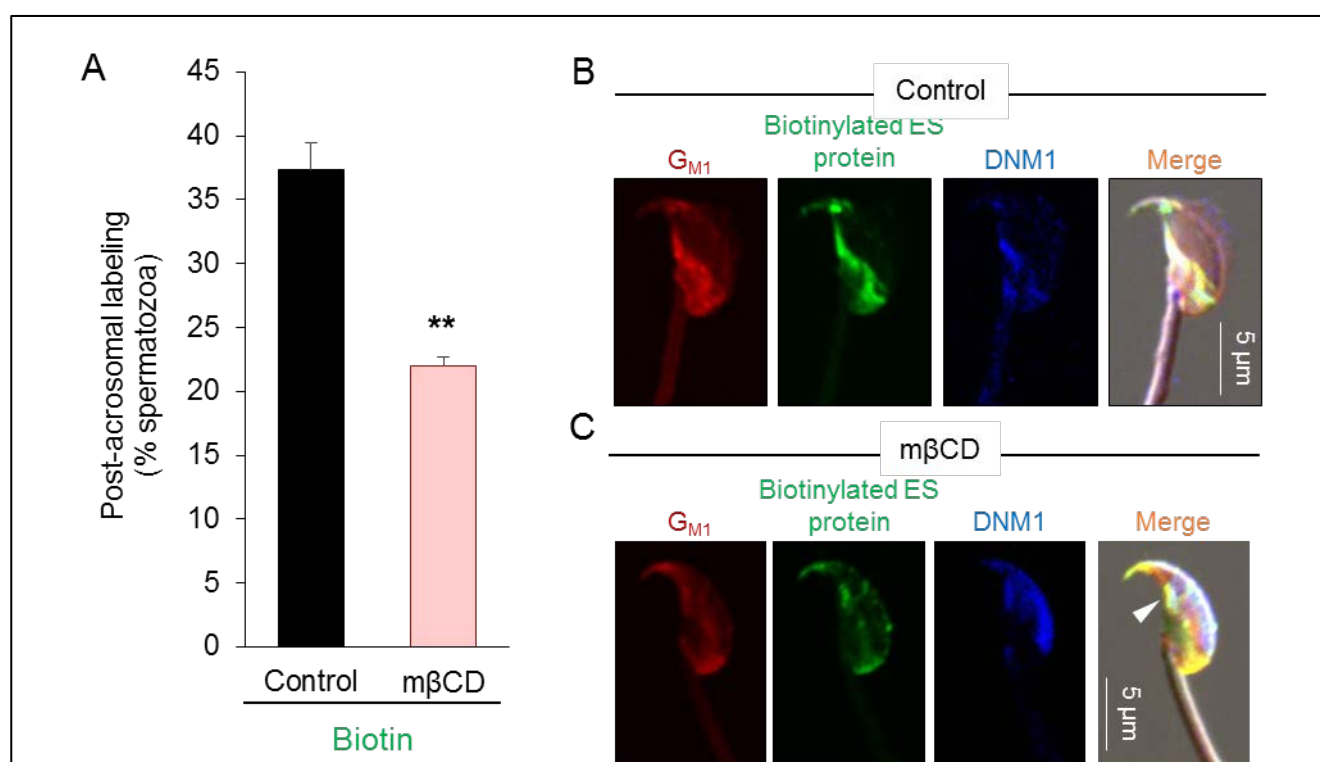


**Figure 9. Disruption of sperm lipid rafts compromises the efficacy of DNMI translocation and epididymosome-sperm interaction.** To examine the role of lipid rafts in mediation of epididymosome-sperm interactions, cells were pre-treated with m $\beta$ CD to sequester membrane cholesterol and disrupt lipid raft integrity. Thereafter, spermatozoa were incubated with biotinylated (membrane impermeant) epididymosomes for 1 h. Spermatozoa were then fixed and subjected to immunofluorescence detection. (A) A significant reduction in the number of cells with post-acrosomal biotin labeling was observed in spermatozoa pre-treated with m $\beta$ CD vs those of untreated controls. Post-acrosomal labeling was assessed in a minimum of 100 cells per treatment group, with these experiments being replicated three times. Each replicate comprised pooled material from at least three mice. The results are presented as the mean  $\pm$  S.E.M.  $**P < 0.01$  compared to control. Individual data points for each replicate are provided in Additional file 7: Raw data. (B, C) Representative immunofluorescence images of triple stained caput spermatozoa: G<sub>M1</sub> (red; rafts), biotin (green) and DNMI (blue). Compared to untreated control (B), m $\beta$ CD treatment (C) elicited a loss of raft integrity with G<sub>M1</sub> being heterogeneously dispersed throughout the sperm head. In these cells, DNMI was mainly retained in the acrosomal domain, but did display a tendency to co-localize with G<sub>M1</sub> and biotinylated proteins (white arrowheads).

indispensable for DNMI relocation. Such changes manifest in a significant ( $P < 0.01$ ) reduction in the efficacy  
315 of biotinylated epididymosome protein transfer to the post-acrosomal sheath compared to the untreated control  
group (Fig. 9A). Instead, biotinylated epididymosome proteins were distributed diffusely throughout the head  
of the m $\beta$ CD-treated spermatozoa, effectively mirroring the localization of G<sub>M1</sub> and thus adding further  
circumstantial evidence that lipid rafts do indeed facilitate epididymosome-sperm interactions. The specificity  
of triple immunofluorescence staining was confirmed by separate dual staining of two targets (all  
320 combinations for DNMI, biotin and G<sub>M1</sub>) through Alexa Fluor-488 and 594 fluorescence (data not shown).

## DISCUSSION

The epididymis fulfills an essential role in promoting sperm maturation and their subsequent storage via the  
creation of a complex intraluminal milieu, a key component of which are epididymosomes [30]. These small  
325 extracellular vesicles have attracted considerable attention owing to their important role in the transfer of  
fertility modulating proteins and regulatory classes of RNA to maturing spermatozoa [8]. To date however,  
little is known of the mechanistic basis by which epididymosomes deliver their cargo to the maturing sperm  
cell. In previous work, we have identified that the post-acrosomal domain of mouse spermatozoa represents  
the predominant site for initial epididymosome-sperm interaction [19]. Here, we have confirmed and extended  
330 these observations via the use of a combination of lipophilic fluorophores and biotinylation reagents (both  
membrane permeant and impermeant) to differentially label epididymosome cargo. This strategy has provided  
evidence that epididymosome-sperm interactions are likely resolved into two sequential phases. Thus, a rapid  
vesicular docking, which is primarily restricted to the SAR / post-acrosomal domain of the sperm head, is  
followed by a transient vesicular fusion. The latter presumably facilitates cargo delivery prior to its  
335 bidirectional dispersal into the anterior region of the sperm head and mid-piece of the flagellum. Moreover,  
our data demonstrate that endogenous DNMI is relocated to the post-acrosomal domain, through association  
with lipid rafts, to facilitate the transient fusion of epididymosome-sperm membranes.

Spermatozoa possess a unique membrane architecture, with the head of these cells being broadly  
divided into apical membrane, and post-acrosomal membrane, domains. Delimiting these two domains are  
340 topographical features known as the equatorial sub-segment (EqSS) and the SAR [31, 32]. Both of these

structures have been implicated as specialized diffusion barriers, which limit lateral mixing of membrane components and thus establish heterogeneous molecular compartments in the sperm head with discrete roles in the fertilization cascade [33, 34]. Indeed, it has been suggested that the dense cytoskeletal structure of the SAR restricts anterior movement of membrane lipids into the apical plasma membrane domain. Moreover, the EqSS, which is dynamically assembled during sperm descent through the caput epididymis (i.e. increases in prevalence from ~30% of testicular sperm to ~78% of caput epididymal spermatozoa) [35], serves as a putative organizing center responsible for the assembly of multimolecular complexes that contribute to fusion competence in this area of the plasma membrane [35]. While we remain uncertain as to why epididymosomes may preferentially interact with the SAR, the imposition of EqSS and SAR may account for the subsequent segregation of epididymosome membrane proteins (i.e. those labeled with membrane impermeant biotin) into the anterior post-acrosomal domain; a phenomenon recorded in our study that also bears striking resemblance to that of independent evidence in the bovine model [18]. The post-acrosomal sheath is formed during the latter stages of spermatogenesis [36] as the spermatid head undergoes elongation and flattening, with its components providing structural reinforcement to maintain the acrosomal and nuclear domains and notably, this region has also gained interest owing to its importance in initiating oocyte activation during mammalian fertilization [37, 38]. Thus, it has been argued that proteins selectively residing in the post-acrosomal sheath [e.g. post-acrosomal sheath protein WW domain-binding protein (PAWP)] enter the oocyte during fertilization and thereafter mediate meiotic resumption and oocyte activation [38, 39]. Such evidence provides a clear imperative for further investigation of the contribution of epididymosomes to establishing the proteomic specialization of both the plasma membrane overlying the post-acrosomal sheath as well as the cytoplasmic content of this domain.

Downstream of the rapid adhesion of epididymosomes to spermatozoa, which took place in as little as one minute of co-culture, we recorded a more gradual, bi-directional transferal of biotinylated epididymosome proteins into the anterior region of the sperm head and the mid-piece of the flagellum. Notably however, this phenomenon was restricted to the use of the membrane permeant biotin reagent, which would be expected to label both the epididymosome membrane and encapsulated cargo. This staining pattern was reminiscent of that achieved following co-incubation of mouse spermatozoa with epididymosomes preloaded with CFSE, an

amine reactive dye that undergoes intracellular catalytic conversion into a highly fluorescent tracer with a propensity to form stable conjugates with proteins [7]. It is also more in keeping with independent reports that dye-labeled mouse epididymosomes can deliver the dye to the acrosomal domain of the head and mid-piece of the flagellum, albeit in caudal spermatozoa [24]. On the basis of these data, we infer that vesicular docking may precede internalization and redistribution, of at least a portion of the epididymosome cargo, to their sites of action in the maturing sperm cell. Whilst the precise details of how sperm achieve this internalization have yet to be completely resolved, evidence is mounting for a transient fusogenic mechanism between the respective epididymosome and sperm membranes. Indeed, there is general consensus that spermatozoa lack the machinery to participate in endocytosis, as is commonly witnessed in exosome-somatic cell interactions. Rather, elegant imaging techniques such as super-resolution structured illumination microscopy [40] and transmission immunoelectron microscopy have revealed compelling evidence for the formation of fusion stalk-like projections forming at sites of interaction between epididymosomes and spermatozoa. Moreover, proteomic analyses of epididymosomes, and spermatozoa themselves, have identified a myriad of complementary trafficking proteins [e.g. soluble N-ethylmaleimide-sensitive factor activating protein receptor (SNARE) proteins, Ras-like proteins and DNM] as might be expected in fusogenic competent vesicles / cells [16, 19, 22, 25].

One such family of proteins that we have investigated here is that of DNM, mechanoenzymes that have been implicated in a variety of vesicular trafficking pathways [25, 41]. While DNM has been best studied in the context of regulating clathrin-coated endocytosis [42], it has also been implicated in clathrin independent pathways. Notably, these pathways include that of a “kiss and run” model that is compatible with the transient fusogenic mechanism proposed for epididymosome-sperm interaction. Within this model, DNM is held to polymerize into large oligomeric helices, which stabilize the formation of the vesicular fusion pores and thus regulate the release of their cargo [43]. Indeed, our recent ultrastructural data has revealed evidence for the formation of stalk-like projections at the site of epididymosome-sperm interaction [19]; a classic template attracting DNM to polymerize into rings / helices [44]. As an important precedent for our own findings implicating DNM in epididymosome fusion, independent work has confirmed a role of DNM in regulating exosome interaction with recipient cells such as B lymphocytes [45]. In this context, pharmacological

395 inhibition of DNM (i.e. Dynasore) led to an impressive ~88% reduction in exosome uptake [45]. Similarly, DNM has also been shown to exert influence over the exosome receptivity of hepatic stellate and placental trophoblast cells [46, 47], with its inhibition leading to a pronounced suppression of their downstream functionality. Also, compatible with our own data is the notion that DNM-mediated regulation of exosome interaction is intimately tied to lipid rafts and their associated proteins [45].

400 Indeed, one of the most intriguing findings of our study was the demonstration that DNM1 is repositioned to the post-acrosomal sheath where epididymosome interacting with the spermatozoa during co-culture. Our collective evidence suggests that such relocation is mediated, at least in part, by DNM1 association with lipid rafts; with the depletion of membrane cholesterol causing a chain of lipid raft disruption, inhibition of DNM1 translocation and reduction in the efficacy of epididymosome cargo incorporation into  
405 the sperm proteome. A particular curiosity of this response is the fact that the caput spermatozoa sourced for *in vitro* co-culture had already encountered epididymosomes *in vivo*. How these cells retain DNM1 in their peri-acrosomal domain after isolation, yet reposition the protein following exposure to an exogenous supply of epididymosomes, remains a perplexing question for which we can only speculate on the answer. One possible explanation for these dichotomous results is that DNM1 translocation is a dynamic event, such that  
410 the removal of spermatozoa from the epididymal luminal environment in which they are normally extremely highly concentrated, leads to an attendant loss of the stimulus that drives DNM1 localization. In seeking to reconcile this model, our transmission immunoelectron microscopy data revealed that DNM1 is almost exclusively localized to the post-acrosomal domain of spermatozoa *in situ*. Additionally, elegant studies by Jones and colleagues have shown that mammalian spermatozoa exhibit a mechanosensitive response that  
415 serves to concentrate important molecules to appropriate sites on the sperm surface [48]. Specifically, porcine spermatozoa experienced a phenomenon referred to as ‘contact induced coalescence’, whereby physical contact such as that experienced during sperm agglutination, promoted a rapid repositioning of lipid rafts; away from the apical ridge overlying the acrosome and clustering at the sites of contact [48]. By analogy, it is tempting to speculate that an equivalent diffusion of rafts may have been triggered via adhesion of excess  
420 epididymosomes to the post-acrosomal domain of cultured spermatozoa, bringing with them essential fusion machinery such as DNM1. However, the validity of this model awaits further investigation, as does the finding

that DNM2 fails to undergo a similar relocation; instead remaining within the peri-acrosomal domain of caput spermatozoa during epididymosome co-culture.

These findings contrast the overlapping localization and functions of DNM1 and DNM2 that have been reported in somatic cells [49]. Nevertheless, despite sharing 80% sequence identity, DNM1 and DNM2 have previously been implicated in discrete functional roles within the male reproductive system. Thus, selective ablation of DNM2 leads to an age-dependent loss of spermatogonia in the mouse testis [50]. Similarly, DNM2 is under-represented, and linked a reduced ability to complete acrosomal exocytosis, in poor quality human spermatozoa [3]. In both scenarios, DNM1 expression is unchanged yet fails to compensate for the loss of DNM2. Based on these data, we infer that DNM1 may be involved in the regulation of epididymal maturation (i.e. regulating epididymosome-sperm interactions), while DNM2 participates in early germ cell development and the downstream functional activation of the mature spermatozoon. It will be of interest to determine whether this specificity is mediated by unique protein- interaction networks.

## CONCLUSIONS

In summary, this study has provided mechanistic insights into epididymosome-sperm interactions, revealing both the spatial and temporal specificity of this process. Such specificity is mediated, at least in part, via the action of lipid rafts owing to their ability to concentrate important molecules to sites of epididymosome interaction. Moreover, we have identified a novel role for vesicle trafficking machinery such as the DNM1 mechanoenzyme, which is likely to support / stabilize the formation of transient fusion pores compatible with the delivery of epididymosome cargo. As an important caveat however, our study is based on the application of an *in vitro* co-culture system and we therefore encourage caution in direct extrapolation of our model of epididymosome-sperm interactions to the equivalent events occurring *in situ* within the epididymal lumen. Further studies aimed at overcoming these limitations and resolving how the proteomic inventory that epididymosomes convey to spermatozoa are able to modulate their function are now warranted if we are to realize the diagnostic and therapeutic potential of these insights.

## METHODS

## **Antibodies and reagents**

450 Unless otherwise stated, chemicals were purchased from Sigma-Aldrich (St. Louis, MO, USA) or Thermo Fisher Scientific (Waltham, MA, USA) and were of molecular biology or research grade. Full details of the primary and secondary antibodies used throughout this study are reported in Additional file 4: Table S1.

## **Mouse epididymosome isolation and characterization**

455 Highly enriched populations of mouse caput epididymosomes were isolated and validated as previously described [7, 51]. Briefly, adult male mice (8-12 weeks old) were euthanized and immediately perfused with pre-warmed phosphate buffered saline (PBS) to minimize the possibility of blood contamination. Caput epididymides were then removed, separated from fat and connective tissue and rinsed with modified Biggers, Whitten, and Whittingham media (BWW; pH 7.4, osmolarity 300 mOsm/kg) [52] before being pooled; the  
460 number of pooled epididymides was adjusted in accordance with the downstream application (please see details provided in relation to each protocol), but generally incorporated tissue from at least three mice. Following incisions with a razor blade, luminal contents were allowed to disperse into the BWW media and filtered through a 70  $\mu$ m membrane. The resultant suspension was sequentially centrifuged with increasing velocity at 4 °C (500  $\times$  g, 5 min; 2,000  $\times$  g, 5 min; 4,000  $\times$  g, 5 min; 8,000  $\times$  g, 5 min; 17,000  $\times$  g, 20 min; and  
465 finally 17,000  $\times$  g for an additional 10 min) to eliminate all cellular debris. The supernatant was layered onto a discontinuous OptiPrep gradient (40%, 20%, 10%, and 5%), diluted with a solution of 0.25 M sucrose, 10 mM Tris. Density gradients were ultracentrifuged (160,000  $\times$  g, 18 h, 4 °C) after which twelve equivalent fractions were collected and diluted in PBS before being subjected to a final ultracentrifugation (100,000  $\times$  g, 3 h, 4 °C). Epididymosomes were subsequently collected from fractions 9 and 10 and characterized in  
470 accordance with the minimal experimental requirements for the definition of extracellular vesicles [53], featuring analysis of their purity and overall homogeneity, as previously described (Additional file 5: Figure S4) [7]. After assessment, pooled preparations of epididymosomes were apportioned between the different experimental treatment groups as described below.

475 **Transfer of epididymosome protein cargo to mouse spermatozoa**

Following isolation, caput epididymosomes were resuspended in PBS. Two different biotin reagents were then applied to label either the subset of membrane-accessible epididymosome proteins (i.e. membrane impermeant EZ-Link sulfo-NHS-LC-Biotin, Thermo Fisher Scientific) or those residing in both the membrane and encapsulated within the epididymosome (i.e. membrane permeant EZ-Link BMCC-Biotin, Thermo Fisher Scientific) with the use of both biotin reagents conforming to manufacturer's recommendations. Biotinylation reactions were conducted for 30 min at room temperature followed immediately by overnight incubation at 4 °C. As a vehicle control for the use of membrane permeant BMCC-biotin, a population of epididymosomes were prepared with an equivalent volume of vehicle [Dimethyl sulfoxide (DMSO)]. Following incubation, epididymosome suspensions were diluted into 50 mM glycine / PBS to quench the biotinylation reaction and excess biotin was removed via ultracentrifugation ( $100,000 \times g$ , 18 h, 4 °C). The resultant biotinylated epididymosome pellets were suspended in modified BWW in preparation for co-incubation with caput epididymal spermatozoa; isolated as previously described [54]. Treatment groups included spermatozoa pre-incubated with either: (i) 0.5 mM m $\beta$ CD; to sequester membrane cholesterol and thereby disrupt membrane rafts [29] for 1 h, (ii) 100  $\mu$ M Dynasore (inhibits DNM1 and DNM2 with equivalent efficacy) for 30 min, or (iii) 100  $\mu$ M Dyngo- $\Theta$  (an inactive analogue of Dynasore) for 30 min. Unless otherwise stated, biotinylated epididymosomes were added at a ratio of 1:1 (i.e. pooled epididymosomes isolated from three mice were subdivided into three equivalent fractions, and one of these fractions was incubated with spermatozoa isolated from a single mouse). Co-incubations were conducted in an atmosphere of 5% CO<sub>2</sub> using the conditions specified in each figure legend. After incubation, cells were washed three times by gentle centrifugation ( $500 \times g$ , 3 min) in modified BWW to remove any unbound or loosely adherent epididymosome, before being subjected to 4% paraformaldehyde (PFA) fixation (for immunofluorescent staining) or protein extraction (for silver stain or immunoblotting as previously described) [41]. Controls for these experiments included spermatozoa directly labeled with both biotin reagents (i.e. in the absence of any epididymosomes) to discriminate the specificity of epididymosome-mediated protein delivery, as well as spermatozoa incubated with unlabeled epididymosomes in order to control for the possibility of endogenous biotin expression.

### **Transfer of lipophilic dyes between epididymosomes and spermatozoa**

A PKH26 Fluorescent Cell Linker Mini Kit (MINI26, Sigma-Aldrich) was used to label epididymosome membranes. For this purpose, caput epididymosomes (from 3 mice) were resuspended in 0.5 ml Diluent C and incubated with PKH26 (2  $\mu$ l dye diluted into 0.5 ml Diluent C, then mixed 1:1 with epididymosomes suspension) for 2 min at room temperature with gentle agitation; thereby achieving irreversible labeling of the epididymosome lipid bilayer. After incubation, excess PKH26 dye was quenched by adding 1 ml of 1% bovine serum albumin (BSA) / PBS and suspensions were ultracentrifuged ( $100,000 \times g$ , 3 h, 4 °C) to pellet PKH26 labeled epididymosomes. Isolated caput epididymal spermatozoa were co-incubated with PKH26 labeled epididymosomes under identical conditions to those described for biotin labeled epididymosomes. The spermatozoa were then split into two equivalent samples, which were subjected to either confocal time-lapse imaging or 4% PFA fixation (for preservation and later-stage imaging). Additional controls were included in which spermatozoa were either directly labeled with PKH26 or incubated with unlabeled, Diluent C treated epididymosomes (negative control).

#### **Affinity and immunofluorescent labeling of spermatozoa**

Following incubation, spermatozoa were preloaded with Alexa Fluor 594 conjugated cholera toxin B subunit at 37 °C for 30 min to selectively label the abundant sperm lipid raft marker,  $G_{MI}$  ganglioside (if applicable). After that, cells were fixed in 4% PFA, washed in 50 mM glycine / PBS and settled onto poly-L-lysine treated coverslips at 4 °C overnight. They were then permeabilized with ice-cold methanol for 10 min and blocked with 3% BSA in PBS at 37 °C for 1 h. Coverslips were then incubated with primary antibodies at 4°C overnight (for specific dilution rates of all antibodies see Additional file 4: Table S1). After three washes in PBS, coverslips were incubated with appropriate secondary antibodies or streptavidin conjugated to Alexa Fluor 488 at 37 °C for 1 h. Following additional washes in PBS, cells were counterstained with FITC-conjugated PNA (1 mg/ml) at 37°C for 15 min (if applicable). Coverslips were then mounted in 10% Mowiol 4-88 (Merck Millipore, Darmstadt, Germany) with 30% glycerol in 0.2 M Tris (pH 8.5) and 2.5% 1,4-diazabicyclo-(2.2.2)-octane. Confocal microscopy (Olympus IX81) was used for detection of fluorescent-labeling patterns with settings for excitation and emission filters being provided in Additional file 6: Table S2.

530 **Electron microscopy**

Mouse caput epididymal tissue was fixed in 4% (w/v) PFA containing 0.5% (v/v) glutaraldehyde. The tissue was then processed via dehydration, infiltration, and embedding in LR White resin. Sections (100 nm) were cut with a diamond knife (Diatome Ltd., Bienne, Switzerland) on an Ultracut S microtome (Reichert-Jung, Leica; Solms, Germany) and placed on 150-mesh nickel grids. For DNMI detection, sections were blocked in 3% (w/v) BSA in PBS (30 min at 37 °C). Subsequent washes were performed in PBS (pH 7.4) containing 1% BSA. Sections were sequentially incubated with anti-DNMI antibodies (overnight at 4 °C), and an appropriate secondary antibody conjugated to 10 nm gold particles (2 h at 37 °C). Labeled sections were then counterstained in 1% (w/v) uranyl acetate. Micrographs were taken on a JEOL 1200 EX II transmission electron microscope (JEOL, Japan) at 80 kV.

540

**Statistical analyses**

All experiments were replicated a minimum of three times, with pooled samples of spermatozoa and epididymosomes having been obtained from at least three male mice. For the purpose of assessing biotin labeling profiles,  $\geq 100$  spermatozoa were counted in each sample through blind assessment (with treatment conditions having been replaced with a random number) and the corresponding percentage of cells with post-acrosomal domain or whole head / mid-piece labeling was determined. Densitometric analyses of immuno/affinity blots were conducted using Image J software (version ImageJ2) [55]. Graphical data are presented as mean values  $\pm$  SEM, which were calculated from the variance between samples. Statistical significance was determined by using one-way ANOVA with a significance threshold of  $P < 0.05$ .

550

## LIST OF ABBREVIATIONS

BSA	bovine serum albumin
BWW	Biggers, Whitten, and Whittingham media
CFSE	carboxyfluorescein diacetate succinimidyl ester
555 DMSO	Dimethyl sulfoxide
DNM	dynamain
DNM1	dynamain 1
DNM2	dynamain 2
EqS	equatorial segment
560 EqSS	equatorial sub-segment
m $\beta$ CD	methyl- $\beta$ -cyclodextrin
MFGE8	Milk fat globule-EGF factor 8 protein
PAWP	post-acrosomal sheath protein WW domain-binding protein
PBS	phosphate buffered saline
565 PFA	paraformaldehyde
PNA	peanut agglutinin
SAR	sub-acrosomal ring
SNARE	Soluble N-ethylmaleimide-sensitive factor activating protein receptor
sncRNA	small non-coding RNAs

## **DECLARATIONS**

### **Ethics approval and consent to participate**

All experimental procedures involving animals were conducted with the approval of the University of Newcastle's Animal Care and Ethics Committee (approval number A-2013-322), in accordance with the Society for the Study of Reproduction's specific guidelines and standards. Inbred Swiss mice were housed under a controlled lighting regime (16L: 8D) at 21–22 °C and supplied with food and water *ad libitum*. Prior to dissection, animals were sacrificed via CO<sub>2</sub> inhalation.

### **Availability of Data and Materials**

All data generated during this study are included in either the published article or its Additional files. Raw data for Figs. 6, 7, and 9 can be found in 'Additional file 7: Raw data'.

### **Consent for publication**

All authors have given consent for publication.

### **Competing interests**

The authors declare that they have no conflicts of interest.

### **Funding**

This work was supported by National Health and Medical Research Council of Australia Project Grants: APP1103176, awarded to BN and EAM, and APP1147932, awarded to BN and MDD.

### **Authors' contributions**

WZ conducted the experiments and generated the manuscript. SJS and ALA provided technical assistance. GNDI, EAM and MDD contributed to study conception and design, data interpretation and manuscript editing. AM provided Dyngo- $\Theta$ , the instruction of the usage of DNM inhibitor. BN conceived of this study and

contributed to study design, data interpretation, and manuscript preparation. All authors have approved the final version and submission of this article.

600

## Acknowledgments

The authors would like to thank Electron Microscope and X-Ray Unit from the University of Newcastle for providing technical support for electron microscopy analysis.

## 605 REFERENCES

1. Hermo L, Jacks D. Nature's ingenuity: bypassing the classical secretory route via apocrine secretion. *Mol Reprod Dev.* 2002; 63(3):394-410.
2. Sullivan R, Frenette G, Girouard J. Epididymosomes are involved in the acquisition of new sperm proteins during epididymal transit. *Asian J Androl.* 2007; 9(4):483-91.
- 610 3. Zhou W, Anderson AL, Turner AP, De Iuliis GN, McCluskey A, McLaughlin EA, Nixon B. Characterization of a novel role for the dynamin mechanoenzymes in the regulation of human sperm acrosomal exocytosis. *Mol Hum Reprod.* 2017; 23(10):657-73.
4. Eickhoff R, Baldauf C, Koyro H-W, Wennemuth G, Suga Y, Seitz J, Henkel R, Meinhardt A. Influence of macrophage migration inhibitory factor (MIF) on the zinc content and redox state of protein-bound sulphhydryl groups in rat sperm: indications for a new role of MIF in sperm maturation. *Mol Hum Reprod.* 2004; 10(8):605-11.
- 615 5. Frenette G, Girouard J, Sullivan R. Comparison between epididymosomes collected in the intraluminal compartment of the bovine caput and cauda epididymidis. *Biol Reprod.* 2006; 75(6):885-90.
6. Kirchhoff C, Hale G. Cell-to-cell transfer of glycosylphosphatidylinositol-anchored membrane proteins during sperm maturation. *Mol Hum Reprod.* 1996; 2(3):177-84.
- 620 7. Reilly JN, McLaughlin EA, Stanger SJ, Anderson AL, Hutcheon K, Church K, Mihalas BP, Tyagi S, Holt JE, Eamens AL. Characterisation of mouse epididymosomes reveals a complex profile of microRNAs and a potential mechanism for modification of the sperm epigenome. *Sci Rep.* 2016; 6:31794.
8. Sharma U, Conine CC, Shea JM, Boskovic A, Derr AG, Bing XY, Belleannée C, Kucukural A, Serra RW, Sun F. Biogenesis and function of tRNA fragments during sperm maturation and fertilization in mammals. *Science.* 2015; 351(6271):391-6.
- 625 9. Belleannée C, Calvo É, Caballero J, Sullivan R. Epididymosomes convey different repertoires of microRNAs throughout the bovine epididymis. *Biol Reprod.* 2013; 89(2):30.
10. Hutcheon K, McLaughlin EA, Stanger SJ, Bernstein IR, Dun MD, Eamens AL, Nixon B. Analysis of the small non-protein-coding RNA profile of mouse spermatozoa reveals specific enrichment of piRNAs within mature spermatozoa. *RNA Biol.*

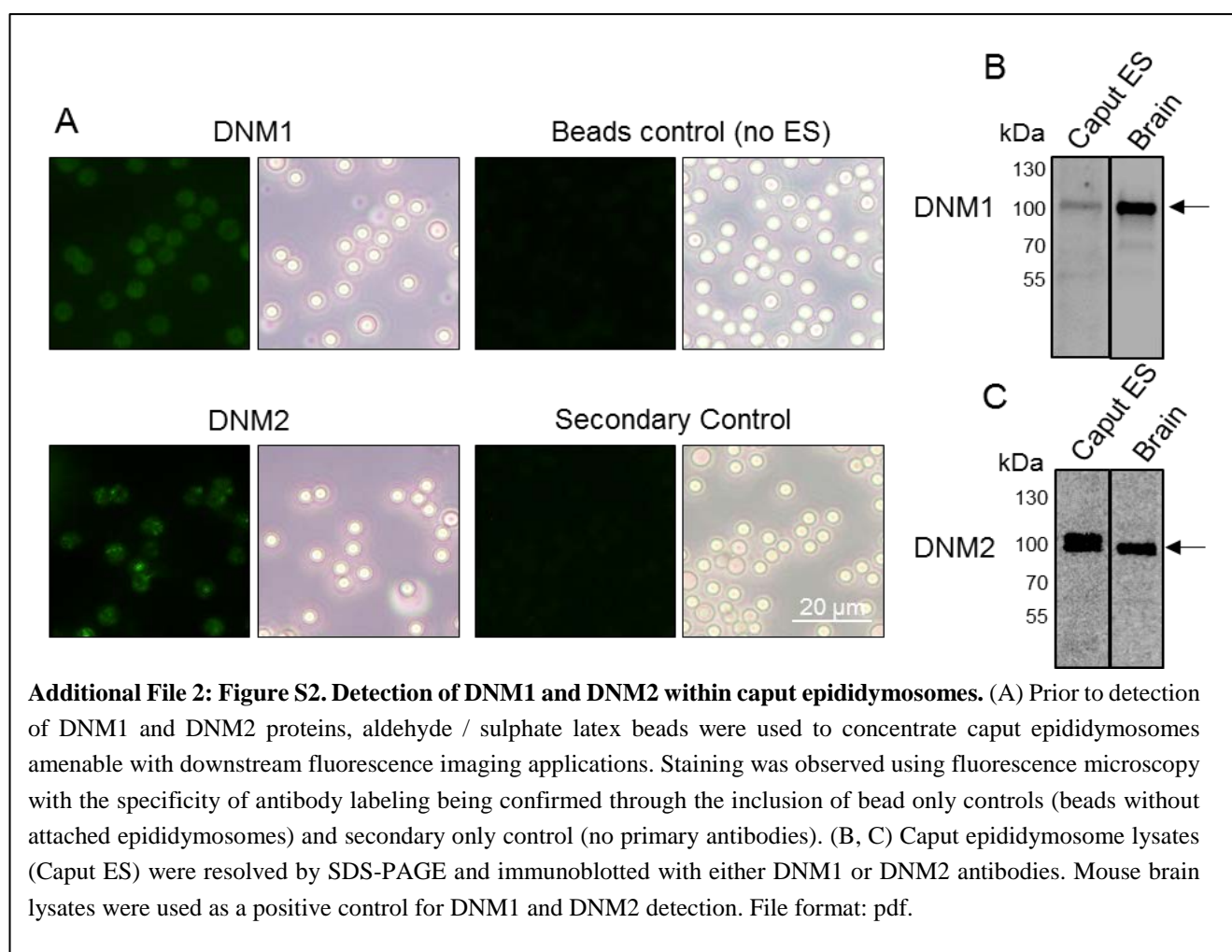
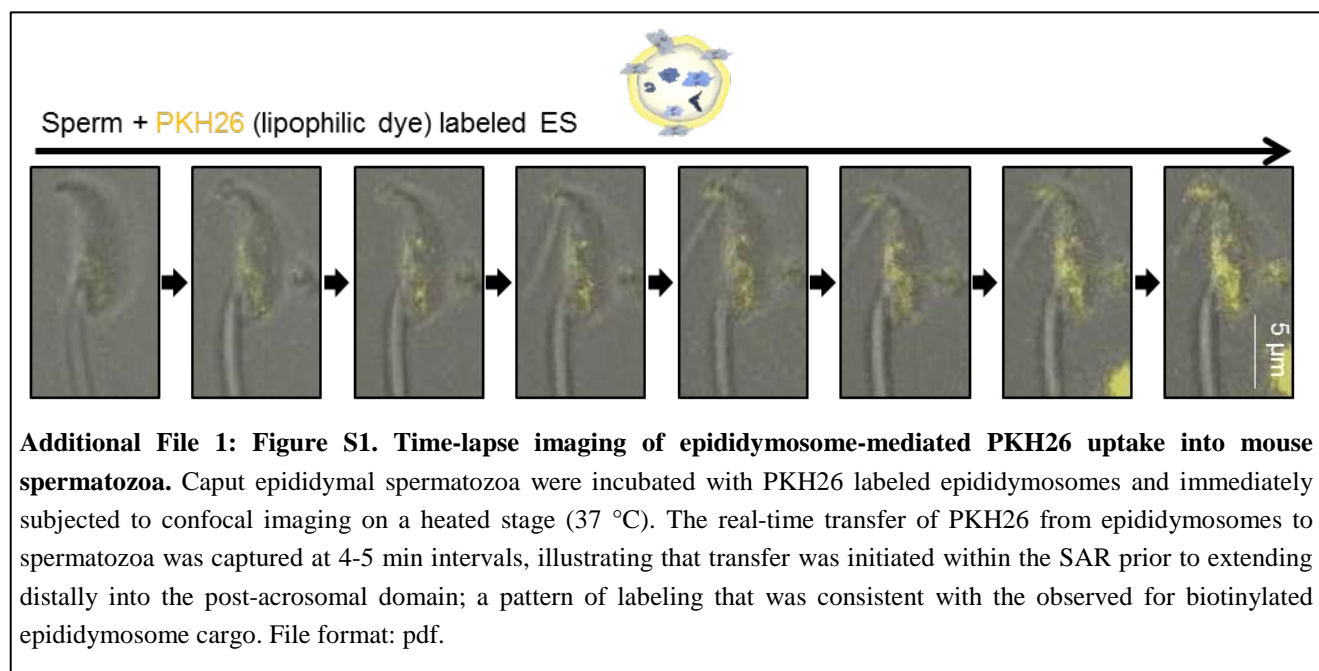
2017; 14(12):1776-90.

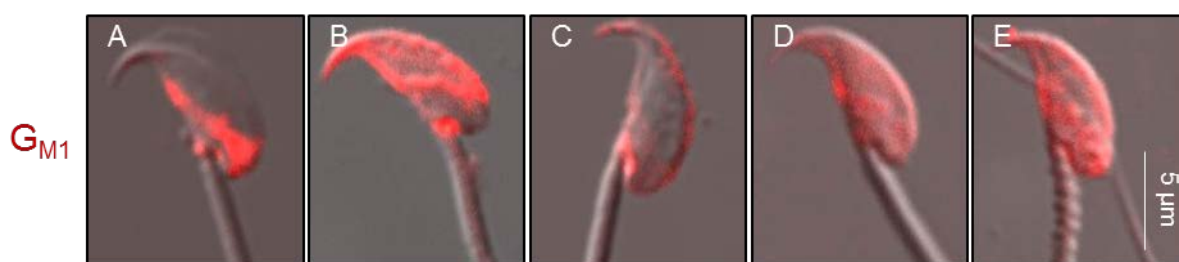
- 630 11. Eaton SA, Jayasooriah N, Buckland ME, Martin DI, Cropley JE, Suter CM. Roll over Weismann: extracellular vesicles in the transgenerational transmission of environmental effects. *Epigenomics*. 2015; 7(7):1165-71.
12. Frenette G, Girouard J, D'Amours O, Allard N, Tessier L, Sullivan R. Characterization of two distinct populations of epididymosomes collected in the intraluminal compartment of the bovine cauda epididymis. *Biol Reprod*. 2010; 83(3):473-80.
- 635 13. Grigor'eva A, Dyrkheeva N, Bryzgunova O, Tamkovich S, Chelobanov B, Ryabchikova E. Contamination of exosome preparations, isolated from biological fluids. *Biomed Khim*. 2017; 11(3):265-71.
14. Caballero JN, Frenette G, Belleannée C, Sullivan R. CD9-positive microvesicles mediate the transfer of molecules to bovine spermatozoa during epididymal maturation. *PloS one*. 2013; 8(6):e65364.
15. D'Amours O, Frenette G, Bordeleau L-J, Allard N, Leclerc P, Blondin P, Sullivan R. Epididymosomes transfer epididymal sperm binding protein 1 (ELSPBP1) to dead spermatozoa during epididymal transit in bovine. *Biol Reprod*. 2012; 87(4):94.
- 640 16. Girouard J, Frenette G, Sullivan R. Comparative proteome and lipid profiles of bovine epididymosomes collected in the intraluminal compartment of the caput and cauda epididymidis. *Int J Androl*. 2011; 34(5pt2):e475-86.
17. Rejraji H, Sion B, Prensier G, Carreras M, Motta C, Frenoux J-M, Vericel E, Grizard G, Vernet P, Drevet JR. Lipid remodeling of murine epididymosomes and spermatozoa during epididymal maturation. *Biol Reprod*. 2006; 74(6):1104-
- 645 13.
18. Schwarz A, Wennemuth G, Post H, Brandenburger T, Aumüller G, Wilhelm B. Vesicular transfer of membrane components to bovine epididymal spermatozoa. *Cell Tissue Res*. 2013; 353(3):549-61.
19. Nixon B, De Iuliis GN, Hart HM, Zhou W, Mathe A, Bernstein I, Anderson AL, Stanger SJ, Skerrett-Byrne DA, Jamaluddin MFB. Proteomic profiling of mouse epididymosomes reveals their contributions to post-testicular sperm maturation. *Mol Cell Proteomics*. 2018; doi:10.1074/mcp.RA118.000946.
- 650 20. Gatti J-L, Métayer S, Belghazi M, Dacheux F, Dacheux J-L. Identification, proteomic profiling, and origin of ram epididymal fluid exosome-like vesicles. *Biol Reprod*. 2005; 72(6):1452-65.
21. Zhou W, De Iuliis GN, Dun MD, Nixon B. Characteristics of the epididymal luminal environment responsible for sperm maturation and storage. *Front Endocrinol (Lausanne)*. 2018; 9:59.
- 655 22. Thimon V, Frenette G, Saez F, Thabet M, Sullivan R. Protein composition of human epididymosomes collected during surgical vasectomy reversal: a proteomic and genomic approach. *Hum Reprod*. 2008; 23(8):1698-707.
23. Harroun TA, Katsaras J, Wassall SR. Cholesterol is found to reside in the center of a polyunsaturated lipid membrane. *Biochemistry*. 2008; 47(27):7090-6.
24. Griffiths GS, Galileo DS, Reese K, Martin-DeLeon PA. Investigating the role of murine epididymosomes and uterosomes in GPI-linked protein transfer to sperm using SPAM1 as a model. *Mol Reprod. Dev* 2008; 75(11):1627-36.
- 660

25. Reid AT, Lord T, Stanger SJ, Roman SD, McCluskey A, Robinson PJ, Aitken RJ, Nixon B. Dynamin regulates specific membrane fusion events necessary for acrosomal exocytosis in mouse spermatozoa. *J Biol Chem.* 2012; 287(45):37659-72.
26. Girouard J, Frenette G, Sullivan R. Compartmentalization of proteins in epididymosomes coordinates the association of epididymal proteins with the different functional structures of bovine spermatozoa. *Biol Reprod.* 2009; 80(5):965-72.
27. Hinshaw J. Dynamin and its role in membrane fission. *Annu Rev Cell Dev Biol.* 2000; 16(1):483-519.
28. Boarelli P. Simultaneous Study of Cholesterol and GM1 Ganglioside by Specific Probes: Lipid Distribution during Maturation, Capacitation and the Acrosome Reaction. *J Cytol Histol.* 2016; 7:412.
29. Nixon B, Bielanowicz A, McLaughlin EA, Tanphaichitr N, Ensslin MA, Aitken RJ. Composition and significance of detergent resistant membranes in mouse spermatozoa. *J Cell Physiol.* 2009; 218(1):122-34.
30. Sullivan R. Epididymosomes: a heterogeneous population of microvesicles with multiple functions in sperm maturation and storage. *Asian J Androl.* 2015; 17(5):726-9.
31. Jones R, James PS, Howes L, Bruckbauer A, Klenerman D. Supramolecular organization of the sperm plasma membrane during maturation and capacitation. *Asian J Androl.* 2007; 9(4):438-44.
32. James PS, Hennessy C, Berge T, Jones R. Compartmentalisation of the sperm plasma membrane: a FRAP, FLIP and SPFI analysis of putative diffusion barriers on the sperm head. *J Cell Sci.* 2004; 117(26):6485-95.
33. Selvaraj V, Asano A, Buttke DE, Sengupta P, Weiss RS, Travis AJ. Mechanisms underlying the micron-scale segregation of sterols and GM1 in live mammalian sperm. *J Cell Physiol.* 2009; 218(3):522-36.
34. Flesch FM, Gadella BM. Dynamics of the mammalian sperm plasma membrane in the process of fertilization. *Biochim Biophys Acta.* 2000; 1469(3):197-235.
35. Jones R, James PS, Oxley D, Coadwell J, Suzuki-Toyota F, Howes EA. The equatorial subsegment in mammalian spermatozoa is enriched in tyrosine phosphorylated proteins. *Biol Reprod.* 2008; 79(3):421-31.
36. Wu AT, Sutovsky P, Xu W, van der Spoel AC, Platt FM, Oko R. The postacrosomal assembly of sperm head protein, PAWP, is independent of acrosome formation and dependent on microtubular manchette transport. *Dev Biol.* 2007; 312(2):471-83.
37. Sutovsky P, Manandhar G, Wu A, Oko R. Interactions of sperm perinuclear theca with the oocyte: Implications for oocyte activation, anti-polyspermy defense, and assisted reproduction. *Microsc Res Tech.* 2003; 61(4):362-78.
38. Wu AT, Sutovsky P, Manandhar G, Xu W, Katayama M, Day BN, Park K-W, Yi Y-J, Xi YW, Prather RS. PAWP, A sperm specific ww-domain binding protein, promotes meiotic resumption and pronuclear development during fertilization. *J Biol Chem.* 2007; 282(16):12164-75.
39. Aarabi M, Balakier H, Bashar S, Moskovtsev SI, Sutovsky P, Librach CL, Oko R. Sperm-derived WW domain-binding protein, PAWP, elicits calcium oscillations and oocyte activation in humans and mice. *FASEB J.* 2014; 28(10):4434-40.

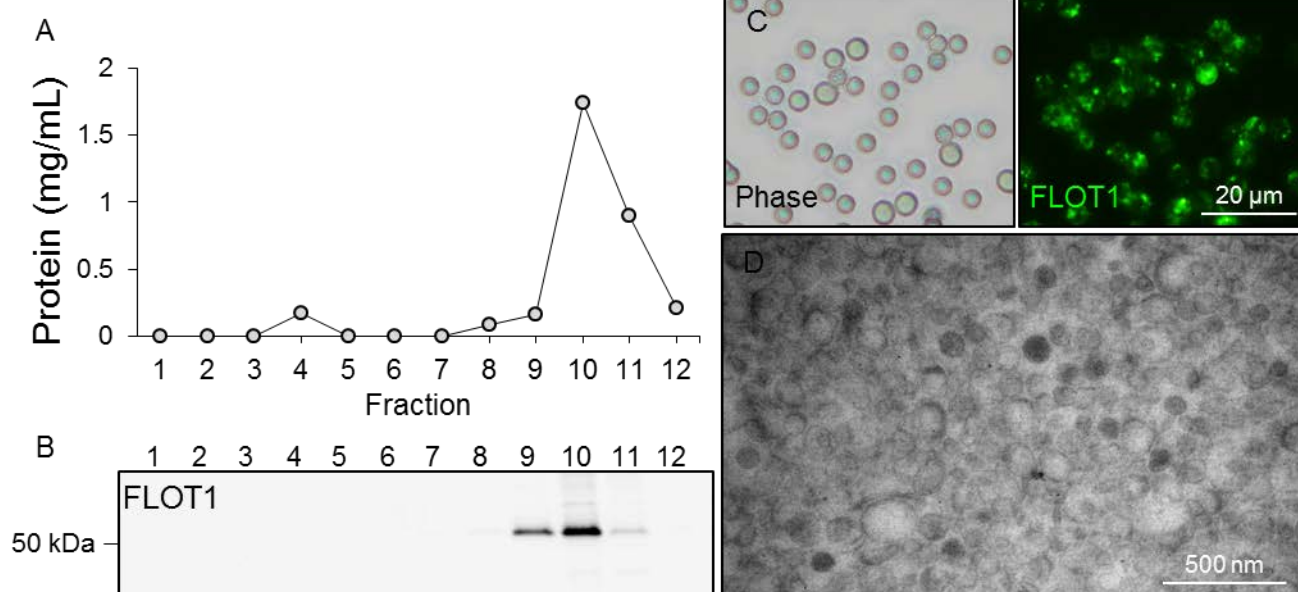
40. Al-Dossary AA, Caplan JL, Martin-Deleon PA. The contribution of exosomes/microvesicles to the sperm proteome. *Mol Reprod Dev.* 2015; 82(2):79.
- 695 41. Zhou W, De Iuliis GN, Turner AP, Reid AT, Anderson AL, McCluskey A, McLaughlin EA, Nixon B. Developmental expression of the dynamin family of mechanoenzymes in the mouse epididymis. *Biol Reprod.* 2016; 96(1):159-73.
42. Merrifield CJ, Feldman ME, Wan L, Almers W. Imaging actin and dynamin recruitment during invagination of single clathrin-coated pits. *Nat Cell Biol.* 2002; 4(9):691-8.
43. Chan S-A, Doreian B, Smith C. Dynamin and myosin regulate differential exocytosis from mouse adrenal chromaffin cells. *Cell Mol Neurobiol.* 2010; 30(8):1351-7.
- 700 44. Takei K, McPherson PS, Schmid SL, De Camilli P. Tubular membrane invaginations coated by dynamin rings are induced by GTP- $\gamma$ S in nerve terminals. *Nature.* 1995; 374(6518):186-90.
45. Hazan-Halevy I, Rosenblum D, Weinstein S, Bairey O, Raanani P, Peer D. Cell-specific uptake of mantle cell lymphoma-derived exosomes by malignant and non-malignant B-lymphocytes. *Cancer Lett.* 2015; 364(1):59-69.
- 705 46. Wang R, Ding Q, Yaqoob U, de Assuncao TM, Verma VK, Hirsova P, Cao S, Mukhopadhyay D, Huebert RC, Shah VH. Exosome adherence and internalization by hepatic stellate cells triggers sphingosine 1-phosphate dependent migration. *J Biol Chem.* 2015; 290(52):30684-96.
47. Holder B, Jones T, Sancho Shimizu V, Rice TF, Donaldson B, Bouqueau M, Forbes K, Kampmann B. Macrophage exosomes induce placental inflammatory cytokines: a novel mode of maternal-placental messaging. *Traffic.* 2016; 17(2):168-78.
- 710 48. Jones R, Howes E, Dunne PD, James P, Bruckbauer A, Klenerman D. Tracking diffusion of GM1 gangliosides and zona pellucida binding molecules in sperm plasma membranes following cholesterol efflux. *Dev Biol.* 2010; 339(2):398-406.
49. Raimondi A, Ferguson SM, Lou X, Armbruster M, Paradise S, Giovedi S, Messa M, Kono N, Takasaki J, Cappello V. Overlapping role of dynamin isoforms in synaptic vesicle endocytosis. *Neuron.* 2011; 70(6):1100-14.
- 715 50. Redgrove KA, Bernstein IR, Pye VJ, Mihalas BP, Sutherland JM, Nixon B, McCluskey A, Robinson PJ, Holt JE, McLaughlin EA. Dynamin 2 is essential for mammalian spermatogenesis. *Sci Rep.* 2016; 6:35084.
51. Zhou W, Sipilä P, De GI, Dun M, Nixon B. Analysis of Epididymal Protein Synthesis and Secretion. *J Vis Exp.* 2018; doi: 10.3791/58308.
52. Biggers J, Whitten W, Whittingham D. The culture of mouse embryos in vitro. *Cult Mouse Embryos In Vitro.* 1971:86-116.
- 720 53. Lötvall J, Hill AF, Hochberg F, Buzás EI, Di Vizio D, Gardiner C, Gho YS, Kurochkin IV, Mathivanan S, Quesenberry P. Minimal experimental requirements for definition of extracellular vesicles and their functions: a position statement from the International Society for Extracellular Vesicles. *J Extracell Vesicles.* 2014; 3:26913.
54. Nixon B, Stanger SJ, Mihalas BP, Reilly JN, Anderson AL, Tyagi S, Holt JE, McLaughlin EA. The microRNA signature

55. Rueden CT, Schindelin J, Hiner MC, DeZonia BE, Walter AE, Arena ET, Eliceiri KW. ImageJ2: ImageJ for the next generation of scientific image data. *BMC Bioinformatics.* 2017; 18(1):529.





**Additional File 3: Figure S3.** Immunofluorescence detection of  $G_{M1}$  gangliosides (an abundant lipid raft marker) was facilitated by labeling of caput epididymal spermatozoa with Alexa Fluor 594 conjugated cholera toxin B subunit. (A - E) A myriad of fluorescence staining patterns for  $G_{M1}$  were observed using confocal microscopy and the dominant profiles are depicted. File format: pdf.



**Additional File 5: Figure S4. Epididymosome purity assessment.** A suite of assays were employed to assess the enrichment of epididymosomes, including: (A) quantitative assessment of the protein content in the twelve equal fractions recovered after density ultracentrifugation; (B) immunoblotting to detect the distribution of the epididymosome marker FLOT1 within each of the twelve fractions; (C) detection of FLOT1 in epididymosomes concentrated via adhesion to aldehyde / sulphate beads; and (D) TEM assessment of the ultrastructure of the epididymosome population isolated from the pooling of fractions 9 and 10. Based on this analysis, epididymosomes partitioning into fractions 9 and 10 were pooled and used throughout the reported studies. File format: pdf.

**Additional File 4: Table S1: Details of antibodies used throughout this study**

Antibody	Final concentration (dilution of stock solution) <sup>1</sup>			Company	Catalogue No. (RRID) <sup>2</sup>	Batch No.	Stock Concentration
	IF	IB	EM				
<b>Primary antibodies</b>							
Dynamin 1	1 µg (1:50)	1.5 µg (1:1000)	-	Abcam	ab108458	GR107528-1	1 mg/mL
Dynamin 1	1.25 µg (1:40)	-	0.83 µg (1:20)	Abcam	ab13251 (AB_299794)	GR283893-2	1 mg/mL
Dynamin 2	0.2 µg (1:50)	-	-	Santa Cruz Biotechnology	sc-6400 (AB_639943)	L0712	0.2 mg/mL
Dynamin 2	-	0.4 µg (1:1000)	-	Thermo Fisher Scientific	PA5-19800 (AB_10983803)	QK2113152	0.27 mg/mL
Flotillin 1	2 µg (1:100)	1.5 µg (1:1000)	-	Sigma-Aldrich	F1180 (AB_1078893)	124M4804V	1 mg/mL
α-Tubulin	-	2.85 µg (1:3000)	-	Sigma-Aldrich	T5168 (AB_477579)	103M4773V	5.7 mg/mL
Cholera Toxin Subunit B 594 conjugate	0.125 µg (1:400)	-	-	Thermo Fisher Scientific	C34777	-	1 mg/mL
<b>Secondary antibodies</b>							
Anti-rabbit Alexa Fluor 488	0.25 µg (1:400)	-	-	Thermo Fisher Scientific	A11008 (AB_143165)	1678787	2 mg/mL
Anti-goat Alexa Fluor 488	0.25 µg (1:400)	-	-	Thermo Fisher Scientific	A11055 (AB_142672)	1369678	2 mg/mL
Anti-goat Alexa Fluor 594	0.25 µg (1:400)	-	-	Thermo Fisher Scientific	A11058 (AB_142540)	1180089	2 mg/mL
Anti-mouse Alexa Fluor 594	0.25 µg (1:400)	-	-	Thermo Fisher Scientific	A11005 (AB_141372)	1219862	2 mg/mL
Anti-mouse Alexa Fluor 555	0.25 µg (1:400)	-	-	Thermo Fisher Scientific	A21422 (AB_141822)	-	2 mg/mL
Dylight-405 anti-mouse	0.375 µg (1:200)	-	-	Jackson ImmunoResearch	715-475-150 (AB_2340839)	130441	1.5 mg/mL
Streptavidin, Alexa Fluor 633	0.25 µg (1:400)	-	-	Thermo Fisher Scientific	S21375 (AB_2313500)	-	2 mg/mL
Streptavidin, Alexa Fluor 488	0.25 µg (1:400)	-	-	Thermo Fisher Scientific	S11223 (AB_2336881)	1733116	2 mg/mL
HRP-Streptavidin	-	N/A (1:1000)	-	Millipore	SA202	ME9AN875 1	N/A
Anti-rabbit HRP	-	1.3 µg (1:1000)	-	Millipore	DC03L (AB_437852)	-	0.13 mg/mL
Anti-mouse HRP	-	0.15 µg (1:4000)	-	Santa Cruz Biotechnology	sc-2005 (AB_631736)	B1616	0.4 mg/mL
Anti-mouse-Gold antibody	-	-	N/A (1:10)	Sigma-Aldrich	G7652 (AB_259958)	127k1520	N/A

<sup>1</sup> IF, immunofluorescence; IB, immunoblot; EM, electron microscopy; -, not applicable; N/A, information not available from manufacturer

<sup>2</sup> RRID: Research Resource Identifier

**Additional File 6: Table S2: Excitation and emission wavelengths used for detection of the different combinations of fluorophores in this study.**

<b>Fluorescent dye combination</b>	<b>Excitation</b>	<b>Emission</b>
Alexa Fluor 488	473 nm	485-545 nm
Alexa Fluor 594	559 nm	570-670 nm
Alexa Fluor 488	473 nm	485-585 nm
Alexa Fluor 633	635 nm	650-750 nm
FITC (PNA)	473 nm	485-545 nm
Alexa Fluor 555	559 nm	570-625 nm
Alexa Fluor 633	635 nm	655-755 nm
DyLight 405	405 nm	425-460 nm
Alexa Fluor 488	473 nm	485-545 nm
Alexa Fluor 594	559 nm	575-675 nm
PKH26	559 nm	570-670 nm

## Additional File 7: Raw data values for experiments in which n < 6

### Figure 6C

	Pixel Intensity (DNM1)		Normalized against Pixel Intensity for Tubulin		Normalized against 'Sperm only'	
	Sperm only	Sperm+epididymosome	Sperm only	Sperm+epididymosome	Sperm only	Sperm+epididymosome
Replicate 1	5805.175	7298.317	0.227401996	0.297481386	1	1.308174032
Replicate 2	12541.853	14770.924	0.594897398	0.683206254	1	1.148443843
Replicate 3	9575.418	12256.054	0.433619643	0.509238783	1	1.174390485
	Sperm only	Sperm+epididymosome				
Mean	1	1.21033612				
SEM	0	0.060611467				

### Figure 7B

	Pixel Intensity (DNM2)		Normalized against Pixel Intensity for Tubulin		Normalized against 'Sperm only'	
	Sperm only	Sperm+epididymosome	Sperm only	Sperm+epididymosome	Sperm only	Sperm+epididymosome
Replicate 1	7421.418	7489.468	0.290713935	0.305272753	1	1.050079533
Replicate 2	8624.368	9982.761	0.40907943	0.461737177	1	1.128722549
Replicate 3	7212.974	8824.267	0.326561818	0.366648106	1	1.122752526
	Sperm only	Sperm+epididymosome				
Mean	1	1.100518203				
SEM	0	0.030959287				

### Figure 9C

	% Sperm with post-acrosomal biotin labeling			% Sperm with post-acrosomal biotin labeling	
	Control	mβCD treated		Control	mβCD treated
Replicate 1 <sup>1</sup>	38	22	Mean	37.3333333	22
Replicate 2	40	21	SEM	2.1602469	0.707106781
Replicate 3	34	23			

<sup>1</sup> In each replicate, 100 sperm cells were counted and the number of cells with biotin labeling of the post-acrosomal domain recorded

# CHAPTER 5

---

*Characterization of a novel role for the dynamin  
mechanoenzymes in the regulation of human sperm acrosomal  
exocytosis*

**Published:** Molecular Human Reproduction (2017) 23 (10): 657-673

**Authors:** Wei Zhou<sup>1</sup>, Amanda L. Anderson<sup>1</sup>, Adrian P. Turner<sup>2</sup>, Geoffry N. De Iulius<sup>1</sup>, Adam McCluskey<sup>3</sup>, Eileen A. McLaughlin<sup>1,2</sup> and Brett Nixon<sup>1\*</sup>

<sup>1</sup>Priority Research Centre for Reproductive Biology, School of Environmental and Life Sciences, University of Newcastle, Callaghan, NSW 2308, Australia.

<sup>2</sup>School of Biological Sciences, University of Auckland, Auckland, New Zealand.

<sup>3</sup>Priority Research Centre for Chemical Biology, School of Environmental and Life Sciences, University of Newcastle, Callaghan, NSW 2308, Australia.

\*Correspondence: [brett.nixon@newcastle.edu.au](mailto:brett.nixon@newcastle.edu.au)

## Chapter 5: Overview

Following epididymal maturation, mammalian spermatozoa must complete a series of biochemical changes during their passage through the female reproductive tract, which eventually culminate in the ability to undergo an acrosome reaction; a unique exocytotic event that allows sperm to penetrate the outer vestments of the oocyte and initiate fertilization. Notably, failure to complete an acrosome reaction represents a common aetiology underpinning the defective sperm function witnessed in infertile males. In recent studies conducted in the mouse model, our laboratory has firmly implicated the dynamin family as important regulators of acrosomal exocytosis. In the studies described in this chapter, we aimed to investigate the regulation of human sperm acrosomal exocytosis by the dynamin family of mechanoenzymes.

In completing these studies, we have provided the first evidence that the three canonical dynamin isoforms (DNM1, DNM2, and DNM3) are present in mature human spermatozoa. Further, the localization of DNM1 and DNM2 to the peri-acrosomal domain of human sperm ideally positions these isoforms to exert regulatory control over acrosomal exocytosis. Consistent with such a role, we demonstrate that pharmacological inhibition of DNM1 and DNM2 is able to significantly suppress the rates of acrosomal exocytosis achieved following progesterone stimulus. In contrast, no such inhibition was observed when acrosomal exocytosis was induced via a calcium ionophore, which is capable of bypassing physiological control of this exocytotic reaction. The importance of such findings was further emphasized by the apparent reduction in DNM2 recorded among poor quality sperm that were refractory to the induction of a progesterone-stimulated acrosome reaction. In addition to providing important mechanistic insight into the control of human sperm acrosomal exocytosis, this study identifies dynamin (i.e. dynamin 2) as a potential biomarker of male fertility with important diagnostic implications for the stratification of infertility patients into appropriate therapeutic options.

# Characterization of a novel role for the dynamin mechanoenzymes in the regulation of human sperm acrosomal exocytosis

Wei Zhou<sup>1</sup>, Amanda L. Anderson<sup>1</sup>, Adrian P. Turner<sup>2</sup>,  
Geoffry N. De Luliis<sup>1</sup>, Adam McCluskey<sup>3</sup>, Eileen A. McLaughlin<sup>1,2</sup>,  
and Brett Nixon<sup>1,\*</sup>

<sup>1</sup>Priority Research Centre for Reproductive Science, School of Environmental and Life Sciences, Discipline of Biological Sciences, University of Newcastle, University Drive, Callaghan, NSW 2308, Australia <sup>2</sup>School of Biological Sciences, University of Auckland, Symonds Street, Auckland Central 1010, New Zealand <sup>3</sup>School of Environmental and Life Sciences, Discipline of Chemistry, The University of Newcastle, University Drive, Callaghan, NSW 2308, Australia

\*Correspondence address. Brett Nixon, Priority Research Centre for Reproductive Science, School of Environmental and Life Sciences, Discipline of Biological Sciences, University of Newcastle, University Drive, Callaghan, NSW 2308, Australia. Tel: +61-2-4921-6977; Fax: +61-2-4921-6308; E-mail: Brett.Nixon@newcastle.edu.au

Submitted on April 28, 2017; resubmitted on June 23, 2017; editorial decision on July 26, 2017; accepted on July 27, 2017

**STUDY QUESTION:** Does dynamin regulate human sperm acrosomal exocytosis?

**SUMMARY ANSWER:** Our studies of dynamin localization and function have implicated this family of mechanoenzymes in the regulation of progesterone-induced acrosomal exocytosis in human spermatozoa.

**WHAT IS KNOWN ALREADY:** Completion of an acrosome reaction is a prerequisite for successful fertilization in all studied mammalian species. It follows that failure to complete this unique exocytotic event represents a common aetiology in the defective spermatozoa of male infertility patients that have failed IVF in a clinical setting. Recent studies have implicated the dynamin family of mechanoenzymes as important regulators of the acrosome reaction in murine spermatozoa. The biological basis of this activity appears to rest with the ability of dynamin to polymerize around newly formed membrane vesicles and subsequently regulate the rate of fusion pore expansion. To date, however, the dynamin family of GTPases have not been studied in the spermatozoa of non-rodent species. Here, we have sought to examine the presence and functional significance of dynamin in human spermatozoa.

**STUDY DESIGN, SIZE, DURATION:** Dynamin expression was characterized in the testis and spermatozoa of several healthy normozoospermic individuals. In addition, we assessed the influence of selective dynamin inhibition on the competence of human spermatozoa to undergo a progesterone-induced acrosome reaction. A minimum of five biological and technical replicates were performed to investigate both inter- and intra-donor variability in dynamin expression and establish statistical significance in terms of the impact of dynamin inhibition.

**PARTICIPANTS/MATERIALS, SETTING, METHODS:** The expression and the localization of dynamin in the human testis, epididymis and mature spermatozoa were determined through the application of immunofluorescence, immunoblotting and/or electron microscopy. Human semen samples were fractionated via density gradient centrifugation and the resultant populations of good and poor quality spermatozoa were induced to capacitate and acrosome react in the presence or absence of selective dynamin inhibitors. The acrosome integrity of live spermatozoa was subsequently assessed via the use of fluorescently conjugated *Arachis hypogea* lectin (PNA). The influence of dynamin phosphorylation and the regulatory kinase(s) responsible for this modification in human spermatozoa were also assessed via the use of *in situ* proximity ligation assays and pharmacological inhibition. In all experiments,  $\geq 100$  spermatozoa were assessed/treatment group and all graphical data are presented as the mean values  $\pm$  SEM, with statistical significance being determined by ANOVA.

**MAIN RESULTS AND THE ROLE OF CHANCE:** Dynamin 1 (DNM1) and DNM2, but not DNM3, were specifically localized to the acrosomal region of the head of human spermatozoa, an ideal position from which to regulate acrosomal exocytosis. In keeping with this notion, pharmacological inhibition of DNM1 and DNM2 was able to significantly suppress the rates of acrosomal exocytosis stimulated by

progesterone. Furthermore, our comparison of dynamin expression in good and poor quality spermatozoa recovered from the same ejaculate, revealed a significant reduction in the amount of DNM2 in the latter subpopulation of cells. In contrast, DNM1 was detected at equivalent levels in both subpopulations of spermatozoa. Such findings are of potential significance given that the poor quality spermatozoa proved refractory to the induction of a progesterone stimulated acrosome reaction. In seeking to identify the regulatory influence of progesterone on DNM2 function, we were able to establish that the protein is a substrate for CDK1-dependent phosphorylation. The functional significance of DNM2 phosphorylation was illustrated by the fact that pharmacological inhibition of CDK1 elicited a concomitant suppression of both DNM2-Ser764 phosphorylation and the overall rates of progesterone-induced acrosomal exocytosis.

**LARGE SCALE DATA:** N/A.

**LIMITATIONS REASONS FOR CAUTION:** This was an *in vitro* study performed mainly on ejaculated human spermatozoa. This experimental paradigm necessarily eliminates the physiological contributions of the female reproductive tract that would normally support capacitation and acrosomal responsiveness.

**WIDER IMPLICATIONS OF THE FINDINGS:** This study identifies a novel causative link between dynamin activity and the ability of human spermatozoa to complete a progesterone-induced acrosome reaction. Such findings encourage a more detailed analysis of the contribution of dynamin dysregulation as an underlying aetiology in infertile males whose spermatozoa are unable to penetrate the zona pellucida.

**STUDY FUNDING/COMPETING INTEREST(S):** This research was supported by a National Health and Medical Research Council of Australia Project Grant (APPI103176) awarded to B.N. and E.A.M. The authors report no conflict of interest.

**Key words:** acrosome reaction / dynamin / human spermatozoa / infertility / sperm maturation

## Introduction

In all mammalian species that have been studied, completion of an acrosome reaction is accepted as a prerequisite for successful fertilization *in vivo* (Florman et al., 2004; Avella and Dean, 2011). This unique exocytotic process is initiated by multiple fusion events between the outer acrosomal membrane and the overlying plasma membrane (Barros et al., 1967). As this wave of vesiculation spreads across the anterior region of the sperm head, it facilitates the destabilization of the acrosomal structure, formation of hybrid membrane vesicles and the concomitant release of acrosomal contents (Barros et al., 1967). This, in turn, enables sperm penetration of the resilient zona pellucida matrix, and provides the cell with access to the oocyte plasma membrane. Recent work has drawn into question the long held view that the acrosome reaction proceeds in an 'all or none' manner, with accumulating evidence suggesting that the process may instead comprise several intermediate phases, each with their own set of functional consequences (Buffone et al., 2012, 2014). Irrespective of this, several features of acrosomal exocytosis, including the relatively slow kinetics at which it proceeds, underscore the highly specialized nature of this secretory process and the prospect that is governed by complex molecular mechanisms (Belmonte et al., 2016).

In keeping with this notion, the capacity to complete a physiological acrosome reaction necessitates that spermatozoa have first completed a process of functional maturation, known as capacitation, during their ascent of the female reproductive tract (Stival et al., 2016). Among the many biochemical and biophysical changes that accompany capacitation, the sperm membrane becomes increasingly fusogenic, owing to alterations in its lipid architecture and the release of decapacitation factors (Nixon et al., 2006; Aitken and Nixon, 2013). These combined events serve to modulate intracellular ion concentrations leading to hyperpolarization of the sperm plasma membrane and triggering complex signalling cascades that culminate in increased protein phosphorylation (Visconti et al., 2011). While these processes prime the cell for completion of an acrosome reaction, the precise physiological stimulus

responsible for the induction of this exocytotic event remains a matter of some controversy (Buffone et al., 2014). Indeed, the long held view that zona pellucida ligands act as the key stimulus for induction of acrosomal exocytosis have recently been drawn into question (Baibakov et al., 2007) in favour of alternative models, which suggest that the timing of the acrosomal exocytosis may actually precede that of zona adhesion (Inoue et al., 2011). Such timing may account for the ability of progesterone, a signalling molecule that sperm encounter within the oviduct prior to zona adhesion, to elicit the induction of acrosomal exocytosis in various species, including the human (Meyers et al., 1995; Meizel et al., 1997; Thérien and Manjunath, 2003). Progesterone, in turn, reportedly acts via its ability to modulate an increase in cytosolic  $\text{Ca}^{2+}$  levels (Blackmore et al., 1990).

The impetus for further investigation of the regulation of acrosomal exocytosis in human spermatozoa stems, at least in part, from the recognition that a failure to complete this event represents a relatively common aetiology associated with the defective spermatozoa of male infertility patients. Indeed, diagnosis of sperm dysfunction suggests that such a defect may account for almost one-third of all cases of failed IVF in couples seeking recourse to assisted reproductive programs due to male factor infertility (Muller, 2000; Liu and Baker, 2003). Notably, these patients commonly present with otherwise normal semen characteristics, suggesting that the defect may be associated with the molecular machinery responsible for the control of acrosomal exocytosis rather than overt morphological defects in their spermatozoa. While such machinery is undoubtedly complex, our recent work in the mouse model has raised the prospect that the dynamin family of mechanoenzymes may hold a critical role in the regulation of the acrosome reaction (Reid et al., 2012; 2015).

The dynamin family of proteins comprise a group of large GTPases that have been extensively researched in the context of their ability to manipulate membrane vesicles during the combined processes of endo- and exo-cytosis (Shpetner and Vallee, 1989; Williams and Kim, 2014; Jackson et al., 2015). Such functions are largely attributed to the

ability of dynamín to self-oligomerize into cylindrical helices around the neck of nascent vesicles (Antonny *et al.*, 2016). In one of the most widely accepted models of dynamín action, GTP hydrolysis subsequently drives conformational changes that lead to constriction of both the polymer and the membrane beneath, thus promoting vesicle scission and release from the parent membrane (Morlot and Roux, 2013). It has also been shown that dynamín has the ability to regulate the rate of fusion pore expansion between the membranes and newly formed vesicles, thus controlling the amount of cargo released from the vesicles (Anantharam *et al.*, 2011; Jackson *et al.*, 2015). Such a model is in keeping with the protracted timeframe, and progressive release, of the acrosomal contents that have been documented during acrosomal exocytosis in mammalian spermatozoa (Buffone *et al.*, 2014; Belmonte *et al.*, 2016).

The existence of three canonical dynamín members (DNM1, DNM2 and DNM3), as well as several dynamín-like proteins, has been recorded in mammalian species (Antonny *et al.*, 2016). Being encoded by three different genes, DNM1, DNM2 and DNM3 are characterized by differential patterns of expression within distinct tissues of the body. In this context, DNM1 is predominantly found in the central nervous system (Ferguson *et al.*, 2007), DNM2 is ubiquitously expressed throughout the body (Cook *et al.*, 1994) and DNM3 appears to reside mainly in the brain and testis (Cao *et al.*, 1998). Studies conducted in our own, and independent laboratories, have recently begun to explore the expression and functional significance of dynamín in the male reproductive tract of murine models (Iguchi *et al.*, 2002; Lie *et al.*, 2006; Kusumi *et al.*, 2007; Vaid *et al.*, 2007; Zhao *et al.*, 2007; Reid *et al.*, 2012; 2015; Redgrove *et al.*, 2016; Zhou *et al.*, 2017). Thus, prominent expression of DNM2 has been documented in the mouse testes where the protein appears to localize to developing germ cells (Redgrove *et al.*, 2016). Accordingly, conditional ablation of the *Dnm2* gene leads to the complete arrest of spermatogenesis and a corresponding phenotype of male infertility (Redgrove *et al.*, 2016). DNM1 has been identified in mouse germ cells where it appears to be restricted to the developing acrosome of round spermatids (Reid *et al.*, 2012). However, unlike *Dnm2*, the targeted ablation of *Dnm1* did not precipitate overt changes in germ cell development or male infertility (Redgrove *et al.*, 2016). In contrast, DNM3 expression within the testis appears to have minimal overlap with the germ cell population (Vaid *et al.*, 2007; Reid *et al.*, 2012). Importantly in the context of this study, we have also shown that both DNM1 and DNM2, but not DNM3, are retained in mature mouse spermatozoa where they co-localize within the peri-acrosomal region of the sperm head (Reid *et al.*, 2012). From this position, DNM1 and DNM2 appear to exert an important regulatory influence over acrosomal exocytosis, such that their selective pharmacological inhibition significantly compromises the ability of mouse spermatozoa to complete a progesterone-induced acrosome reaction (Reid *et al.*, 2012). In agreement with such findings, independent research has shown the DNM2 also forms productive interactions with complexin I (Zhao *et al.*, 2007), an important element of the SNARE family of proteins that themselves have been implicated in regulation of acrosomal exocytosis (Buffone *et al.*, 2014). Accordingly, this interaction has been mapped to the acrosomal region of mouse spermatozoa (Zhao *et al.*, 2007).

Notwithstanding promising data generated thus far in rodent models, to the best of our knowledge, there is presently no research directly exploring the presence and/or functional significance of dynamín

isoforms in human spermatozoa. Thus, the aim of this study was to characterize the expression pattern of the canonical dynamín family members (DNM1, DNM2 and DNM3) in the human testis and ejaculated spermatozoa, as well as assess their potential role in the regulation of acrosomal exocytosis in our own species.

## Materials and Methods

### Ethics statement

The experiments described in this study were conducted with human semen samples obtained with informed written consent from a panel of healthy normozoospermic donors (University student volunteers) assembled for the Reproductive Science Group at the University of Newcastle. All experiments were performed in accordance with protocols approved by the University of Newcastle Human Research and Ethics Committee.

### Reagents

Unless specified, chemical reagents were purchased from Sigma-Aldrich (St. Louis, MO, USA) and were of molecular biology or research grade. Rabbit polyclonal antibody against dynamín 1 (ab108458) was purchased from Abcam (Cambridge, England, UK); goat polyclonal antibody against dynamín 2 (sc-6400) and IZUMO1 (sc-79 543), mouse monoclonal antibody against CDC2 (CDK1) (sc-54) and rabbit polyclonal antibody against CDK5 (sc-173) were from Santa Cruz Biotechnology (Dallas, TX, USA); rabbit polyclonal anti-dynamín 2 (PA5-19 800) and sheep polyclonal anti-phospho-dynamín 1 (Ser-778) antibodies were from Thermo Fisher Scientific (Eugene, OR, USA); rabbit polyclonal antibody against dynamín 3 (14 737-1-AP) was purchased from Proteintech Group (Chicago, IL, USA); mouse monoclonal antibody against  $\alpha$ -tubulin (T5168) was from Sigma-Aldrich. Alexa Fluor 594-conjugated goat anti-rabbit, donkey anti-goat and goat anti-mouse, Alexa Fluor 488-conjugated donkey anti-sheep and goat anti-rabbit were all purchased from Thermo Fisher Scientific. Anti-rabbit immunoglobulin G (IgG) conjugated to horse radish peroxidase (HRP) was supplied by Millipore (Chicago, IL, USA) and anti-sheep IgG-HRP was supplied by Abcam. Full details of the primary and secondary antibodies are also provided in Supplementary Table S1. Bovine serum albumin (BSA) was purchased from Research Organics (Cleveland, OH, USA). D-glucose was supplied by Ajax Finechem (Auburn, NSW, Australia). Percoll, HEPES and nitrocellulose were from GE healthcare (Buckinghamshire, England, UK). Precast 4–20% polyacrylamide gels were purchased from Bio-Rad Laboratories (Gladesville, NSW, Australia). Minicomplete protease inhibitor cocktail tablets were supplied by Roche (Sandhoferstrasse, Mannheim, Germany). Mowiol 4–88 was from Calbiochem (La Jolla, CA, USA), paraformaldehyde (PFA) was obtained from ProSciTech (Thuringowa, QLD, Australia). Human testis lysate was purchased from Santa Cruz Biotechnology. CDK1 inhibitor (217 695) was from Millipore. Dynamín inhibitors, Dynasore and Dyngo 4a were purchased from Tocris Bioscience (Bristol, England, UK) and Abcam, respectively. Dyngo- $\Theta$  (an inactive chemical analogue of both the Dynasore and Dyngo 4a inhibitors) was generated in our laboratory as previously described (McCluskey *et al.*, 2013).

### Human semen analysis

All semen samples used in this study were assessed according a specialized methodological checklist (Björndahl *et al.*, 2015). Briefly, semen samples were collected following sexual abstinence of at least 2 days. After collection, all samples were kept at 37°C and were de-identified prior to delivery to the laboratory except for assignment of a unique identification number. Sample analysis was initiated after completion of liquefaction and within 1 h of ejaculation. At least 100 cells were assessed in each of two duplicates for determination of cell motility, viability and morphology, with at least

five microscope fields of view being examined in each duplicate count. Sperm morphology was assessed in accordance with WHO criteria (World Health Organization, 2010) in the absence of papanicolaou, Shorr or Diff-Quik staining using  $\times 400$  magnification and bright field microscopy (Olympus CX40, Olympus, Sydney, Australia). Motility assessment was performed using phase contrast microscope optics ( $\times 400$  magnification), with cells being classified as either motile (i.e. sperm that displayed any form of motility ranging from rapid progressive to non-progressive) or immotile. The aliquot of semen used for assessment of sperm concentration was sampled using a positive displacement pipette with care taken to avoid the introduction of bubbles during aspiration. No assessment of anti-sperm antibodies was performed, however, all samples were free of abnormal clumping (aggregates and agglutinates) and the presence of excessive inflammatory cells ( $< 1$  million/ml). No biochemical markers for prostatic, seminal vesicle or epididymal secretions were analysed owing to our focus on spermatozoa.

## Human spermatozoa preparation and capacitation

Human semen samples were fractionated over a discontinuous Percoll density gradient (comprising 40 and 80% Percoll suspensions) by centrifugation at  $500 \times g$  for 30 min (Redgrove et al., 2012). After centrifugation, two fractions comprising the interface of the 40 and 80% Percoll suspensions and the pellet at the base of the 80% Percoll suspension were collected individually prior to being resuspended in a non-capacitating (non-cap) formulation of Biggers, Whitten and Whittingham medium (BWW) (Biggers et al., 1971) containing 1 mg/ml polyvinyl alcohol (PVA) but prepared without  $\text{HCO}_3^-$  (osmolarity of 290–310 mOsm/kg) (Bromfield et al., 2015a). A subset of these cells were assessed for motility and concentration while the remainder were washed by centrifugation at  $500 \times g$  for 15 min. The sperm cells collected from the base of the 80% Percoll suspension are nominally referred as 'good quality' or 'mature' spermatozoa, whereas those partitioning at the 40/80% Percoll interface are referred to as 'poor quality' spermatozoa (Aitken et al., 1993). Unless otherwise stated, good quality spermatozoa were used throughout our experiments following their resuspension in medium appropriate to experimental requirements.

To induce capacitation *in vitro*, spermatozoa were incubated in a formulation of BWW (91.5 mM NaCl, 4.6 mM KCl, 1.7 mM  $\text{CaCl}_2 \cdot 2 \text{H}_2\text{O}$ , 1.2 mM  $\text{KH}_2\text{PO}_4$ , 1.2 mM  $\text{MgSO}_4 \cdot 7 \text{H}_2\text{O}$ , 25 mM  $\text{NaHCO}_3$ , 5.6 mM D-glucose, 0.27 mM sodium pyruvate, 44 mM sodium lactate, 5 U/ml penicillin, 5 mg/ml streptomycin, 20 mM HEPES buffer, 1 mg/ml PVA (substituted for BSA; osmolarity of 290–310 mOsm/kg), 3 mM pentoxifylline and 5 mM dibutyl-yl cyclic adenosine monophosphate) that has previously been optimized for the induction of human sperm capacitation as assessed via tyrosine phosphorylation status, zona pellucida-binding competence and, importantly in the context of this study, the ability to complete an acrosome reaction (Mitchell et al., 2007). Where indicated, the capacitating medium was supplemented with either dimethyl sulfoxide (DMSO) (vehicle control), Dynasore, Dyngo 4a or Dyngo- $\ominus$ . Spermatozoa were incubated at a concentration of  $10 \times 10^6$  cells/ml at  $37^\circ\text{C}$  under an atmosphere of 5%  $\text{CO}_2$ :95% air for 3 h with a gentle inversion every 30 min to prevent settling of the cells (Mitchell et al., 2007; 2008; Redgrove et al., 2011). After incubation, spermatozoa were prepared for assessment of their capacity to undergo an acrosomal reaction utilizing the assay protocols outlined below.

## Acrosomal reaction assays

Following appropriate incubation, spermatozoa (non-capacitated, capacitated, dynamin inhibited or Dyngo- $\ominus$  treated) were induced to acrosome react by supplementation of media with either  $2.5 \mu\text{M}$  A23187 for 30 min or  $15 \mu\text{M}$  progesterone (pH 7.00–7.05) for 2 h in the presence of dynamin

inhibitors or vehicle controls prepared at the same concentration as utilized during the initial capacitation incubation. The spontaneous rates of acrosome loss were assessed via the inclusion of a capacitated sperm control group (designated Cap control), which were prepared under identical incubation conditions with the exception that they did not receive an A23187 or progesterone stimulus. At the completion of this induction period, sperm motility and viability were assessed (Bromfield et al., 2015a) to ensure neither parameter was compromised by any of the treatments. The cells were then incubated in pre-warmed hypo-osmotic swelling media (HOS; 0.07% w/v sodium citrate; 1.3% w/v fructose) for another 30 min at  $37^\circ\text{C}$ . After being fixed in 4% PFA, spermatozoa were aliquoted onto 12-well slides, air-dried and permeabilized with ice cold methanol for 10 min. Cells were then incubated with fluorescein isothiocyanate (FITC)-conjugated PNA ( $1 \mu\text{g}/\mu\text{l}$ ) at  $37^\circ\text{C}$  for 15 min, and the acrosomal status of viable cells (possessing coiled tails as a result of incubation in HOS medium) were verified using fluorescence microscopy (Zeiss Axio Imager A1, Jena, Thuringia, Germany). The wavelengths of the microscopic filters used for excitation and emission were 474 and  $\sim 527$  nm.

## Immunofluorescent localization

Human testis and epididymis sections used in this study were kindly provided by Dr Zhuo Yu of Shanghai Jiaotong University. These tissues were collected from donors diagnosed with prostatic carcinoma but showing normal morphology of both the testis and epididymis. Tissues were fixed in fresh Bouin's solution, embedded in paraffin and sectioned at  $5 \mu\text{m}$  thickness. Embedded tissue was dewaxed, rehydrated and then subjected to antigen retrieval as previously reported (Zhou et al., 2017). After being blocked with 3% BSA/phosphate-buffered saline (PBS) at  $37^\circ\text{C}$  for 1 h, slides were incubated with primary antibodies at  $4^\circ\text{C}$  overnight (for specific dilution rates of all antibodies see Supplementary Table S1). After three washes in PBS, slides were incubated with appropriate Alexa Fluor conjugated secondary antibodies at  $37^\circ\text{C}$  for 1 h. Following additional washes, slides were incubated with PNA at  $37^\circ\text{C}$  for 15 min and counter-stained with nuclear dyes; propidium iodide ( $5 \mu\text{g}/\text{ml}$ ) or 4',6-diamidino-2-phenylindole ( $2 \mu\text{g}/\text{ml}$ ). Slides were then washed and mounted with a 10% Mowiol 4–88 with 30% glycerol in 0.2 M Tris (pH 8.5) and 2.5% 1, 4-diazabicyclo-(2.2.2)-octane (DABCO). Staining patterns were recorded using fluorescence microscopy (Zeiss Axio Imager A1). The wavelengths of the microscopic filters used for excitation and emission were 474 nm and  $\sim 527$  nm (Alexa Fluor 488 and propidium iodide), and 585 nm and  $\sim 615$  nm (Alexa Fluor 594). Alternatively, confocal microscopy (Olympus IX81) was used for detection of fluorescent-labelling patterns using excitation and emission filters of wavelength 473 nm and 485–545 nm (Alexa Fluor 488), and 559 nm and 570–670 nm (propidium iodide).

For immunofluorescent staining of human spermatozoa, cells were fixed in 4% (w/v) PFA for 15 min at room temperature, washed in 0.05 M glycine/PBS and settled onto poly-L-lysine treated coverslips at  $4^\circ\text{C}$  overnight. For detection of the CDK1 kinase, cells were then subjected to antigen retrieval via immersion in 100 mM Tris, 5% urea (pH 9.5) at  $90^\circ\text{C}$  for 10 min (Reid et al., 2015) and permeabilized with 0.1% Triton X-100 for 10 min. For detection of all other proteins, spermatozoa were permeabilized with ice cold methanol for 10 min (no antigen retrieval required). Following PBS washes, cells were blocked with 3% BSA/PBS and immunolabelled as described for human testis and epididymis slides.

## Electron microscopy

Human spermatozoa were fixed in 4% (w/v) PFA containing 0.5% (v/v) glutaraldehyde. Cells were then processed via dehydration, infiltration and embedding in LR White resin. Sections (80 nm) were cut with a diamond knife (Diatome Ltd, Bienne, Switzerland) on an EM UC6 ultramicrotome (Leica Microsystems, Vienna, Austria) and placed on 200-mesh nickel

grids. Subsequent washes were performed using PBS containing 1% foetal calf serum (FCS). After being blocked with 10% FCS + 1% cold water fish gelatin in PBS (30 min), sections were incubated with primary antibodies overnight at 4°C. An appropriate secondary antibody conjugated to 10 nm (anti-goat) gold particles was incubated on grids for 90 min at room temperature. Sections were counterstained in 2% (w/v) uranyl acetate. Micrographs were taken on a Tecnai 12 transmission electron microscope (FEI Company) at 120 kV.

## SDS-PAGE and immunoblotting

Protein was extracted from human spermatozoa via boiling in SDS extraction buffer (0.375 M Tris pH 6.8, 2% w/v SDS, 10% w/v sucrose, protease inhibitor cocktail) at 100°C for 5 min. Insoluble material was removed by centrifugation (17 000 × g, 10 min, 4°C) and soluble protein remaining in the supernatant was quantified using a BCA protein assay kit (Thermo Fisher Scientific). Extracellular vesicles were isolated from seminal plasma using an optimized OptiPrep density gradient protocol (Reilly *et al.*, 2016) and proteins were extracted and quantified as described for human sperm samples. Equivalent amounts of protein (10 µg) were boiled in SDS-PAGE sample buffer (2% v/v mercaptoethanol, 2% w/v SDS, and 10% w/v sucrose in 0.375 M Tris, pH 6.8, with bromophenol blue) at 100°C for 5 min, prior to be resolved by SDS-PAGE (150 V, 1 h) and transferred to nitrocellulose membranes (350 mA, 1 h). Similar protocols were also used in order to prepare human testis protein (sc-363 781) for immunoblotting. Membranes were then blocked and incubated with appropriate antibodies raised against target proteins by using optimized conditions as previous described (Zhou *et al.*, 2017). Briefly, blots were washed three times × 10 min with either PBS supplemented with 0.5% (v/v) Tween-20 (PBST) (dynamín 1), or Tris-buffered saline with 0.1% (v/v) Tween-20 (TBST) (dynamín 2, dynamín 3, dynamín pSer778 and  $\alpha$ -tubulin), before being probed with appropriate HRP-conjugated secondary antibodies (see Supplementary Table S1). After three additional further washes, labelled proteins were detected using an enhanced chemiluminescence kit (GE Healthcare). Where appropriate labelled protein band intensity was determined by densitometry using Image J-win64 software (Gassmann *et al.*, 2009; Xia *et al.*, 2016).

## Immunoprecipitation

Capacitated spermatozoa were progesterone treated for 1 h. After treatment, cell lysis was performed on a total population of  $\sim 100 \times 10^6$  cells in 200 µl cell lysis buffer (10 mM CHAPS, 10 mM HEPES, 137 mM NaCl and 10% glycerol supplemented with a protease inhibitor cocktail) at 4°C for 2 h. Following centrifugation (15 000 × g, 4°C for 10 min), the supernatant containing soluble protein was transferred to a clean tube and precleared by incubation with 50 µl aliquots of a protein G Dynabead slurry at 4°C for 30 min. A total of 3 µg of anti-DNM2 antibody was then added to the pre-cleared cell lysate followed by overnight incubation at 4°C with constant rotation. At the completion of this incubation period, protein G Dynabeads were added and the suspension returned to rotation for a further 30 min at 4°C to facilitate the precipitation of target antigens. The beads were subsequently washed three times in PBS, prior to resuspension in SDS loading buffer and boiling for 5 min to elute target proteins. These proteins were then subjected to immunoblotting with either anti-DNM2 or anti-DNM1 serine-778 antibodies.

## Duolink proximity ligation assay

Human spermatozoa were prepared for Duolink *in situ* proximity ligation assays (PLAs) as previously described. In brief, capacitated populations of human spermatozoa were incubated in the presence or absence of progesterone (15 µM) for 1 h. Non-capacitated cells were incubated for

the same time period in non-cap BWV medium alone. Following incubation, sperm motility and viability were recorded and the cells were then fixed, washed and settled onto poly-L-lysine treated coverslips at 4°C overnight. After antigen retrieval and permeabilization (see immunofluorescence; all antibodies used for PLA were first assessed via immunofluorescence for compatibility of antigen retrieval conditions), PLA labelling was conducted according to the manufacturers' instructions (OLINK Biosciences, Uppsala, Sweden) using pairs of primary antibodies comprising anti-CDK1 and anti-DNM2, anti-CDK1 and anti-DNM1 or anti-CDK1 and anti-IZUMO1 (irrelevant antibody control). Appropriate synthetic oligonucleotide-conjugated secondary antibodies (OLINK Biosciences) were subsequently applied for incubation at 37°C 1 h. After ligation and amplification, sperm cells were viewed using fluorescence microscopy (Zeiss Axio Imager A1). In this assay, target proteins residing within a maximum distance of 40 nm from each other are detected via the generation of foci of red fluorescent dots. A threshold of three or more fluorescent foci within the sperm head was set for the recording of positive PLA signals (Bromfield *et al.*, 2015b). Using this criterion, a total of 100 spermatozoa were assessed per sample ( $n = 5$ ) and the percentage of PLA positive cells was recorded.

## Statistics

Experiments reported in this study were repeated on at least five unique biological samples, with each sample representing semen collected from a single healthy normozoospermic donor. For the purpose of assessing acrosome reaction status and dynamín labelling profiles,  $\geq 100$  spermatozoa were counted in each sample and the corresponding percentage of acrosome reacted or positively labelled cells, respectively were determined dividing by the total number of cells counted. Graphical data are presented as the mean values  $\pm$  SEM, which were calculated from the variance between samples. Statistical significance was determined by using an ANOVA.

## Results

### Detection of dynamín isoforms in human testis and mature spermatozoa

The presence of the three canonical dynamín isoforms (DNM1, DNM2 and DNM3) was assessed in lysates prepared from human testis and ejaculated spermatozoa. For this purpose, testis lysate was purchased from a commercial source (Santa Cruz Biotechnology) and Percoll fractionated spermatozoa were isolated from the semen of at least five donors of known fertility. In the case of DNM1, a predominant band of the anticipated size ( $\sim 100$  kDa) was detected in the mature sperm lysate (Fig. 1A). Notably however, an equivalent protein was not detected in human testis lysate (Fig. 1A). To discount the possibility of protein degradation within the testis lysate, these samples were further assessed by stripping of the membranes and re-probing with anti- $\alpha$ -tubulin antibody. This approach confirmed both the integrity of the testis protein sample and the equivalent protein loading achieved between testis and sperm lysates. To address the alternative possibility of relatively low DNM1 expression in human testes, the quantity of testis protein was increased three fold (i.e. 30 µg versus 10 µg for sperm lysate) but there was no associated increase in the detection of DNM1 (data not shown).

The detection of a doublet of around 100 kDa for DNM1 in sperm lysates (Fig. 1A, arrowheads) also prompted a further investigation of the potential for this band to represent a phosphorylated form of the

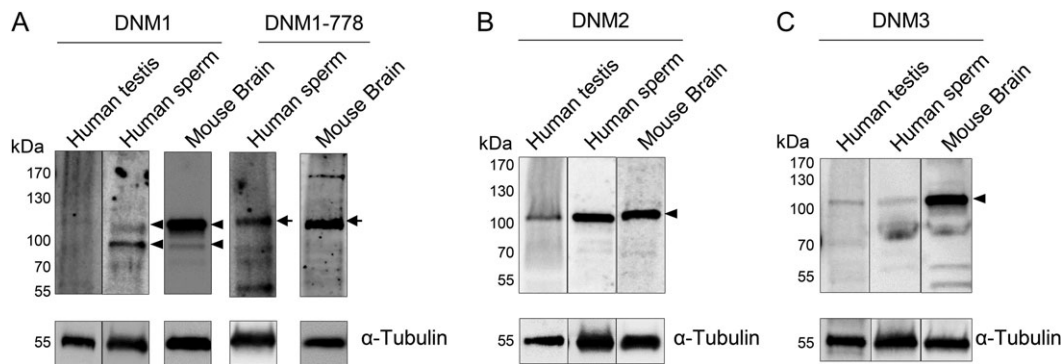


**Figure 1** Identification of dynamin isoforms in human testis and sperm lysates. Human testis and sperm lysates were analysed for the presence of (A) dynamin 1 (DNMI), (B) dynamin 2 (DNM2) and (C) dynamin 3 (DNM3) using standard immunoblotting protocols. Mouse brain tissue homogenates were resolved alongside the human samples as a positive control for dynamin expression. After initial dynamin labelling, blots were stripped and re-probed with anti- $\alpha$ -tubulin antibody to confirm equivalent protein loading of each sample. (A) The detection of a doublet of  $\sim 100$  kDa for DNMI (arrowheads) prompted a further investigation of the potential for post-translational phosphorylation of this isoform. For this purpose, anti-phospho-DNMI-778 antibody was used to probe the same samples of mouse brain and human sperm lysates, revealing positive labelling of the higher molecular weight band (arrows). These experiments were repeated on spermatozoa obtained from five different healthy normozoospermic donors and representative immunoblots are shown. In contrast, testicular lysates were obtained from a commercial supplier and represent material prepared from a single healthy donor.

protein. For this purpose, additional immunoblotting was conducted on the same homogenates of mouse brain (a tissue in which abundant phosphorylated DNMI is present), and human spermatozoa using an antibody that detects phosphorylated DNMI serine-778. Labelling with this antibody was restricted to the higher molecular weight band (Fig. 1A, arrows) potentially indicating that the basal level of DNMI phosphorylation differs depending on the tissue from which the protein is isolated.

Notwithstanding some minor cross-reactivity, dominant protein bands corresponding to those of the predicted size for DNM2 and DNM3 (also  $\sim 100$  kDa) were detected in both the human testis and sperm lysates (Figs 1B and 1C, arrowheads). In all cases, an additional positive control consisting of mouse brain lysate was subsequently probed for DNMI, DNM2 and DNM3, revealing the labelling of the same size band in this tissue (Fig. 1).

### Immunolocalization of dynamin isoforms in human testis

In view of the detection of dynamin expression in the human testis and/or sperm lysates, we next sought to investigate the specific localization of these enzymes within histological sections of human testes. Immunofluorescence was applied in this study in combination with a peanut agglutinin (PNA) counterstain of the developing sperm acrosome (Mortimer et al., 1987), and representative micrographs illustrating the expression patterns of dynamin are shown in Fig. 2. Consistent with the immunoblotting of testis lysate, immunofluorescence failed to reveal any significant DNMI expression in human testis sections (Fig. 2A–C). The absence of DNMI labelling persisted despite the application of a variety of antigen retrieval techniques in combination with trials to optimize incubation time and antibody concentration (data not shown). These data contrast those obtained for DNM2 immunolabelling, with distinct fluorescence foci being readily detected

for DNM2 in the developing germ cell population of the human testes. While the quality of the testis sections precluded the precise determination of the temporal expression of DNM2, spatially, the protein was clearly co-localized with PNA in round and elongating spermatids (Fig. 2E–G). Such findings implicate DNM2 in acrosomal biogenesis during the later stages of the spermatogenic cycle. Additional DNM2 immunofluorescence was also detected, albeit considerably weaker, within the Sertoli cells of the seminiferous tubules. In the case of DNM3, a punctate pattern of localization was observed throughout the seminiferous tubules and, whilst this labelling did appear in the vicinity of the developing germ cells (Fig. 2I–K), we failed to detect any direct co-localization of DNM3 and PNA in germ cell populations. These later findings agree with those reported in the mouse testis (Reid et al., 2012), and suggest that DNM3, like that of DNMI, is unlikely to participate in the morphogenesis of the acrosomal vesicle in human spermatozoa. The specificity of all immunolabelling studies was confirmed through the inclusion of negative controls comprising secondary antibodies only (Fig. 2D, H, L) and anti-dynamin antibodies that had been pre-absorbed with excess immunizing peptide (where available, Supplementary Fig. S1A). As anticipated, none of these controls revealed any labelling of testis sections.

### Immunolocalization of dynamin isoforms in human spermatozoa

Immunofluorescent localization of dynamin was also performed on the isolated spermatozoa of normozoospermic donors (Fig. 3). In order to account for the possibility of either inter- and intra-donor variability in dynamin expression, these studies were conducted on spermatozoa obtained from at least five different donors, as well as on the spermatozoa purified from multiple ejaculates obtained from the same donor, respectively. Among the notable findings from this analysis was the detection of strong DNMI labelling throughout the entire

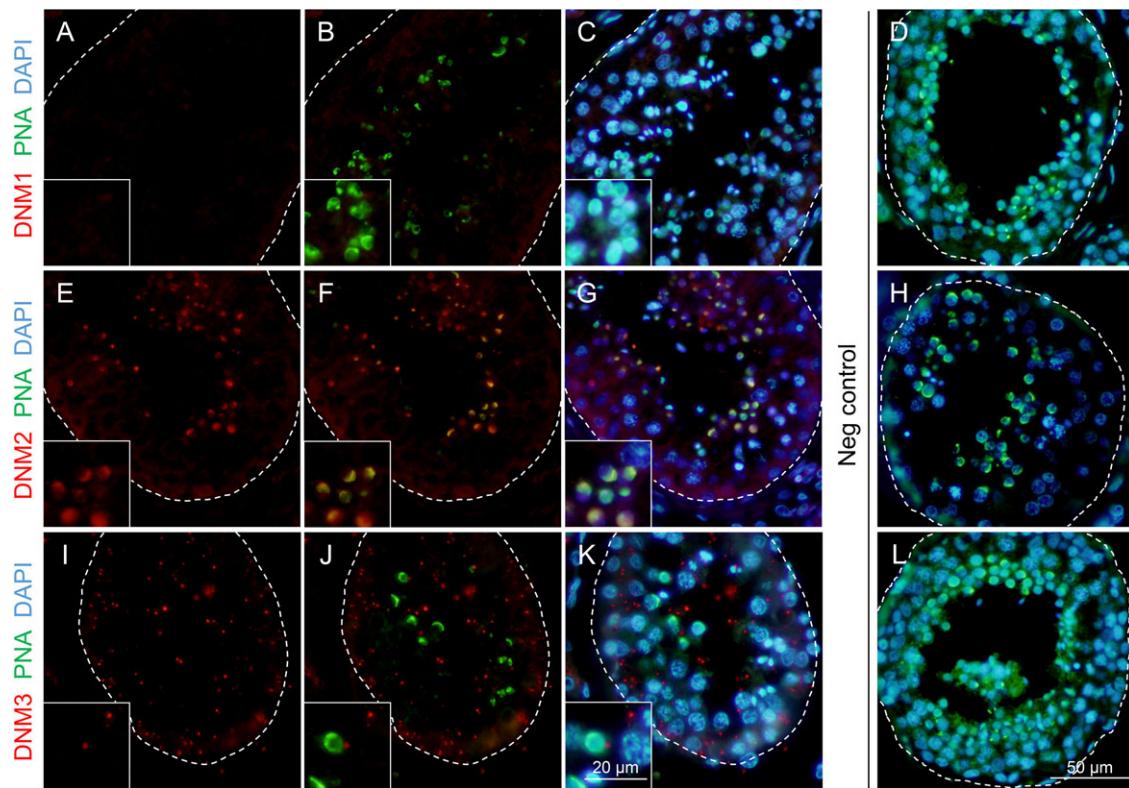


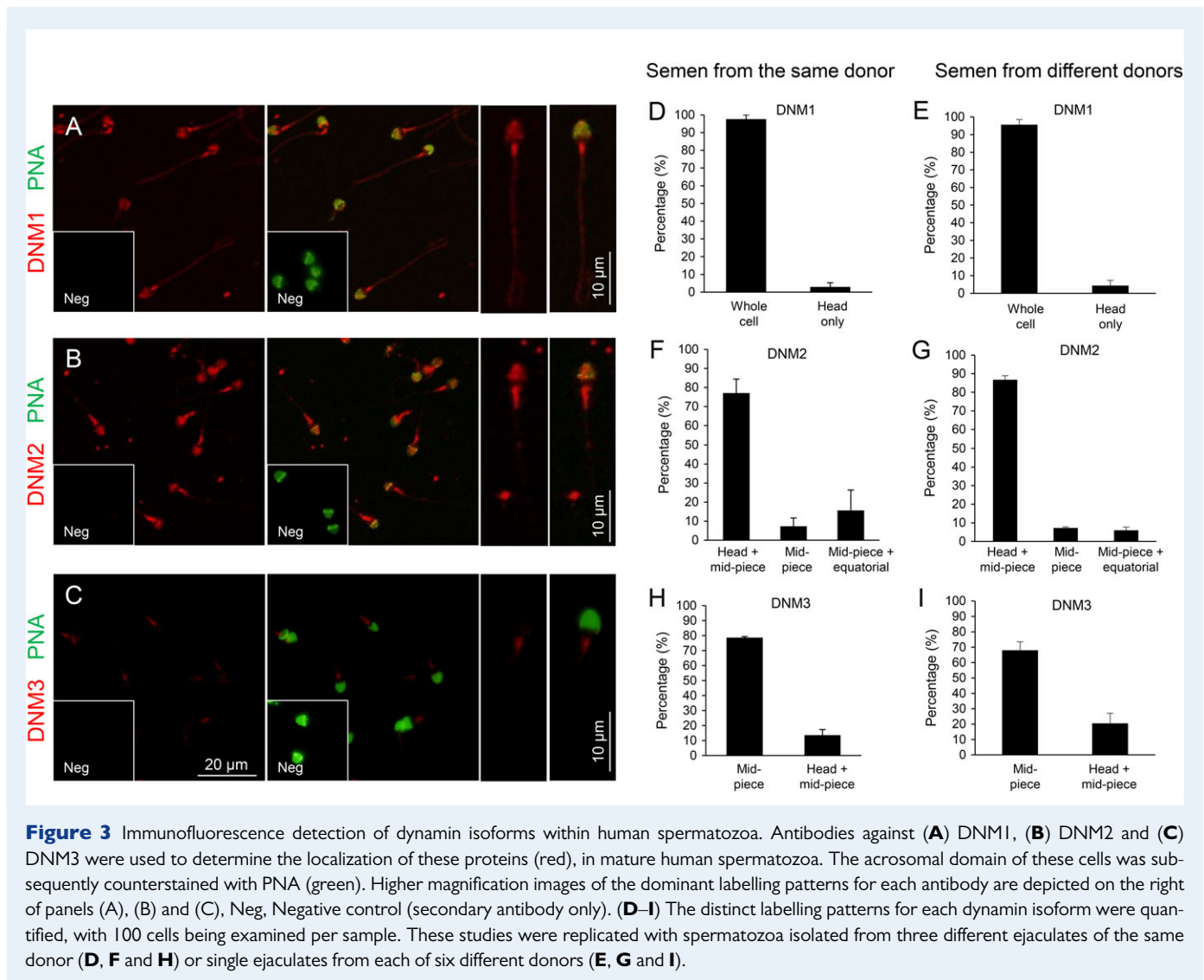
**Figure 2** Immunofluorescence detection of dynamín isoforms within the human testis. Antibodies against (A, B and C) DNMI1, (E, F and G) DNMI2 and (I, J and K) DNMI3 were used to determine the localization of these proteins (red) in human testis sections. These sections were subsequently counterstained with PNA (green) and DAPI to reveal the acrosome, and the cell nuclei (blue) of developing germ cells, respectively. For clarity, the structure of seminiferous tubules has been outlined. Among the three dynamín isoforms examined, only DNMI2 was found to co-localize with the developing acrosomal vesicle. (D, H and L) The specificity of antibody labelling was confirmed through the inclusion of negative controls (Neg) in which antibody buffer was substituted for the primary antibody. These experiments were replicated on material from three human donors and representative immunofluorescence images are shown. Insets are of equivalent sections shown at higher magnification.

spermatozoon (Fig. 3A). Importantly, this pattern of localization was present in virtually all cells examined, irrespective of whether they were sourced from multiple ejaculates of the same, or different, donors (Fig. 3D and E). While such results clearly contrast those obtained in human testis sections (Fig. 2A–C), they nevertheless accord with the positive DNMI1 protein band labelled in human sperm lysates (Fig. 1A). Since spermatozoa leaving the testis are incapable of either gene transcription or protein translation, such findings raise the prospect that DNMI1 may be acquired by spermatozoa from the external environment in which they are bathed during their functional maturation in the epididymis.

To begin to investigate this possibility, human epididymal sections were subjected to immunofluorescence labelling under identical conditions to those described for the testes. This analysis revealed positive DNMI1 staining throughout the cytoplasm of the epithelial cells lining the epididymal duct (Supplementary Fig. S2A). Additional labelling was also detected in the lumen of the epididymis and, at least a portion of this, was found to co-localize with sperm heads (Supplementary Fig. S2A). Although we failed to source a reliable supply of human epididymal fluid, we were able to detect a positive signal for DNMI1 by immunoblotting of whole seminal fluid (Supplementary Fig. S2B).

A similar DNMI1 band was also present in fractionated seminal fluid samples prepared using an OptiPrep density gradient protocol that has been optimized for the isolation of extracellular vesicles (Supplementary Fig. S2B). While further experimentation is required before definitive conclusions can be drawn, such data offer tentative support for the delivery of DNMI1 to maturing human spermatozoa during their post-testicular maturation.

Similar to DNMI1, DNMI2 was also readily detected in human spermatozoa. In this case however, the most common pattern of labelling placed DNMI2 in the sperm head and the mid-piece of their flagellum, with essentially no labelling being detected in the principal-piece of the flagellum (Fig. 3B, F and G). The labelling of DNMI2 in the head was further verified by electron microscopy, which demonstrated positive immunogold labelling within the acrosomal domain (Supplementary Fig. S3). In contrast with DNMI2, only very weak DNMI3 staining was recorded in human spermatozoa. In the majority of cells, this labelling appeared restricted to the mid-piece of the flagellum, but in ~20% of the population it was accompanied by additional labelling within the sperm head (Fig. 3C, H and I). Such weak labelling of DNMI3 raises the prospect that DNMI1 and/or DNMI2 fulfil the predominant functional role(s) of dynamín in mature spermatozoa.



In all cases, dynamin labelling was highly reproducible and displayed minimal variation among the biological replicates examined. Similarly, the inclusion of negative controls in which spermatozoa were incubated with either secondary antibodies only (Fig. 3A–C, insets) or anti-dynamin antibodies that had been pre-absorbed with excess immunizing peptide (where available, Supplementary Fig. S1B) also supported the specificity of the immunofluorescent staining we documented across these samples.

### Inhibition of dynamin 1 and 2 suppresses the induction of acrosomal exocytosis *in vitro*

The localization of DNMI and DNM2 in the anterior region of the head of mature human spermatozoa ideally positions these two isoforms to participate in the regulation of acrosomal exocytosis, consistent with the putative function of the enzymes in mouse spermatozoa (Reid et al., 2012). We therefore investigated whether pharmacological inhibition of DNMI and DNM2 could compromise the *in vitro* induction of acrosomal exocytosis in human spermatozoa. However, prior to implementing these experiments, we first sought to optimize

an assay capable of eliciting an acrosome reaction independent of the use of a calcium ionophore. For this purpose, capacitated populations of human spermatozoa were primed with progesterone during incubation in capacitating BWW media formulated to encompass the pH range of 6.4–7.8. Live cells were subsequently assessed for their acrosomal status by labelling with FITC-conjugated PNA, with those cells displaying curled tails (induced by incubation in HOS medium) and green fluorescence over the complete peri-acrosomal domain being classified as acrosome intact (Cheng et al., 1996). In contrast, acrosome reacted spermatozoa were defined as those in which PNA was either absent or restricted to the equatorial domain (Cheng et al., 1996; Esteves et al., 1998). By imposing these criteria, we consistently achieved optimal acrosome reaction rates in BWW with a pH of 7.00–7.05 (Supplementary Fig. S4).

Using these optimized conditions, populations of human spermatozoa were found to be significantly inhibited in their capacity to undergo a progesterone-induced acrosome reaction if capacitation medium was supplemented with the dynamin inhibitors of Dynasore or Dyngo 4a (Fig. 4A,  $P < 0.05$ ), compared to spermatozoa from the capacitated + vehicle (DMSO) control group. The inclusion of Dyngo- $\Theta$ , an inactive

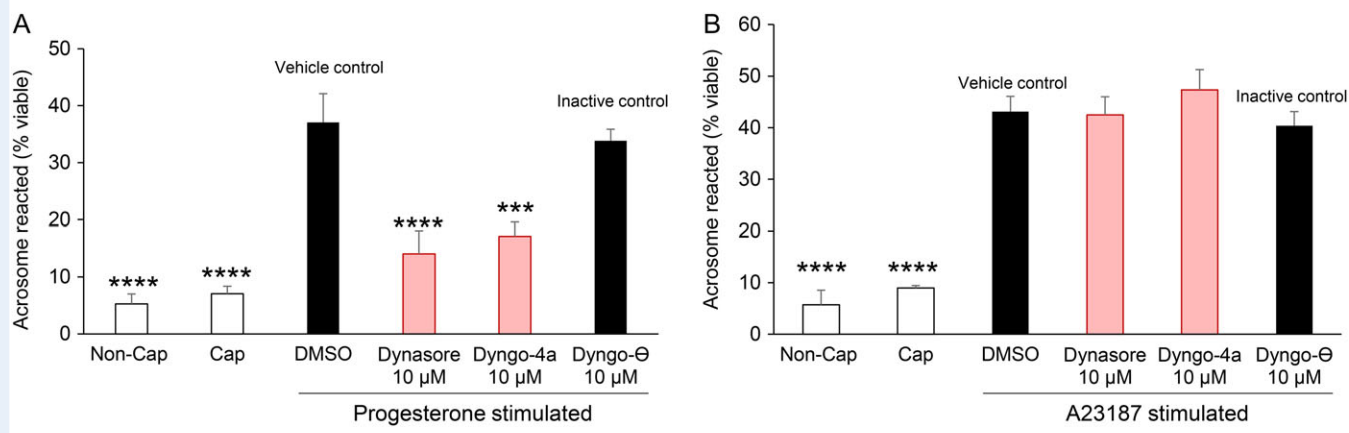


**Figure 4** Examination of the effect of dynamín inhibition on the ability of human spermatozoa to engage in acrosomal exocytosis. PNA staining was applied to record the acrosomal status of viable spermatozoa from each of several treatment groups. Cells were induced to acrosome react via either a (A) progesterone (15 μM) or (B) calcium ionophore (A23187, 2.5 μM) stimulus. (A) A significant reduction in the number of acrosome reacted cells was observed in the presence of dynamín inhibitors (Dynasore or Dyngo, 10 μM) when compared to treatment with either the vehicle control (DMSO) or an inactive isoform control (Dyngo-Θ). (B) No such reduction was detected when acrosomal exocytosis was induced via A23187 challenge. Five biological replicates were conducted for each experiment and the results are presented as the means ± S.E.M. \*\*\*\* $P < 0.001$ ; \*\*\*\*\* $P < 0.0001$  compared to vehicle control (DMSO).

chemical analogue of Dynasore and Dyngo 4a, did lead to a modest suppression of acrosome reaction rates. Importantly however, this reduction did not prove to be significantly different from that of either of the positive control treatment groups (capacitated ± DMSO), but did differ significantly ( $P < 0.05$ ) compared to both Dynasore and Dyngo 4a groups, thus precluding the possibility of non-specific pharmacological inhibition.

The selectivity of inhibition was reinforced by the demonstration that neither Dynasore nor Dyngo 4a could prevent the induction of acrosomal exocytosis by the calcium ionophore, A23187. Indeed, no significant differences were recorded in levels of A23187 induced acrosome reaction rates among the capacitated populations of spermatozoa treated with either Dynasore, Dyngo 4a, Dyngo-Θ or DMSO (Fig. 4B). Further, neither of the dynamín inhibitors nor the inactive isoform control had a detrimental impact on sperm viability, which consistently remained above 75% in all treatment groups. In the case of Dyngo 4a, we did record a modest reduction in overall sperm motility (Supplementary Fig. S5). However, an equivalent reduction in sperm motility was not observed in the cells treated with Dynasore. Overall, these results are consistent with our previous reports of the response of mouse spermatozoa to dynamín inhibition (Reid *et al.*, 2012), indicating a conserved relationship between the activity of this enzyme and the ability of spermatozoa to undergo a progesterone-induced acrosome reaction.

### Comparison of dynamín expression in populations of good and poor quality human spermatozoa

The ability to modulate acrosomal responsiveness in human spermatozoa through selective inhibition of dynamín prompted a more detailed evaluation of this enzyme in good and poor quality human sperm cells.

To achieve this, semen samples from healthy normozoospermic individuals were fractionated via Percoll density gradient centrifugation into two discrete populations, referred to as a poor quality fraction (i.e. spermatozoa that partitioned at the interface of the 40–80% Percoll suspension) and a good quality fraction (i.e. high quality spermatozoa that pelleted at the base of 80% Percoll suspension). These two populations of human spermatozoa have been well characterized in previous reports and shown to possess significant differences in morphology ( $P < 0.03$ ), motility and competence to fuse with the oolemma ( $P < 0.001$ ) (Aitken *et al.*, 1993). The presence of contaminating cellular debris, immature germ cells and other components within the poor quality fraction precluded the use of immunoblotting to accurately determine the relative amount of the dynamín isoforms in each subpopulation of spermatozoa. Thus, immunofluorescence was applied with a view to determining the percentage of spermatozoa harbouring DNMI and DNMI2 within the anterior head.

As illustrated in Fig 5A and B, a similar proportion of spermatozoa displayed DNMI head labelling irrespective of whether they were recovered from the poor or good quality subpopulations. In marked contrast, a dramatic underrepresentation of DNMI2 was recorded in spermatozoa that partitioned into the lower quality subpopulation. Notably, this highly significant reduction in DNMI2 labelling was restricted to the sperm head, with the majority of these cells retaining DNMI2 labelling in the mid-piece of their flagellum (Fig. 5C and D).

To begin to explore the functional consequences of reduced DNMI2 expression in the head of poor quality spermatozoa, we compared the ability of our subpopulations to undergo an acrosome reaction in response to either a progesterone or calcium ionophore (A23187) stimulus. This analysis was again conducted using FITC-PNA labelling to assess acrosomal integrity and only live spermatozoa (possessing coiled tails as a result of incubation in HOS medium) were counted. Consistent with the reduction of DNMI2 in the sperm head, those cells

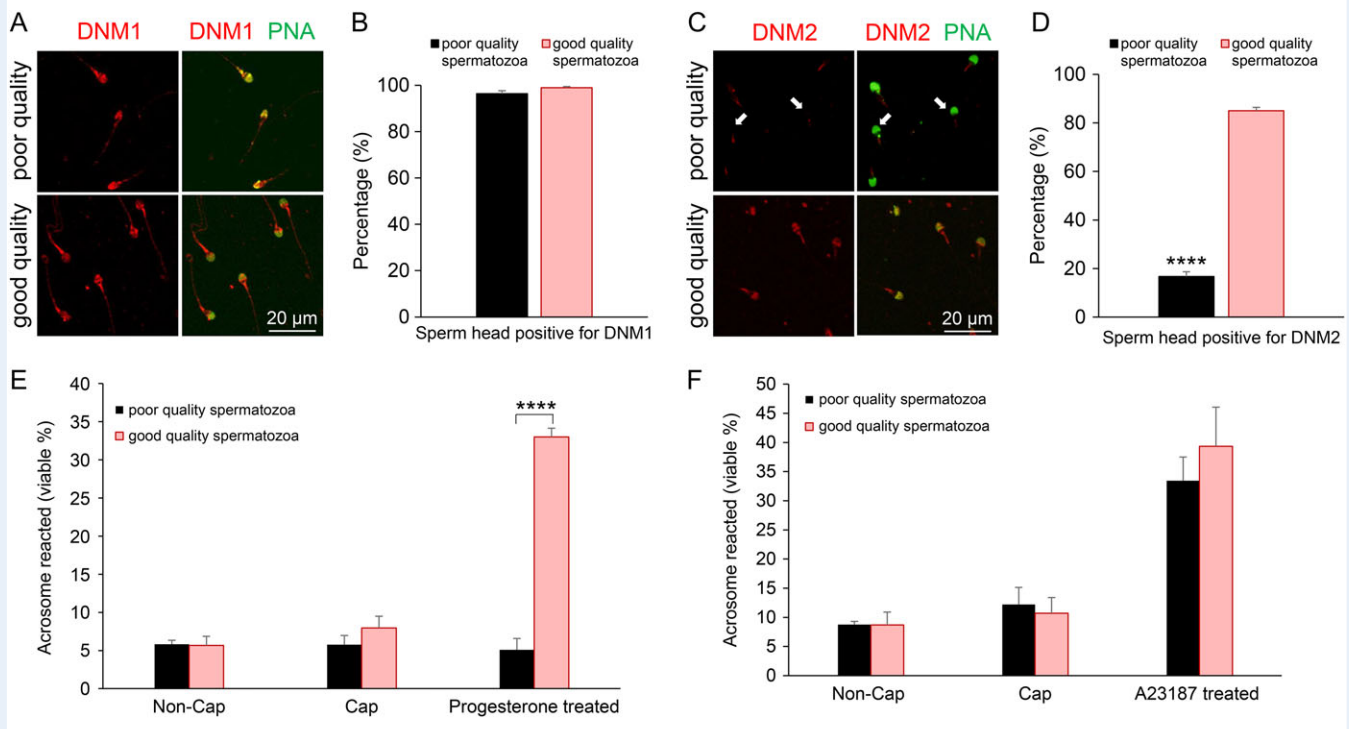


**Figure 5** Comparison of dynamin expression in populations of good and poor quality human spermatozoa. Two subpopulations comprising good and poor quality spermatozoa were generated via Percoll density gradient centrifugation of semen from the same donor. (A and B) Immunolabelling of DNMI revealed an equivalent staining pattern in both good and poor quality subpopulations of mature spermatozoa. (C and D) By contrast, immunolabelling of DNM2 demonstrated an apparent reduction in the amount of this protein in the head of poor quality spermatozoa (arrows) versus that of the good quality subpopulation of cells. Spermatozoa from each of the two subpopulations were induced to acrosome react with either (E) progesterone (15  $\mu$ M) or (F) calcium ionophore (A23187, 2.5  $\mu$ M) stimulus. (E and F) The poor quality spermatozoa were significantly compromised ( $P < 0.0001$ ) in their capacity to complete a progesterone, but not an A23187, induced acrosome reaction compared to good quality spermatozoa. Non-Cap: the spermatozoa in these samples were not capacitated prior to the addition of progesterone or A23187. Cap: the spermatozoa in these samples were capacitated yet received no additional progesterone or A23187 stimulus. Five biological replicates were conducted with quantification of dynamin labelling and acrosomal status being performed across 100 cells per sample. Results are presented as the means  $\pm$  S.E.M. \*\*\*\* $P < 0.0001$ .

that were separated into the poor quality fraction proved entirely refractory to progesterone stimulus (Fig. 5E). Notably, the highly significant diminution in the response of these poor quality cells occurred despite the apparent retention of DNMI in the sperm head (Fig. 5A and B). It also contrasted with the results obtained with the good quality subpopulation, over 35% of which were induced to acrosome react following progesterone challenge (Fig. 5E). Importantly, this lack of responsiveness was restricted to progesterone-induced acrosome reactions, such that no equivalent decrease was observed following exposure to calcium ionophore (A23187) (Fig. 5F).

### CDKI regulates the human sperm acrosome reaction through dynamin phosphorylation

It is well established that dynamin function is regulated through alternating cycles of phosphorylation/de-phosphorylation. We therefore sought to investigate if DNMI and DNM2 activity in human spermatozoa is also regulated through phosphorylation. Specifically, we focused on the characterization of CDKs (CDK1 and CDK5), serine/threonine kinases that reportedly target DNM2 Ser-764 and DNMI Ser-778 for

phosphorylation in somatic cells (Tan et al., 2003; Chircop et al., 2011). Through the use of immunofluorescence labelling, we found CDK1 was detected in the peri-acrosomal region of the human sperm head (Fig. 6A). In contrast, CDK5 displayed a restricted profile of localization within the mid-piece of the flagellum with no accompanying head labelling being detected irrespective of the functional status (non-capacitated, capacitated and progesterone treated) of the sperm samples analysed (Fig. 6B illustrates the representative labelling detected in non-capacitated spermatozoa). This raises the possibility of CDK1 targeting the substrates of DNMI and/or DNM2 in the peri-acrosomal domain.

An *in situ* PLA was therefore employed to assess the co-localization of DNMI/DNM2 and CDK1 using the criterion of  $\geq 3$  punctate red fluorescent spots within the sperm head as a threshold for positive PLA labelling (Bromfield et al., 2015b) (Fig. 7). The combination of anti-CDK1 and anti-DNM2 antibodies, generated positive PLA signals that were primarily distributed over the anterior region of the sperm head. Although the percentage of CDK1/DNM2 PLA positive cells did not change following the induction of capacitation, it was significantly increased (from  $\sim 5$  to  $\sim 30\%$ ,  $P < 0.01$ ) upon the receipt of a

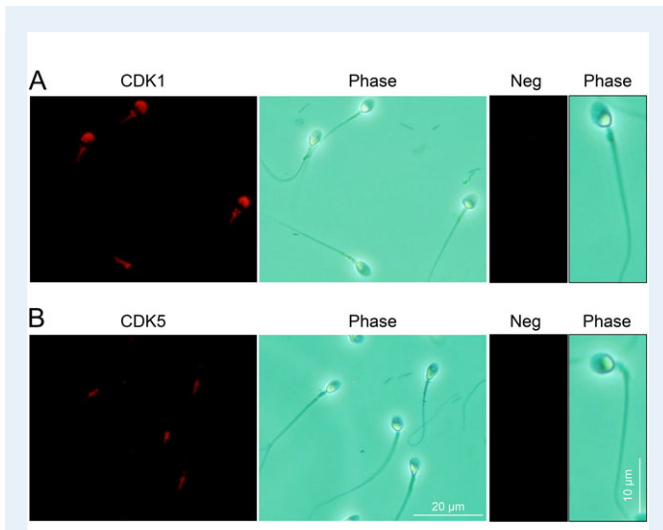


**Figure 6** Immunofluorescence detection of cyclin dependent kinases (CDK1 and CDK5) in human spermatozoa. **(A)** Immunolabelling of human spermatozoa with anti-CDK1 antibodies revealed the strong labelling of the protein within the acrosomal and mid-piece domains. **(B)** Equivalent immunolabelling with anti-CDK5 antibodies demonstrated a restricted pattern of localization within the mid-piece of the flagellum and no accompanying head labelling. (A and B) The specificity of antibody labelling was confirmed through the inclusion of negative controls (Neg) in which antibody buffer was substituted for the primary antibody. Three biological replicates were conducted and representative images are shown.

progesterone stimulus. In contrast, minimal PLA labelling was detected for the combination of anti-CDK1 and anti-DNM1 antibodies irrespective of the functional status of the spermatozoa (Fig. 7A, C and Supplementary Fig. S6). Similarly, the irrelevant combination of anti-CDK1 and anti-IZUMO1 (Fig. 7B) or anti-DNM1 and anti-BAG6 antibodies (data not shown) also failed to generate positive PLA signals.

Having secured evidence for a putative interaction between CDK1 and DNM2, we next sought to investigate whether pharmacological inhibition of CDK1 could compromise phosphorylation of DNM2 and consequently result in reduced rates of acrosomal exocytosis following progesterone stimulation. Previous reports indicate that the dominant site for DNM2 phosphorylation site is the residue Ser-764, which is homologous to the phosphorylation site of Ser-778 in DNM1 (Chircop *et al.*, 2011). Thus, we treated human spermatozoa with 10  $\mu\text{M}$  CDK1 inhibitor ( $\text{IC}_{50} = 5.8 \mu\text{M}$ ; Andreani *et al.*, (2000)) prior to assessing DNM1 Ser-778/DNM2 Ser-764 phosphorylation status with an antibody (anti-DNM1 Ser-778) that also recognizes the phosphorylated form of DNM2 Ser-764 residue (Supplementary Fig. S7). As shown in Fig 8A and B, spermatozoa treated with the CDK1 inhibitor experienced a significant reduction in the levels of phosphorylated DNM1 Ser-778/DNM2 Ser-764. Importantly, this reduction in phospho-labelling was restricted to the sperm head, coinciding with the location of CDK1 (Supplementary Fig. S8), and was not attributed to the loss of acrosomal contents, which were readily labelled with PNA in these spermatozoa (Fig. 8C). (Loss of acrosomal contents has also been associated with loss of DNM1 Ser-778/DNM2 Ser-764 in the acrosomal region; Supplementary Fig. S9). The impact of CDK1

inhibition also extended to a significant reduction in the rates of acrosomal exocytosis elicited in response to progesterone challenge (Fig. 8D) compared to that of the vehicle control (DMSO) group. Taken together, these data implicate the necessity for dynamín phosphorylation in the regulatory control of human sperm acrosomal exocytosis.

## Discussion

The completion of an acrosome reaction is a prerequisite for successful fertilization and accordingly, failure to complete this unique exocytotic event represents a common aetiology underpinning the defective sperm function of infertile males (Muller, 2000; Liu and Baker, 2003). In support of recent studies implicating the dynamín family of mechanoenzymes as important regulators of the acrosome reaction in murine spermatozoa (Reid *et al.*, 2012), we have provided evidence that this function may also be conserved in the spermatozoa of our own species. Specifically, our study has revealed that the canonical dynamín isoforms of DNM1, DNM2 and DNM3 are each represented among the proteome of ejaculated human spermatozoa. Further, DNM1 and DNM2 are ideally positioned within the anterior portion of the sperm head to enable them to exert an important regulatory influence over the acrosomal status of human spermatozoa. Accordingly, we report that the loss, or pharmacological inhibition of this enzyme, is associated with a concomitant reduction in the ability of human spermatozoa to complete a progesterone-induced acrosome reaction. The selectivity of such inhibition was supported by absence of an equivalent impact on acrosomal exocytosis induced by the calcium ionophore, A23187, which has the ability to bypass key physiological mechanisms required for acrosomal exocytosis (Buffone *et al.*, 2014).

The presence of dynamín isoforms within human spermatozoa has previously been recorded among the inventories arising from large scale proteomic profiling studies of fertile donors (Wang *et al.*, 2013; Amaral *et al.*, 2014). Indeed, these studies have revealed that human sperm harbour dynamín 2 and 3, in addition to the dynamín-like isoforms such as dynamín 1 like protein, dynamín-like 120 kDa protein S1. However, to the best of our knowledge, our study represents the first to confirm the presence of the three canonical dynamín isoforms and report their spatial expression profiles in the human testis, epididymis and ejaculated spermatozoa. Our findings raise the prospect that this family of mechanoenzymes may fulfil diverse, yet evolutionary conserved roles in the support of male germ cell development and function. Notwithstanding this possibility, we also observed some variation in the expression patterns of dynamín isoforms anticipated on the basis of previous observations in rodent models.

One particular curiosity was our inability to detect appreciable levels of dynamín 1 in human testis sections despite the relatively strong labelling of the protein in ejaculated spermatozoa (confirmed by both immunofluorescence and immunoblotting). Among the possible explanations for this observation is that DNM1 is either unmasked, or alternatively, uniquely acquired during the post-testicular maturation of spermatozoa. Arguing against the former explanation is the fact that we were unable to detect DNM1 in testis sections despite the application of a variety of antigen retrieval steps that have previously been successfully implemented in the mouse (Zhou *et al.*, 2017). Further, transcript and protein expression data sourced from public databases (Gene Expression Omnibus profile and the European Bioinformatics Institute) also indicate that DNM1 is not expressed in the human

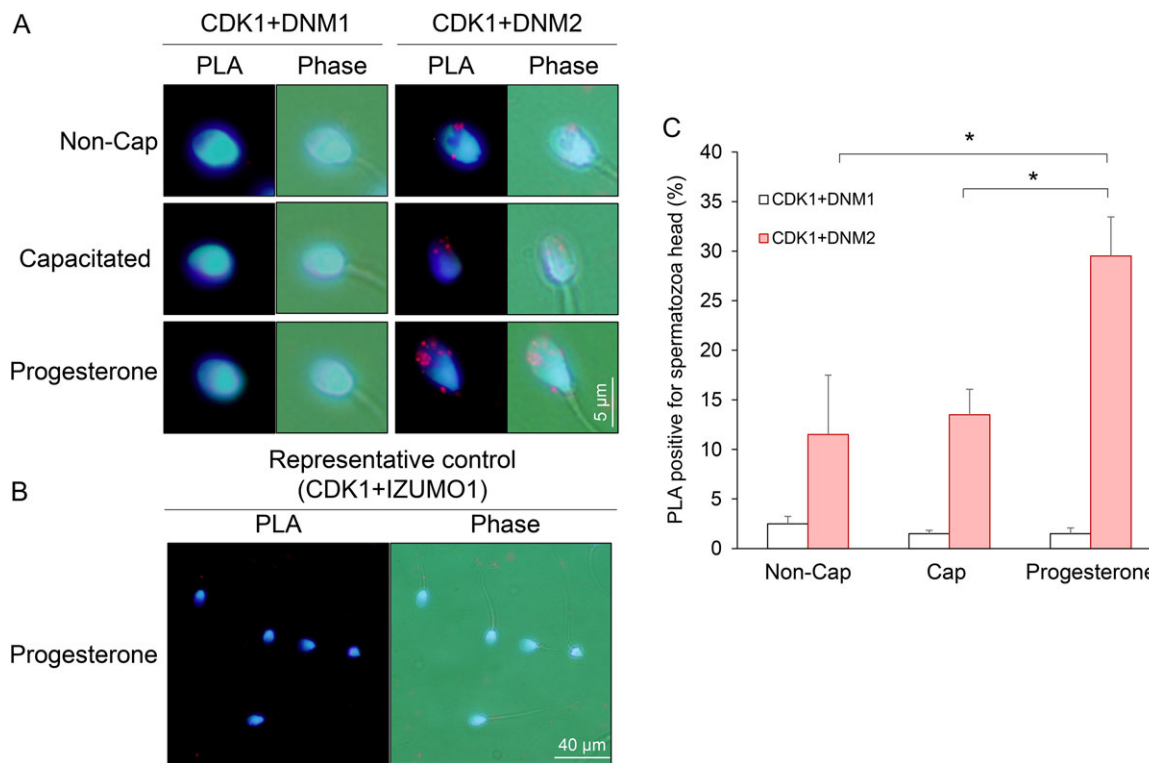
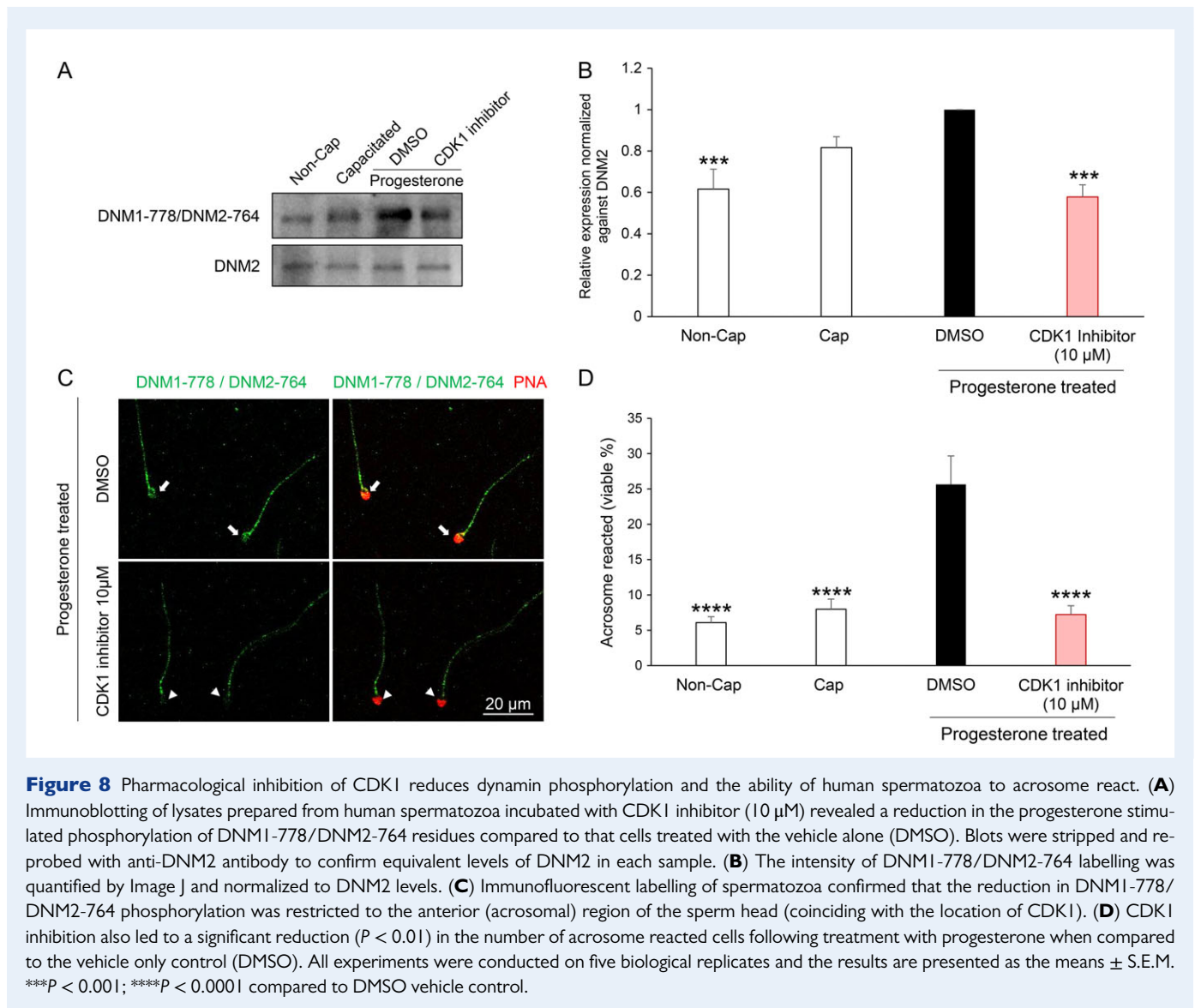


**Figure 7** Analysis of CDK1/dynamin 1 and CDK1/dynamin 2 interaction in human spermatozoa. PLAs were applied to investigate the putative interaction between CDK1/DNM1 and CDK1/DNM2 in the anterior region of the human sperm head. This assay generates punctate red fluorescent signals when the targeted pair of proteins reside within a maximum of 40 nm from each other. A threshold of  $\geq 3$  red fluorescent spots within the sperm head was set for recording of positive PLA labelling. For clarity, cells were counterstained with the nuclear stain, DAPI. **(A)** Representative PLA images demonstrating that CDK1 resides in close proximity to DNM2, but not DNMI1, in the anterior region of the sperm head. **(B)** The specificity of this interaction was confirmed through the use of antibodies targeting IZUMO1, a protein that is not expected to be a substrate of CDK1. **(C)** Data from this assay were quantified by recording the percentage of PLA positive spermatozoa, with 100 cells being examined per sample. Experiments were conducted on five biological replicates and the results are presented as the means  $\pm$  S.E.M. \* $P < 0.05$  compared to progesterone treatment (CDK1/DNM2).

testes. On the other hand, the tenet that DNMI1 may be transferred to maturing spermatozoa draws on a wealth of evidence that the sperm proteome is substantially modified during their transit of the epididymis (Dacheux et al., 2006, 2016; Sullivan and Miesusset, 2016). One of the principle mechanisms implicated in this form of intercellular communication is the interaction formed between spermatozoa and a population of extracellular vesicles, known as epididymosomes, which are secreted into the epididymal lumen (Sullivan, 2015). In support of this mechanism, we detected DNMI1 in whole seminal fluid as well as an extracellular vesicle fraction isolated from this material. While the validity of this model of DNMI1 acquisition awaits further investigation, the labelling of the protein in the peri-acrosomal domain of ejaculated spermatozoa suggests that it may work in tandem with DNMI2, which occupies a similar location, to regulate the release of the acrosomal contents during a progesterone-induced acrosome reaction. Such functional redundancy is a relatively common feature of dynamin expression in somatic cells (Altschuler et al., 1998), and is also commensurate with the overall importance of the acrosome reaction in terms of securing successful fertilization.

Notwithstanding the potential for overlapping function between DNMI1 and DNMI2, our collective data lead us to conclude that DNMI2 is likely to fulfil the dominant role in terms of both male germ cell development and function. Indeed, the conditional ablation of this ancestral form of the enzyme, which is most closely related to the dynamin-like proteins detected in lower organisms (Chircop et al., 2011), leads to a complete arrest of early germ cell development (Redgrove et al., 2016). In contrast, the loss of DNMI1 at a similar stage of germ cell development had no discernible effect on either germ cell development or the fertility of the null males (Redgrove et al., 2016). It is also noted that during latter phases of germ cell development, the DNMI2 protein co-localizes with PNA at a time when Golgi-derived vesicles begin to fuse to form a single large secretory vesicle that eventually gives rise to the acrosome (Kierszenbaum et al., 2003). This agrees with data implicating DNMI2 as a key regulator of newly formed vesicles and post-Golgi vesicle exocytosis in various somatic cell types (Jones et al., 1998; Kreitzer et al., 2000; Grimmer et al., 2005; Kessels et al., 2006; Jaiswal et al., 2009). On the basis of similar patterns of localization in human testis, it is tempting to suggest that DNMI2 may



fulfil an equivalent role in our species. In a similar vein, the expression of DNM2 detected within the epididymal epithelium suggests that the protein may also exert an influence over the secretion of proteins into the epididymal lumen and, in so doing, influence the maturation of spermatozoa (Zhou *et al.*, 2017).

The possibility that such functional conservation extends to the control of mature human spermatozoa is supported by selective pharmacological inhibition, which led to a significant reduction in the ability of these cells to complete an acrosome reaction. However, in seeking to discern the relative importance of DNMI and DNM2 in this response, it is notable that the dynamins inhibitors employed in this study target both isoforms with equivalent efficacy owing to their selective inhibition of the GTPase activity of these enzymes (Macia *et al.*, 2006; McCluskey *et al.*, 2013). Despite this, the importance of DNM2 is underscored by the dramatic underrepresentation of this isoform, but not DNMI, in the subpopulation of poor quality spermatozoa recovered from healthy donors following density gradient centrifugation. Importantly, the apparent loss of DNM2 was correlated with reduced ability of these

cells to complete a progesterone-induced acrosome reaction. The fact that these cells retained the competence to complete a calcium ionophore induced acrosome reaction, which is relatively forgiving of the functional status of the cell, indicates that this was not associated with compromised structural integrity of the acrosomal vesicle. While such findings would clearly benefit from further validation across an expanded cohort of patients with zona pellucida penetration defects, they nevertheless support the importance of the DNM2 in governing the acrosomal responsiveness of human spermatozoa.

An important caveat to this interpretation is that the putative importance of progesterone as a physiologically relevant stimulus to prime human spermatozoa for induction of acrosomal exocytosis remains the subject of active debate (Buffone *et al.*, 2014). Recent evidence mounts a compelling case in favour of this hypothesis by revealing that progesterone can interact either directly (Lishko *et al.*, 2011; Strunker *et al.*, 2011), or indirectly with CATSPER channels in human spermatozoa (Miller *et al.*, 2016). In the latter model, it is suggested that progesterone binds to abhydrolase domain containing 2 (ABHD2). This lipid hydrolase

is highly expressed in human spermatozoa where it is responsible for the degradation of endocannabinoid 2-arachidonoylglycerol (2AG), and hence its depletion from the plasma membrane. Since 2AG inhibits CATSPER, its progesterone-dependent removal (Miller et al., 2016) serves to modulate intracellular calcium levels as necessitated for the induction of acrosomal exocytosis (Beltrán et al., 2016). However, the fact that both CATSPER channels and ABHD2 are restricted to the flagellum of human spermatozoa (Lishko et al., 2011; Strünker et al., 2011; Miller et al., 2016) raises the question of whether the CATSPER initiated calcium fluxes could be propagated to the anterior region of the sperm head. Tentative support for this model rests with the demonstration that mouse spermatozoa challenged with solubilised ZP proteins responded via the propagation of a CATSPER-dependent calcium wave that progressed from the flagellum toward the head (Ren and Xia, 2010). An alternative possibility is that progesterone could induce acrosomal exocytosis via interaction with progesterone receptors (Aquila and De Amicis, 2014) that are known to be located in the mid-piece/neck region of human spermatozoa (Thomas et al., 2009). A further consideration is the prospect that the spermatozoa of different species may respond differently to progesterone stimulus. For instance, unlike their human counterparts, the CATSPER harbored by mouse spermatozoa is reportedly refractory to progesterone stimulus. Similarly, 2AG is removed from the plasma membrane of mouse spermatozoa prior to their completion of epididymal transit (Miller et al., 2016). Despite this, mouse spermatozoa do retain the capacity to respond to progesterone through induction of an acrosome reaction (Osman et al., 1989).

Irrespective of the pathways employed, our data emphasize the importance of downstream events tied to progesterone stimulus via the demonstration that dynamin phosphorylation can promote the induction of acrosomal exocytosis in the spermatozoa both humans and mice. Indeed, in our hands progesterone challenge led to an increase in phosphorylation of DNMI Ser-778/DNM2 Ser-764 in human spermatozoa. The consequences of the phosphorylation of these dynamin residues has been studied extensively in the context of membrane remodelling and vesicle scission in somatic cells. In neural tissue, replacement of DNMI and DNM3 with DNMI dephospho- or phospho-mimetic mutations can either accelerate or decelerate the endocytotic process (Armbruster et al., 2013). Similarly, DNM2 phosphorylation in endothelial cells has proven to be essential for scission of caveolae (Shajahan et al., 2004). In our own studies, we have previously reported a substantive increase in dynamin phosphorylation in the peri-acrosomal region of mouse spermatozoa following progesterone challenge (Reid et al., 2012). On the basis of these data we hypothesized that dynamin phosphorylation may slow the rate of expansion and/or stabilize the formation of fusion pores between the outer acrosomal membrane and plasma membrane thereby prolonging the exocytosis process consistent with the protracted kinetics of this unique secretory process. Our data from this study suggest that dynamin phosphorylation may also play a pivotal role in the modulation of its function in human spermatozoa. Further work is now needed to reconcile the differences in progesterone action in the spermatozoa of these two species.

In order to initiate these studies, we sought to identify the kinase responsible for dynamin phosphorylation, with our data revealing that CDK1 is a likely candidate in the phosphorylation of DNM2, but not DNMI, within the acrosomal region of progesterone stimulated spermatozoa. This result is consistent with independent studies identifying

CDK1 as the principle kinase responsible for DNM2 phosphorylation in somatic cells and in mouse germ cells (Chircop et al., 2011; Ferguson and De Camilli, 2012; Redgrove et al., 2016). While we sought to confirm the CDK1/DNM2 interaction using reciprocal co-immunoprecipitation, regrettably this interaction proved recalcitrant to this strategy irrespective of whether CDK1 or DNM2 were used as the bait. Among the possible explanations, we consider that the transient nature of the kinase/substrate interaction, which is typically measured in milliseconds, precluded the capture of this event. Nevertheless, we did confirm that CDK1 co-localizes with DNM2 in the anterior region of the sperm head and that the selective inhibition of this kinase suppressed the ability of these cells to respond to progesterone challenge in terms of both DNM2 phosphorylation (at Ser-764) and acrosomal exocytosis. In accounting for these findings, it is noteworthy that dynamin phosphorylation is known to regulate the enzymes GTPase activity and hence the scission of vesicles in neuronal tissues (Robinson et al., 1993). These findings encourage speculation of a causative link between the suppression of DNM2 Ser-764 phosphorylation and the GTPase-dependent conformational change in the protein that putatively regulates acrosomal exocytosis. However, we are cognizant that CDK1 has the potential to phosphorylate multiple substrates (Ubersax et al., 2003) and we remain uncertain what, if any, role(s) these additional targets have in the regulation of sperm function; thus, these data must be interpreted with caution.

In summary, the collective findings described in this, and our preceding studies of dynamin function, lead us to propose that this family of mechanoenzymes may hold conserved roles in the regulation of several aspects of male fertility. Chief among these are the support of acrosome formation during germ cell development and the regulated exocytotic release of the acrosomal contents that precedes fertilization. Such activity appears to be intimately tied to the phosphorylation status of the protein, with our current study identifying CDK1 as a key regulatory kinase in the phosphorylation of DNM2. Our study has also provided evidence that the underrepresentation of DNM2 is associated with poor quality spermatozoa that fail to complete acrosomal exocytosis. Although the causative nature of these phenomenon awaits further investigation, this study stimulates further research into the potential of dynamin as a novel molecular target to assist with diagnosis of male infertility and the establishment of discrete criteria for the stratification of infertility patients into appropriate therapeutic options.

## Supplementary data

Supplementary data are available at *Molecular Human Reproduction* online.

## Acknowledgements

The authors are grateful to Jodie Powell for orchestrating the panel of healthy donors used in this research and Dr Zhuo Yu of Shanghai Jiaotong University for the supply of human testis and epididymis sections.

## Authors' roles

W.Z. conducted the experiments and generated the manuscript. A.L.A. provided technical assistance. A.P.T. conducted the electron microscopy experiment. G.N.D.I. and E.A.M. contributed to study conception and design, data interpretation and manuscript editing. A.M. provided

Dyngo-Θ, the instruction of the usage of dynamín inhibitors. B.N. conceived this study and contributed to study design, data interpretation, and manuscript preparation. All authors approved the final version and submission of this article.

## Funding

National Health and Medical Research Council of Australia Project Grant (APPI 103176 B.N. and E.A.M).

## Conflict of interest

The authors declare that they have no conflicts of interest.

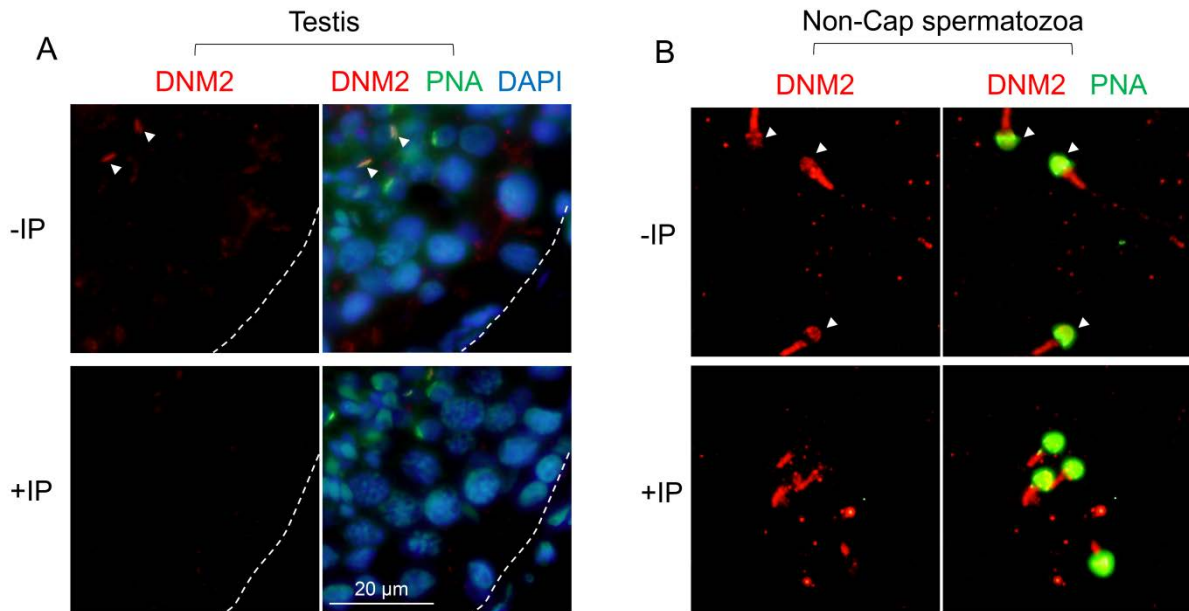
## References

- Aitken RJ, Harkiss D, Buckingham D. Relationship between iron-catalysed lipid peroxidation potential and human sperm function. *J Reprod Fertil* 1993;**98**:257–265.
- Aitken RJ, Nixon B. Sperm capacitation: a distant landscape glimpsed but unexplored. *Mol Hum Reprod* 2013;**19**:785–793.
- Altschuler Y, Barbas SM, Terlecky LJ, Tang K, Hardy S, Mostov KE, Schmid SL. Redundant and distinct functions for dynamín-1 and dynamín-2 isoforms. *J Cell Biol* 1998;**143**:1871–1881.
- Amaral A, Castillo J, Ramalho-Santos J, Oliva R. The combined human sperm proteome: cellular pathways and implications for basic and clinical science. *Hum Reprod Update* 2014;**20**:40–62.
- Anantharam A, Bittner MA, Aikman RL, Stuenkel EL, Schmid SL, Axelrod D, Holz RW. A new role for the dynamín GTPase in the regulation of fusion pore expansion. *Mol Biol Cell* 2011;**22**:1907–1918.
- Andreani A, Cavalli A, Granaiola M, Leoni A, Locatelli A, Morigi R, Rambaldi M, Recanatini M, Garnier M, Meijer L. Imidazo [2, 1-b] thiazolymethylene-and indolylmethylene-2-indolinones: a new class of cyclin-dependent kinase inhibitors. Design, synthesis, and CDK1/cyclin B inhibition. *Anti-Cancer Drug Des* 2000;**15**:447–452.
- Antony B, Burd C, De Camilli P, Chen E, Daumke O, Faelber K, Ford M, Frolov VA, Frost A, Hinshaw JE. Membrane fission by dynamín: what we know and what we need to know. *EMBO J* 2016;**35**:2270–2284.
- Aquila S, De Amicis F. Steroid receptors and their ligands: effects on male gamete functions. *Exp Cell Res* 2014;**328**:303–313.
- Armbruster M, Messa M, Ferguson SM, De Camilli P, Ryan TA. Dynamín phosphorylation controls optimization of endocytosis for brief action potential bursts. *eLife* 2013;**2**:e00845.
- Avella MA, Dean J. Fertilization with acrosome-reacted mouse sperm: Implications for the site of exocytosis. *Proc Natl Acad Sci* 2011;**108**:19843–19844.
- Baibakov B, Gauthier L, Talbot P, Rankin TL, Dean J. Sperm binding to the zona pellucida is not sufficient to induce acrosome exocytosis. *Development* 2007;**134**:933–943.
- Barros C, Bedford JM, Franklin LE, Austin CR. Membrane vesiculation as a feature of the mammalian acrosome reaction. *J Cell Biol* 1967;**34**:C1–C5.
- Belmonte SA, Mayorga LS, Tomes CN. The molecules of sperm exocytosis. In: Buffone M (ed). *Sperm Acrosome Biogenesis and Function During Fertilization. Advances in Anatomy, Embryology and Cell Biology*, Vol. 220, Cham: Springer, 2016, 71–92.
- Beltrán C, Treviño CL, Mata-Martínez E, Chávez JC, Sánchez-Cárdenas C, Baker M, Darszon A. Role of ion channels in the sperm acrosome reaction. In: Buffone M (ed). *Sperm Acrosome Biogenesis and Function During Fertilization. Advances in Anatomy, Embryology and Cell Biology*, Vol. 220, Cham: Springer, 2016, 35–69.
- Biggers JD, Whitten WK, Whittingham DG. Culture of mouse embryos in vitro. In: Daniel J.C. Jr (ed). *Methods in Mammalian Embryology*. San Francisco: Freeman, 1971:86–116.
- Björndahl L, Barratt CL, Mortimer D, Jouannet P. 'How to count sperm properly': checklist for acceptability of studies based on human semen analysis. *Hum Reprod* 2015;**31**:227–232.
- Blackmore PF, Beebe SJ, Danforth DR, Alexander N. Progesterone and 17 alpha-hydroxyprogesterone. Novel stimulators of calcium influx in human sperm. *J Biol Chem* 1990;**265**:1376–1380.
- Bromfield EG, Aitken RJ, Anderson AL, McLaughlin EA, Nixon B. The impact of oxidative stress on chaperone-mediated human sperm–egg interaction. *Hum Reprod* 2015a;**30**:2597–2613.
- Bromfield EG, Aitken RJ, Nixon B. Novel characterization of the HSPA2-stabilizing protein BAG6 in human spermatozoa. *Mol Hum Reprod* 2015b;**21**:755–769.
- Buffone MG, Hirohashi N, Gerton GL. Unresolved questions concerning mammalian sperm acrosomal exocytosis. *Biol Reprod* 2014;**90**:1–8.
- Buffone MG, Ijiri TW, Cao W, Merdiushev T, Aghajanian HK, Gerton GL. Heads or tails? Structural events and molecular mechanisms that promote mammalian sperm acrosomal exocytosis and motility. *Mol Reprod Dev* 2012;**79**:4–18.
- Cao H, Garcia F, McNiven MA. Differential distribution of dynamín isoforms in mammalian cells. *Mol Biol Cell* 1998;**9**:2595–2609.
- Cheng FP, Fazeli A, Voorhout WF, Marks A, Bevers MM, Colenbrander B. Use of peanut agglutinin to assess the acrosomal status and the Zona pellucida-induced acrosome reaction in stallion spermatozoa. *J Androl* 1996;**17**:674–682.
- Chircop M, Sarcevic B, Larsen MR, Malladi CS, Chau N, Zavortink M, Smith CM, Quan A, Anggono V, Hains PG. Phosphorylation of dynamín II at serine-764 is associated with cytokinesis. *Biochim Biophys Acta* 2011;**1813**:1689–1699.
- Cook TA, Urrutia R, McNiven MA. Identification of dynamín 2, an isoform ubiquitously expressed in rat tissues. *Proc Natl Acad Sci* 1994;**91**:644–648.
- Dacheux JL, Belghazi M, Lanson Y, Dacheux F. Human epididymal secretome and proteome. *Mol Cell Endocrinol* 2006;**250**:36–42.
- Dacheux JL, Dacheux F, Druart X. Epididymal protein markers and fertility. *Anim Reprod Sci* 2016;**169**:76–87.
- Esteves SC, Sharma RK, Thomas AJ, Agarwal A. Cryopreservation of human spermatozoa with pentoxifylline improves the post-thaw agonist-induced acrosome reaction rate. *Hum Reprod* 1998;**13**:3384–3389.
- Ferguson SM, Brasnjo G, Hayashi M, Wölfel M, Collesi C, Giovedi S, Raimondi A, Gong LW, Ariel P, Paradise S. A selective activity-dependent requirement for dynamín I in synaptic vesicle endocytosis. *Science* 2007;**316**:570–574.
- Ferguson SM, De Camilli P. Dynamín, a membrane-remodelling GTPase. *Nat Rev Mol Cell Biol* 2012;**13**:75–88.
- Florman HM, Jungnickel MK, Sutton KA. Regulating the acrosome reaction. *Int J Dev Biol* 2004;**52**:503–510.
- Gassmann M, Grenacher B, Rohde B, Vogel J. Quantifying western blots: pitfalls of densitometry. *Electrophoresis* 2009;**30**:1845–1855.
- Grimmer S, Ying M, Wälchli S, van Deurs B, Sandvig K. Golgi vesiculation induced by cholesterol occurs by a dynamín-and cPLA2-dependent mechanism. *Traffic* 2005;**6**:144–156.
- Iguchi H, Watanabe M, Kamitani A, Nagai A, Hosoya O, Tsutsui K, Kumon H. Localization of dynamín 2 in rat seminiferous tubules during the spermatogenic cycle. *Acta Med Okayama* 2002;**56**:205–209.
- Inoue N, Satouh Y, Ikawa M, Okabe M, Yanagimachi R. Acrosome-reacted mouse spermatozoa recovered from the perivitelline space can fertilize other eggs. *Proc Natl Acad Sci* 2011;**108**:20008–20011.
- Jackson J, Papadopoulos A, Meunier FA, McCluskey A, Robinson PJ, Keating DJ. Small molecules demonstrate the role of dynamín as a bi-directional

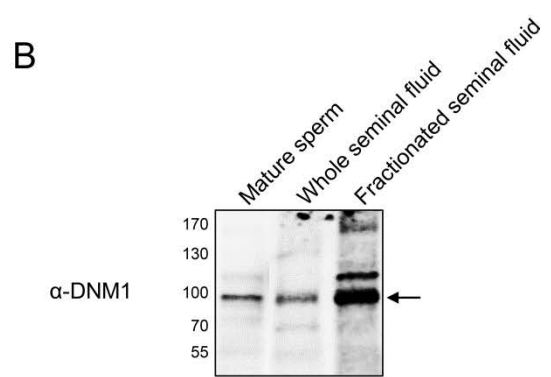
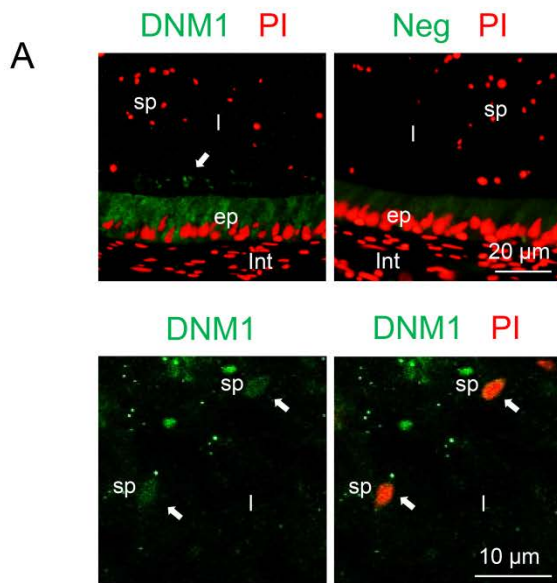
- regulator of the exocytosis fusion pore and vesicle release. *Mol Psychiatry* 2015;**20**:810–819.
- Jaiswal JK, Rivera VM, Simon SM. Exocytosis of post-Golgi vesicles is regulated by components of the endocytic machinery. *Cell* 2009;**137**:1308–1319.
- Jones SM, Howell KE, Henley JR, Cao H, McNiven MA. Role of dynamin in the formation of transport vesicles from the trans-Golgi network. *Science* 1998;**279**:573–577.
- Kessels MM, Dong J, Leibig W, Westermann P, Qualmann B. Complexes of syndapin II with dynamin II promote vesicle formation at the trans-Golgi network. *J Cell Sci* 2006;**119**:1504–1516.
- Kierszenbaum AL, Rivkin E, Tres LL. Acroplaxome, an F-actin–keratin-containing plate, anchors the acrosome to the nucleus during shaping of the spermatid head. *Mol Biol Cell* 2003;**14**:4628–4640.
- Kreitzer G, Marmorstein A, Okamoto P, Vallee R, Rodriguez-Boulan E. Kinesin and dynamin are required for post-Golgi transport of a plasma-membrane protein. *Nat Cell Biol* 2000;**2**:125–127.
- Kusumi N, Watanabe M, Yamada H, Li SA, Kashiwakura Y, Matsukawa T, Nagai A, Nasu Y, Kumon H, Takei K. Implication of amphiphysin I and dynamin 2 in tubulobulbar complex formation and spermatid release. *Cell Struct Funct* 2007;**32**:101–113.
- Lie PP, Xia W, Wang CQ, Mruk DD, Yan HH, Wong CH, Lee WM, Cheng CY. Dynamin II interacts with the cadherin-and occludin-based protein complexes at the blood–testis barrier in adult rat testes. *J Endocrinol* 2006;**191**:571–586.
- Lishko PV, Botchkina IL, Kirichok Y. Progesterone activates the principal Ca<sup>2+</sup> channel of human sperm. *Nature* 2011;**471**:387–391.
- Liu DY, Baker HW. Disordered zona pellucida–induced acrosome reaction and failure of in vitro fertilization in patients with unexplained infertility. *Fertil Steril* 2003;**79**:74–80.
- Macia E, Ehrlich M, Massol R, Boucrot E, Brunner C, Kirchhausen T. Dynasore, a cell-permeable inhibitor of dynamin. *Dev Cell* 2006;**10**:839–850.
- McCluskey A, Daniel JA, Hadzic G, Chau N, Clayton EL, Mariana A, Whiting A, Gorgani NN, Lloyd J, Quan A. Building a better dynasore: the dyngo compounds potently inhibit dynamin and endocytosis. *Traffic* 2013;**14**:1272–1289.
- Meizel S, Turner KO, Nuccitelli R. Progesterone triggers a wave of increased free calcium during the human sperm acrosome reaction. *Dev Biol* 1997;**182**:67–75.
- Meyers SA, Overstreet JW, Liu IK, Drobnis EZ. Capacitation in vitro of stallion spermatozoa: comparison of progesterone-induced acrosome reactions in fertile and subfertile males. *J Androl* 1995;**16**:47–54.
- Miller MR, Mannowetz N, Iavarone AT, Safavi R, Gracheva EO, Smith JF, Hill RZ, Bautista DM, Kirichok Y, Lishko PV. Unconventional endocannabinoid signaling governs sperm activation via the sex hormone progesterone. *Science* 2016;**352**:555–559.
- Mitchell LA, Nixon B, Aitken RJ. Analysis of chaperone proteins associated with human spermatozoa during capacitation. *Mol Hum Reprod* 2007;**13**:605–613.
- Mitchell LA, Nixon B, Baker MA, Aitken RJ. Investigation of the role of SRC in capacitation-associated tyrosine phosphorylation of human spermatozoa. *Mol Hum Reprod* 2008;**14**:235–243.
- Morlot S, Roux A. Mechanics of dynamin-mediated membrane fission. *Annu Rev Biophys* 2013;**42**:629–649.
- Mortimer D, Curtis EF, Miller RG. Specific labelling by peanut agglutinin of the outer acrosomal membrane of the human spermatozoon. *J Reprod Fertil* 1987;**81**:127–135.
- Muller CH. Rationale, interpretation, andrology lab corner validation, and uses of sperm function tests. *J Androl* 2000;**21**:10–30.
- Nixon B, MacIntyre DA, Mitchell LA, Gibbs GM, O'Bryan M, Aitken RJ. The identification of mouse sperm-surface-associated proteins and characterization of their ability to act as decapacitation factors. *Biol Reprod* 2006;**74**:275–287.
- Osman RA, Andria ML, Jones AD, Meizel S. Steroid induced exocytosis: the human sperm acrosome reaction. *Biochem Biophys Res Commun* 1989;**160**:828–833.
- Redgrove KA, Anderson AL, Dun MD, McLaughlin EA, O'Bryan MK, Aitken RJ, Nixon B. Involvement of multimeric protein complexes in mediating the capacitation-dependent binding of human spermatozoa to homologous zonae pellucidae. *Dev Biol* 2011;**356**:460–474.
- Redgrove KA, Bernstein IR, Pye VJ, Mihalas BP, Sutherland JM, Nixon B, McCluskey A, Robinson PJ, Holt JE, McLaughlin EA. Dynamin 2 is essential for mammalian spermatogenesis. *Sci Rep* 2016;**6**:35084.
- Redgrove KA, Nixon B, Baker MA, Hetherington L, Baker G, Liu DY, Aitken RJ. The molecular chaperone HSPA2 plays a key role in regulating the expression of sperm surface receptors that mediate sperm-egg recognition. *PLoS One* 2012;**7**:e50851.
- Reid AT, Anderson AL, Roman SD, McLaughlin EA, McCluskey A, Robinson PJ, Aitken RJ, Nixon B. Glycogen synthase kinase 3 regulates acrosomal exocytosis in mouse spermatozoa via dynamin phosphorylation. *FASEB J* 2015;**29**:2872–2882.
- Reid AT, Lord T, Stanger SJ, Roman SD, McCluskey A, Robinson PJ, Aitken RJ, Nixon B. Dynamin regulates specific membrane fusion events necessary for acrosomal exocytosis in mouse spermatozoa. *J Biol Chem* 2012;**287**:37659–37672.
- Reilly JN, McLaughlin EA, Stanger SJ, Anderson AL, Hutcheon K, Church K, Mihalas BP, Tyagi S, Holt JE, Eamens AL. Characterisation of mouse epididymosomes reveals a complex profile of microRNAs and a potential mechanism for modification of the sperm epigenome. *Sci Rep* 2016;**6**:31794.
- Ren D, Xia J. Calcium signaling through CatSper channels in mammalian fertilization. *Physiology* 2010;**25**:165–175.
- Robinson PJ, Sontag JM, Liu JP, Fykse EM, Slaughter C, McMahan H, Südhof TC. Dynamin GTPase regulated by protein kinase C phosphorylation in nerve terminals. *Nature* 1993;**365**:163–166.
- Shajahan AN, Timblin BK, Sandoval R, Tirupathi C, Malik AB, Minshall RD. Role of Src-induced dynamin-2 phosphorylation in caveolae-mediated endocytosis in endothelial cells. *J Biol Chem* 2004;**279**:20392–20400.
- Shpetner HS, Vallee RB. Identification of dynamin, a novel mechanochemical enzyme that mediates interactions between microtubules. *Cell* 1989;**59**:421–432.
- Stival C, Molina LdCP, Paudel B, Buffone MG, Visconti PE, Krampf D. Sperm capacitation and acrosome reaction in mammalian sperm. In: Buffone M (ed). *Sperm Acrosome Biogenesis and Function During Fertilization. Advances in Anatomy, Embryology and Cell Biology*, Vol. 220, Cham: Springer, 2016, 93–106.
- Strünker T, Goodwin N, Brenker C, Kashikar ND, Weyand I, Seifert R, Kaupp UB. The CatSper channel mediates progesterone-induced Ca<sup>2+</sup> influx in human sperm. *Nature* 2011;**471**:382–386.
- Sullivan R. Epididymosomes: Role of extracellular microvesicles in sperm maturation. *Front Biosci (Schol Ed)* 2015;**8**:106–114.
- Sullivan R, Miesusset R. The human epididymis: its function in sperm maturation. *Hum Reprod Update* 2016;**22**:574–587.
- Tan TC, Valova VA, Malladi CS, Graham ME, Berven LA, Jupp OJ, Hansra G, McClure SJ, Sarcevic B, Boadle RA. Cdk5 is essential for synaptic vesicle endocytosis. *Nat Cell Biol* 2003;**5**:701–710.
- Thérien I, Manjunath P. Effect of progesterone on bovine sperm capacitation and acrosome reaction. *Biol Reprod* 2003;**69**:1408–1415.
- Thomas P, Tubbs C, Garry VF. Progesterin functions in vertebrate gametes mediated by membrane progesterin receptors (mPRs): identification of mPR $\alpha$  on human sperm and its association with sperm motility. *Steroids* 2009;**74**:614–621.
- Übersax JA, Woodbury EL, Quang PN, Paraz M, Blethrow JD, Shah K, Shokat KM, Morgan DO. Targets of the cyclin-dependent kinase Cdk1. *Nature* 2003;**425**:859–864.

- Vaid KS, Guttman JA, Babyak N, Deng W, McNiven MA, Mochizuki N, Finlay BB, Vogl AW. The role of dynamín 3 in the testis. *J Cell Physiol* 2007;**210**:644–654.
- Visconti PE, Krapf D, de la Vega-Beltrán JL, Acevedo JJ, Darszon A. Ion channels, phosphorylation and mammalian sperm capacitation. *Asian J Androl* 2011;**13**:395–405.
- Wang G, Guo Y, Zhou T, Shi X, Yu J, Yang Y, Wu Y, Wang J, Liu M, Chen X. In-depth proteomic analysis of the human sperm reveals complex protein compositions. *J Proteomics* 2013;**79**:114–122.
- Williams M, Kim K. From membranes to organelles: emerging roles for dynamín-like proteins in diverse cellular processes. *Eur J Cell Biol* 2014;**93**:267–277.
- World Health Organization *WHO Laboratory Manual for the Examination and Processing of Human Semen*, 5th edn. Switzerland: WHO, 2010.
- Xia Q, Chesí A, Manduchi E, Johnston BT, Lu S, Leonard ME, Parlin UW, Rappaport EF, Huang P, Wells AD. The type 2 diabetes presumed causal variant within TCF7L2 resides in an element that controls the expression of ACSL5. *Diabetologia* 2016;**59**:2360–2368.
- Zhao L, Shi X, Li L, Miller DJ. Dynamín 2 associates with complexins and is found in the acrosomal region of mammalian sperm. *Mol Reprod Dev* 2007;**74**:750–757.
- Zhou W, De Iuliis GN, Turner AP, Reid AT, Anderson AL, McCluskey A, McLaughlin EA, Nixon B. Developmental expression of the dynamín family of mechanoenzymes in the mouse epididymis. *Biol Reprod* 2017;**96**:159–173.

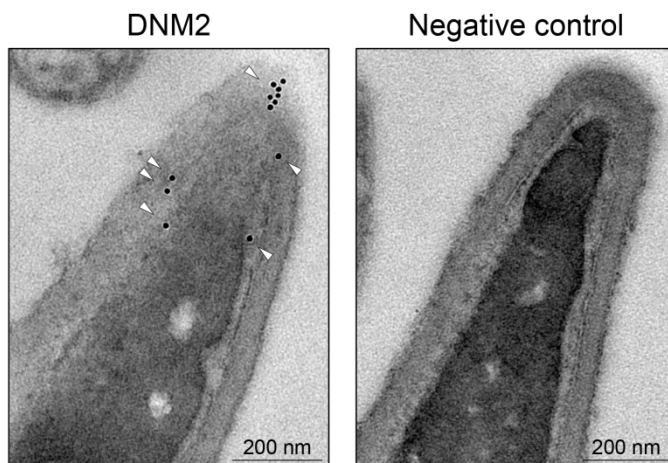
## Chapter 5: Supplementary material



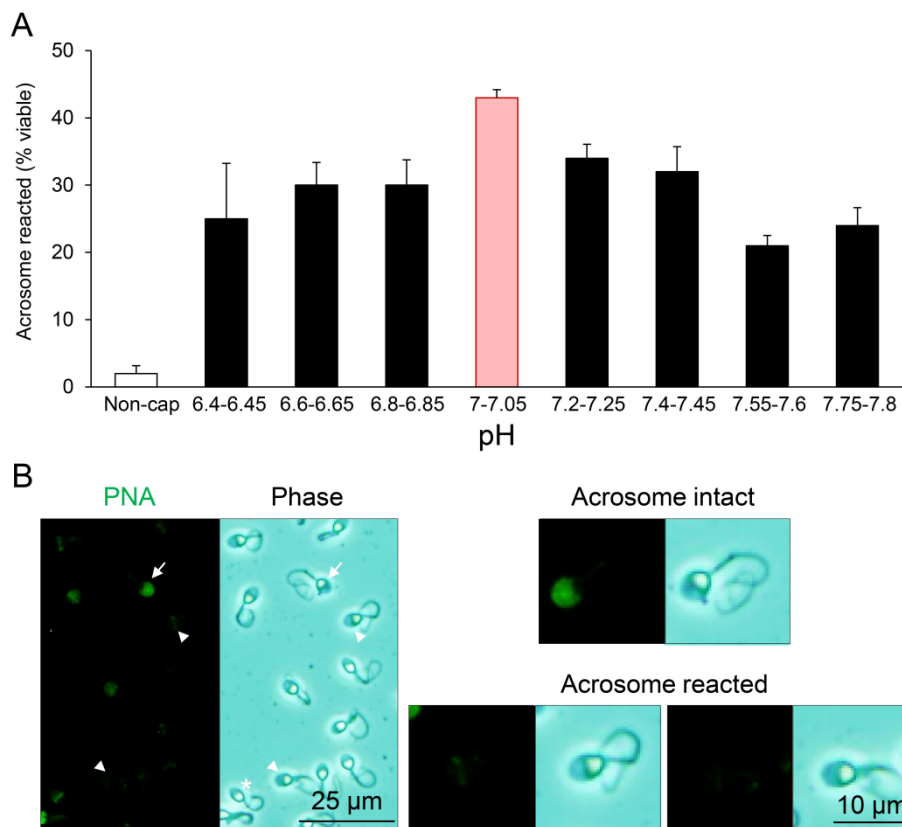
**Supplementary Figure S1 Examination of the specificity of anti-dynamin 2 antibody localisation patterns.** Representative immunofluorescence images indicate that DNM2 is (A) localised to the developing sperm acrosome in testicular tissue (arrowheads), and to the (B) corresponding anterior region of the mature sperm head (arrowheads). (A and B) Both of these localisation patterns were abolished following pre-absorption of the antibody with excess immunizing peptide (+IP). (B) In contrast an additional focus of mid-piece labelling that was detected in mature spermatozoa persisted despite the pre-absorption of the anti-DNM2 antibody with immunizing peptide, suggesting that this is non-specific. (A) DAPI and (A and B) PNA were used to counterstain cells to and detect nuclei (blue) and acrosome, respectively. For clarity, the peripheral structure of seminiferous tubules are outlined with dotted lines.



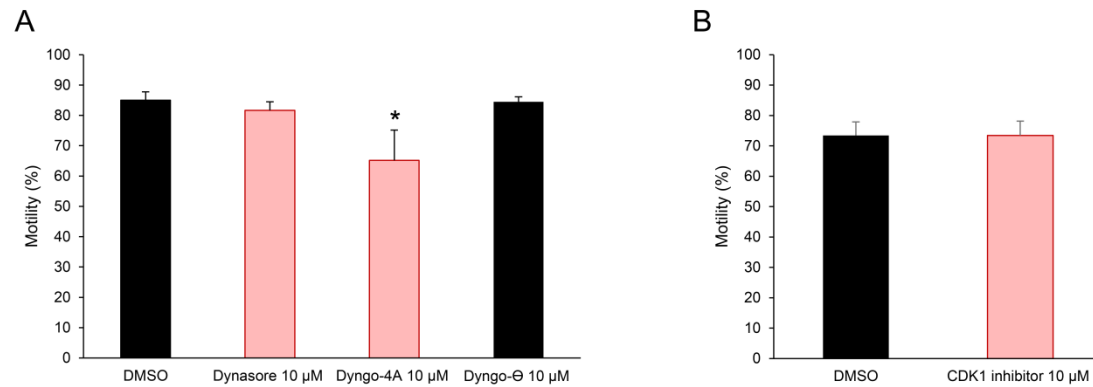
**Supplementary Figure S2 Detection of dynamin 1 in the human epididymis.** (A) The localisation of DNM1 (arrows) was examined in human epididymal sections by sequential labelling with anti-DNM1 antibody and propidium iodide (PI, red). Epithelial cells lining the epididymal duct and spermatozoa within the epididymal lumen were found to both display DNM1 labelling. Representative negative control (Neg, secondary antibody only) images are included to demonstrate the specificity of antibody labelling. ep, epithelial cells; sp, sperm; int, interstitium; l, lumen. (B) Immunoblotting was also employed to detection the presence of DNM1 in whole seminal fluid as well as an extracellular vesicle fraction isolated from seminal fluid via Optiprep density gradient centrifugation.



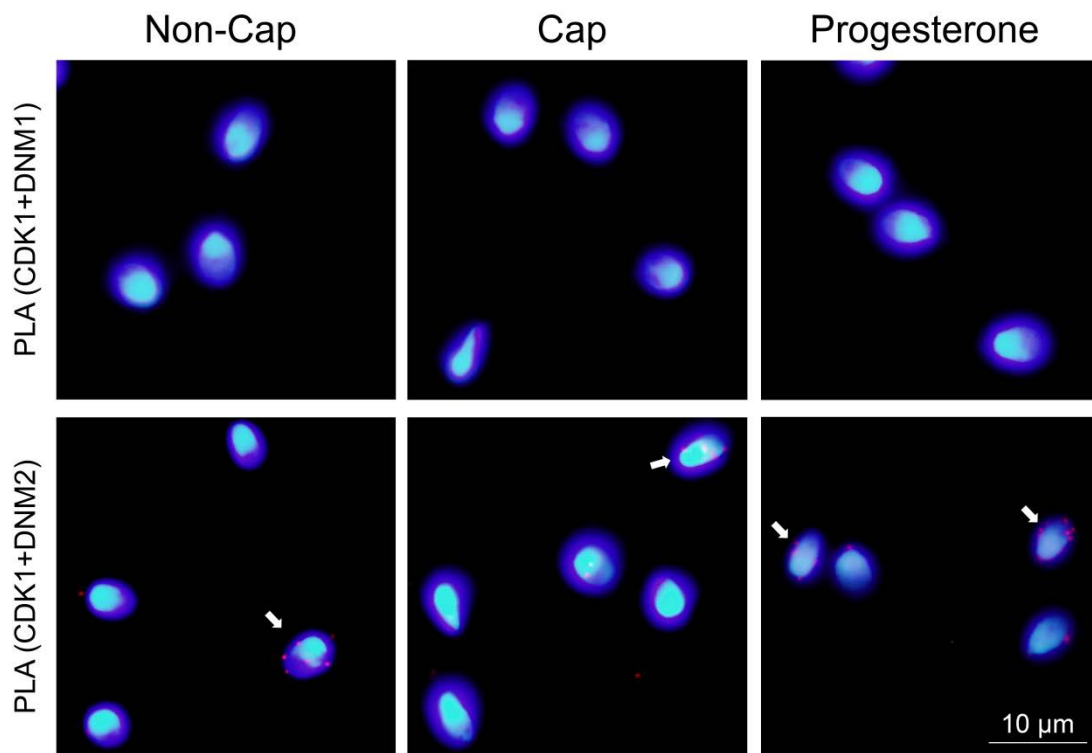
**Supplementary Figure S3 Immunogold labelling of dynamin 2 in head of human spermatozoa.** Electron microscopy was used in conjunction with immunogold secondary antibody to investigate the ultrastructural localisation of DNM2 in the acrosomal domain of human spermatozoa. No equivalent labelling was observed in the negative control samples (Neg) probed with secondary antibody only.



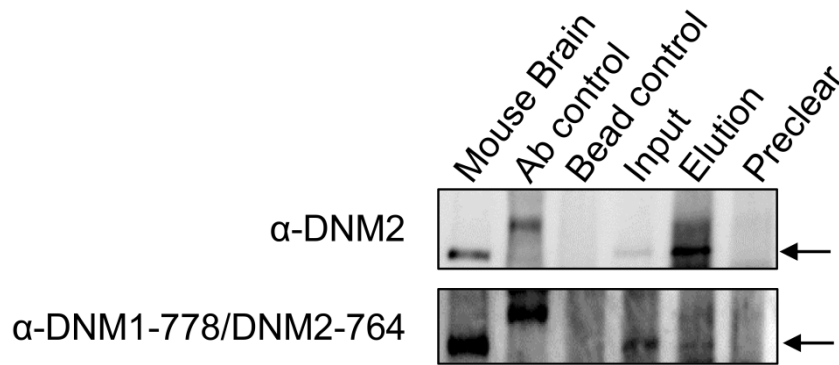
**Supplementary Figure S4** Optimisation of a robust, progesterone-induced acrosome reaction assay via manipulation of the pH (6.4 - 7.8) of the BWB incubation medium. (A) Acrosome reaction rates were found to be consistently elevated in BWB with an adjusted pH of 7.00 - 7.05; thus, these conditions were applied for all subsequent acrosome reaction assays. (B) Representative images illustrative of the PNA labelling criteria used to determine acrosome status; a complete absence of PNA labelling, or restriction of PNA labelling to the equatorial domain, was used to define acrosome reacted sperm cells. Three biological replicates were conducted.



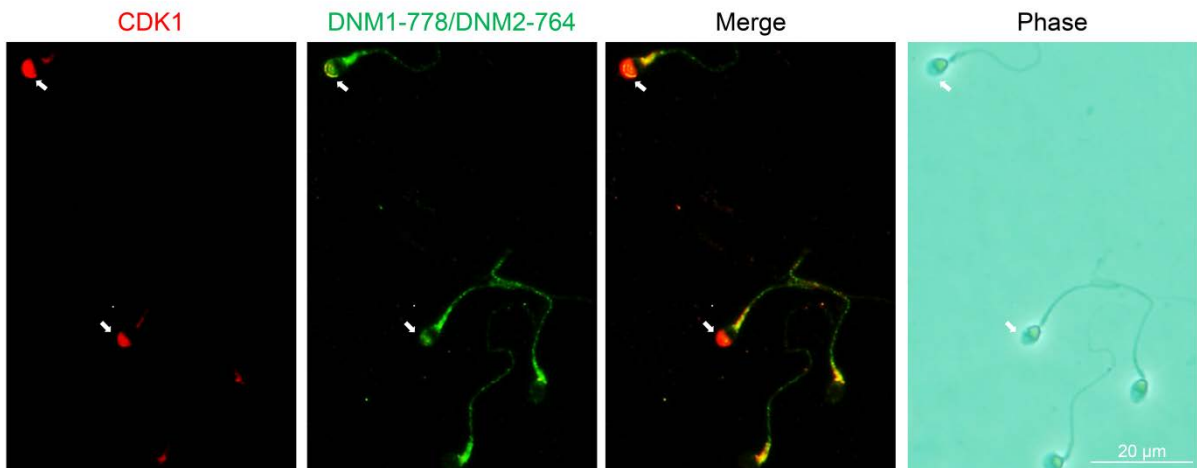
**Supplementary Figure S5 Effect of pharmacological inhibitors on sperm motility.** (A and B) Of all the pharmacological inhibitors used in this study, only Dyngo 4a (10 μM) was found to have a significant negative impact on human sperm motility ( $P < 0.05$ ) compared to DMSO vehicle control. Importantly, this reduction in motility was not accompanied by an equivalent reduction in cell vitality, which remained above 75% in all treatment groups.  $\geq 5$  biological replicates were conducted and quantification of results are presented as the means  $\pm$  S.E.M. \*,  $P < 0.05$ .



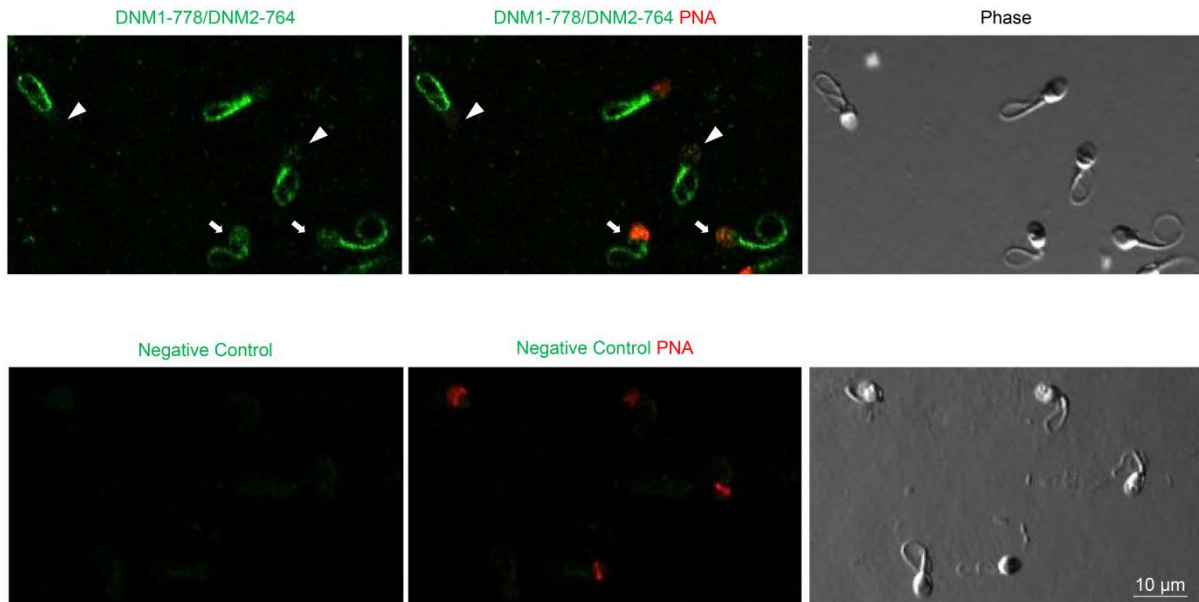
**Supplementary Figure S6** Analysis of CDK1/dynamin 1 and CDK1/dynamin 2 interaction in human spermatozoa. Representative cell population images were shown.



**Supplementary Figure S7 Confirmation that anti-DNM1-Ser778 antibody also recognises phosphorylated DNM2-Ser764.** An immunoprecipitation strategy with anti-DNM2 antibody was used to pull-down DNM2 from sperm lysates. Captured protein were eluted from protein G beads and immunoblotting was used to detect DNM2 and DNM2-Ser764 by anti DNM2 and DNM1-Ser778 antibodies. Alongside with elution are antibody-only control (Ab control), bead-only control (Bead control), progesterone treated sperm lysate (Input) and precleared control (Preclear), Mouse brain lysate was used as positive control to indicate the location of the band.



**Supplementary Figure S8 Colocalisation of CDK1 and phospho-DNM1-778/DNM2-764 in capacitated populations of human spermatozoa treated with progesterone.** Representative immunofluorescence images depicting spermatozoa positively labelled with anti-CDK1 (red) and anti-phospho-DNM1-778/DNM2-764 antibodies. Colocalisation of the target antigens was detected in the anterior region of the sperm head (arrows) and the neck/mid-piece of the flagellum.



**Supplementary Figure S9** Colocalisation of phospho-DNM1-778/DNM2-764 and PNA in capacitated populations of human spermatozoa treated with progesterone. Representative immunofluorescence images depicting spermatozoa positively labelled with PNA in the acrosomal region. These acrosome intact cells were also positively labelled with anti-DNM1-778/DNM2-764 antibodies (arrow). In contrast, the loss of acrosomal contents (denoted by an absence of PNA labelling, arrow heads) was accompanied by a reduction/loss of anti-DNM1-778/DNM2-764 antibody labelling within this domain. Negative control: secondary antibody only.

Antibody	Final concentration <sup>1</sup>			Company	Catalogue N <sup>o</sup> .	Batch N <sup>o</sup> .	Concentration (stock)
	IF	IB	EM				
<b>Primary antibodies</b>							
Dynamin 1	20 µg/ml	1 µg/ml	NA	Abcam	ab108458	GR107528-1	1 mg/ml
Dynamin 2	4 µg/ml	NA	2 µg/ml	Santa Cruz	sc-6400	#L0712	0.2 mg/ml
Dynamin 2	NA	0.27 µg/ml	NA	Thermo	PA5-19800	#QK2113152	0.27 mg/ml
Dynamin 3	3 µg/ml	0.15 µg/ml	NA	Proteintech	14737-1-AP	NA	0.15 mg/ml
Dynamin pSer778	57.8 µg/ml	5.78 µg/ml	NA	Thermo	PA1-4621	QJ2096151	5.78 mg/ml
CDC2 (CDK1)	4 µg/ml	NA	NA	Santa Cruz	sc-54	K1915	0.2 mg/ml
CDK5	4 µg/ml	NA	NA	Santa Cruz	sc-173	A2513	0.2 mg/ml
IZUMO1	4 µg/ml	NA	NA	Santa Cruz	sc-79543	#B1309	0.2 mg/ml
α-Tubulin	NA	1.9 µg/ml	NA	Sigma	T5168	103M4773V	5.7 mg/ml
<b>Secondary antibodies</b>							
Anti rabbit Alexa Fluor 594	5 µg/ml	NA	NA	Thermo	A11012	1608464	2 mg/ml
Anti rabbit Alexa Fluor 488	5 µg/ml	NA	NA	Thermo	A11008	1678787	2 mg/ml
Anti goat Alexa Fluor 594	5 µg/ml	NA	NA	Thermo	A11058	1180089	2 mg/ml
Anti sheep Alexa Fluor 488	5 µg/ml	NA	NA	Thermo	A11015	1567206	2 mg/ml
Anti mouse Alexa Fluor 594	5 µg/ml	NA	NA	Thermo	A11005	1219862	2 mg/ml
Anti rabbit HRP	NA	0.13 µg/ml	NA	Millipore	DC03L	NA	0.13 mg/ml
Anti mouse HRP	NA	0.1 µg/ml	NA	Santa Cruz	sc-2005	B1616	0.4 mg/ml
Anti sheep HRP	NA	2 µg/ml	NA	Abcam	Ab6747	GR238704-1	2 mg/ml
Gold label anti Goat 10 nm	NA	NA	NA	Sigma	G5402	SLBP7446V	NA
PLA probe anti-Mouse PLUS	NA	NA	NA	Sigma	PUO92001	A43902/1	NA
PLA probe anti-Goat MINUS	NA	NA	NA	Sigma	PUO92006	A43108/1	NA
PLA probe anti-Rabbit PLUS	NA	NA	NA	Sigma	PUO92002	A51303/1	NA
PLA probe anti-Mouse MINUS	NA	NA	NA	Sigma	PUO92004	A32705	NA

<sup>1</sup> IF, immunofluorescence; IB, immunoblot; EM, electron microscopy, NA, not applicable / not available

### Supplemental Table S1 Details of antibodies used throughout this study

## Checklist for acceptability of studies based on human semen analysis

### Patients

- × For clinical studies: The patient population (e.g. patients, volunteers, students) has been declared in the manuscript, together with the recruitment method and inclusion and exclusion criteria. If the study concerns couples being investigated for infertility then the following must be specified in the manuscript: fertility status of female partner; and primary, secondary or other level of investigation of the man.
- × If used in the manuscript, the term ‘male factor’ must be completely defined.

### General aspects

- × Patients were instructed to maintain 2–7 days of sexual abstinence before collecting a sample for investigation. *≥ 2 days*
- × Patients were informed about the importance of reporting any missed early ejaculate fractions, and men's answers were noted on the laboratory form. *Verbal confirmation*
- × For specimens not collected at the laboratory, patients were instructed to avoid cooling or heating of the semen sample during transport to the laboratory.
- × Samples were kept at 37°C before initiation of and during the analysis in case of sperm motility assessment.
- □ For samples collected adjacent to the laboratory, analysis was initiated after completion of liquefaction and within 30 min after ejaculation. *Analysis was commenced within 1 h after ejaculation*
- □ Liquefaction was first checked within 30 min after ejaculation. *Liquefaction was checked within 1 h after ejaculation*
- × Volume was determined either by weighing or using a wide-bore volumetric pipette.
- × Viscosity was measured using either a wide-bore pipette or a glass rod. *Wide-bore pipette*
- × All staff members who performed the analyses have been trained in basic semen analysis (ESHRE Basic Semen Analysis Course—or equivalent—and further in-house training) and participate regularly in internal quality control.
- × If more than one method can be recommended for a particular characteristic (e.g. to measure volume), only one should be used in a given study.

### Sperm concentration assessment

- × Semen aliquot to be diluted for sperm concentration assessment was taken with a positive displacement pipette (i.e. a ‘PCR pipette’) using a recommended diluent (state which diluent: *0.37% paraformaldehyde, 0.6M NaHCO<sub>3</sub> in Milli-Q dH<sub>2</sub>O*).

- × Only standard dilutions were used (1:50, 1:20, or 1:10). *1:20*
- × Sperm concentration was assessed using haemocytometers with improved Neubauer ruling.
- × Haemocytometers were allowed to rest for 10–15 min in a humid chamber to allow sedimentation of the suspended spermatozoa onto the counting grid before counting.
- × Sperm counting was done using phase contrast microscope optics (200–400×).
- × Comparisons were made between duplicate counts, and counts re-done when the difference exceeded the acceptance limits.
- □ Typically at least 200 spermatozoa were counted in each of the duplicate assessments.  $\geq 100$

### **Sperm motility assessment**

- × Motility assessments were performed at  $37^{\circ}\text{C} \pm 0.5^{\circ}\text{C}$ .
- × Motility assessments were done using phase contrast microscope optics (200–400×).
- □ Sperm motility was classified using a four-category scheme: rapid progressive, slow progressive, non-progressive, and immotile (World Health Organization, 1999; Björndahl *et al.*, 2010; Barratt *et al.*, 2011).
- × Motility assessments were done in duplicate and compared; counts were re-done on new preparations when the difference between duplicates exceeded the acceptance limits.
- × The wet preparation was made with a drop of 10  $\mu\text{l}$  and a 22  $\times$  22 mm coverslip to give a depth of ~20  $\mu\text{m}$  (must be at least 10  $\mu\text{m}$ , but not too deep so as to allow spermatozoa to move freely in and out of focus; typically *ca.* 20  $\mu\text{m}$ ).
- □ At least 200 spermatozoa were assessed in each duplicate motility count.  $\geq 100$
- × At least 5 microscope fields of view were examined in each duplicate count.

### **Sperm vitality assessment**

- × A validated supravital staining, appropriate to the type of microscope optics utilized, was used to assess sperm vitality.
- □ At least 200 spermatozoa were evaluated in each sample.  $\geq 100$
- □ Assessments were done under high magnification ( $\times 1000$ – $1250$ ) using a  $100\times$  high resolution oil immersion objective and bright field microscope optics (Köhler illumination). *40  $\times$  objective;  $\times 400$  magnification*

### **Sperm morphology assessment**

- × Tygerberg Strict Criteria were used for the evaluation of human sperm morphology.

Note: Another classification could be used for scientific studies with specific aims if the classification is described or referenced. Depending on the aim of the study, the evaluation of particular abnormal forms might be useful. *Reference: WHO laboratory manual for human semen analysis with no staining being applied.*

- Abnormalities are recorded for all four regions of the spermatozoon (head, neck/midpiece, tail and cytoplasmic residue) and the Teratozoospermia Index or 'TZI' was calculated (Björndahl *et al.*, 2010; Barratt *et al.*, 2011).
- If the laboratory claims to use Tygerberg Strict Criteria for the evaluation of human sperm morphology, then the laboratory must participate in an external quality assurance scheme to verify that its assessments comply with these criteria.
- The Papanicolaou staining method adapted for the assessment of human sperm morphology was used. For specific aims other staining methods could be used, but must then be declared and explained.
- At least 200 spermatozoa were assessed in each ejaculate.  $\geq 100$
- Assessments were done under high magnification ( $\times 1000$ – $1250$ ) using a  $100\times$  high resolution oil immersion objective and bright field microscope optics (Köhler illumination).  $40\times$  objective;  $\times 400$  magnification

### **Other findings**

- The presence of abnormal clumping (aggregates and agglutinates) was recorded.
- Abnormal viscosity was recorded.
- The presence of inflammatory cells was recorded and reported if more than 1 million/ml.
- For the purpose of classifying infertility status (World Health Organization, 2010), antisperm antibodies were examined with a validated screening test (state which method was used: \_\_\_\_\_).

### **Analysing data**

- The actual duration of sexual abstinence (in 'hours' or 'days') was recorded for each sample and included in the data reported in the manuscript.  $\geq 2$  days
- As a minimum in clinical studies, semen volume, sperm concentration, total number of spermatozoa/ejaculate, and abstinence time are given to reflect sperm production and output; only samples identified as having been collected completely can be included in the study.
- Confounding factors have been considered for statistical analysis: e.g. abstinence time and age, to evidence secular or geographical variations in sperm concentration or sperm count.

- If appropriate, optional biochemical markers for prostatic, seminal vesicular and epididymal secretions were analysed and reported both as concentration and total amount.
- Signs of active infection/inflammation were noted and considered in the analysis of data in the study (e.g. inflammatory cells, impaired sperm motility, possibly also antisperm antibodies and reduction of secretory contributions).

# CHAPTER 6: FINAL DISCUSSION AND FUTURE RESEARCH DIRECTIONS

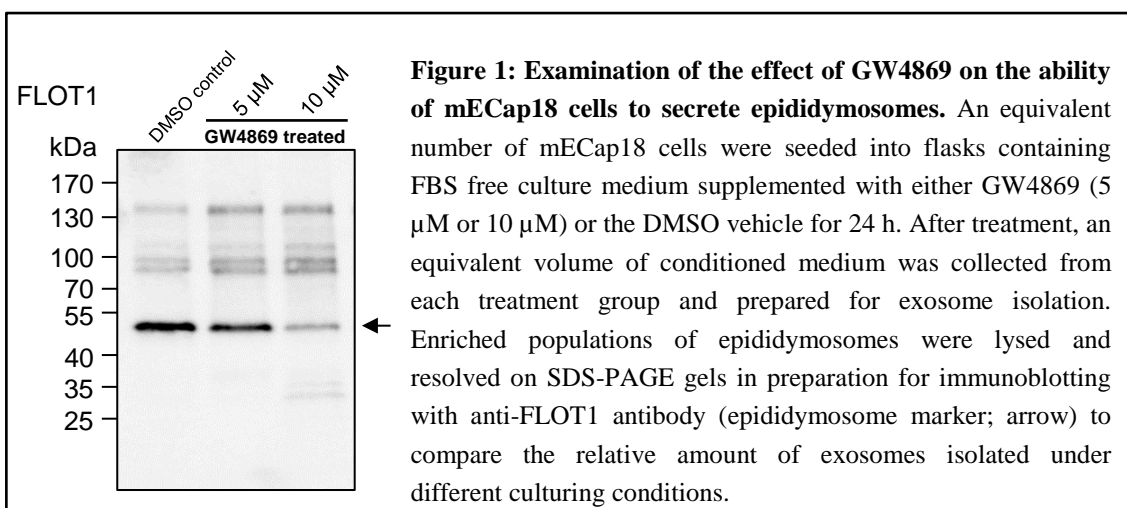
---

The functional development of mammalian sperm is an exceptionally complex process that is initiated with the testes but overtly influenced by their subsequent exposure to the extrinsic milieu within both the male and female reproductive tracts. While a focus for studies of sperm function has been identifying the proteomic components responsible for promoting their motility and ability to interact with the oocyte, comparatively less is known about the regulatory mechanisms responsible for creation of the epididymal microenvironment or those that allow efficient transferral of proteins and other macromolecular cargo to the maturing cell. Improved understanding in this area has potential benefits in terms of informing novel approaches for fertility intervention. Accordingly, my PhD project has focused on dynamin, a protein family with well-characterized roles in the control of membrane trafficking events. Indeed, the overarching hypothesis that was tested is that the dynamin family of enzymes regulate multiple aspects of sperm maturation and function.

During my candidature, I firstly characterized the localization of three dynamin isoforms in the mouse epididymis (Chapter 3). Our data suggest that, instead of overlapping localization, each isoform displays unique patterns of distribution. Notably, dynamin 2 strongly co-localizes with the Golgi apparatus of principal cells within zones 2 to 5 (i.e. the caput segment) of the epididymis. Such a finding is of interest as this epididymal segment is not only most active in terms of protein secretion, but it also coincides with the region in which sperm acquire the potential to display forward progressive motility and to recognize the zona pellucida [1-3]. Implicating dynamin in these processes, we were able to demonstrate that pharmacological inhibition of dynamin led to reduced protein secretion by an *in vitro* caput epididymal cell line. There are a number of potential strategies to build on these observations and further explore the functionality of dynamin in regulating the epididymal microenvironment *in vivo*. Chief among these would be the use of a conditional knockout strategy to selectively ablate the *dynamain 2* gene in the principal epithelial cells of the caput epididymis. Ideally, this knockout mouse model would incorporate the use of Cre/lox recombination driven by a *Lcn5* promoter [4], which directs the segment-specific expression of *Cre* recombinase in caput epididymis of transgenic mice. An additional important property of the *Lcn5* promoter is that it has a relatively late onset of expression,

thus making it an ideal choice to reduce the likelihood of unwanted developmental defects brought about by elimination of dynamin 2 during epididymal differentiation [4]. Access to the *Lcn5-Cre* transgenic mice has been approved by Prof Zhang and studies are currently being planned to utilize this model to directly address the question of whether dynamin 2 is involved in regulating the caput epididymal environment and its downstream effects on sperm functionality.

As a complementary approach, we have also begun to explore the possibility of using microinjection methods to directly deliver dynamin inhibitors into the epididymis via the efferent ducts. Similar methods are well established for the retrograde transplant of spermatogonial stem cells into the testis [5] and have also proven to be applicable for the introduction of reagents into the epididymal lumen [6]. An advantage of this approach is that it is permissive of direct assessment of the impact of dynamin inhibition on sperm functionality; with endpoint analyses focusing on sperm motility and ability to bind to the zona pellucida. As an alternative to dynamin inhibition, this strategy could also be used to introduce reagents such as N-SMase inhibitor GW4869 into the epididymal lumen and thereby focus on the contribution of epididymosomes to sperm functionality [7]. Indeed, the GW4869 reagent has been used extensively to inhibit neutral sphingomyelinases, and thus exosome production and secretion, in a variety of somatic cells [8, 9]. In proof-of-concept pilot studies, we have shown exosome secretion by the mECap18 cell line can be suppressed in a dose-dependent manner via pre-treatment with GW4869 (Figure 1). Importantly, our unpublished data indicates that the exosomes harvested from the mECap18 cell line possesses

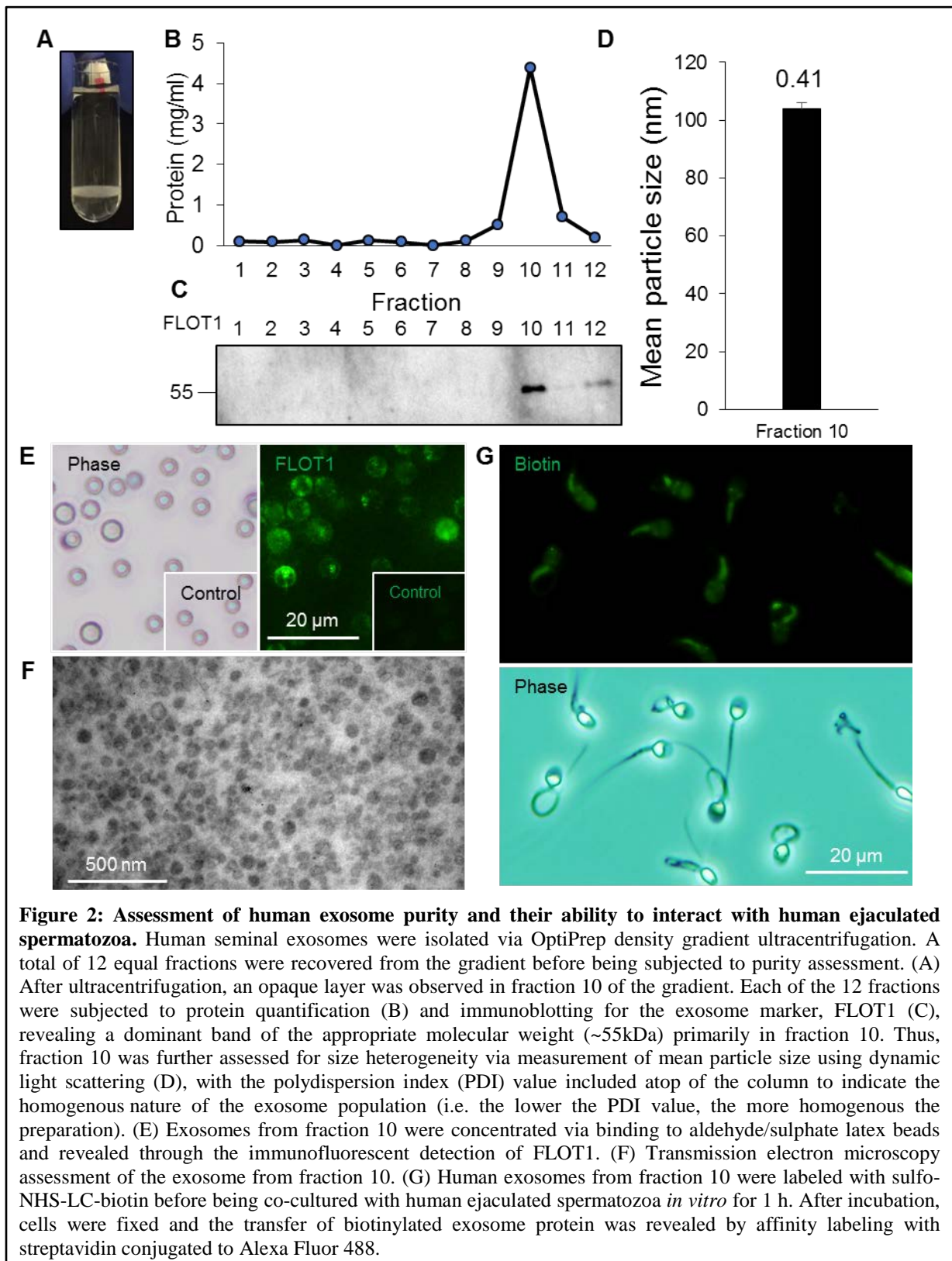


virtually identical physical properties to those epididymosomes harvested from the caput epididymis. Thus, the combination of selective dynamin and exosome inhibition should

enable us to determine the precise role of membrane trafficking / extracellular vesicles in promoting epididymal sperm maturation.

A fascinating phenomenon that has been witnessed during epididymosome-sperm interaction (Chapter 4) is that the lipid rafts are able to selectively relocate dynamin 1 (but not dynamin 2) to the post-acrosomal sheath to facilitate the epididymosome cargo uptake. It is worth mentioning that these two dynamin isoforms not only share over 80% amino acid sequence homology, but also localize to similar domains in mouse spermatozoa [10]. It is therefore tempting to speculate that dynamin 1, but not dynamin 2, selectively partitions into lipid raft microdomains, which coordinate its delivery to sites of epididymosome interaction [11, 12]. Further analysis of lipid raft composition, the mechanistic basis by which they sequester specific elements of the sperm proteome and how they respond to mechanosensitive stimuli remains as exciting avenues for further research. Such studies will benefit from previous independent research [13-15], as well as that of our own group [16], which has reported the successful isolation and preliminary characterization of lipid rafts from spermatozoa.

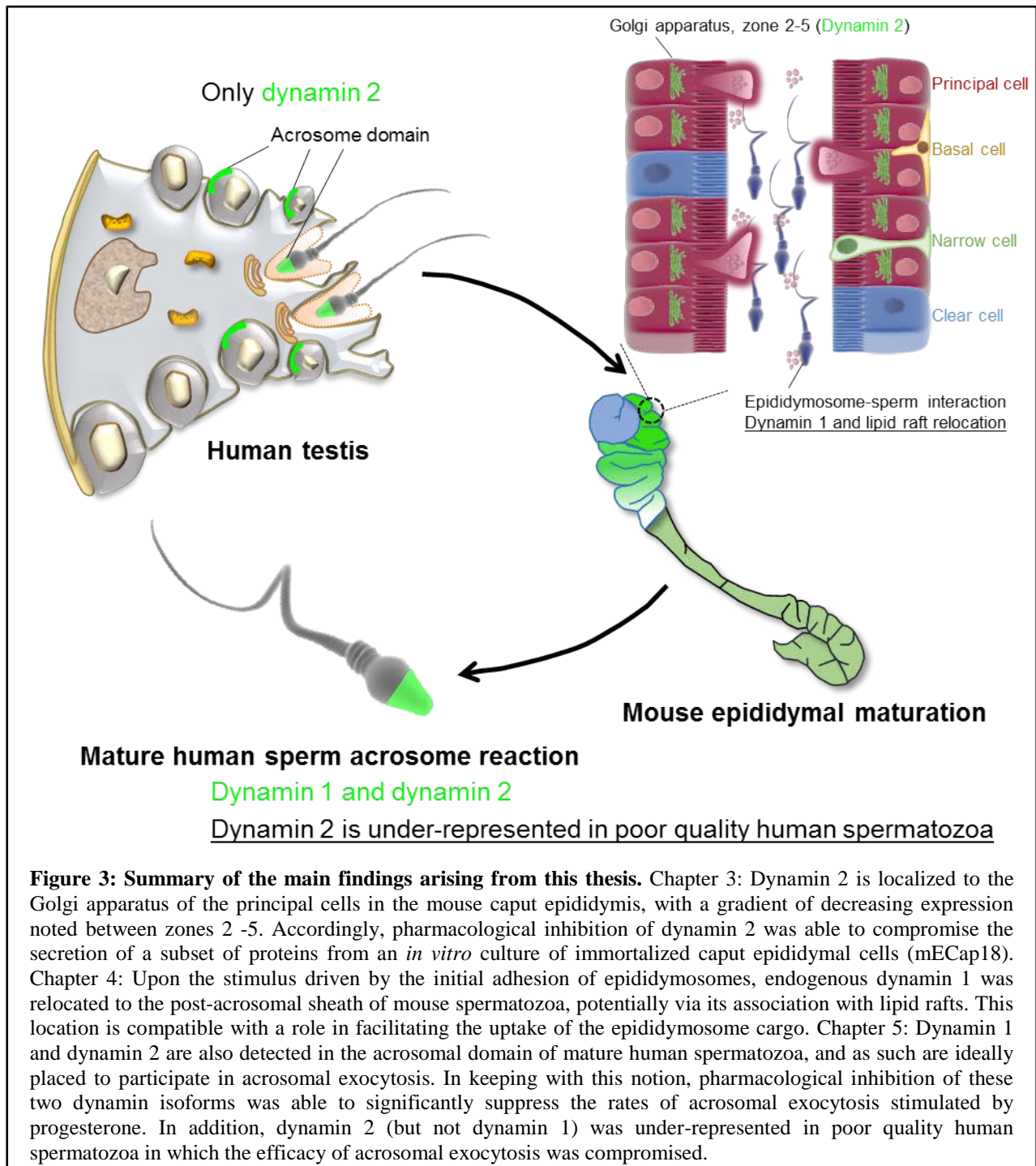
As the ultimate goal of research, we are seeking to translate our understanding of the biological function of dynamin and epididymosomes into human sperm models. Due to an inability to access sufficient quantities of human epididymal fluid, we are instead beginning to purify the exosome population present in human seminal plasma [17]. We acknowledge that a limitation of this approach is that seminal exosomes represent mixed population of extracellular vesicles originating not only from the epididymis, but also from the prostate and seminal vesicles [18]. Nevertheless, seminal exosomes have been implicated in the transfer of protein cargo to sperm, which promotes their motility, ability to capacitate, and complete acrosomal exocytosis [19]. We now have secured pilot data to confirm that the isolation methodology we developed for mouse epididymosomes is suitable for enrichment of human seminal exosomes. As shown in Figure 2, we have conducted preliminary characterization of these exosomes in accordance with the minimal experimental requirements for the definition of extracellular vesicles [20]; with a specific focus on their size, heterogeneity, ultrastructure and detection of FLOT1 (a known exosome marker). In comparison to our work on mouse epididymosomes, we readily isolated an abundance of exosomes from human seminal plasma. Indeed, in a sample of only 100  $\mu$ L of seminal plasma, we were able to visualize an opaque layer corresponding to the partitioning of seminal exosomes within our density gradients (Figure 2A). Furthermore, *in vitro* culturing of these exosomes with human ejaculated sperm, revealed the transfer of biotin (membrane impermeable) labeled proteins to



the head and mid-piece, two sites responsible for sperm-egg interaction and motility, respectively (Figure 2G). Excitingly, *in vitro* culturing of human exosomes with immature mouse caput sperm revealed interaction with a conserved domain within the post-acrosomal region of the head (data not shown). These data raise the prospect of shared mechanisms of

epididymosome-sperm interaction existing in both the human and mouse models. While it remains uncertain whether the epididymosome cargo that is delivered is influenced by the developmental status of the recipient sperm, a deeper understanding of the nature of epididymosome-sperm interactions may contribute to realization of the intriguing possibility that human seminal exosomes could be harnessed as a delivery vehicle to rescue the dysfunctional spermatozoa of infertile individuals.

Finally in Chapter 5, we extended our research focus into the functionality of mature human spermatozoa by assessing factors that regulate acrosomal exocytosis in these cells. This event is compulsory to facilitate sperm penetration of the zona pellucida and hence fertilization of an oocyte. Indeed, failure to complete an acrosome reaction represents a relatively common aetiology among males with idiopathic infertility [21, 22]. Specifically, our study explored the localization of dynamin family members in the human spermatozoa leading to the identification of both dynamin 1 and 2 in the acrosomal domain. Moreover, we demonstrated that pharmacological inhibition of dynamin 1 and dynamin 2 was able to significantly reduce the ability of human spermatozoa to undergo acrosome reaction in response to a progesterone (physiological) stimulus. As an extension of these findings, we also revealed that the poorer quality spermatozoa within an ejaculate have significantly less dynamin 2 within their acrosomal domain compared to that of their higher quality counterparts. Notably, these poorer quality cells were also characterized by a reduction in their ability to complete a progesterone-induced acrosome reaction. These combined findings suggest that dynamin 2 may play a dominant role in regulating this unique exocytotic event and that, despite occupying a similar domain in human spermatozoa, dynamin 1 is not able to compensate for the loss of dynamin 2. In view of these findings, future studies will seek to explore whether the dysfunctional spermatozoa of male IVF patients that present with lesions in egg penetration/acrosome reaction also have reduced levels of dynamin 2. In pilot studies based on two individuals that fit these criteria, we have indeed shown that their spermatozoa have an under-representation of dynamin 2 (data not shown), thus encouraging the recruitment of additional patients to allow the reliability of this putative biomarker of male fertility to be more thoroughly assessed.



### Concluding remarks:

The main findings arising from this thesis are summarized in Figure 3, which serves to illustrate that, consistent with our overarching hypothesis, dynamin mechanoenzymes do play multiple, non-redundant roles in male reproductive biology. This conclusion contrasts that of somatic cell literature in which the dynamin isoforms have commonly been shown to display overlapping patterns of distribution and the ability to functionally compensate for

each other [23]. Such findings suggest that unique protein-protein interaction networks may exist within the male reproductive system that are responsible for tightly regulating the complex development and maturation of the male gamete. An improved understanding of the mechanistic basis of these processes promises to shed light on the aetiology of clinical infertility cases. Indeed, independent evidence implicating dynamin in the regulation of male fertility has been afforded by studies of the antipsychotic agent, chlorpromazine, which disrupts dynamin-dependent endocytotic pathways and results in compromised male fertility; a side-effect that has yet to be directly explored [24]. Although further studies are clearly needed to resolve the complete spectrum of functional roles that dynamin plays in male reproduction, the studies described in this thesis provide the impetus to pursue such goals with potential benefits including improved diagnostic and therapeutic options for male infertility patients.

#### **Additional references:**

1. Dacheux J-L, Belleannée C, Jones R, Labas V, Belghazi M, Guyonnet B, Druart X, Gatti JL, Dacheux F: **Mammalian epididymal proteome**. *Molecular and cellular endocrinology* 2009, **306**(1-2):45-50.
2. Dacheux J-L, Dacheux F: **New insights into epididymal function in relation to sperm maturation**. *Reproduction* 2014, **147**(2):R27-R42.
3. Aitken RJ, Nixon B, Lin M, Koppers AJ, Lee YH, Baker MA: **Proteomic changes in mammalian spermatozoa during epididymal maturation**. *Asian journal of andrology* 2007, **9**(4):554-564.
4. Xie S, Xu J, Ma W, Liu Q, Han J, Yao G, Huang X, Zhang Y: **Lcn5 promoter directs the region-specific expression of cre recombinase in caput epididymidis of transgenic mice**. *Biology of reproduction* 2013, **88**(3):71, 71-78.
5. Brinster RL, Avarbock MR: **Germline transmission of donor haplotype following spermatogonial transplantation**. *Proceedings of the National Academy of Sciences* 1994, **91**(24):11303-11307.
6. Qu B, Gu Y, Shen J, Qin J, Bao J, Hu Y, Zeng W, Dong W: **Trehalose maintains vitality of mouse epididymal epithelial cells and mediates gene transfer**. *PloS one* 2014, **9**(3):e92483.
7. Marchesini N, Luberto C, Hannun YA: **Biochemical properties of mammalian neutral sphingomyelinase2 and its role in sphingolipid metabolism**. *Journal of Biological Chemistry* 2003, **278**(16):13775-13783.
8. Kosaka N, Iguchi H, Yoshioka Y, Takeshita F, Matsuki Y, Ochiya T: **Secretory mechanisms and intercellular transfer of microRNAs in living cells**. *Journal of Biological Chemistry* 2010:jbc. M110. 107821.
9. Trajkovic K, Hsu C, Chiantia S, Rajendran L, Wenzel D, Wieland F, Schwille P, Brügger B, Simons M: **Ceramide triggers budding of exosome vesicles into multivesicular endosomes**. *Science* 2008, **319**(5867):1244-1247.
10. Reid AT, Lord T, Stanger SJ, Roman SD, McCluskey A, Robinson PJ, Aitken RJ, Nixon B: **Dynamin regulates specific membrane fusion events necessary for acrosomal exocytosis in mouse spermatozoa**. *J Biol Chem* 2012:37659-37672.

11. Girouard J, Frenette G, Sullivan R: **Compartmentalization of proteins in epididymosomes coordinates the association of epididymal proteins with the different functional structures of bovine spermatozoa.** *Biol Reprod* 2009, **80**(5):965-972.
12. Griffiths GS, Galileo DS, Reese K, Martin-DeLeon PA: **Investigating the role of murine epididymosomes and uterosomes in GPI-linked protein transfer to sperm using SPAM1 as a model.** *Mol Reprod Dev* 2008, **75**(11):1627-1636.
13. Chamberlain LH: **Detergents as tools for the purification and classification of lipid rafts.** *FEBS letters* 2004, **559**(1-3):1-5.
14. Foster LJ, de Hoog CL, Mann M: **Unbiased quantitative proteomics of lipid rafts reveals high specificity for signaling factors.** *Proceedings of the National Academy of Sciences* 2003, **100**(10):5813-5818.
15. Macdonald JL, Pike LJ: **A simplified method for the preparation of detergent-free lipid rafts.** *Journal of lipid research* 2005, **46**(5):1061-1067.
16. Nixon B, Bielanowicz A, Mclaughlin EA, Tanphaichitr N, Ensslin MA, Aitken RJ: **Composition and significance of detergent resistant membranes in mouse spermatozoa.** *J Cell Physiol* 2009, **218**(1):122-134.
17. Vojtech L, Woo S, Hughes S, Levy C, Ballweber L, Sauteraud RP, Strobl J, Westerberg K, Gottardo R, Tewari M: **Exosomes in human semen carry a distinctive repertoire of small non-coding RNAs with potential regulatory functions.** *Nucleic acids research* 2014, **42**(11):7290-7304.
18. Piehl LL, Fischman ML, Hellman U, Cisale H, Miranda PV: **Boar seminal plasma exosomes: effect on sperm function and protein identification by sequencing.** *Theriogenology* 2013, **79**(7):1071-1082.
19. Tompkins AJ, Chatterjee D, Maddox M, Wang J, Arciero E, Camussi G, Quesenberry PJ, Renzulli JF: **The emergence of extracellular vesicles in urology: fertility, cancer, biomarkers and targeted pharmacotherapy.** *Journal of extracellular vesicles* 2015, **4**(1):23815.
20. Lötvall J, Hill AF, Hochberg F, Buzás EI, Di Vizio D, Gardiner C, Ghossein YS, Kurochkin IV, Mathivanan S, Quesenberry P: **Minimal experimental requirements for definition of extracellular vesicles and their functions: a position statement from the International Society for Extracellular Vesicles.** In: *J Extracell Vesicles*; 2014: 26913.
21. Liu DY, Baker HG: **Disordered zona pellucida-induced acrosome reaction and failure of in vitro fertilization in patients with unexplained infertility.** *Fertility and sterility* 2003, **79**(1):74-80.
22. Liu DY, Clarke GN, Martic M, Garrett C, Baker HG: **Frequency of disordered zona pellucida (ZP)-induced acrosome reaction in infertile men with normal semen analysis and normal spermatozoa-ZP binding.** *Human Reproduction* 2001, **16**(6):1185-1190.
23. Raimondi A, Ferguson SM, Lou X, Armbruster M, Paradise S, Giovedi S, Messa M, Kono N, Takasaki J, Cappello V: **Overlapping role of dynamin isoforms in synaptic vesicle endocytosis.** *Neuron* 2011, **70**(6):1100-1114.
24. Hong C, de Saintonge DC, Turner P: **Effects of chlorpromazine and other drugs acting on the central nervous system on human sperm motility.** *European journal of clinical pharmacology* 1982, **22**(5):413-416.